
Char Slurries as a Fuel for Developing Countries

James Michael Hammerton

Submitted in accordance with the requirements for the degree
of Doctor of Philosophy



The University of Leeds
School of Chemical and Process Engineering

September 2018

Declaration

The candidate confirms that the work submitted is his own, except where work which has formed part of jointly authored publications has been included. The contribution of the candidate and the other authors to this work has been explicitly indicated below. The candidate confirms that appropriate credit has been given within the thesis where reference has been made to the work of others.

Publications

J. Hammerton, L.R. Joshi, A.B. Ross, B. Pariyar, J.C. Lovett, K.K. Shrestha, B. Rijal, H. Li, P.E. Gasson; Characterisation of biomass resources in Nepal and assessment of potential for increased charcoal production, Journal of Environmental Management, Volume 223, 2018, Pages 358-370, <https://doi.org/10.1016/j.jenvman.2018.06.028>.

Research produced for the article appears in chapters 3 and 4. Parts attributable to the thesis author are related to the chemical analysis of the samples collected and analysis of biomass supply and demand. Contributions by co-authors in this thesis are related to the selection and harvesting of samples.



This copy has been supplied on the understanding that it is copyright material and that no quotation from the thesis may be published without proper acknowledgement.



Acknowledgements

I would firstly like to thank my supervisors Dr Andrew Ross, Dr Hu Li, Prof. Paul Williams and Prof. Jonathan Lovett for their continued support throughout the research project. Thank you to Dr Adrian Cunliffe and Karine Alves Thorne in the ERI Analytical lab for training on equipment. I am also very grateful for the assistance provided by Simon Lloyd in the laboratories. I would like to take this opportunity to acknowledge the training in the Particles lab provided to me by Dr Ben Douglas and Susanne Patel.

Without the hard work of the technicians in helping me build the engine test facility, this project could not have been completed. I am especially grateful for the work by Jonathan Stephenson who sadly passed away before the project was completed. Thank you also to Gurdev Bhogal and Scott Prichard for further assistance required for the final years of work on the test facility.

A special thanks to Dr BK Sharma and Dr Bidhya Kunwar for agreeing to host me at the University of Illinois for a month. Also, I would like to thank the technicians and researchers for assisting me and making my short time there, fruitful.

I would like to pay tribute to the other members of the Doctoral Training Centre in Low Carbon Technologies and researchers in SCAPE for helping me find my feet at the University of Leeds. I would also like to thank Post-doctoral Researchers Dr Patrick Biller and Dr Surjit Singh for getting me started on my project.

I am very appreciative of the funding for this project from the Engineering and Physical Sciences Research Council (grant number: EP://G036608/1) . I would also like to acknowledge the funding provided by the Economic and Social Research Council (grant number: ES/K011812/1) for the fieldwork in Nepal, and the Royal Society- DFID Africa Capacity Building Initiative (grant number: AQ150063) for further equipment.

For helping in the collection and analysis of biomass samples in Nepal, and preparation of the journal manuscript, I thank Prof. Krishna Shrestha, Bishnu Rijal and Laxmi Joshi at Tribhuvan University. I would also like to thank Dr Pete Gasson at the Royal Botanic Gardens, Kew, and Bishnu Pariyar and Rachel Gasior at the School of Geography, University of Leeds for their contributions to the study.

Thank you to my family for their endless support and love during some challenging points on the journey. This Thesis is dedicated to my partner, Deborah Brindley for her constant encouragement.

Abstract

The purpose of the thesis was to investigate if producing a slurry made from char particles could be used as a locally sourced alternative to diesel in developing countries for making electricity with engine generators. The lack of access to electricity in many areas of developing countries is seen as one of the biggest barriers to economic development.

The research investigated all aspects of char slurry fuels including sourcing suitable feedstocks, conversion to char, micronisation and combustion in an engine. A slurry fuel testing facility was built for the purpose encompassing a small diesel engine generator, typical of what is available in developing countries for producing electricity.

Analysis of a wide selection of chars made from several types of material showed that woody biomass was the most suitable for producing slurry fuels. The majority of chars made from agricultural residues were not suitable as the silicon content is likely to cause wear issues in engines. The grindability of chars made from biomass was good and the energy requirements to micronise to particle sizes suitable for an engine were small enough to make producing slurry fuels economically viable. It was recommended that low pyrolysis temperatures are used to make char for slurry fuels because they burn better in an engine whilst still having a high grindability.

Two 10%wt. char-diesel slurry fuels were tested, one using a pyrolysis char, the other using a hydrothermal carbonisation (HTC) char. It was found that the HTC char burned better, producing less CO, THC and soot than the pyrolysis char based fuel because the carbon was less recalcitrant. Issues were found with the engine when using slurry fuels, particularly the injector needle which would seize. Investigating better injector design and engine construction materials is a priority to make slurry fuels viable for developing countries.

Table of contents

List of figures and tables	8
Abbreviations	13
Glossary	14
Chapter 1: Introduction	15
1.1 Background	15
1.2 Aims and objectives	21
1.3 Thesis outline	24
1.4 References	26
Chapter 2: Literature review	29
2.1 Introduction	29
2.2 A history of micronised fuels	30
2.2.1 The first micronised fuels	30
2.2.2 Slurry fuel development in the 20 th century	32
2.2.3 Current notable research	34
2.3 Desired characteristics for micronised fuel	35
2.3.1 Low hardness of fuel	35
2.3.2 Organic composition	37
2.3.3 Good grindability	39
2.3.4 High energy content	41
2.3.5 Summary of desired characteristics	42
2.4 Charcoal vs. coal	43
2.5 Thermal treatment of materials	43
2.5.1 Pyrolysis	44
2.5.2 Charcoal making reactor design	46
2.5.3 Hydrothermal carbonisation (HTC)	48
2.5.4 HTC mechanisms	48
2.5.5 HTC reactors	50
2.6 Micronisation	51
2.7 Liquid media	54
2.8 Rheology	55
2.9 Surfactants	57
2.10 Combustion chemistry	61
2.10.1 Combustion of liquid fuels	62
2.10.2 Combustion of solid particles	64
2.11 Diesel additives	66
2.12 Conclusions	67
2.13 References	68
Chapter 3: Materials and methods	79
3.1 Introduction	79
3.2 Selection criteria for slurry fuel feedstocks	79
3.2.1 Scoping potential feedstocks from a range of material	79
3.2.2 Sampling of an important agricultural residue in developing countries	80
3.2.3 Assessment of potential feedstocks in Nepal, a developing country	80

3.3 Preparation of char and samples	81
3.3.1 Preparation of samples for analysis and processing	81
3.3.2 Pyrolysis	82
3.3.3 Hydrothermal carbonisation (HTC)	83
3.4 Char and feedstock analysis	86
3.4.1 Proximate analysis	86
3.4.2 Ultimate analysis	86
3.4.3 Preparation for inorganic analysis	87
3.4.4 Atomic adsorption spectroscopy (AAS)	87
3.4.5 Inductively coupled plasma – optical emission spectroscopy (ICP-OES)	88
3.4.6 Determination of phosphorus by colorimetry	88
3.4.7 X-ray fluorescence (XRF)	88
3.4.8 Temperature programmed oxidation (TPO)	88
3.4.9 Solid state C13 nuclear magnetic resonance (NMR)	89
3.5 Milling of chars and stability of slurries	90
3.5.1 Grindability of chars	90
3.5.2 Processing of chars for slurring	90
3.5.3 Stability analysis and surfactants	90
3.5.4 Measuring char density through pycnometry	91
3.6 Analysis of liquid fuels	91
3.6.1 Elemental analysis	91
3.6.2 Gas chromatography-flame ionisation detection (GC-FID)	91
3.6.3 FAME analysis by GC-MS	92
3.7 Engine test facility	92
3.7.1 Selection of diesel engine	92
3.7.2 Test bed monitoring	94
3.7.3 Andersen cascade impactor	96
3.7.4 Single stage filter for PM ₁₀	97
3.7.5 Horiba stack gas analyser	97
3.7.6 Zirconia sensor	97
3.7.7 Particle size distribution	97
3.7.8 Engine speed	98
3.7.9 Fuel consumption	98
3.7.10 Air-fuel ratio	98
3.7.11 Development of software	98
3.7.12 Engine test procedure	100
3.7.13 Offline analysis	101
3.8 Conclusions	101
3.9 References	102
Chapter 4: Feedstock and char properties.....	103
4.1 Introduction	103
4.2 Biomass availability in a case study country: Nepal	104
4.3 Shea as a feedstock for char in African developing countries	110

4.4 Properties of chars produced from six potential feedstocks for slurry fuels	113
4.4.1 Proximate and ultimate analysis of preliminary candidates for slurry fuels	113
4.4.2 Trace element analysis of potential feedstocks	118
4.4.3 Chars chosen for engine tests	121
4.4.4 Structure and ignition temperature of chars	123
4.5 Conclusions	130
4.6 References	131
Chapter 5: Slurryability of char	135
5.1 Introduction	135
5.2 Effect of milling parameters	136
5.3 Larger scale milling	145
5.4 Power consumption of milling process	149
5.5 Stability	150
5.6 Conclusions	154
5.7 References	155
Chapter 6: Using char as an additive to conventional fuel	157
6.1 Introduction	157
6.2 Chemical composition of fuels used	158
6.2.1 Biodiesel analysis	158
6.2.2 Diesel analysis	160
6.3 Baseline tests using conventional fuels	161
6.3.1 Diesel baseline	161
6.3.2 Biodiesel from waste cooking oil (WCOME) baseline	163
6.4 Char additive tests at 0.1%wt.	167
6.4.1 Gaseous emissions from 0.1%wt. slurries	169
6.4.2 0.1%wt. slurries particle emissions	175
6.4.3 Presence of ash in soot samples	181
6.5 1%wt. char slurries	182
6.5.1 Modification before tests	182
6.5.2 1%wt. slurry fuel consumption	184
6.5.3 Gaseous emissions from 1%wt. slurries	186
6.5.4 Particle emissions from 1%wt. slurries	191
6.6 Conclusions	195
6.7 References	196
Chapter 7: Testing char-diesel slurry fuels	201
7.1 Introduction	201
7.2 Initial studies	202
7.2.1 More modification to the injector	202
7.2.2 Engine cylinder wear	205
7.2.3 Analysis of lubrication oil after engine failure	208
7.2.4 Replacement engine and recommissioning	211
7.3 Testing 10%wt. slurries	211
7.3.1 Properties of fuels tested	211

7.3.2 Particulate emission baseline	212
7.3.3 Effect of using 10%wt. slurries on engine generation efficiency	215
7.3.4 Effect of using 10%wt. slurries on engine gaseous emissions	217
7.3.5 Particle emissions from using 10%wt. slurries	222
7.3.6 Lubrication oil analysis	226
7.4 Conclusions	227
7.5 References	229
Chapter 8: Energy and economics	231
8.1 Introduction	231
8.2 Energy requirements for the production of electricity with a slurry engine	231
8.3 Energy requirements for producing electricity through an engine gasification alternative	235
8.4 Projected cost of microgeneration systems	238
8.5 Conclusions	245
8.6 References	246
Chapter 9: Conclusions	249
9.1 Summary	249
9.1.1 Selection of char	249
9.1.2 Using char slurries	251
9.1.3 Energy and economics	254
9.2 Review of objectives	256
9.3 Limitations	259
9.4 Recommendations for further work	260
9.5 References	263
Appendix 1: Images of reactors and equipment	265
Appendix 2: Labview program for datalogging engine test data	269
Appendix 3: Supplementary tests undertaken on biomass and chars from Nepal	271

List of figures and tables

Figures

1-1 Outline of the slurry making process	18
1-2 Micronized slurry fuel classifications	19
2-1 Diesel's coal dust injection system	30
2-2 Coal Dust Injector invented by Pawilkowski	31
2-3 Products of cellulose pyrolysis	45
2-4 Design of a Brazilian beehive kiln	47
2-5 Lignocellulosic material carbonising into hydrochar microspheres which re-attach to parts of the initial feed that remain during the process of HTC	50
2-6 One half of a twin-screw extruder used for continuous HTC	51
2-7 Jet milling comminution chamber	53
2-8 Viscosity of three water slurries as a function of solid loading	57
2-9 Anionic surfactant molecules interacting with the surface of a coal particle	58
2-10 Cystine didodecyl ester salt- an example of a Gemini Surfactant	59
2-11 Four-stroke diesel engine	62
3-1 Schematic of the pyrolysis reactor used. Showing insert, containing nickel crucibles, used for some tests (top middle)	82
3-2 Pyrolysis reactor used for producing pyrochar	83
3-3 Schematic of the HTC reactors used	84
3-4 600ml hydrothermal reactor	84
3-5 Flow diagram of analysis performed on char and feedstock Samples	85
3-6 An example of a proximate analysis curve produced using a TGA	86
3-7 Typical TPO curve of biomass material	89
3-8 Schematic of engine generator and peripherals	92
3-9 Injector used in the diesel engine selected	94
3-10 Engine generator setup used for char-slurry tests	95
3-11 Andersen cascade impactor and single stage filter	96
3-12 Data and control connections on the engine rig	99
3-13 Schematic of the data handling process in the software	100
4-1 Proximate analysis, mass yield and calorific value of shea residue and chars produced using it	111
4-2 Trace element analysis of shea feedstock and the two chars derived from it	112
4-3 Proximate analysis, mass yields and higher heating values of chars produced from the initial biomass types	114
4-4 Trace element analysis of pyrolysis chars produced from the four most promising initial samples	119
4-5 Trace elemental analysis of hydrothermal chars produced at two different temperatures	121
4-6 Temperature programmed oxidation profiles of solid fuels used in slurry tests	125

4-7 Carbon-13 NMR of chars produced from rhododendron	127
4-8 Carbon-13 NMR of chars produced from chlorella	129
5-1 Cumulative undersize (weight percent) of Rhododendron chips after pyrolysis at 600°C	135
5-2 Lognormal volume distribution of Rhododendron 600°C pyrolysis char after milling for 1 hour using a single 10mm steel ball at different frequencies	136
5-3 Comparison of Rhododendron 600°C pyrolysis char milled at two frequencies for different times	137
5-4 Effect of ball size on the lognormal volume distribution of Rhododendron 600°C pyrolysis charcoal at 25Hz	138
5-5 Effect of thermal treatment on Rhododendron char	139
5-6 Rhododendron 400°C pyrolysis char milled in various concentrations of dispersants	140
5-7 Milling Rhododendron 250°C hydrochar at different dispersant ratios	142
5-8 Milling behaviour of Shea 400°C pyrolysis char	140
5-9 Shea 250°C hydrochar milling behaviour	143
5-10 Chlorella 400°C pyrochar milling behaviour	144
5-11 Chlorella 250°C hydrochar milling behaviour	145
5-12 Disc milling shea 400°C at 1000rpm for different timespans	146
5-13 Shea 400°C pyrolysis char milled in a stirred reactor at 10% wt. solids in diesel at 500 rpm	147
5-14 Particle size distribution of shea 400°C pyrolysis char milled in a stirred reactor at 10%wt. solids in diesel with variation of milling speed	148
5-15 Power curve for the stirred media mill used for wet milling Experiments	149
6-1 FAME analysis of the two biodiesels used	159
6-2 Carbon number distribution of compounds in red and white diesel	160
6-3 Baseline emissions using white diesel fuel	161
6-4 Specific exhaust particle size distributions at varying engine load when using white diesel	163
6-5 Variation in particle emissions with power when using white diesel	163
6-6 Biodiesel from waste cooking oil consumption, generation efficiency and emission characteristics	164
6-7 Particle size distribution of soot emission from the engine running on biodiesel	165
6-8 Particle emissions from the engine using biodiesel	165
6-9 Particle emissions on a mass basis. Circles and triangles represent data for diesel and biodiesel respectively	166
6-10 Fuel consumption of 0.1% wt. slurries	168
6-11 CO ₂ emissions from 0.1%wt. slurries	169
6-12 NO _x emissions from 0.1%wt. slurries	170

6-13 NO ₂ emissions from 0.1% wt. slurries used in a diesel engine	172
6-14 CO emissions from slurry fuels containing 0.1%wt. char	173
6-15 THC emissions from 0.1%wt. slurry	174
6-16 Particle size distribution of soot produced at different loads. Left: diesel baseline, and right: biodiesel baseline	175
6-17 Difference in particle size distribution of 0.1%wt. diesel chars from the neat diesel baseline in figure 6-15	176
6-18 Difference in particle size distribution of 0.1%wt. biodiesel chars from the baseline	178
6-19 shows the total particle emission over all loads for the 0.1%wt. slurries tested	179
6-20 Cut through injector nozzle body and needle with key sections labelled	183
6-21 SEM images of the needle guide area at 80x magnification	181
6-22 Fuel consumption of 1%wt. slurries compared to a diesel baseline containing the lecithin surfactant used	185
6-23 Raw data from balance measuring fuel mass change of diesel with 0.1%wt. lecithin at full load	186
6-24 CO ₂ emissions of 1%wt. slurries	187
6-25 CO emissions of 1%wt. slurries	187
6-26 Exhaust manifold temperature during the operation of the genset using 1%wt. chars in diesel	188
6-27 Total hydrocarbon emissions versus load when using 1%wt. slurries	189
6-28 Oxides of nitrogen emissions from 0.1%wt. slurries	187
6-29 Particle emissions from 0.1%wt. lecithin in diesel baseline test	191
6-30 Change in particle emissions from the baseline when using 1 %wt. slurries	192
6-31 Particle number emission from 1%wt. slurries versus load	194
7-1 Development of injector for 10%wt. slurries	203
7-2 Performance of modified injectors from figure 7-1 operating on a 10% wt. shea pyrochar slurry at idle	204
7-3 Performance of injector 4 across all loads	205
7-4 Inspection of the internal surfaces of the engine cylinder after failure	206
7-5 Worn big end	207
7-6 Worn piston imaged from: a) major, and b) minor thrust side	207
7-7 Particle size distribution of char used in the 10%wt. char-slurry diesel tests	212
7-8 Particle number emission distribution using pure diesel	213
7-9 Particle number emission distribution using diesel containing the surfactant dosage used in 10%wt. slurries -0.5% lecithin	214
7-10 Electrical generation efficiency of the engine using diesel and 10%wt. slurry fuels	215

7-11 Exhaust temperature occurring at different loads using different fuels	216
7-12 CO ₂ emissions using 10%wt. slurries	217
7-13 Carbon monoxide emissions produced by the engine when using 10%wt. slurries	218
7-14 Total hydrocarbon emissions (THC) from using 10%wt. slurries	218
7-15 NO _x emission concentration in the exhaust of the engine generator when using 10%wt. slurries	219
7-16 Nitric oxide emissions when using 10%wt. slurry fuels	220
7-17 Nitrogen dioxide emissions from 10%wt. slurries	221
7-18 Particle number emission concentration in the exhaust when using 10%wt. slurries	222
7-19 Particle number distribution map across the full load range. a) Neat diesel fuel, and b) diesel and 0.5%wt. lecithin	223
7-20 Particle number distribution of soot in the exhaust gas. a) 10%wt. rhododendron pyrochar slurry, and b) 10%wt. rhododendron hydrochar slurry	224
7-21 Change in particle size distribution of soot compared to the tests using the diesel and surfactant mixture. a) 10%wt. rhododendron pyrochar in diesel, and b) 10%wt. rhododendron hydrochar in diesel	224
8-1 Sankey diagram showing input energy and losses associated with producing 1MJ net of electricity via an engine slurry generator	232
8-1 Sankey diagram for the production of electricity using a slurry engine based on the best practice processes in literature which are feasible in a developing country	233
8-3 Sankey diagram based on all available technologies for running a slurry engine for electricity generation	234
8-4 An example of a diesel generator converted to run on syngas	236
8-5 Sankey diagram showing the energy flow for producing electricity through an engine gasifier system	238
8-6 Estimated cost of electricity for diesel engine conversions to biofuels	240
8-7 Cost breakdown of electricity produced by 10kW, operating at a capacity factor of 75%	242
8-8 Cost variation of electricity generated versus the cost of surfactant used for the slurry	243
8-9 Prediction of the economic feasibility of slurry fuel generation systems based on the cost of diesel and the proportion of char used to create electricity	244

Tables

2-1 Hardness of oxides commonly found in ash	36
2-2 Summary of some of the desired properties of solid fuels for engine combustion	42
2-3 Summary of the classification of pyrolysis processes	44
2-4 Properties of media which could be used in a slurry fuel	55
3-1 Temperatures and thermal conversion method used for each set of samples	81
3-2 Properties of the surfactants used	91
3-3 Prediction of the suitability of different types of diesel engine	93
4-1 Total forestry above-ground growing stocks of common species by region	105
4-2 Yearly production of residues from some common crops	106
4-3 Proximate and ultimate analysis of pyrolysis chars produced at 400°C from types of biomass commonly found in Nepal	107
4-4 Trace element analysis of untreated samples collected from Nepal	109
4-5 Ultimate analysis of shea chars produced and feedstock used	111
4-6 Ultimate analysis and energy recovery of the chars produced	117
4-7 Trace elemental analysis of fuels used for tests	122
4-8 Recalcitrance index and chemical shift of methanol sorbed to char	124
5-1 Properties of the two fuels used as a matrix for char particles	150
5-2 Stability of char in diesel and RME at 10%wt. solid loadings	151
5-3 Stability observed of surfactant, liquid and char mixtures	152
5-4 Surfactant blends tested in a 10%wt. rhododendron 400°C diesel slurry	153
6-1 Carbon number and elemental analysis of the two biodiesel fuels used	158
6-2 Elemental analysis of diesel fuels used	160
6-3 Total suspended particles below 10µm (PM10) at full load testing	180
6-4 Particle emissions PM ₁₀ from 1%wt. slurry fuels in diesel	193
7-1 Inorganic analysis by XRF of engine oil before and after testing for 180 hours	209
7-2 Commercial analysis of lubrication oil from test engine	210
7-3 Properties of fuels tested	212
7-4 Particle mass emission from the combustion of 10%wt. slurries in an engine generator	225
7-5 Lubrication oil analysis before and after the 10%wt. slurry tests	226
8-1 Efficiency reported of engine gasifier systems	237
8-2 Economic model assumptions for a 10kW system	239
8-3 Cost of diesel in a number of developing countries as of August 2018	245

9-1 Percentage change in emissions from adding rhododendron char to diesel at three different concentrations when the engine is operated at 3.5kW, the highest power achieved with the highest concentration of particles 251

Abbreviations

AAS	Atomic adsorption spectroscopy
cc	Cubic centimetre
CO	Carbon monoxide
CO ₂	Carbon dioxide
CPMAS	Cross-polarisation magic angle spinning
CV	Calorific value
CWS	Coal-water slurries
DAF	Dry ash free
DB	Dry basis
DI	Deionised
DPMAS	Direct-polarisation magic angle spinning
EDL	Electrical double layer
EDM	Electrical discharge machining
EDX	Energy dispersive x-ray
FTIR	Fourier transform infrared spectroscopy
GDP	Gross Domestic Product
ICP-OES	Inductively coupled plasma- optical emission spectroscopy
HLB	Hydrophillic-lipophilic balance
kW(h)	Kilowatt (hour)
HTC	Hydrothermal carbonisation
MW	Megawatt
NMR	Nuclear magnetic resonance
NO _x	Oxides of nitrogen
NO	Nitric oxide
NO ₂	Nitrogen dioxide
OD	Outer diameter
PM	Particulate matter
PPM	Parts per million
RME	Rapeseed methyl ester
RPM	Revolutions per minute
SEM	Scanning electron microscopy
TGA	Thermal gravimetric analysis
THC	Total hydrocarbons
TPO	Temperature programmed oxidation
WCO	Waste cooking oil
WCOME	Waste cooking oil methyl ester
Wt.	Weight
XRF	X-ray fluorescence

Glossary

Amphoteric	Surfactant containing groups of positive and negative charge. Also known as zwitterionic.
Anionic	Surfactant with solely negatively charged ions.
Capacity factor	The average power produced divided by the rated peak power.
Cationic	Surfactant with solely positively charged ions.
Char	Carbonised material produced from a biomass material.
Cold gas efficiency	Ratio of energy in the feedstock used versus the energy in the syngas produced during gasification.
Dp	Diameter of particle.
Feedstock	Raw material used in manufacturing process.
Genset	Engine generator.
Hydrochar	A char produced via the thermochemical route of hydrothermal carbonisation.
Lignocellulosic	Containing lignin, cellulose and hemicellulose. Terrestrial plant matter.
Load	Resistance to the engine applied externally. Absorbs the power produced.
Pyrochar	A char produced by pyrolysis. Commonly known as charcoal.
Slurry	A mixture of fine particles suspended in a liquid matrix.
Specific emissions	Emissions produced normalised to the useful work performed by the engine.

Chapter 1: Introduction

1.1 Background

The provision of electricity to rural areas in developing countries is a necessity to stimulate development. Electrification assists in reducing energy poverty, improving quality of life, reducing rural-urban migration and improving education as a lot of studying occurs after daylight because children work in the daytime to provide extra income for their families (Javadi et al., 2013; Cherni and Preston, 2007; Mulder and Tembe, 2008). The region with the lowest access to electricity is Sub-Saharan Africa where 62.5% of the population, a total of 609 million people do not have access to electricity (World Bank, 2017). South Asia is another key region for electrification with 20% of people without access. Other lacking areas are East Asia and the Pacific (3.5%), Latin America (3%) and the Middle East and North Africa (3%) (World Bank, 2017). Providing electricity through the burning of fossil fuels is prohibitively expensive for many people and contributes to global warming (Silva Herran and Nakata, 2012). With the cost of small photovoltaics, micro-hydro and wind turbines decreasing, the feasibility of these systems are ever increasing (Cowan and Daim, 2009). Additionally, biomass is an energy source often readily available in rural areas including sewage, agricultural residues and animal dung from subsistence farming and wood from local forestry sources. The use of renewable energy for rural electrification is, therefore, cheaper than fossil fuels in most areas.

Biomass is an incredibly important part of the energy mix in the majority of developing countries. Only oil-producing states in the north of Africa gain less than 10% of their energy from biomass. A total of 7 out of 25 nations assessed by International Energy Agency (2017) in Africa obtained 75% of energy from biomass. In South Asia, 25% of energy consumption is from biomass and Nepal has the highest contribution with 80% (International Energy Agency, 2017).

There are several obstacles to rural electrification. These include poor policy, lack of subsidy and low population density (Barnes, 2011; Mulder and Tembe, 2008). It is often the case that electrification does not extend to the poorest and most remote areas where the cost of interconnections and the lack of demand makes it uneconomical (Barnes, 2011). Micro-grids and home systems can remove the cost of interconnections making them an alternative to national centralised grids (Williams et al., 2015). It is also possible to link micro-grids in the future once they have grown and spread across a large area until there are very small gaps between them. Another key issue is the intermittency of electricity supply. In Sub-Saharan Africa, interruptions cumulate to three months a year and in developing countries overall it is a month causing a significant loss to GDP (Rao, 2013). Interruptions are also generally unevenly distributed to affect rural areas more often.

Despite a collapse in crude oil prices in 2014, fossil fuels remain an expensive source for electricity generation in developing countries. The primary source of electricity in most rural areas is from diesel generators (Inyang, 2008). As diesel is rarely produced locally, the availability is vulnerable either through supply chain disruption or volatility in the price of oil (Williams et al., 2015). Often these diesel generators are converted to run on locally produced fuels to avoid supply issues and reduce costs. A range of liquid and gaseous fuels can be used with few adaptations. The flexibility of the diesel generator makes it very useful for overcoming intermittency problems.

The easiest alternative fuel to use is biodiesel through the transesterification of locally produced oils. However, the process is complicated and expensive (Hoque et al., 2011). It is, however, possible to run a diesel engine on untreated vegetable oil (Satyanarayana and Muraleedharan, 2012). The use of vegetable oil as a feedstock for engine fuels, however, raises an issue of food vs. fuel. The advantage of either vegetable oil or biodiesel as a fuel is that they can be stored for periods of months and used without modification of the generator.

Gaseous fuels such as syngas and biogas can be used in a diesel generator with modification. A gas mixer is required on the intake manifold to add the gaseous fuel to the intake air of the engine. To ignite the fuel in the combustion chamber either pilot injection of diesel to co-fuel the engine or installation of a spark plug into the cylinder is needed (Oh et al., 2018). The range of biomass that can be converted into these gaseous fuels is vast but storing an appreciable amount is very difficult especially with syngas which contains large amounts of carbon monoxide. Gasifiers producing syngas need time to heat up before fuel is produced meaning that it cannot be produced immediately on demand. Anaerobic digesters used to produce biogas often fail to produce gas as a result of poor management and cold weather (Lahav and Morgan, 2004). The supply of this gas is often unreliable and seasonal (Rosenblum et al., 2015).

A novel fuel for diesel generators is char slurry. It consists of micronised charcoal in a liquid medium of water or another fuel which is combustible in a diesel engine, such as diesel. A small amount of additive may also be added to improve the rheological properties and to keep the particles in suspension. By adding charcoal, the longevity of the supply of expensive diesel can be increased. Mixing micronised charcoal with water creates a slurry which can be an alternative to diesel.

Figure 1-1 shows a flow diagram of the general slurry making process. Suitable biomass material must first be found and is cut or chipped so that it fits into the reactor used for carbonisation. Parts of the biomass that contain higher ash may also be screened out. Before converting the material to charcoal it may also be leached to further remove ash present.

Next, the carbonisation process converts the material to charcoal which is less fibrous and so can be easier milled to the ultrafine level needed. Milling then occurs which may happen dry or wet depending on the sample chosen. The micronised charcoal might then be separated, removing the higher ash fragments while retaining the higher grade for use in an engine. The high ash charcoal could be used for other purposes.

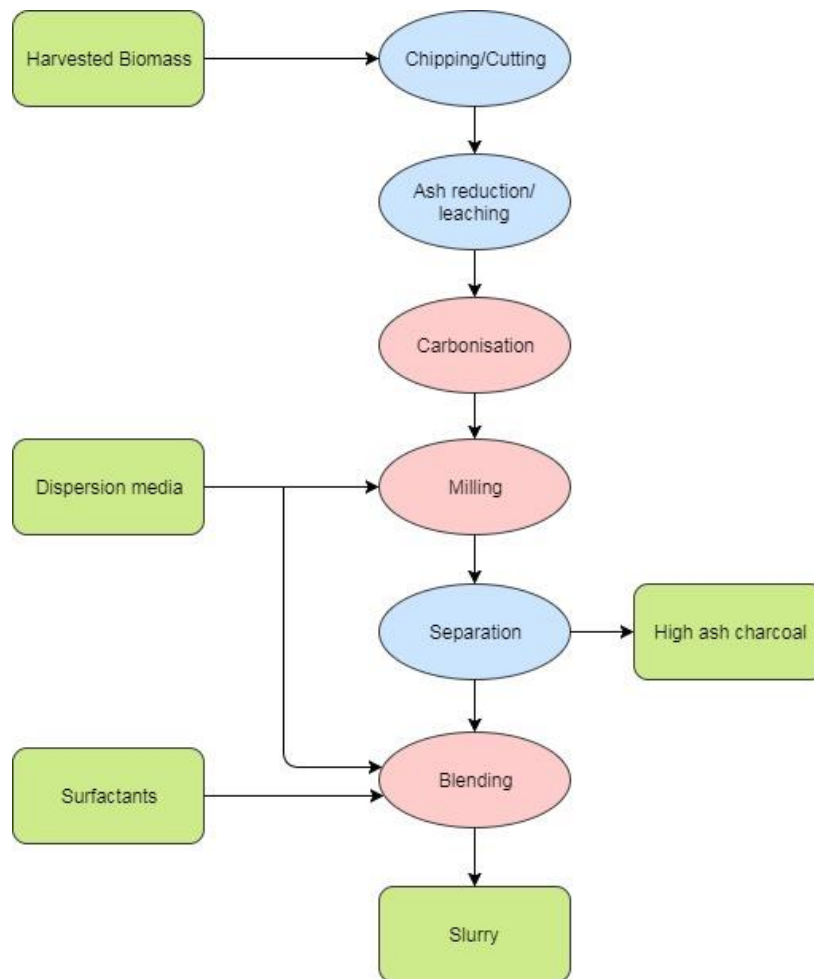


Figure 1-1 Outline of the slurry making process. Inputs and outputs are shown in green, compulsory processes in red and optional processes in blue

Next is a blending stage where further dispersion media is added, as well as surfactants to improve stability and other rheological properties. After this, the fuel is ready to be used.

Charcoal is produced in large quantities in many developing countries and involves a relatively simple process. Access to charcoal, a ball mill to micronise it and a diesel generator to convert the slurry to energy is what is required- all of which are available in most areas of developing countries except for a mill.

Some modification of the diesel generator used might be needed to prepare it for using slurry fuels. Injectors are sometimes hardened to reduce abrasion from the slurry particles and the fuel line heated to reduce viscosity (Patton et al., 2009). One of the most important advantages of this fuel is that it can be stored for long periods, (although it sometimes needs to be remixed) unlike gaseous biofuels. It could, therefore, be used to reduce blackouts when other fuels run out. It can also be produced from a host of biomass resources, unlike other liquid fuel options that demand oil which may therefore not be available all year. The biggest obstacles to implementation are ensuring the fuel does not excessively wear the engine and that the energy required in production is low enough to be economical.

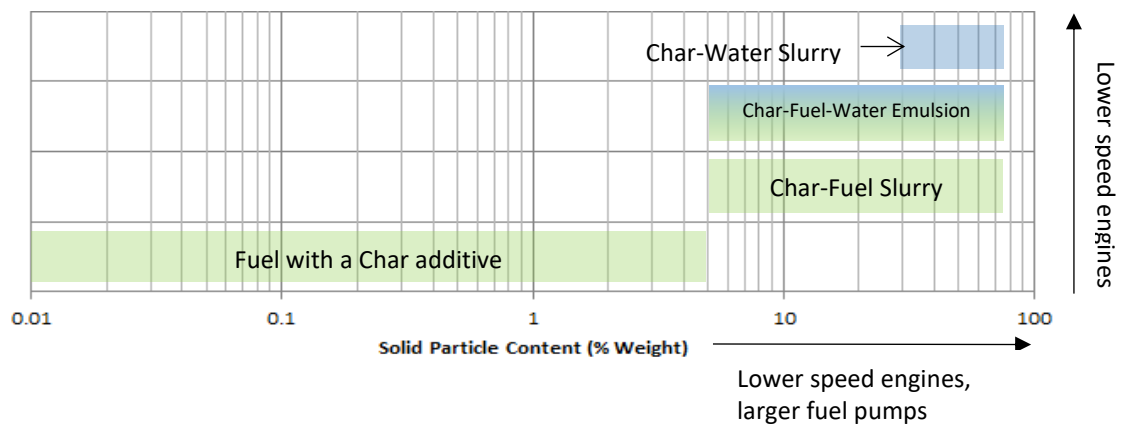


Figure 1-2 Micronised slurry fuel classifications

Slurry fuels can be categorised by the amount of solids and the liquid medium in which they are in (figure 1-2). At low concentrations, below 5%, the majority of effects caused by the addition relate to how the particles interact with the fuel. The presence of trace elements in the char can affect how the fuel burns. At higher solid particle concentrations, the way the charcoal itself burns becomes more important. Also, significant fuel savings can be made by introducing the char, displacing fossil fuels. Depending on the material and particle size distribution, up to 75% by weight can be added (Papachristodoulou and Trass, 1987). The char is either added to a pure fuel or a fuel water emulsion/mixture. By emulsifying with water, the amount of liquid fuel used with respect to the amount of char can be reduced. In the most common example, diesel, the addition of water also changes the emission concentrations-decreasing oxides of nitrogen but increasing carbon monoxide and particulates (Subramanian, 2011). A novel mixture relevant to developing countries would be to add charcoal to a water-ethanol solution produced by fermentation. Another method used to co-fuel char with a liquid fuel is to use two injection systems into one cylinder - one feeding in a char-water slurry, the other acting as a pilot, using diesel, to help ignite the slurry (Urban et al., 1988).

The need for diesel can be completely removed by dispersing charcoal particles solely in water. As the liquid medium does not impart energy itself during the combustion cycle, the amount of solid must be higher. Char-water slurries are most suited to larger, low-speed engines (300rpm or less) as the fuel takes longer to combust than conventional diesel and oils most commonly used (Wamankar and Murugan, 2015; Zhu et al., 2017). The significant reduction in calorific value of char-water slurries compared to conventional fossil fuels means that they are not suitable for road vehicles and small-medium vessels which require a level of output power and lack the fuel tank capacity required. With increasing solids content comes higher viscosity, which means that conventional fuel pumps begin to struggle, possibly being replaced with specially adapted ones for slurries. The slower burn of charcoal becomes an increasing issue especially when the amount of diesel in the mix decreases which helps initiate combustion.

The solid fuel material used for slurring must meet two vital criteria- it must be possible to micronise it easily and must be low in ash. The two criteria are to an extent a trade-off because improvements to grindability are made by increasing the carbonisation temperature, which in turn raises the concentration of ash. The process of carbonisation also raises the calorific value of the initial feedstock, which in the case of lignocellulosic and agricultural residue biomass is far less than that of diesel which it replaces (Öner and Altun, 2009; Nanda et al., 2013). Other important criteria for the solid fuel material are low levels of nitrogen and sulphur, high volatile matter and can form a stable suspension in the carrier liquid. There are two routes to carbonise biomass- pyrolysis and hydrothermal carbonisation (HTC). Pyrolysis involves heating biomass in an inert atmosphere to above 300°C whereas as HTC involves heating in water under pressure to between 100°C and 300°C (Libra et al., 2011).

The complex chemical composition of charcoal means that a small addition to a fuel, such as diesel, could have a significant impact on the emissions and combustion characteristics. The presence of metals in small quantities (≤ 100 ppm) such as magnesium, manganese, zinc and copper- which are present in the ash of many biomasses- can have a significant effect on emissions (Lenin et al., 2013; Keskin et al., 2008; Javed et al., 2016). Organic material in additives ≥ 1000 ppm can have an effect on the fuel consumption and emissions (Hernández et al., 2012; İleri and Koçar, 2013). Whilst pyrolysis chars usually have monolithic aromatic structures with little functionality, hydrothermal chars have more functionality, oxygen and nitrogen which may have a large effect on emissions. Hydrothermal synthesis, a process which is similar to hydrothermal carbonisation, is used as a way of creating highly functional materials such as catalysts (Trejda et al., 2011; Narasimharao et al., 2014).

There are many viable technologies for microgeneration in developing countries. In terms, of the typical bioresource availability in rural locations, there is not one process that can convert the wide range of materials to fuels. Anaerobic digestion is suited to wet materials such as sewage and grasses which do not meet the low ash requirements for slurry fuels. Ethanol requires sugars and biodiesel is produced from oils. These three process routes to biofuels can be used to generate electricity but are not in competition for the same feedstocks as slurry fuels. The most comparable routes to biofuels are gasification and direct combustion which also use lignocellulosic material. It is, therefore, necessary for slurry fuels to have advantages over these two routes, either in cost or simplicity.

Currently, very little research has been done on the use of charcoal slurry fuels and it has not previously been mooted as a fuel for developing countries. There is at present research in some countries, particularly Australia, that investigates using coal-water slurries to generate electricity in large marine engines. Generally, low-grade coal is used and is dewatered and deashed through a hydrothermal process before milling (Cui et al., 2008).

1.2 Aims and objectives

The overall aim of the thesis is to assess whether charcoal slurries are a viable fuel for diesel generators in developing countries. The whole process is investigated from feedstock selection to combustion emissions. The charcoal slurry pathway to electricity is then compared to alternatives, most notably gasification.

- ***Objective 1: Conduct a literature review***

The first objective is to conduct a literature review of previous work on slurry fuels and connected areas such as micronised fuels. The thermal conversion routes of pyrolysis and hydrothermal carbonisation are also studied. More general previous work into the combustion chemistry in engines is used to predict how slurry fuels will burn because studies on slurry fuel combustion are limited. A review of biomass availability in Nepal is also included.

- ***Objective 2: Investigation of suitable feedstocks and thermal conversion routes***

The next objective is to investigate what types of biomass can be used to produce chars with the desired properties. Various types of plant-based biomass are analysed to find which could be used. Wood, grass, agricultural residue, microalgae and macroalgae are investigated. From each, chars are made via HTC and pyrolysis at different temperatures and their chemical properties analysed to find the optimum processing conditions. The carbon structure is studied, which can be used to predict how efficiently the fuel will burn in a diesel engine. Trace elements are also quantified during the investigation. Many of these elements can affect the

chemical reactions occurring in the engine. Furthermore, and most importantly, trace elements such as silicon and aluminium cause wear to parts in the engine. Based on the results of these tests, suitable chars are selected for further study.

As a case study, the resource availability in Nepal, a developing country, is performed to gauge how much supply of suitable feedstock there could be for the implementation of slurry fuel generation technologies. The different types of biomass are evaluated in terms of their elemental and proximate values.

- *Objective 3: Achieving suitable micronisation with selected chars for slurrying*

Once suitable materials are found in terms of elemental composition, the physical properties relevant to slurry fuels are investigated. The grindability is one such property which is evaluated in a small mill to compare different materials under the same conditions. Grindability is important because the particle size of the char must be small to pass through the injection system. Higher grindability means that less energy must be used to achieve the requisite particle size. Milling tests are performed in dry and wet modes. The ratio of sample to liquid dispersant and the type of dispersant are altered during the wet mode test. The particle size distribution of the samples from each test are measured using dynamic light scattering.

The next part is to upscale the process to one which can produce enough fuel for engine tests. The process must also mimic one that fits the technological constraints of developing countries. Using what was learned from the grindability tests and literature, appropriate mills are selected. Ball size, milling time, media to sample ratio, frequency, energy use and dispersants are the parameters studied during the tests. Ball, disc and stirred media mills are all investigated.

- *Objective 4: Formulate slurries with sufficient stability for use in a diesel engine*

For storage and use it is vital that the particles remain in suspension for a period of time as sedimentation would lead to uneven fuel quality injected into the cylinder during operation. Surfactants are certainly required to provide a stability which is acceptable. It is also important to optimise the additive package as surfactants increase the cost of the slurry. One or a mixture of surfactants must be used to achieve this. They can also have other effects such as altering viscosity and surface tension. Different dosages and mixtures are investigated to improve stability. A dispersion analyser is used to quantify the shelf life of the slurries. It will also be assessed if different micronised fuels need different surfactant packages or if one can suit all.

- *Objective 5: Design and construct a slurry engine test bed*

The next aim is to test the fuels in a laboratory environment using a diesel engine generator which is of a design typical to what is found in a developing country. The first part is to create a test cell around a diesel generator which can measure key emissions such as soot and NO_x, fuel consumption, temperature and power output. Once the test bed is built, it is commissioned using standard fuels as a baseline for performance. Slurry fuels are compared with respect to this baseline.

- *Objective 6: Use char as an additive to conventional fuel*

The first slurry tests will assess if charcoal can be used as an additive to improve fuel efficiency or reduce emissions. The tests will show if the charcoal interacts with the liquid fuel to produce a catalytic benefit. The amount added will be 0.1% wt. meaning it will have minimal effect on the calorific value of the fuel or gaseous emissions from its own combustion. After the tests are completed, a sample of the lubricant oil will be taken to see if the charcoal contaminates it with carbon or ash.

The next stage is to test fuels at 1% wt. charcoal. This value is an intermediary stage between using the charcoal as an additive and a fuel. At this point, a surfactant package is added because the stability will begin to drop with increased charcoal addition. At this level of addition, it is predicted that the emissions from the charcoal itself will become apparent.

The amount of ash passing through the cylinder will be several times higher than the amount of soot formed normally. It should be apparent at this point if the ash is exiting the exhaust, by weighing a filter paper in the exhaust flow or entering the lube oil. A lube oil sample is also taken at this point for analysis to check if ash has entered. A conclusion can be made at this point if an exhaust particulate filter or lube oil cleaner would be needed.

- *Objective 7: Use a char-diesel slurry as a fuel for a diesel engine*

The next objective is to test the use of charcoal as a fuel by increasing the loading to 10% wt.. Whilst the loading can be significantly higher than this, the level was chosen for several practical reasons. Firstly, the amount of charcoal that can be made in the lab scale reactors is limited especially for hydrothermal carbonisation and so to produce enough would be time-consuming. Secondly, increasing the solid loading begins to have a marked impact on the viscosity of the fuel and so surfactant improvers have to be added to reduce this which is beyond the scope of the project. Thirdly, the engine is a small high rpm engine and so the fuel has less time to combust than in a larger engine. Increasing the solid content beyond 10% wt. will affect ignition delay more. The amount added, however, should provide insights into many of the practicalities of using slurry fuels such as wear and jamming of components. The

emissions will likely change at this point as the charcoal composes a significant proportion of the fuel. It is predicted that emissions such as CO, soot and total hydrocarbon (THC) will increase and NO_x will decrease as combustion times will likely be longer, reducing the peak cylinder temperature. The test cell does not have a pressure transducer and so how the rate of combustion changes with crank angle is not directly measured. Nevertheless, the emissions, fuel consumption and exhaust manifold temperature will be able to provide a prediction of ignition delay and other combustion parameters. After these tests, the lube oil is once again analysed. Soot during the 10% tests is analysed using a particle size analyser, Andersen impactor and single stage filter to give a measure of distribution from 5nm to 10000nm. The majority of soot from burning diesel in an engine is below 1000nm but in the case of slurry fuels, it may be higher.

- *Objective 8: Compare with other energy generation technologies used in developing countries*

An economic assessment of the technology is made in comparison to the more mature alternative option of gasification, a method of converting biomass to a gaseous fuel for use in a diesel engine. Both technologies can theoretically remove the need for fossil fuel but in reality, it is difficult. The analysis shows how much diesel must be replaced with char before converting equipment to run on char slurries is financially viable. The outcome shows where slurry fuels fit in the fuel mix - as the preferred fuel on cost grounds, or as an emergency backup when others are unavailable.

Another comparison made is the amount of raw biomass feedstock is required per unit of electricity. Preserving forestry natural resources is important in rural areas as it is a source for fuelwood and economic activities.

1.3 Thesis outline

Chapter 2 is a literature review and addresses Objective 1. It firstly gives a brief history of using micronised fuels as an engine fuel, including slurries and dust fumigation methods of injection. The history of these fuels is long and coal dust was in fact amongst the first fuels used in a diesel engine. The next topic covered is the thermal processes which are used to convert fibrous biomass into amorphous carbon, which is more easily micronised. Past research on producing a slurry is reviewed including micronisation, selection of the liquid phase, rheology and stability. With growing concerns about air quality from diesel engines, current research on additives is investigated. Previous engine test work using slurries is also reviewed to predict the behaviour of the fuels made in this study.

Chapter 3 provides details of the methods used during the thesis and is referred to in later chapters. The methods follow chronologically in the order in which they are used in the chapters and the order used in producing the fuel, starting from harvested biomass. Included also is the commissioning and development of the engine test bed used for testing the slurries made which is Objective 5 of the thesis.

Chapter 4 is the first results chapter and investigates the feedstocks and processes to discover which combinations are appropriate for creating a viable slurry fuel. In this section, various methods are used to analyse the carbon structure which is important for predicting the rate particles will burn in the engine. The inorganic composition is also assessed which is an important consideration when attempting to minimise wear to the engine. From the species tested, conclusions are made about the type of feedstock which is suitable. Chapter 4 focusses on Objective 2 of the thesis.

In Chapter 5 the preparation of chars deemed suitable in Chapter 4 is investigated. Chapter 5 aims to address the points of Objective 3 and 4. First, small-scale milling investigations are performed, which give an indication of the relative grindability of each of the materials. The particle size distributions of the different milled powders are compared. The scaling up of the process needed to create enough slurry for engine testing is investigated. The energy use of the larger mill is measured to calculate the energy input needed to produce the fuel. The final section is based on research into the stability of slurries produced using different dispersal media and surfactants.

Chapter 6 investigates if the presence of chars as an additive can improve the combustion behaviour of diesel and biodiesel, which is Objective 6 of the thesis. Fuels are selected based on the findings of the previous two result chapters. 0.1% and 1% by weight of char are added to diesel or biodiesel, creating a slurry. Gaseous emissions, particle number, particulate matter, engine temperature and fuel consumption are measured for each of the tests, giving an indication as to how the addition of char affects the combustion of the liquid fuel.

The topic of Chapter 7 examines using the chars in a 10%wt. fuel blend. Diesel is used as the liquid media for the char particles. Two fuels are tested- one made with a pyrolysis char and one using a hydrochar made from the same feedstock. Emissions, fuel consumption, efficiency, wear and contamination of the lube oil are investigated. The implications for engine wear from long-term slurry use are investigated and suggestions made to minimise this. Chapter 7 focuses on achieving Objective 7.

Chapter 8 pertains to the economic side of using slurry fuels. The extra cost in modifying and maintaining a slurry engine must be less than the cost of simply buying diesel. A comparison is

also made with gasification which is the main alternative to diesel for powering generators in developing countries. Also, gasification uses similar feedstocks to slurry fuels and thus there is a direct comparison that can be made. The amount of char that must be added to the diesel to account for the modifications and extra processing equipment needed to produce a slurry. A Sankey diagram also shows the energy input needed to produce a kilowatt-hour of electricity. This section is related to Objective 8 of the thesis.

Chapter 9 concludes if any of the fuels or additives tested have the potential for use in developing countries. The practicality of using such fuels is also determined. It reviews to what extent the objectives are met by the research completed. Recommendations are made for further research which is needed to increase the confidence that slurry fuels could be used as an alternative to other technologies for producing energy in developing countries.

1.4 References

- Barnes, D.F. 2011. Effective solutions for rural electrification in developing countries: Lessons from successful programs. *Current Opinion in Environmental Sustainability*. **3**(4), pp.260-264.
- Cherni, J.A. and Preston, F. 2007. Rural electrification under liberal reforms: the case of Peru. *Journal of Cleaner Production*. **15**(2), pp.143-152.
- Cowan, K.R. and Daim, T. 2009. Comparative technological road-mapping for renewable energy. *Technology in Society*. **31**(4), pp.333-341.
- Cui, L.An, L. and Jiang, H. 2008. A novel process for preparation of an ultra-clean superfine coal–oil slurry. *Fuel*. **87**(10), pp.2296-2303.
- Hernández, D.Fernández, J.J.Mondragón, F. and López, D. 2012. Production and utilization performance of a glycerol derived additive for diesel engines. *Fuel*. **92**(1), pp.130-136.
- Hoque, M.E.Singh, A. and Chuan, Y.L. 2011. Biodiesel from low cost feedstocks: The effects of process parameters on the biodiesel yield. *Biomass and Bioenergy*. **35**(4), pp.1582-1587.
- İleri, E. and Koçar, G. 2013. Effects of antioxidant additives on engine performance and exhaust emissions of a diesel engine fueled with canola oil methyl ester–diesel blend. *Energy Conversion and Management*. **76**, pp.145-154.
- International Energy Agency. 2017. *Statistics*. [Online]. [Accessed 29/6/17]. Available from: <http://www.iea.org/statistics/statisticssearch/>.
- Inyang, H. 2008. Decommissioning of Diesel-Fueled Electric Power Generators in Developing Countries. *Journal of Energy Engineering*. **134**(1), pp.1-1.
- Javadi, F.S.Rismanchi, B.Sarraf, M.Afshar, O.Saidur, R.Ping, H.W. and Rahim, N.A. 2013. Global policy of rural electrification. *Renewable and Sustainable Energy Reviews*. **19**(0), pp.402-416.
- Javed, S.Satyanarayana Murthy, Y.V.V.Satyanarayana, M.R.S.Rajeswara Reddy, R. and Rajagopal, K. 2016. Effect of a zinc oxide nanoparticle fuel additive on the emission reduction of a hydrogen dual-fuelled engine with jatropha methyl ester biodiesel blends. *Journal of Cleaner Production*. **137**, pp.490-506.
- Keskin, A.Gürü, M. and Altıparmak, D. 2008. Influence of tall oil biodiesel with Mg and Mo based fuel additives on diesel engine performance and emission. *Bioresource Technology*. **99**(14), pp.6434-6438.
- Lahav, O. and Morgan, B.E. 2004. Titration methodologies for monitoring of anaerobic digestion in developing countries—a review. *Journal of Chemical Technology & Biotechnology*. **79**(12), pp.1331-1341.

- Lenin, M.A.Swaminathan, M.R. and Kumaresan, G. 2013. Performance and emission characteristics of a DI diesel engine with a nanofuel additive. *Fuel*. **109**, pp.362-365.
- Libra, J.A.Ro, K.S.Kammann, C.Funke, A.Berge, N.D.Neubauer, Y.Titirici, M.-M.Fühner, C.Bens, O.Kern, J. and Emmerich, K.-H. 2011. Hydrothermal carbonization of biomass residuals: a comparative review of the chemistry, processes and applications of wet and dry pyrolysis. *Biofuels*. **2**(1), pp.71-106.
- Mulder, P. and Tembe, J. 2008. Rural electrification in an imperfect world: A case study from Mozambique. *Energy Policy*. **36**(8), pp.2785-2794.
- Nanda, S.Mohanty, P.Pant, K.K.Naik, S.Kozinski, J.A. and Dalai, A.K. 2013. Characterization of North American Lignocellulosic Biomass and Biochars in Terms of their Candidacy for Alternate Renewable Fuels. *BioEnergy Research*. **6**(2), pp.663-677.
- Narasimharao, K.Malik, M.A.Mokhtar, M.M.Basahel, S.N. and Al-Thabaiti, S.A. 2014. Iron oxide supported sulfated TiO₂ nanotube catalysts for NO reduction with propane. *Ceramics International*. **40**(3), pp.4039-4053.
- Oh, G.Ra, H.W.Yoon, S.M.Mun, T.Y.Seo, M.W.Lee, J.-G. and Yoon, S.J. 2018. Syngas production through gasification of coal water mixture and power generation on dual-fuel diesel engine. *Journal of the Energy Institute*.
- Öner, C. and Altun, Ş. 2009. Biodiesel production from inedible animal tallow and an experimental investigation of its use as alternative fuel in a direct injection diesel engine. *Applied Energy*. **86**(10), pp.2114-2120.
- Papachristodoulou, G. and Trass, O. 1987. Coal slurry fuel technology. *The Canadian Journal of Chemical Engineering*. **65**(2), pp.177-201.
- Patton, R.Steele, P. and Yu, F. 2009. Coal vs. Charcoal-fueled Diesel Engines: A Review. *Energy Sources, Part A: Recovery, Utilization, and Environmental Effects*. **32**(4), pp.315-322.
- Rao, N.D. 2013. Does (better) electricity supply increase household enterprise income in India? *Energy Policy*. **57**, pp.532-541.
- Rosenblum, J.Bisesi, M.Castano, J.Tamkin, A.Ciotola, R.Lee, J. and Martin, J. 2015. Influence of seasonal fluctuation and loading rates on microbial and chemical indicators during semi-continuous anaerobic digestion. *Environmental Technology*. **36**(10), pp.1308-1318.
- Satyanarayana, M. and Muraleedharan, C. 2012. Experimental Studies on Performance and Emission Characteristics of Neat Preheated Vegetable Oils in a DI Diesel Engine. *Energy Sources, Part A: Recovery, Utilization, and Environmental Effects*. **34**(18), pp.1710-1722.
- Silva Herran, D. and Nakata, T. 2012. Design of decentralized energy systems for rural electrification in developing countries considering regional disparity. *Applied Energy*. **91**(1), pp.130-145.
- Subramanian, K.A. 2011. A comparison of water–diesel emulsion and timed injection of water into the intake manifold of a diesel engine for simultaneous control of NO and smoke emissions. *Energy Conversion and Management*. **52**(2), pp.849-857.
- Trejda, M.Stawicka, K. and Ziolek, M. 2011. New catalysts for biodiesel additives production. *Applied Catalysis B: Environmental*. **103**(3), pp.404-412.
- Urban, C.M.Mecredy, H.E.Ryan, I.T.W.Ingalls, M.N. and Jett, B.T. 1988. Coal–Water Slurry Operation in an EMD Diesel Engine. *Journal of Engineering for Gas Turbines and Power*. **110**(3), pp.437-443.
- Wamankar, A.K. and Murugan, S. 2015. Review on production, characterisation and utilisation of solid fuels in diesel engines. *Renewable and Sustainable Energy Reviews*. **51**, pp.249-262.
- Williams, N.J.Jaramillo, P.Taneja, J. and Ustun, T.S. 2015. Enabling private sector investment in microgrid-based rural electrification in developing countries: A review. *Renewable and Sustainable Energy Reviews*. **52**, pp.1268-1281.
- World Bank. 2017. *State of Electricity Access Report*. Washington DC: World Bank.

Zhu, M.Zhang, Z.Zhang, Y.Setyawan, H.Liu, P. and Zhang, D. 2017. An experimental study of the ignition and combustion characteristics of single droplets of biochar-glycerol-water slurry fuels. *Proceedings of the Combustion Institute*. **36**(2), pp.2475-2482.

Chapter 2: Literature review

2.1 Introduction

Previous studies pertaining to using slurry fuels as an alternative to diesel in internal combustion engines focus on the use of coal. Despite being a different material to chars produced from biomass, it is similar and still relevant to the research. The most notable research into char slurry fuels has been performed at Curtin University, Australia (although not being produced for diesel engines) and Georgia Southern University, USA, which produced a journal article testing a charcoal slurry fuel in a diesel engine. Beyond these two groups, there are few studies on the topic of char slurries. No previous work has hypothesised that these types of fuels could be particularly relevant to microgeneration in developing countries. Furthermore, the use of chars produced by hydrothermal carbonisation as a fuel for diesel engines has not been investigated.

One of the key advantages of using char instead of coal is that it can be argued to be carbon neutral providing that the resource used for the raw material is restocked. Additionally, the availability of coal is limited by geography and geology, whereas biomass is available in nearly all rural developing areas at a low price because agriculture is the main economic activity and settlements are often close to forests for access to firewood. Char is, therefore, a more suitable fuel from an environmental as well as an economic perspective in most areas of developing countries.

The first section of the review investigates the history of using micronised fuels in diesel engines, which is as long as the history of the diesel engine itself. The history includes work conducted on using powders, as well as micronised particles suspended in a liquid, i.e. a slurry. After this section, the desired characteristics of a micronised fuel are investigated which is then used to appraise what are the advantages and disadvantages of using char instead of more commonly used coal. The next part of the review investigates the whole production process beginning with the raw feedstock and finishing with a slurry fuel which is ready to be used. The review of thermochemical conversion routes looks at what properties the chars produced have and what reactions are occurring during the process. Finally, the review investigates the combustion chemistry of particles and liquid fuels in diesel engines. Literature is reviewed pertaining to how solid particles combust and how the presence of trace inorganic elements can act as an additive changing how liquid fuels burn.

2.2 A history of micronised fuels

2.2.1 The first micronised fuels

Micronised fuels for use in an internal combustion engine date all the way back to the 19th Century and the first tests performed by Rudolf Diesel on his eponymous engine. Figure 2-1 shows Diesel's design for using coal dust as a fuel which was filed for patent in 1895 (Diesel, 1898). Labelled on the diagram, coal dust in a hopper, T, is metered into a tube with a rotating valve, r. As the valve at n lifts, compressed air in L draws the dust with it into the cylinder. Eventually, the idea was dropped in favour of using oils. Presumably, from the patented design, it is hard to achieve a constant mass of dust into the cylinder each time because the powder is unlikely to flow well into the fast-moving rotary valve each time. It is possible that the air would not entrain all the dust added also. Excessive wear has also been reported as a reason for the work ceasing, which could certainly be a problem especially if the particles were large and high in ash (Nicol, 2014). Wear is likely because the powder fuel enters on the intake stroke with air leading to more opportunity to contact with the inner surface of the cylinder, valves and piston crown.

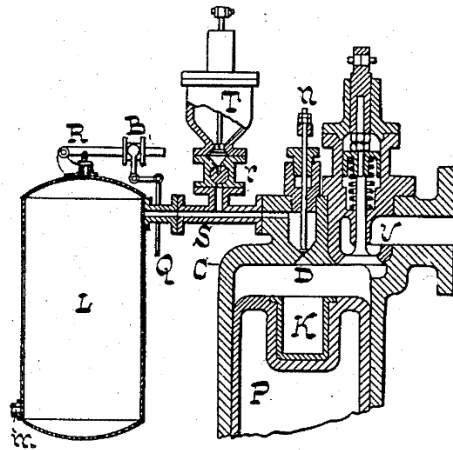


Figure 2-1 Diesel's coal dust injection system (Diesel, 1898)

A newspaper article in 1928 claimed that a man named Rudolph Pawlikowski, a former assistant to Diesel, had run an engine on coal dust for 12 years (Klein, 1928). Other engineers of the time were sceptical because of the possibility of wear and accumulation of powder in the cylinder, but Pawlikowski reported no such problems. It was reported that more lubricating oil was used which was the key to reducing engine wear. The particle size of the coal dust used in the experiments was 25-250 μm . A patent filed by Pawlikowski in 1924 shows several distinct differences to Diesel's design (Pawlikowski, 1924). Firstly, the coal dust is not aspirated into the inlet valve air. Secondly, the injection system is direct and is designed to ignite the coal dust almost instantaneously. Figure 2-2 shows the upper head assembly

containing the injector. Worm gears labelled 32 and 33 provide coal dust to a small pre-chamber, 3, via a valve between the two. Oil is heated in the chamber, labelled 51, beneath. The valve in the injection system leading to the engine cylinder is opened so the oil followed by the coal dust is forced into the cylinder at 30 bar. The oil ignites nearly instantly as it enters the combustion chamber, and the coal dust is ignited by passing through the oil flame. The patent eludes to another important difference between oils and coal dusts- that the autoignition temperature of the latter is higher, hence the need for another fuel to aid combustion. Finally, a valve between the hopper and chamber, labelled 3, is designed to blow coal dust out of the area around the valve seat. A lot of the ash was believed to have ended up in the lubricating oil, so a system was designed to remove it during operation.

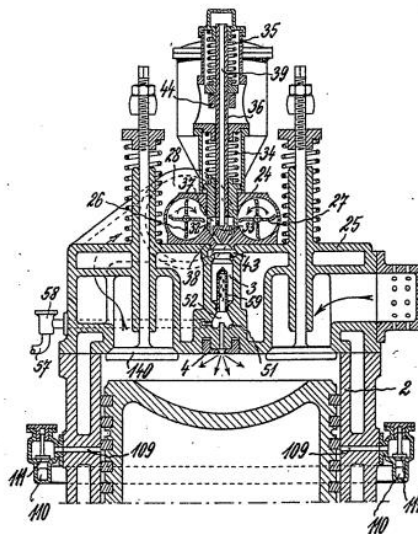


Figure 2-2 Coal Dust Injector invented by Pawilkowski

Despite successful tests by Pawilkowski the idea all but died out. The reason is somewhat unclear but has been suggested to be as a result of the relatively low price of petroleum products, which are easier to use than solid powders and cause less engine wear (Soehngen et al., 1976). Furthermore, it is difficult to see how the concept would work in a vehicle, one of the most common uses of a diesel engine, as the engine is more complex and larger. Also, the amount of coal dust required to be stored has two serious hazards, inhalation and self-heating. From both these early tests, Arthur D. Little INC. (1995) noted that many of the patents arising were regarding prevention of contact between dust and the oil wetted cylinder which would prevent the material from burning and causing wear to the rings and liner. Also, development of hardened materials for piston rings and cylinder liners occurred. A hardened cast iron was produced and used by many coal engine manufacturers.

2.2.2 Slurry fuel development in the 20th century

Mixing coal dust with water to create a slurry fuel removes the hazards involved with powder handling. The use of slurry fuels quickly became the predominant method of delivering solid carbon into an engine cylinder. Slurry fuels also cause less wear than using the dust directly (Ryan, 1994). Development of coal-water slurry fuels started in the 1940s and was the most intensive from 1970-1990 due to the oil crisis (Feng et al., 2016).

The first coal-oil slurry fuels were developed in the USA from 1945. Arthur D. Little INC. (1995) found that very little characterisation of particle size and flow properties were performed and so it is harder to put the results into context. It was also found that injection systems, liners and rings had wear issues which could be somewhat reduced by increasing clearances. Combustion efficiency was noted to be worse using slurries, although this may be a result of the damage to injection systems.

In the 1970s Wärtsilä and B&W tested coal-diesel mixtures in large low-speed diesel engines. They also found wear of injector nozzles and cylinders was severe (Nicol, 2014).

Downie and Bandopadhyay (1988) prepared de-ashed coal-diesel mixtures up to 30% wt. solid loading as a way of extending the life of the diesel. It was found that there was no apparent increase in exhaust smoke but there were operating regions where energy consumption increased, questioning the diesel fuel saving. This occurred at higher brake mean effective pressures. Exhaust temperature was reported to increase at high engine speeds for the slurry fuels suggesting late burning.

Several technical papers were produced by members of the Southwest Research Institute, USA during the 1980s and early 1990s. Several solid materials were experimented in slurries with diesel, including biomass in the form of cellulose and flour (Ryan et al., 1980). In terms of performance, it was found that adding carbon black of approximately 7.5% wt. was optimal for improving thermal cycle efficiency because the combustion kinetics of the diesel fuel were improved. It was suggested that atomisation of 10%wt. slurries were no worse than diesel fuel. Poor atomisation is associated with high soot emissions and poor combustion efficiency. Ryan et al. (1982) found that atomisation of 20%wt. carbon black slurries were worse as the cone angle was found to be smaller and the jet penetrated further. Longer penetration of the injector jet is particularly bad as it increases the chance of unburnt injected carbon black and ash contacting the liner. Most of their tests were on carbon-diesel slurries but some 50% wt. coal-water slurries were also used (Schwalb et al., 1994).

Despite issues around wear, development continued in the 1990s until the present day, focusing on the use of coal-water slurries (CWS) because the total removal of diesel fuel makes

it more commercially attractive. Collaborative work between Arthur D. Little INC., Cooper-Bessemer and the USA Department of Energy in 1992-1993 claimed several key advances toward making the technology viable (Arthur D. Little INC. , 1995). Large low-speed engines (1800kW, 400rpm) were used for the testing of these fuels. Of all the advances, durable injection nozzles which showed very little wear after hundreds of hours of testing were probably the most important. The injector was mainly made of titanium nitrided steel, with some tungsten carbide in more delicate areas such as the tip of the injection nozzle valve and the nozzle seat. The injector orifices were filled with sapphire inserts. Others have also reported adding very hard materials to the orifices such as diamond (Nicol, 2014). A tungsten carbide coating was also used on the cylinder liner and piston rings. Wear on the exhaust valves was still a problem not solved during the project. The emissions from the coal-water slurry engine were competitive with electricity generation alternatives such as gas turbines at the time of the study. Ultra-low ash coal produced by chemical cleaning was deemed commercially unviable and so lower cost slurries were used. It was found that 2%wt. ash or less, 88 micron top size and 12-15 μm mean particle size was acceptable. The report estimated that CWS engines would be cheaper and more efficient than conventional coal power. It can also be viable for smaller installations of approximately 10 MW.

Following on from this first major pilot success was the clean coal demonstration project running from 1994 to 2006 (Wilson, 2007). A 6.2 MW 18-cylinder, 512 rpm rated 4-stroke compression ignition engine, incorporating a special CWS injector and standard diesel pilot injector in each cylinder. The pilot injector was used to help with cold starting and to improve ignition control. An alternative is to use a glow plug but the disadvantage of this is torque loss which has been reported as approximately 20% (Gurney, 1984). Another option would be to increase the in-cylinder temperature to evaporate the water and burn the coal quicker by increasing the compression ratio or turbocharger pressures. 4-5% pilot injection of diesel by total energy of fuel (diesel and slurry) injected was found to be optimal. Burn time was about 6-7 crank angle degrees longer than diesel but, in this case, did not affect efficiency or power. It was also noted that before proper optimisation, embers travelled through exhaust and set the baghouse filters alight. After optimisation, this problem did not occur again. In this study, the wear of exhaust valves was significantly reduced using a chromium carbide coating compared to the 1992-1993 tests. However, it was tested for just 90 hours and so does not provide a stronger estimate for part lifespan. Hydrothermal treatment of sub-bituminous coals was also studied as a way of utilising lower rank coals. The study found that making two products from low-rank coal, 33% a high engine grade coal and 66% a lower boiler grade, was more economical than aiming to produce entirely an engine grade.

2.2.3 Current notable research

The most prominent current research is being undertaken by the Commonwealth Scientific and Industrial Research Organisation (CSIRO) in Australia since 2008. The research revolves around producing a higher-grade engine coal from lignite than previously obtained. They are also investigating the use of two-stroke diesel engines as well which have larger clearances and longer combustion time (Nicol, 2014). Like the latest research in the USA, the main motivation is to utilise cheap lignite which is upgraded by several processes including hydrothermal carbonisation (HTC). Biochar, algae and coke have also been used. Another motivation is that it provides a lot more flexibility to the electricity grid because slurry engines need little start-up time, unlike traditional coal-fired steam turbines which are often limited to providing base load (Wibberley, 2014). Water consumption is also lower than steam turbines which is useful in many countries. Using air blast injection to improve atomisation has been suggested.

With CO₂ emissions a major concern, it is uncertain if CWS using a fossil fuel will be used commercially. However, the process can still utilise renewable biomass sources. Little research has studied using charcoal slurries at present with just one journal article investigating the performance of a diesel engine powered by the fuel (Soloiu et al., 2011). The fuel tested consisted of 25% wt. wood charcoal, 72.2% diesel, 2.8% water and some surfactants. The slurry was used in a 1L single cylinder 1200rpm engine. Fatty acid surfactants were added to the formulation to stabilise the slurry, and water to minimise the amount of surfactant required. The charcoal was produced from Cedar wood at 300 and 400°C. Little information is available on the charcoal characteristics, except O/C ratio determined by EDX (0.06) and TGA which shows volatile content to be between 10 and 20%. Ash was found to be between 0.8 and 1.4% which is less than the 1.7% in the raw feedstock. It is not explained why this was. The motivation for creating a charcoal-diesel slurry is somewhat unclear except for the fact that wood waste is cheap and widely available. During the initial tests, the standard injector would stick open as deposits would form between the needle and seat. The problem was partially overcome by reducing the average charcoal particle size from 10.5µm to 5µm and modifying the injector with a lubricating oil channel through the nozzle body towards the needle stem. Although sticking was prevented with the modifications, wear rate was estimated to be 4-8 times faster than when using diesel fuel alone. It was claimed that the addition of charcoal reduced the amount of smoke evaluated by the Bosch method by roughly 60%, ignition delay increased, fuel droplet diameter increased, NO_x decreased (but was not compared with a diesel emulsion with an equivalent amount of water) and thermal efficiency remained the same once issues with the injector were solved. The smoke reduction was attributed to the oxygen content of the charcoal. Whilst NO_x was decreased, this was after altering the injection

timings to a more optimal setup. The increase in NO_x compared to diesel at the same injection times is likely because the ignition delay increased. The use of the char-diesel slurry fuel without affecting the thermal efficiency is promising as it shows that it can supplement the supply of diesel.

Currently, no research has linked slurry fuels with the problem of providing electricity in developing countries where conventional fuels are scarce and grid power intermittency is an issue. The motivations behind previous research are, however, similar. The advantage of providing load flexibility compared to coal-fired steam turbines is the main attraction for past research, which is comparable to the need to reduce intermittency in the supply of electricity from the grid or from other renewable technologies, in developing countries. Also, the modularity of being able to increase capacity simply by installing more engines in a power station is similar to the need in developing countries to be able to increase supply as economic development increases.

2.3 Desired characteristics for micronised fuel

2.3.1 Low hardness of fuel

Previous studies have shown that the most common problem with micronised fuel is wear of the injectors and also the pistons and cylinder liner. To some extent, the problem can be alleviated by hardening the construction materials at some expense. Another is to reduce the hardness of the micronised fuel used. The main culprit is the ash within the fuel being used and so should be selected based on low content, as well as containing only small amounts of the most abrasive elements. Abrasiveness grows with increased content of ash, smaller rounding radii of particles and greater immobility of abrasive particles (Kashcheev and Yampolsky, 1981).

Table 2-1 shows the hardness of some materials that may be present in the ash of coal and charcoal and the hardness of cylinder liners and hardened steel which is used for many components like fuel injectors. The most important abrasives are silicon dioxide and aluminium (IV) oxide followed by oxides of iron, titanium and magnesium. In coals, the majority of ash is aluminium and silicon, the most abrasive minerals. Charcoals from lignocellulosic materials generally contain low levels of these two elements. Magnesium is an important element for plants and so is often present in large quantities, potentially causing abrasion. Calcium is also common in biomass but is softer than cylinder liners, so the rate of wear caused would be less than elements such as magnesium. Other common elements present in charcoal ash are potassium and sodium. The literature review found no recordings of the hardness of the oxides of these elements, but it can be predicted to be low. Hardness is

related to the strength of the ionic structure created (Railsback, 2012). The charge of both these elements is +1 but they have large ionic radii similar in size to oxygen meaning that the compactness of the structure is low compared to that of aluminium which can fit in the voids between oxygen anions. Also common in biomass is phosphorus which has a high charge to atomic radii ratio, but this produces high cation-cation repulsion reducing hardness (Railsback, 2012).

Table 2-1 Hardness of oxides commonly found in ash.

<i>Material</i>	<i>Hardness (Vickers) (kgf/mm²)</i>	<i>Hardness (Knoop)(kgf/mm²)</i>	<i>Mohs Scale</i>
<i>Cast iron cylinder liner</i>	200-350 _{5,6}		4-5 ₅
<i>Hardened steel</i>	725-825 ₉		
<i>Aluminium Oxide (Al₂O₃)</i>	2600-2720 ₁	2000-2050 ₁	9 _{1,2}
<i>Calcium Oxide (CaO)</i>		560 ₁	3.5 ₂
<i>Magnesium Oxide (MgO)</i>	400-825 ₄		5.5 _{1,2}
<i>Silicon Dioxide (SiO₂)</i>	1040-1300 ₁	710-790 ₁	7 ₂
<i>Titanium Oxide (TiO₂)</i>	712-1121 ₁	713-1121 ₁	5.5-6.5 ₂
<i>Iron (II) Oxide (FeO)</i>	300 ₃		
<i>Iron (III) Oxide (Fe₂O₃)</i>	600 ₃		

Subscripts: 1) (Shackelford and Alexander, 2001) 2) (Nickel and Nichols, 1991) 3)(Takeda et al., 2009) 4)(Ishigaki and Buckley, 1981) 5)(Jensen et al., 2002) 6)(Schläpfer et al., 1990) 9)(Das et al., 2010)

The amount of ash can be reduced by treatment of the initial feedstock or the produced charcoal. Elements such as sodium, potassium and phosphorus can be removed in large amounts from biomass as well as some magnesium through water leaching (Wu et al., 2011). The removal rates of magnesium and calcium are much higher when a dilute acid solution is used instead (Liaw and Wu, 2013).

Another option is to use mechanical separation which is the only option for removing elements like silicon and aluminium. Methods such as froth flotation and ultrasound can be used although much of the combustible material is lost with the inorganic material (Wibberley, 2015; Ambedkar et al., 2011). These higher ash fragments can still be used for other purposes other than an engine fuel. In developing countries and on a small scale many of these technological options are unavailable; however, certain parts of biomass such as the bark can be removed to lower the ash content. Additional ash reduction can also be performed if the material is chipped prior to carbonisation by sieving out fractions known to contain high ash (Lacey et al., 2016). Similarly, these parts could be used to produce heat for carbonisation or sold as a fuel for cooking.

The presence of ash can alter the rheology and stability of slurries. Wang et al. (2013a) found that the addition of CaO to wastewater sludge decreased viscosity and increased hydrophobicity, improving slurryability. Trace metals present in the liquid phase either originating from the slurried solid or added later, therefore, influence the stability and viscosity.

2.3.2 Organic composition

The organic elemental composition is also an important property for solid fuels. It is important to keep the amount of nitrogen and sulphur low as the oxides of these are released into the atmosphere during combustion. It should be noted, however, that the amount of oxides of nitrogen released from the thermal reaction of oxygen and nitrogen in the air inside the combustion chamber will be significantly higher than that from the fuel. Sulphur emissions may be significantly increased using solid fuels instead of diesel. In most developed countries, regulations have massively limited the amount of sulphur in diesel fuel. In the European Union, the EN 590 diesel fuel standard limits sulphur to 10ppm in white and red diesel (BSI, 2013). In developing countries, however, levels can be much higher, up to 3000ppm (Ross, 2016). The sulphur limits required for diesel in many places is lower than is often found in solid fuels and therefore could be easily surpassed, a potential environmental issue from using slurries. The oxygen content has importance but is less clear as to what value is desired. Soloiu et al. (2011) suggested that oxygen content in the fuel reduced total smoke as it suppresses the formation of soot in the centre of the injected fuel jet which has not mixed with air. It is also known that oxygenated liquid fuels have a similar effect (Iannuzzi et al., 2016; Park et al., 2017). The presence of oxygen increases hydrophilicity, which is seen as undesirable in water slurries because the attraction immobilises water molecules, thereby increasing the viscosity (Fu and Wang, 2014). Whilst previous studies have rarely touched on solid loadings in diesel, it would be logical to assume that the opposite of water would be desirable, that the presence of oxygenated material improves slurryability. The presence of oxygen in the char may improve slurryability in diesel, but it will also reduce calorific value (Wanignon Ferdinand et al., 2012).

The proximate analysis of the char is important for formulating the slurry and the combustion characteristics. Volatile matter within char burns much faster than the fixed carbon component as it can diffuse into the air in the cylinder, whereas the burning of fixed carbon is limited to the surface (McHale et al., 1982). The rate of combustion is especially important when using char as a fuel for IC engines because the residence time is very short. As the particle size is very small in slurries, char combustion should still occur at a rapid rate (Howard and Essenhigh, 1967). Moisture adsorbed into the pores of the char will potentially affect tailpipe emissions. Water has been emulsified with diesel to alter the combustion

characteristics, most notably to reduce NO_x and particulates, the two most concerning emissions. The reason for the reduction in NO_x is because the combustion temperature is reduced and the evaporation of water before ignition creates micro explosions reducing fuel droplet size (Lif and Holmberg, 2006). Lif and Holmberg (2006) found the addition of 10%* water can reduce soot by 50% and NO_x by 10%, with only a small fuel consumption penalty. Water-diesel emulsions are not particularly stable without surfactants and thus a cost can be incurred. In most fully air-dried chars the amount of water is <5% and thus the total amount of water will be small, so the reductions will be more modest. The presence of moisture and volatile matter can, however, make micronisation harder as they may cause particles to stick together.

The surface functionality of chars will likely influence some characteristics of the slurry. This most importantly will affect the stability and rheology of the slurries by the interaction with the surfactants and dispersion media. The ability of pyrolysis chars to adsorb ions has been well studied in terms of use to improve soil nutrient concentrations. The ability to adsorb phosphate and ammonium, a negative and positive ion respectively, are the most studied and is generally found to increase with increasing pyrolysis temperature (Trazzi et al., 2016). It would follow then that anionic and cationic surfactants would have a greater affinity with the surface of more condensed aromatic structures and hence make them more stable in suspension. It has been suggested that the reason the chars from higher temperatures adsorb more is that the surface area is larger, but it has been shown to not be the most important factor (Takaya et al., 2016).

Another important aspect is the type of compounds in the feedstock biomass because they influence the final material. In lignocellulosic material, the amount of lignin, cellulose and hemicellulose affect the final solid yield. Yang et al. (2007) found lignin pyrolysis produced the highest solid residue at 900°C of 45% wt., whereas less than 10% wt. and 30% wt. remained from hemicellulose and cellulose respectively. Similarly, lignin yields the most solid in hydrothermal carbonisation, although the difference between the three components is only a few percent (Kang et al., 2012). Cellulose and hemicellulose, however, produce a hydrochar with a higher heating value than lignin (Kang et al., 2012). Proteins and lipids often found in non-woody biomass such as microalgae, pomace, nuts and shells, have different behaviours during thermal conversion. Lipids are particularly valuable in a fuel because they have a high calorific value (Chia et al., 2013). During pyrolysis of microalgae, the solid residue occurs mainly from the protein and lipids, and both have a similar mass yield (Du et al., 2013). The

* The paper does not specify whether this by weight or volume

process breaks down the lipids into compounds which yield less energy than the starting material which is undesirable (Du et al., 2013). Whilst still yielding significant amounts of char, pyrolysis to aromatic carbons is unlikely to be a good use of valuable lipids. During HTC, however, the lipids remain with little compositional change, whilst the rest of the material changes, meaning the final char has a higher calorific value (Levine et al., 2013).

Hydrochars have more diverse surfaces than pyrolysis chars, with the material containing more hydrogen, nitrogen and oxygen (Dieguez-Alonso et al., 2018). Hydrochar particles generally consist of a solid core of aromatised material, surrounded by a coat of high molecular weight oils and moisture (Donar et al., 2016; Zhu et al., 2017). Once added to a liquid medium, the surface of the hydrochar will certainly change as many of the oils on the surface will be soluble, compared to pyrolysis chars which will largely be unaffected (Zhu et al., 2017). It is, therefore, harder to predict how the surface functionality of hydrochars will affect rheology as it is unclear what will remain on the surface.

2.3.3 Good grindability

The grindability of the material is very important as above a critical size of particles about 50-75 μm will cause damage and seizure to pumps and injectors. It is also important to grind well to reduce the energy expenditure of micronisation. The need for grindability is the main reason that fibrous lignocellulosic biomass is not used as received and is treated prior to slurring. Grindability usually increases with increasing moisture content and ash in coals, however, neither of these are desirable for a micronised fuel (Vuthaluru et al., 2003; Sengupta, 2002). Increasing the pyrolysis temperature used for treating biomass increases the degree of aromatic condensation, improving grindability.

Abdullah and Wu (2009) prepared chars from mallee wood at different temperatures and compared the grinding properties to a sub-bituminous coal. It was found that grindability increases significantly between pyrolysis temperatures of 300-450 $^{\circ}\text{C}$ but very little between 450-500 $^{\circ}\text{C}$. This suggests, given that ash concentrates and volatile matter decreases with pyrolysis temperature, that for the purpose of producing charcoal for engine combustion, 450 $^{\circ}\text{C}$ represents an upper temperature limit for optimal process conditions. The grindability of mallee chars compared to the coal in Abdullah and Wu (2009) was similar, but slightly worse. By elemental carbon and fixed carbon, the mallee char at 500 $^{\circ}\text{C}$ would be considered a higher rank than the coal, but this did not translate to better grindability. Similarly for HTC, Kambo and Dutta (2015a) found that the grindability of miscanthus improved with a temperature between 190-260 $^{\circ}\text{C}$ but with diminishing return.

The feedstock properties affect grindability of the end char. The cellulose, hemicellulose and lignin content in woody biomass is one set of parameters which will likely determine the grindability of carbonised products from the feedstock. A study into the pyrolysis of hemicellulose, cellulose and lignin by Yang et al. (2007) found that decomposition happened between 220-315°C, 315-400°C and 160-900°C respectively. As lignin is the major contributor to the solid residue, it may be a case of the type of lignin present that effects grindability the most. The aromatisation of lignin below 400°C occurs predominantly in guaiacyl and syringyl (type-G and S) lignins (Mu et al., 2013). The presence of condensed type linkages in lignin increases solid residue yields and is why softwood lignins generate larger amounts of residue than hardwood lignins (Mu et al., 2013). Some materials such as microalgae, pomace, nuts and shells can contain lipids and proteins. The decomposition of lipids occurs in a large range of 200-500°C, whereas protein thermal decomposition occurs in the same region as hemicellulose (Bach and Chen, 2017). Lipids and proteins may reduce grindability as the viscous nature of these components may cause agglomeration. Wet milling may therefore be necessary to disperse these sticky compounds. However, proteins and lipids are not as difficult to mill as they are not fibrous like lignocellulose.

Yuchi et al. (2005) found a relationship between several properties of coal and the maximum solid loading in coal water slurry system. High solid loadings are desirable as it reduces the amount of liquid fuel needed or increasing the calorific value. The maximum solid loading, L (max %wt.) was approximated by the equation:

$$L = 37.93 + 0.38C_{daf} - 0.31M_{ad} + 0.049HGI - 0.077S_{Hg} \quad (1)$$

Where C_{daf} is the carbon content (%wt) on a dry ash free basis, M_{ad} is the air equilibrium moisture (%wt), HGI is the Hardgrove grindability index and S_{Hg} is the surface area (m^2/g) determined by a mercury porosimeter. Most of these variables are connected in some way. For example, as carbon increases, the reduction of oxygen and hydrogen inhibits the material's ability to retain moisture. The connection between increasing surface area and solid loadings is logical as the size of voids between particles is larger with smaller particle diameter. Large surface area particles caused by uneven or jagged surfaces will also increase porosity. The equation shows that smooth, rounded particles are more desired than those with a large specific surface area in terms of improving maximum solid loadings.

2.3.4 High energy content

The energy content of the solid fuel is also very important to the process. Diesel, the most common fuel for compression ignition engines has a calorific value in the region of 45 MJ/kg, whereas lignocellulosic material is in the region of just 18 MJ/kg (Amin et al., 2016; Bragadeshwaran et al., 2018; Ozyuguran et al., 2018). The best coal is in the region of 30 MJ/kg meaning that slurry fuels will certainly deliver less per unit mass than diesel (Smart and Riley, 2011; Wynter et al., 2004). As the density is much higher for solid fuels, the calorific values are much closer- coal and charcoal have a density in the region of 1.3-1.5 g/cm³ whereas diesel is approximately 0.85 g/cm³ (Strugała, 2000; Taulbee et al., 1989; Somerville and Jahanshahi, 2015). This means that the volume of fuel injected per stroke can be similar between diesel and slurries because, on a volume basis, the calorific values are close. The differences in density between liquid carriers, such as diesel, and solid, micronised fuels does create practical problems because it means the two components will separate out more easily. The issue of stability arising from the high density of charcoal is less in water (1 g/cm³) but more in ethanol (0.79 g/cm³) with respect to diesel.

2.3.5 Summary of desired characteristics

Table 2-2 shows a summary of some of the most important properties for selecting an appropriate solid fuel. In most cases except for ash, sulphur and nitrogen content there are several trade-offs between properties. Some of the desired properties can be contradictory such as having a highly aromatised structure and high volatile matter because thermal conversion increases aromatisation but causes the volatile matter change to fixed carbon.

Table 2-2 Summary of some of the desired properties of solid fuels for engine combustion.

<i>Characteristic</i>	<i>Benefits</i>	<i>Drawbacks</i>
<i>High lignin content of feedstock</i>	Higher mass yields after carbonisation.	Lignin decomposes at higher temperatures potentially affecting grindability. Specific lignin structure important if hard to measure.
<i>High calorific density</i>	Calorific value of the slurry provided by the char is higher.	Generally, means higher mass density which can decrease slurry stability.
<i>Low moisture</i>	Increased CV, more stable slurry.	NOx and soot reduction benefit of water lost.
<i>High volatile matter (including lipids)</i>	High CV and can disperse into the liquid medium improving combustion. Faster combustion rate.	Causes agglomeration during milling.
<i>Low ash (particularly aluminium and silicon)</i>	Wear reduction and higher CV.	-
<i>Low sulphur and nitrogen</i>	Reduce SOx and NOx tailpipe emissions.	-
<i>Low oxygen</i>	Increased CV, reduced hydrophilicity (for water/ethanol slurries).	Potentially higher soot emissions.
<i>Low particle size</i>	Less likelihood to damage moving parts, more stable slurry.	Reduction in maximum solid loading.
<i>Low surface area</i>	Less use of surfactant, higher solid loading possible.	Less stable.
<i>Highly aromatised by thermal conversion.</i>	Improved milling characteristics.	Higher fixed carbon and thus lower combustion rate.

2.4 Charcoal vs. coal

Whilst coal is the most commonly used micronised fuel because of its price in many developed countries, it is more expensive than charcoal in many developing countries. Charcoal is potentially more attractive as a micronised fuel compared to coal, not only because of the renewable nature, but also the properties.

The main advantage is the lower tendency to wear, caused by two reasons- charcoal generally contains less ash and the constituents are much softer. Previous studies using a coal-water slurry found that silica was the primary abrasive particle and the wear rate was linearly correlated to ash content (Arthur D. Little INC. , 1995). The hardness of the abrasive ash in these tests was 500 kg/mm² and was formed of 89% SiO₂, Al₂O₃ and Fe₂O₃. Charcoal ash contains very little of these hard elements and so the hardness will likely be less than coal ash, increasing the life of components. In combustion more generally, such as in a boiler, the issue of using charcoal and other biomass is the presence of alkaline metals, leading to fouling (Lee et al., 2018). Whilst, no prolonged tests have used charcoal slurries, tests of over 100 hours using a coal-water slurry showed no evidence of fouling (Wibberley, 2014). It is thought to be because high temperatures only occur for a very short time (Wibberley, 2014).

The presence of nitrogen and particularly sulphur vary greatly between charcoal and coal. Sulphur is much higher in coal whilst virtually non-existent in charcoal apart from those made from macroalgae (De Bhowmick et al., 2018; Yu et al., 2017). Nitrogen in coal is quite high typically 1-3%. In biomass, the range is much larger, with woody biomass typically <1% but materials such as sewage sludge and grass can be as high as 3-5% (Abelha et al., 2008). Charcoal from woody biomass represents a much cleaner fuel in terms of NO_x and SO_x emissions than coal (Patton et al., 2009).

2.5 Thermal treatment of materials

There are two thermal treatment routes, pyrolysis and HTC, for producing a micronised fuel and is vital to achieve a grindability which is acceptable. Pyrolysis is a mature technology used for several thousand years, but our understanding is still growing and methods improving. This is the only viable route currently for producing the fuel in developing countries. HTC is more novel and has not reached commercial maturity yet. However, it was included as the fuels produced are very different to pyrolysis and could be more suitable for making slurries. It could in the future be possible to use the method.

2.5.1 Pyrolysis

Pyrolysis is the process of thermally decomposing a material in an inert gas. Solid, liquid and gaseous products are produced and, whilst only the solid is used in slurry fuels, the others have uses and could be used for heating the process. The process can be optimised to produce different proportions of each fuel by changing parameters such as temperature, residence time and heating rate (Aysu and Küçük, 2014). These parameters are used to classify what type of pyrolysis is being performed, a summary of which is given in table 2-3. The heating rate affects the balance of physical states of the products. Slow pyrolysis, with residence times of hours or even days, produces more solid product than when higher heating rates are used and the char burns more cleanly the higher the process temperature used (Kandpal et al., 1995). Higher heating rates, in the range of 10-200°C/sec, favour the production of bio-oil containing large amounts of highly oxygenated compounds (Mohan et al., 2006). High pyrolysis temperature promotes low molecular weight species which inhibits char formation, hence why fast pyrolysis favours bio-oil and gas products (Patwardhan et al., 2011). At even higher heating rates and temperatures ($\approx 1000^\circ\text{C}$) the major product is gas. The equilibrium of gases changes with temperature- more hydrogen at higher temperatures, and more carbon monoxide, carbon dioxide and hydrocarbons at lower temperatures (Basu, 2010). Hence, for charcoal slurries, slow pyrolysis is the optimal process to maximise solid product. It is also the easiest process to use and the technology mature.

Table 2-3 Summary of the classification of pyrolysis processes (Basu, 2010).

<i>Pyrolysis Process</i>	<i>Residence Time</i>	<i>Heating Rate</i>	<i>Final Temperature (°C)</i>	<i>Products</i>
<i>Carbonization</i>	Days	Very low	400	Charcoal
<i>Conventional</i>	5-30 min	Low	600	Char, bio-oil, gas
<i>Fast</i>	<2 s	Very high	~ 500	Bio-oil
<i>Flash</i>	<1 s	High	<650	Bio-oil, chemicals, gas
<i>Ultra-rapid</i>	<0.5 s	Very high	~ 1000	Chemicals, gas
<i>Vacuum</i>	2-30 s	Medium	400	Bio-oil
<i>Hydropyrolysis</i>	<10s	High	<500	Bio-oil
<i>Methano-pyrolysis</i>	<10s	High	>700	Chemicals

The temperature for which slow pyrolysis begins at is approximately 250°C when most of the constituents of lignocellulosic biomass can decompose to some extent. The process forms regions of amorphous carbon which are most importantly, easier to grind down than the elastic and fibrous material that many biomass feedstocks begin as (Di Blasi, 2008). After the initial degradation stage comes repolymerisation causing the aromatic molecules to grow even larger with increasing temperature (Kan et al., 2016; Fisher et al., 2002; Keiluweit et al., 2010). The grindability increases with thermal degradation, but the increasing degree of

polymerisation reduces the suitability of the char as a slurry fuel because the compounds become less volatile and larger, increasing the autoignition temperature and the reaction time. The pyrolysis temperature should, therefore, be minimised to reducing the size of the polymers formed but still improving grindability. During the process oxygen, hydrogen, nitrogen and sulphur become less common in the solid residues (Anca-Couce, 2016; Kan et al., 2016). During pyrolysis, volatile compounds are released. The first is moisture, then tars are formed. The hot volatiles play an important part, providing heat transfer to cooler material and can cause secondary reactions (Demirbas, 2009).

The major products of cellulose pyrolysis, a main component of lignocellulosic biomass is shown in figure 2-3. Cellulose initially decomposes into glucose then glucosan with the elimination of a water molecule (Bradbury et al., 1979). Levoglucosan then forms from the glucose and is the most abundant product (Zhang et al., 2013). The pyrolysis of levoglucosan can leave residual char or react with other volatile material (Bradbury et al., 1979). Cellulose can also produce furfural and hydroxymethylfuran (HMF) between 200 and 300°C (Wang et al., 2017; Antal, 1985). Amorphous cellulose is related more to the formation of char and also produces more furfural and HMF (Wang et al., 2017).

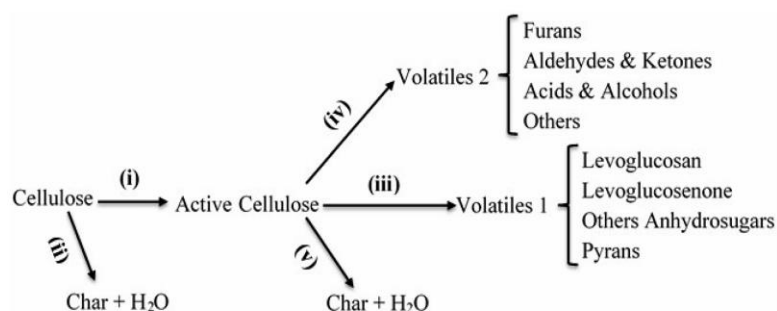


Figure 2-3 Products of cellulose pyrolysis (Bennadji et al., 2018)

Hemicellulose pyrolysis is less well understood as less is known about the structure. Xylose is the most common model compound, but arabinose and mannose are sometimes used (Wang et al., 2013c; Räsänen et al., 2003). The initial stage in the thermal degradation of these is ring opening at the C-O bond (Wang et al., 2013b). Several different reactions occur producing compounds such as furfural and hydroxyacetaldehyde (Wang et al., 2017). Hemicellulose containing high levels of pentose and side branches are thought to produce high char yields because more macromolecular radicals are formed which begin polymerisation (Wang et al., 2015).

Lignin produces more char compared to cellulose and hemicellulose because the structure is already more condensed (Wang et al., 2017). The presence of methoxyl groups prevents polymerisation to char as they stabilise large molecular fragments (Wang et al., 2017).

Methoxyl groups on the aromatic ring of type-S lignin prevent this and so reduce the amount of char yield (Wang et al., 2009). Cleavage of aryl bonds in lignin create phenyl compounds such as phenol and catechol (Wang et al., 2017).

Nitrogen in biomass is mainly in the form of amino acids such as glycine and aspartic acid (Ren et al., 2011). During pyrolysis hydrogen cyanide and ammonia are formed by the cracking of tar components formed from these (Ren et al., 2011). Little nitrogen is left in the solid residue after pyrolysis and so should not contribute significantly to NO_x emissions during slurry combustion (Anca-Couce, 2016).

There are many complicated interactions during pyrolysis creating a whole host of different compounds. Reforming, water gas shift reactions, radicals recombination and dehydration occur during pyrolysis and are a function of residence time, temperature and pressure profile (Demirbas, 2009). During the char formation process dehydrogenation/dehydroxylation occur to form double bonded carbon groups concentrating the carbon content in the solid (Harvey et al., 2012a). The interaction between the three main groups of compounds in lignocellulosic biomass also affects char yields. Cellulose is known to suppress char formation in lignin (Wang et al., 2017).

2.5.2 Charcoal making reactor design

There are many different designs of reactors that can be used for charcoal production. The inert atmosphere needed to prevent combustion is nitrogen, steam, or air depleted of oxygen by combustion. The latter is most commonly used in developing countries as nitrogen is harder to source and steam requires more complicated reactors. The earliest method which is still used today is making charcoal in earth pits which uses soil covering the reaction chamber as a natural barrier to oxygen in the air and preventing heat loss. An air inlet is made at one end, allowing some material to burn, creating the necessary heat and inert atmosphere to convert the remaining material. The quality of the charcoal is very unpredictable with some only partially carbonised and some nearly completely turned to ash (FAO, 1983). Vahrman (1987) reported the charcoal from this method can also get contaminated with dirt, sand and water which could be especially problematic for slurry engines because of silicon. The process is time consuming, gives low yields and reabsorbs bio-oil making it burn with more smoke (FAO, 1983). The reabsorption is certainly bad as a cooking fuel but would be less so for slurry fuels as it would potentially allow the fuel to burn faster.

Brick kilns are also commonly used and have several advantages. They can be made with locally sourced materials, are easier to control than earth pits, can be cooled quickly and are built to last for many years. One of the main disadvantages is that the tars produced are not

burned to heat the process and are released as air pollution (FAO, 1983). Similar to earth pit kilns, part of the fuelwood is burned to provide the heat and inert atmosphere. There are several different versions- one of the most common is the Brazilian beehive kiln shown in figure 2-4. This kiln consists of a round domed structure several metres tall and wide. It has a door for loading and unloading material, chimneys which release the volatile material as smoke and lots of small air inlets at the bottom and middle to exchange air needed to provide heat (Bustamante-García et al., 2013).

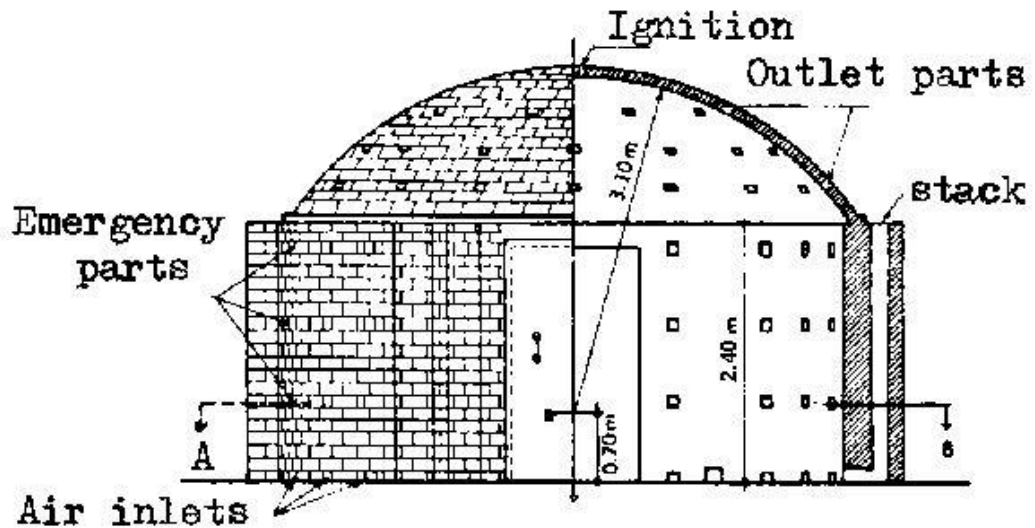


Figure 2-4 Design of a Brazilian beehive kiln

Some metal kilns are also used which often have the advantage of being transportable as they are much lighter. One such example is the “Kon Tiki” kiln- a metal cone which is filled with biomass (Smebye et al., 2017). The top is lit and the flame on the surface creates a curtain of inert gas, protecting the rest of the material from oxygen.

The main issues with these methods are that they rely on a constant flow of air into the feedstock material, increasing the ash of the final charcoal which is undesirable in slurry fuels. Also, they are often wasteful of tars which could be used to heat the process. The Adam retort kiln (Adam, 2009) addresses both by burning a separate material, often of lower quality, in a firebox to create a flow of hot inert air. The volatile tar is also burned to create heat and reduce emissions (Sparrevik et al., 2015). Another common design is to place the feed material in a sealed drum which is then placed in a larger one filled with biomass which is combusted for heat.

Solar pyrolysis is a method which does not need to burn biomass to produce the reaction temperatures needed and is suitable for places with high solar irradiance. Hence, the mass yield of charcoal can be much higher than with more traditional methods. Morales et al. (2014) found that a parabolic trough mirror could provide enough heat needed for pyrolysis on a day

with insolation of 965 W/m². The main setbacks of solar pyrolysis are the initial costs of construction and the unreliability of the weather.

2.5.3 Hydrothermal carbonisation (HTC)

The main feature of HTC is that reactions occur within water at subcritical temperatures. This is a temperature range which is less than the critical point (374°C) and above the boiling point at standard temperature and pressure (STP). The process occurs at elevated pressure keeping the water in a liquid state. The products from HTC are: solid residue, an aqueous phase containing inorganic and organic compounds, and gas (Zhao et al., 2018). Unlike pyrolysis, the medium used for HTC, water, also acts as a reactant (Nizamuddin et al., 2017). A key advantage of this process is the ability to efficiently convert wet streams of biomass into dry fuels, unlike pyrolysis where the moisture severely affects the energy efficiency. An interesting use of the technology is the carbonisation of liquid materials such as glucose to grow structures such as nanospheres and microtubes (Funke and Ziegler, 2010).

The solid residue, hydrochar, is generally the main product and contains most of the organic material from the feedstock (Libra et al., 2011). On a macro scale, hydrochar differs from the feedstock by having a lower O/C ratio, lower H/C ratio, lower moisture (after drying), higher fixed carbon and higher calorific value (Nizamuddin et al., 2017; Funke and Ziegler, 2010). The feedstock material undergoes demineralisation meaning that it is possible to create a hydrochar with less ash than the original biomass (Funke and Ziegler, 2010). The oxygen and hydrogen content are reduced but remain much higher than that of pyrolysis char (Jian et al., 2018). The particles of hydrochar comprise a solid core with a high surface area surrounded by low molecular weight extractables (Funke and Ziegler, 2010). It is made predominantly of aliphatic and aromatic structures formed from benzofuran-like compounds (Guiotoku et al., 2012). The aqueous phase gains further water during the process as it is a reaction product as well as the reactant (Nizamuddin et al., 2017). Much of the ash is leached into the aqueous phase, a major benefit of the process, and some organic material because water also acts as a strong solvent, becoming less polar at higher temperatures (Alghoul et al., 2017). Only about 1-5% wt. of the feed material is converted to gas, mainly CO₂ but also trace amounts of some hydrocarbons and hydrogen (Libra et al., 2011; Berge et al., 2011).

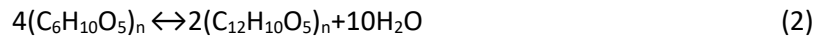
2.5.4 HTC mechanisms

The key to HTC is that the properties of water alter significantly with temperature. At room temperature, water is a polar solvent but the dielectric constant decreases with temperature becoming less polar. During HTC, the dielectric constant of the subcritical water is in the region of methanol or acetone (Kambo and Dutta, 2015b). Also, at 227-327°C water acts as a base and an acid because the ionic product is maximised (Yu et al., 2008).

Similar with pyrolysis, the process of HTC is affected by residence time, temperature, pressure, heating rate and feed particle size. Nizamuddin et al. (2017) provides an overview of how temperature, pressure and residence time affect the process. Temperatures below 200°C massively favours solid product yield. Between 200 and 250°C, there is a significant change in the amount of aqueous product formed. Above this temperature range, more gas is created. More aromatisation occurs in the solid product at higher temperatures. Longer reaction times favour more solid residue as there is more time for repolymerisation and condensation of heavy liquid fractions leached into the aqueous phase (Lei et al., 2016). The mass yields increase up to a residence time of 26 hours. Pressure has little effect on liquid and gas yields, but greatly influences the formation of hydrochar. Processes such as decarboxylation and dehydration are suppressed with pressure. Higher pressures also mean that the water can infiltrate the solid particles better. There is little information on how the heating rate affects the hydrochar. Presumably, less dehydration and decarboxylation reactions will occur during the heating phase and would be reduced when the reactor reaches the hold temperature and maximum pressure. Yan et al. (2014) investigated the effect of particle size (0.6-2.38 mm) on the properties of hydrochar from pine. It was found that the energy yield for smaller particles was lower indicating that mass transfer is a factor during HTC. For this range, however, the overall effect was small.

There are several reaction mechanisms during HTC, the main ones being, hydrolysis, dehydration, decarboxylation, polymerisation and aromatisation (Funke and Ziegler, 2010). Lower temperatures are used for HTC than pyrolysis because the pathway reactions have a lower activation energy (Libra et al., 2011). Hydrolysis is an important initial step in which water reacts with glycosidic groups cleaving ether and ester bonds (Reza et al., 2014; Funke and Ziegler, 2010). The fragments are further hydrolysed to yield compounds such as levulinic, formic and acetic acid. The dehydration reaction is both physical and chemical in that water is released from the pores as the material becomes more hydrophobic and is created by the elimination of hydroxyl groups (Reza et al., 2014). Hence, the O/C and H/C ratios both reduce.

Cellulose, one of the main components of plant-based biomass was found to decompose by dehydration according to (Funke and Ziegler, 2010):



Presence of carbon dioxide and carbon monoxide in the gas product suggests that decarboxylation reactions occur in the process (Funke and Ziegler, 2010). Whilst decarboxylation is important, the ratio between $\text{CO}_2/\text{H}_2\text{O}$ shows that dehydration is the dominant process (Hoekman et al., 2011). The amount of CO_2 present is greater than can be explained by decarboxylation- the rest possibly formed during the decomposition of formic acid or during condensation reactions (Funke and Ziegler, 2010). Polymerisation occurs mainly in the aqueous phase between some of the organic products produced during hydrolysis creating microspheres that may re-attach to the initial feed, shown in figure 2-5 (Lei et al., 2016).

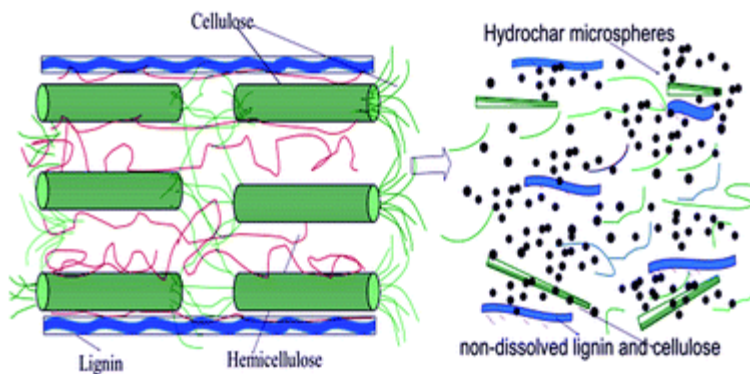


Figure 2-5 Lignocellulosic material carbonising into hydrochar microspheres which re-attach to parts of the initial feed that remain during the process of HTC (Lei et al., 2016).

Condensation polymerisation, specifically aldol condensation, is the main reaction which occurs around the remaining aromatic cores, often from lignin (Funke and Ziegler, 2010). The aromatisation stage needs temperatures higher than the other reactions to occur. Also, aromatic structures exhibit high stability under hydrothermal conditions preventing them from condensing as much as pyrolysis chars (Funke and Ziegler, 2010).

2.5.5 HTC reactors

Most current HTC reactors are small sized (<2l) pressure vessels, heated externally for batch production. Hence, most produce only a small amount of material each time. Designs have appeared for continuous processes which are needed to improve throughput. Hoekman et al. (2017) created a twin-screw extruder, shown in figure 2-6, with changing pitch and thread angle along the shaft depending on the stage. Feed is forced through at one end, heated to carbonisation temperature and then cooled before separating. The HTC process, in this case, was under a minute, much quicker than batch processes. Hoekman et al. (2014) focused on a

similar design but had two auger screws, one to push the dry feed into the reactant water then another to draw it along the reactor area.

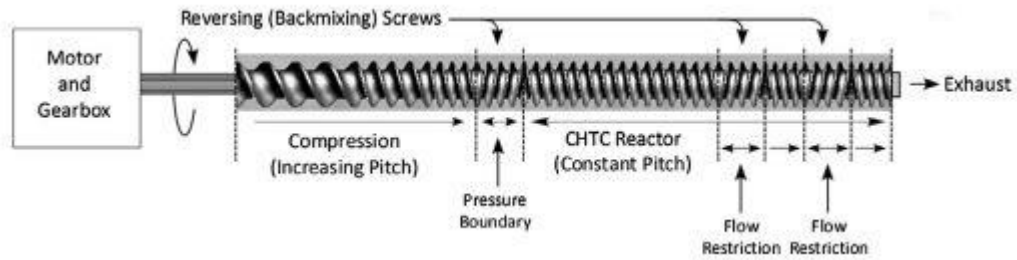


Figure 2-6 One half of a twin-screw extruder used for continuous HTC in Hoekman et al. (2017)

Most work using HTC is at the lab scale, but there are some instances of commercialisation. The first commercial HTC facility in the UK was announced by CPL industries in 2017, with production due to begin in 2018. Also in 2017, a joint venture between Armstrong energy and Licella was announced to use HTC to recycle waste plastics in the UK (Armstrong Energy, 2017). TerraNova is another company with HTC facilities for sewage sludge around the world.

2.6 Micronisation

Micronisation is an important step in the process of creating a slurry because it reduces the possibility of damage to the engine from solid particles and improves the stability of the suspension. The process of micronisation can be energy intensive. Unlike pyrolysis which requires energy from heat that can be relatively easily obtained by burning biomass which is readily available, micronisation requires electricity or mechanical energy, most likely provided by the slurry powered engine. Thus, it can create a drain on the electrical output from the generator, meaning the effective useful output is reduced and more slurry fuel has to be produced to create said energy. There are many types of mill including ball, disc, rotor, rod, hammer and jet.

The most common type used for producing fine powders is the ball mill, of which there are many subtypes. A container is filled with the material to be milled along with a charge of hard balls, usually made of stainless steel. Once agitated, the balls work with the walls of the container to crush the material into smaller particles. The size of balls, quantity, time, material loading and degree of agitation all have an impact on the rate of size reduction and final fineness (Wu et al., 2018). The right ball size depends on the size of the feed itself, with coarser particles requiring larger ball diameters to efficiently mill (Katubilwa et al., 2011). As the initial feed of charcoal is likely to be in the region of several millimetres or even centimetres, needing to be ground down to just a few microns, it may be sensible to split the milling stage into two or more parts using ever smaller balls. The advantage of this is that smaller balls grind fine material to a specified level faster than larger ones, thus saving energy

(Katubilwa et al., 2011). The amount of balls added, commonly known as the charge filling ratio, affects the grinding time, as well as the specific energy consumption (Schnatz, 2004).

There are many methods of agitation that can be employed in ball milling. The most common is to roll the container either on rollers or by rotation. The rotation speed is important as too slow and the balls do not gain the momentum to break the particles, too fast and it begins to act like a centrifuge, with the balls and material forced to the edges of the container, therefore not moving in relation to one another (Watanabe, 1999). At medium speeds, a tumbling motion occurs with the balls being lifted from the bottom of the container, then falling back onto the milling material at speed causing breakage. During planetary milling, the container rotates about its central axis and an offset axis (the sun) simultaneously. It is a form of high-energy milling capable of achieving very small particle sizes (Broseghini et al., 2016).

Stirred ball milling was developed as an ultrafine grinding method which achieves higher energy efficiencies over traditional ball mills because they are operated with smaller milling media, high tip speeds and high filling ratios (Altun et al., 2013). The designs consist of a shaft with paddles or discs which agitate the contents. The most notable commercial example is the Isamill which has been used to create coal slurries (Wibberley and Osborne, 2015).

An important decision is whether the material is milled dry or wet. In this case, as the final product is a slurry, removal of the liquid after milling is not needed, making wet milling more attractive. Also, wet milling prevents dust from forming which, at the final particle size needed, can be harmful (Iyogun et al., 2018). The main advantage of wet milling is that the presence of a liquid can prevent agglomeration, especially important for sticky materials such as hydrochars (Janot and Guérard, 2005). Also, the breakage rate of the largest fraction in the particle size distribution has been found to increase with the introduction of a liquid to the grinding media (Tangsathitkulchai, 2002).

Grinding aids are chemicals which improve grindability and can be used during wet and dry milling. The two main mechanisms for this improvement is the reduction in surface energy of the particles and the alteration in flow and arrangement of the suspension, preventing agglomeration (Choi et al., 2010). These are most often polar organic compounds (Zhao et al., 2016).

Jet milling is an alternative to ball milling for producing ultrafine particles and is solely a wet milling route. Figure 2-7 shows the inside of a jet milling comminution chamber. A slurry is passed at high pressure through the chamber containing tight turns in a pipe, which causes the particles to break. The intensity of the impact load in jet milling is over 40 times that of traditional mills whilst using only 30-50% of the energy (Cui et al., 2007). The process involves

pumping the feed slurry at high pressure through a tube with many tight turns. This causes the particles to collide with each other or the tube walls causing breakage. Cui et al. (2008) used the method to micronise coal achieving a mean diameter of $2.71\mu\text{m}$ whilst using less than a third of the energy of wet ball milling.

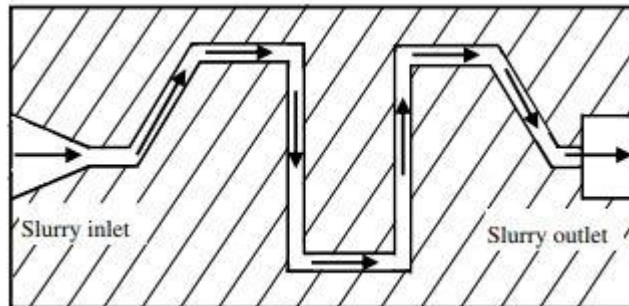


Figure 2-7 Jet milling comminution chamber (Cui et al., 2008)

Various procedures have been used to achieve micronisation. Arthur D. Little INC. (1995) concluded that a combination of an initial crushing ball mill stage followed by a wet stirred ball mill stage is the best method for producing ultrafines. Current research in Australia is focused on using the Isamill which a type of stirred mill (Wibberley, 2014). During the University of Alaska tests, a two-stage milling procedure was selected, beginning with wet ball milling to $250\mu\text{m}$ then to $20\mu\text{m}$ (Wilson, 2007). There is agreement in literature that the final stage of micronisation should be wet stirred media milling, potentially preceded by an initial size reduction.

The particle size determines the overall maximum loading of solid particles. Larger particles mean that the solid loading is higher because the voids between particles are proportionally smaller than those between smaller ones. However, large particles do not form as stable slurries and will not pass through diesel fuel injectors. The mean desired particle size is considered to be below $20\mu\text{m}$ with a maximum of $85\mu\text{m}$ for large engines to allow passage through the fuel system (Nicol, 2014). One option to increase loading is to broaden the particle size distribution or create a bimodal one. This can potentially increase loading because the smaller particles fill voids between larger ones. Ghanooni et al. (2013) improved solid loadings and viscosity by mixing two monodisperse coal fractions with a modal size of 20 and $150\mu\text{m}$. In terms of a process for a developing country, producing a slurry with a broad distribution of particles may add a level of complexity which does not yield a large enough benefit to make it warranted.

2.7 Liquid Media

There are several liquid media that micronised particles can be mixed with to create a working fuel. Table 2-4 gives an outline of several which have been used as part of a liquid mixture or the sole carrier of charcoal and coal to produce a slurry. Diethyl ether is only used as part of the liquid mixture, rather than a sole carrier of particles in a slurry but is valuable as cetane improver. The onset of combustion begins in a diesel engine when the autoignition temperature is reached. With the exception of water, all the examples of liquid media begin to burn before the charcoal that is added. Diethyl ether is often added to improve the cetane number of a fuel and is miscible in both diesel and water. With the addition of charcoal with a high autoignition temperature, diethyl ether could be used to counteract this. Ethanol, an alternative fuel which could be made relatively easy at a small scale in a developing country, has a high autoignition temperature which means that the ignition delay will be longer.

Alternative fuels have a lower higher heating value than diesel which can cause an issue with fuel delivery. Charcoal could, however, improve the calorific value of ethanol on a by weight and volume basis. Charcoal usually has a density higher than that of water and so will be intrinsically unstable in all the potential media as it will always sediment. The least stable char slurries will be ethanol and diethyl ether, the most being biodiesel and water.

The low boiling point and viscosity of ethanol encourages air-fuel mixing in the cylinder, increasing the time for which the char particles are in contact with oxygen in the air (Emiroğlu and Şen, 2018). Water should also disperse well in the cylinder as the boiling point and viscosity are low. The main issue surrounds the fact that it does not itself provide energy and furthermore, absorbs a large amount of amount during the early stages as it has a high latent heat of evaporation. This means the mixture inside the cylinder will take even longer to reach the temperature to initiate combustion of the char particles. Certainly, in medium to high-speed engines, either a pilot injector or a miscible fuel such as ethanol or diethyl ether would have to be used also.

All media with the exception of water have high wettability with charcoal. The reason is that the dielectric constant of water is high in comparison to hydrophobic charcoal.

Table 2-4 Properties of media which could be used in a slurry fuel.

Media	Flash point (°C)	Autoignition temperature (°C)	Higher Heating Value (MJ/kg)	Density (kg/m ³)	Viscosity (mm ² /s)	Dielectric constant	Boiling Point (°C)
Water	N.A.	N.A.	N.A.	1000	1.13	80.4	100
Diesel	55°C	210	44.8	830	3.0	2.1	270
Biodiesel (Rapeseed)	120°C	260	39.5	888	5.89	3.3	369
Ethanol	16.6°C	365	29.7	789	1.52	24.3	78.4
Diethyl Ether	-45°C	160	33.9	713	0.23	4.3	34.6

If wet milling were employed in situ with the final liquid medium, then the flash point becomes more important as flammable vapours make the process potentially dangerous. The first three in table 2-4 are sufficiently high enough because the flash point is beyond the temperature that the mill or air is likely to become. The use of ethanol on its own could potentially be problematic without good ventilation. However, the flash point can be increased by the addition of water.

2.8 Rheology

The rheological properties are very important as the slurry fuel made must be pumped at high pressures and stored before use. The properties are governed by the composition and quantity of particles, the liquid media and the additives present.

The stability of a slurry is the ability to remain homogeneously dispersed within the liquid medium. One way of improving dispersity is to increase the repulsion between char particles. The nature of the electrical double layer (EDL) around the solid particles strongly determines the stability of the slurry through the interparticle repulsion it creates. Most substances that come into contact with a polar medium gain a surface electrical charge as a result of ionisation, ion adsorption or ion dissolution (Williams, 1992). Preferential adsorption to the interface of certain ions can occur as a result of geometries, and the adsorption and orientation of dipolar molecules (Aveyard and Haydon, 1973). The EDL around particles can help to prevent agglomeration by creating repulsive forces which counteract van der Waals attraction (Herman and Papadopoulos, 1990). The most common indicator of this repulsive force is zeta potential which corresponds to the electrical potential at the shear boundary. The absolute magnitude of the zeta potential of the slurried biomass helps to determine the stability of the solution. Larger values correspond to increased stability. Mori et al. (1984) found for a given pH of coal suspensions in water, the zeta potential could be predicted from the ultimate analysis and

weight percent ash of the solid. The equations predicting zeta potential in Mori et al. (1984) had a coefficient of correlation with the observed values of thirteen coals of between 0.770 and 0.972. It was also found that the carbon content of coal decreased in significance for determining the zeta potential with increasing pH whereas oxygen, sulphur and nitrogen increased. For pH = 3, zeta potential could be approximated as (Mori et al., 1984):

$$Z_{(pH=3)} = 0.77x(C) + 3.00x(H) - 2.86x(O) - 11.97x(N) - 5.62x(S) - 1.78(\text{Ash}) \quad (3)$$

As loading increases, viscosity increases and slurries begin to show non-Newtonian properties (Ugwu et al., 2013). Yuchi et al. (2005) found the flow index of a slurry was mainly influenced by ash content, soluble ion content, pore volume and zeta potential. Flow index, N , is a non-dimensional measure of rheological behaviour where $N < 1$ indicates shear thinning and $N > 1$ is dilatant. For a set of sixteen coals Yuchi et al. (2005) found the rheological behaviour of a coal-water slurry with maximum coal content can be estimated using the following equation with a correlation coefficient of 0.917 and standard deviation of 0.139:

$$N = 0.86 - 0.098A_d - 0.0023D_t - 0.291V_{Hg} + 0.011\xi \quad (4)$$

Where A_d is ash content (%wt), D_t is content of soluble ions (mg/g coal), V_{Hg} is pore volume (cc/g) determined by mercury porosimeter and ξ is zeta potential (mV) of the solid. The rheological benefit of ash in coal is caused by clay-based mineral matter creating a gel which is a cross-linked network in the slurry. As the ash in biomass is not clay based this will not occur but could still affect the flow index in another way. Ash also increases the apparent viscosity of slurries (Mishra et al., 2002). Higher viscosity fuels are more likely to form deposits on injectors (Pehan et al., 2009). A large pore volume can also accelerate the transfer of slurries from a soft sediment to a hard sediment through the permeation of the liquid medium into the micropores during storage (Gu et al., 2008).

One of the main challenges of creating a slurry fuel is controlling the rheology. As the solid content increases, the viscosity increases and the fuel becomes non-Newtonian. Non-Newtonian fluids can be problematic because under high shear, like when fuel is injected into an engine, the viscosity changes. Shear-thickening is especially problematic because the increased viscosity leads to poor atomisation. Coal oil slurries are Newtonian at low solid concentrations ($\approx 10\%$ wt.) and become non-Newtonian at approximately 30% wt. (Papachristodoulou and Trass, 1984). Cui et al. (2008) investigated different solid loadings of micronised coal in diesel. It was found that the rheology of slurry changed from shear thinning to thickening between 45 and 50%wt.. Shivaram et al. (2013) prepared a 41%wt. biochar-water slurry with different particle size distributions, finding that all were shear thinning. Yield stress

also decreased with increasing particle size. The stability of charcoal-diesel slurries is in the range of a day to a week (Soloiu et al., 2011).

Higher viscosity fuels are harder to pump and do not produce as fine droplets as pure diesel (Soloiu et al., 2011). The viscosity exponentially increases with solid weighting before becoming virtually unpumpable at approximately 55-80%wt., depending on the material properties. Figure 2-8, shows this phenomenon occurring in coal-water slurries when solid loadings are increased above 55%wt. (Mukherjee et al., 2015). Two methods are commonly employed to overcome this: by broadening the particle size distribution allowing smaller particles to fill the voids between larger ones and by using surfactants (Chen et al., 2011).

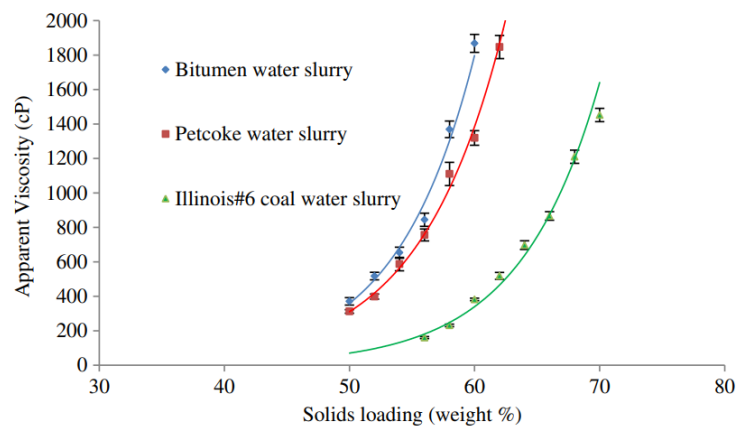


Figure 2-8 Viscosity of three water slurries as a function of solid loading (Mukherjee et al., 2015)

2.9 Surfactants

Surfactants must be used to create a sufficiently stable suspension for the storage of slurries. They are often used to improve flow properties as well. The selected surfactant must interact with both the liquid media and particles and hence they contain both hydrophilic and hydrophobic areas. Figure 2-9 shows how surfactant molecules build up on the surface of particles. In this case, the negatively charged head (meaning that it is anionic) of the surfactant molecule faces into the solution and the non-charged section interacts with the surface. The presence of the negatively charged surfactant on the surface can repel other surfactant molecules on the surface of other particles in the slurry, preventing coalescence.

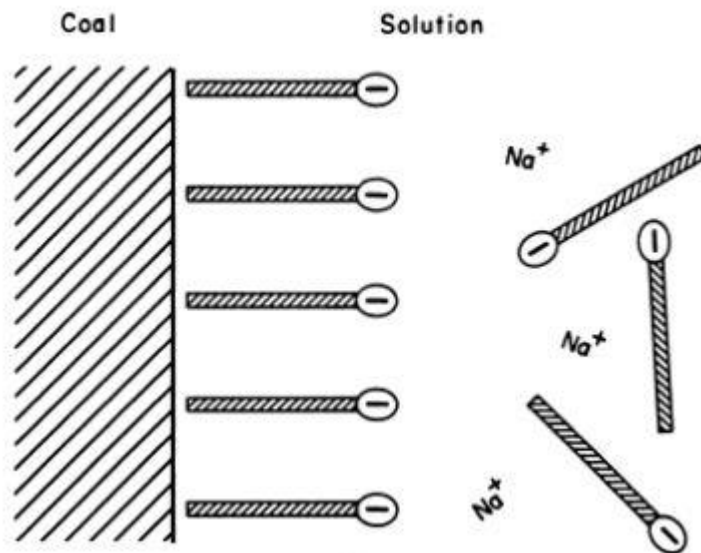


Figure 2-9 Anionic surfactant molecules interacting with the surface of a coal particle (Kilau, 1990)

There are several properties which influence the suitability of surfactants for improving the slurry. One of the most important is the hydrophilic-lipophilic balance (HLB), which expresses the relative strength of polar and non-polar regions. It can be applied to a single compound or a mixture. Whilst not hydrophilic, charcoal is more so than diesel (Herman and Papadopoulos, 1990). The ideal surfactant package for a char-diesel slurry would have a lower HLB than one in which the media is hydrophilic, e.g. water. Wetting agents have an HLB in the region of 7-9 and can improve slurry stability by lowering surface tension (Chang et al., 2015; Song et al., 2014). HLB also gives an indication of the solubility of the surfactant. Above an HLB of 10 indicates it is water soluble.

Another key differentiator is the type of hydrophilic head on the molecule. The hydrophobic tail is a hydrocarbon and can be branched or straight, saturated or unsaturated. The first type of heads are non-ionic which are made hydrophilic by the presence of a dipole created by the presence of electronegative atoms, usually oxygen (Rodríguez-Cruz et al., 2005). Often these are fatty acids and alcohol ethoxylates (Tadros, 2014). The advantage of non-ionic surfactants is that they are usually ashless. The other types are ionic and can be anionic, cationic or amphoteric. Anionic surfactants are the most commonly used because of their cost (Tadros, 2014). The molecules have a negatively charged head bonded to a counterion which is usually sodium, shown in figure 2-9. Cationic surfactants are positively charged, usually by a quaternary ammonium head with a chloride counterion. Amphoteric surfactants contain both cationic and anionic groups. Depending on the pH, these can behave more like an anionic or cationic surfactant. A common naturally occurring example is lecithin, a phospholipid found in eggs and soybeans.

The morphology of the surfactant compounds also determines how the rheology is affected. For example, a straight-chain surfactant with only one charged or dipolar area will make contact with particles at a single point. Another type of surfactant is a graft copolymer, which has a polymeric backbone and several branched chains creating a comb shape (Tadros, 2014). The multitude of attachment sites means that strong adsorption occurs. Other surfactants have long chains with charged heads separated by so-called spacer chains, illustrated by figure 2-10 (Negin et al., 2017). These are sometimes referred to as Gemini surfactants and have a very high efficiency in reducing surface tension and have a low Critical Micelle Concentration (CMC) (Tadros, 2014).

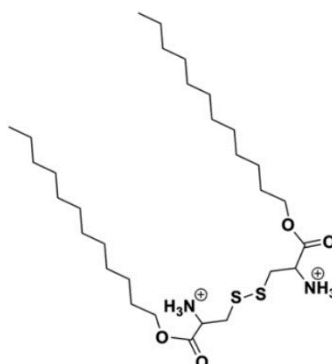


Figure 2-10 Cystine didodecyl ester salt- an example of a Gemini surfactant (Pérez et al., 2014)

The right dosage of surfactant is important as it represents a major cost to the overall slurry. Surfactants should be chosen which can efficiently cover the particle surfaces, preventing agglomeration. Low concentrations of surfactants can increase flocculation as they can create bridges from a particle it is adhered to, to an area of an uncovered particle (Dobiáš and Rybinski, 1999). Too high and the surfactants begin to form micelles whereby they coagulate with the lyophobic sections in the centre (Fares et al., 2013). Previous studies suggest that the amount of surfactant needed for addition to slurries is in the region of 0.25-2%wt. for fuels with a solid content of 10-60%wt. (Soloiu et al., 2011; Arthur D. Little INC. , 1995; Wilson, 2007; Shivaram et al., 2013)

Steric stabilisation is an important mechanism in surfactants to prevent the suspension from flocculating and sedimenting. The collision between two layers of surfactants surrounding a particle can repel in two different ways. Firstly, the amount of surfactant molecules in the surrounding layer increases, thus the number of configurations is reduced (i.e. reduces entropy) (Dobiáš and Rybinski, 1999). This loss of entropy causes an effect called entropic repulsion. Another mechanism is that the concentration of the surfactant increases in the overlapping area causing the particles to separate by osmotic repulsion (Dobiáš and Rybinski, 1999).

Depletion stabilisation occurs when two particles that have a surface saturated with a polymer are very close (Semenov and Shvets, 2015). Any closer would mean that the polymer interface would be displaced. As they are already organised in the most energetically favourable configuration, the free energy would have to increase (Dobiáš and Rybinski, 1999). This creates an area of relatively pure solvent between the particles known as the depletion zone (Semenov and Shvets, 2015). This region can serve to destabilise the overall suspension. A small amount of additional surfactant can cause flocculation by introducing depletion interaction (Kim et al., 2015). By further increasing surfactant concentration, the suspension stabilises again because of the repulsion effect of the ends of the non-adsorbed polymer chains (Semenov and Shvets, 2015).

Essentially, the stability of a suspension can increase and decrease with the amount of surfactant. First, it can reduce with the bridging effect, then increases as steric stabilisation dominates, decreases through depletion flocculation and finally increases with depletion stabilisation.

Most studies have focused on surfactants for (char)coal-water slurries. Shivaram et al. (2013) created a char-water slurry stabilised with poly(butadiene-maleic acid) sodium salt (BMA) and carboxymethylcellulose (CMC) sodium salt. BMA was the most effective at increasing the solid loading but did not completely disperse the char. Wilson (2007) produced a 47.7% wt. coal-water slurry containing xanthan gum and Triton X surfactants to control low and high shear viscosity respectively. Arthur D. Little INC. (1995) used a surfactant package for coal-water slurries using xanthan gum as a stabiliser, and an ammonium salt polymer and Naphthalene sulfonic acid as dispersants. The slurry could be stored for a year, although some remixing was required, and the surfactant package contributed to about 40% of the cost.

There is less information in literature about surfactants for (char)coal-diesel slurries. Soloiu et al. (2011) investigated using fatty acids, alkyl esters and fatty acid soap at 0.5%wt. concentrations to stabilise a charcoal-diesel slurry. It was found a single surfactant was poor at stabilising the slurry and so mixtures were used. The most promising was a fatty acid and fatty acid soap mixture which was stable for 4 days and also reduced viscosity. Kalpesh and Dabhi (2014) used a number of surfactants for a 10%wt. charcoal-diesel slurry concluding that Polyethylene Glycol 400 was the most effective with 25 hours of stability. N'Kpomin et al. (1995) produced a charcoal-diesel slurry with several non-ionic ethoxylated surfactants to reduce viscosity. Water is also sometimes added to reduce the amount of surfactant needed (Kalpesh and Dabhi, 2014; Soloiu et al., 2011; N'Kpomin et al., 1995).

A weakness in the literature is the lack of quantification of the stability of slurries making it harder to reproduce the tests. Some have quantified the zeta potential which can show that a surfactant has been adsorbed to the surface and thus predict if stability improves. Measuring the shelf life of the slurry in literature has been done by a visual assessment of separation and is therefore subjective.

2.10 Combustion chemistry

The ignition of fuel in a diesel engine differs from that of a petrol engine, principally by the absence of a spark plug to begin combustion. Instead, the heat of compression causes the fuel to auto-ignite in the cylinder. Another key difference in modern engines is that the fuel is directly injected into the combustion chamber of the diesel engine, whereas in a petrol engine (although gasoline direct injection is an exception) the fuel is added to the inlet air. The efficiency advantage of diesel engines occurs from the ability to operate with lean fuel mixes (Zheng et al., 2004). This negates the need for a throttle which causes pumping losses and increases the amount of air which expands per unit of fuel burned (Li et al., 2018). Also, higher compression ratios and less friction from lower running speeds improves efficiency (McAllister et al., 2011).

The diesel four-stroke cycle, shown in figure 2-11, first begins at sub image a) by drawing air into the combustion chamber through the inlet valve as the piston moves down from top dead centre (TDC). The inlet valve closes when the piston reaches bottom dead centre (BDC) and begins to compress the air (sub-image b)). Fuel is injected and mixes in the cylinder as the piston approaches TDC. A few crankshaft degrees later and the mixture ignites; the time for this to happen is known as the ignition delay. The higher the cetane number of the fuel, the shorter the ignition delay (Churkunti et al., 2016). This is typically 1-1.5ms in naturally aspirated engines (Binder, 2010). The fuel injector remains open, spraying in further fuel which burns as it enters the chamber and makes contact with oxygen. This stage is known as diffusion combustion. At low loads, most of the combustion is premixed whereas at high loads diffusion dominates (Churkunti et al., 2016). The fuel injector closes at some point after top dead centre and the gases begin to expand and cool. The exhaust valve is opened, and the gases are pushed out by the piston, which is shown in figure 2-11d, before the process repeats.

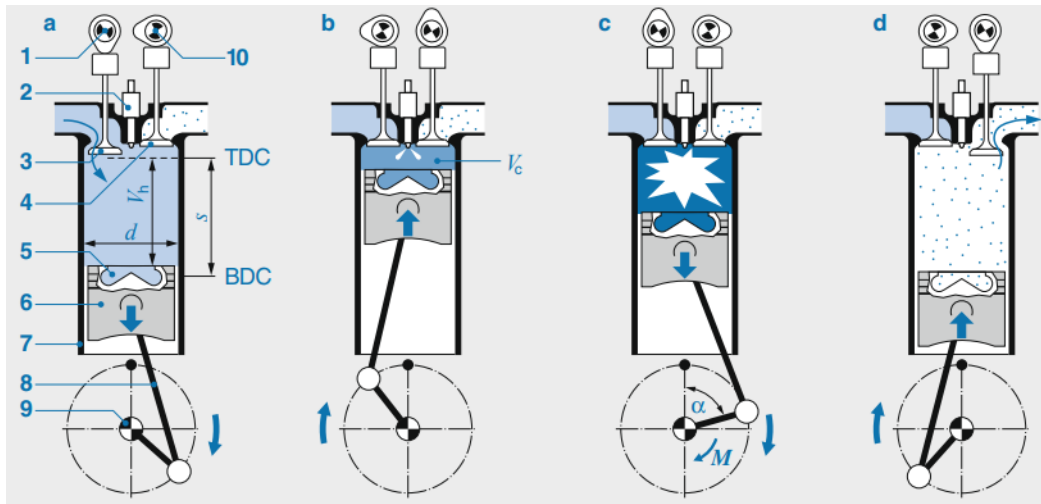


Figure 2-11 Four-stroke diesel engine (Grieshaber and Ratz, 2014)

2.10.1 Combustion of liquid fuels

The time during which the fuel is injected into the engine is the most important part of the 4-stroke cycle and is dependent on the chemical properties of the fuel used. As the fuel mixing occurs in the combustion chamber, the maximum engine rpm is lower for a diesel than a petrol engine (Stone, 1992). Also, because of the heterogeneous charge in the combustion chamber, it is hard to utilise all the oxygen present in the short time combustion occurs, so there is excess air of 5-15% at full load (Binder, 2010). For combustion to begin, fuel must vaporise, mix with the air, and reach the autoignition temperature. There are two parts to this ignition delay, physical and chemical. The physical aspect is the time for the spray to break up into droplets and evaporate into a combustible mix. The injection pressure and injector hole size improves atomisation which is important in reducing the physical ignition delay (Binder, 2010). The presence of solid particles will potentially affect the physical ignition delay in a number of ways. Low temperature volatile compounds (more volatile than the liquid medium) on the char, in particular, water will be released from the surface as a vapour, increasing the pressure within droplets. This will enhance the rate at which droplets break up and mix with air, reducing physical ignition delay. Water added to diesel in small quantities (<20% wt.) reduce NO_x and particulates by this phenomenon known as microexplosions (Lif and Holmberg, 2006). However, CO and THC emissions can increase. Surface tension affects the physical properties of the droplets and will also be affected by the presence of char particles and surfactants (Binder, 2010). The increased viscosity of char slurries compared to diesel as the atomisation will be poorer.

The chemical ignition delay is the time taken for the formation of radicals (e.g. OH) which are needed for combustion reactions to occur. OH radicals are highly reactive and important in the oxidation of soot and NO formation (McAllister et al., 2011; Ikegami and Kamimoto, 2009). Also, larger molecules are cracked into smaller ones. These reactions can occur in the vapour

and liquid phases as opposed to ignition, which only occurs in vapour mixtures (Heywood, 1988). The cracking reactions are potentially important in slurry fuels as the compounds in the char structure are often large and recalcitrant. The char particles provide a source of OH radicals which will affect the overall combustion rate of the diesel component (Blocquet et al., 2013). During the ignition delay, acetylene is formed, which then reacts with other acetylene compounds to form poly-aromatic hydrocarbons, a soot precursor (Ikegami and Kamimoto, 2009).

As the fuel-air mix is heterogeneous, the reaction chemistry is more complex than a petrol engine. There are two important parts to the fuel combustion, premix and diffusion. Premixed combustion occurs from the fuel what is injected before ignition. This fuel has a comparatively long time to mix with air and so there are less oxygen deprived areas. Hence, less soot is produced during premix combustion but a large proportion of the total NO_x is because of the high temperatures in excess air (Binder, 2010). Premix combustion can also be increased by injecting the fuel earlier (McAllister et al., 2011).

Diffusion combustion occurs during the continued injection of fuel after ignition has begun. This period of combustion is longer and the fuel burns slower compared to premix. As the mix at this point is more heterogeneous, there are more areas deprived of oxygen. Furthermore, the temperature within the spray is higher after combustion has begun. Hence, CO and soot are formed in larger quantities. About 14% of the total carbon in the diesel fuel injected is converted to soot (Ikegami and Kamimoto, 2009). The soot particles during this time begin to agglomerate and undergo dehydrogenation. The majority of soot (90-95%) formed is burned within the cylinder before it can be released through the exhaust (Ikegami and Kamimoto, 2009; Binder, 2010).

Soloiu et al. (2011) reported that, for a charcoal-diesel slurry, the ignition delay increases because the atomisation is poorer, caused by the higher viscosity compared to diesel. Without altering the fuel injection timings, the NO_x emission was higher and the smoke lower compared to diesel which fits with the ignition delay being longer. The ignition timing was retarded and it was found that the NO_x could be reduced without a significant increase in smoke which is expected with liquid fuels. The reason for this was attributed to the presence of oxygen in the slurry charcoal. Conventional oxygenated diesel fuel blends show similar combustion properties- the presence of oxygen increases ignition delay (An et al., 2015). Smoke reduces with the addition of oxygenated compounds but does not necessarily lead to an increase in NO_x (Guo et al., 2016). The reason for this is likely the reduction in calorific value leading to lower cylinder pressures and temperatures (An et al., 2015).

2.10.2 Combustion of solid particles

As with the burning of liquid fuels, the combustion kinetics of solid particles are complicated. Models of char particle combustion in an internal combustion engine are lacking but there is some for processes where the heating rate and temperatures are similar to an engine. There are two main stages in solid fuel combustion; the first is volatile (gas phase), the second char combustion (Clery et al., 2018; Vorobiev et al., 2016).

There are two important dimensionless numbers for the combustion of particles. Firstly, the Biot number relates the internal resistance to the flow of heat or mass transfer to that at the surface of the body given by the equation (Schaschke, 2014):

$$Bi = hl/k \quad (5)$$

Where h is the film coefficient, l is the characteristic dimension and k is the thermal conductivity of the solid. If $Bi < 0.1$ then the thermal gradient is negligible. Considering that the particle size, l , in slurry fuels is very small, the temperature can be considered uniform across the particle.

Secondly, the ratio of the rate of chemical reactions compared to the rate at which reactants mix is important. Porosity, size and surface area of the char particles are of great importance as they have a large influence on the rate of combustion. The more porous and larger the specific surface area, the quicker oxygen can diffuse and react with larger parts of the solid particle (Piriou et al., 2013; Dunn-Rankin et al., 1987). Char combustion is the slowest step in burning and so increasing the value of these two parameters can significantly improve reaction rates. There is, however, a point at which higher porosity no longer increases the rate of reaction, as the process becomes a chemically controlled one (Ahmed and Gupta, 2011). Similarly, particle size affects the rate of combustion, as the smaller the particle size the faster air can diffuse throughout the entire volume. Essentially, the importance of porosity and particle size is the ease at which gas reactants can diffuse into the solid fuel particles. These two properties are linked by the Damköhler number (Da) which is the ratio of chemical timescale to transportation rate (Leach et al., 1998). In the case of air reacting with a solid particle transportation rate refers to the diffusivity of the reactant gases within the solid. It is given by (Ahmed and Gupta, 2011):

$$Da = \frac{k(2r_p)^2}{D_o \epsilon^2} \quad (6)$$

Where k is the reaction rate constant (s^{-1}), r_p is particle size (m), D_o is the diffusivity of oxygen in air (m^2/s) and ϵ is the porosity of the solid. For small particle sizes and high porosity, the Damköhler number is low thus the overall reaction rate is limited by chemical processes rather than diffusion. At the particle size required for slurry fuel, the Damköhler number is very low

and therefore the reaction rate is limited by the chemical timescale (Howard and Essenhigh, 1967). High porosity and surface area in the case of slurry fuels are not a particularly desirable property as the amount of surfactants required increases (de Aguiar et al., 2011). It also increases the potential for more of the liquid media to be immobilised on the surface, increasing the viscosity.

Some models exist for the combustion of particles at high temperatures and heating rates although the particle size is 1-2 magnitudes larger than exist in slurry fuels. Mock et al. (2016) investigated the combustion of biomass and coal particles in O₂/N₂ mixes at 1090-1340K and a heating rate of roughly 10⁵ K/s. The particle sizes were 150-500µm, roughly ten times the size of slurry fuel particles. Whilst the heating rate is similar to a diesel engine, the temperature is less and the particle sizes larger meaning that combustion in the study will be slower. The onset of coal volatile combustion was earlier than biomass and was shorter in duration because less volatile matter was present. The flame for coal was found to be sootier than the biomass flame. High volatile matter chars such as hydrochar are therefore likely to produce less soot than coal.

For comparatively large periods of time within the cylinder the particles are in a region of low oxygen. As such, combustion will be limited, but other reactions may occur which are similar to pyrolysis, causing the carbon structure to break down before combustion. For less stable materials such as hydrochar, this is likely a significant phenomenon. Yan et al. (2012) performed rapid pyrolysis on 50µm coal particles in a thermal plasma reactor. Temperatures of 2000K were reached in a few milliseconds during the tests which is similar to diesel engines. In this time, a yield of gaseous product of between 31 and 48% wt. (daf) was achieved from a coal with 41.62% (daf) volatile matter. Over 75% of the gas was hydrogen. The next most abundant was carbon monoxide, then acetylene and methane. The main parameter for increasing gas yield was faster heating rates. During combustion in an engine it is therefore likely that char in areas of low oxygen, like the centre of the spray, will break into gaseous components before combustion, decompose rather than burn when oxygen comes into contact with the surface of particles.

In the latter stages of combustion, soot and the fixed carbon remaining in char will oxidise. Harvey et al. (2012b) analysed the recalcitrance of different carbons. An index was created using the equation:

$$R_{50} = T_{50,x} / T_{50 \text{ graphite}} \quad (7)$$

Where T_{50,x} is the temperature at which half the mass of the carbon is oxidised and T_{50 graphite} is 886°C. It was found that carbon black produced from acetylene, which is very similar to engine soot had an index of 0.85 whereas lignocellulosic biochars produced around 400-600°C had a value of 0.45-0.6. Therefore, the char will have longer to burn than soot because the combustion

chamber does not have to be as hot as it does to burn soot. Whilst late burning is not ideal from an energy efficiency perspective, it will mean less particulate emission from the char will be emitted. Additionally, soot particles formed may agglomerate with char particles as they do with other soot particles. The continued heat produced from the combustion of less recalcitrant char could improve the soot burnout.

2.11 Diesel additives

The presence of inorganic elements in the combustion chamber influences the chemical reactions that take place. Research has investigated using several different elements blended into diesel for emissions reduction and fuel efficiency improvements. Often these are added to the fuel as organic compounds (Gürü et al., 2002). Elements investigated include: Ag, Al, Ca, Cu, Co, Fe, Mg, Mn, Ti and Zr (Gürü et al., 2002; Sajith et al., 2010; Çelik et al., 2015; Soukht Saraee et al., 2015; Yang et al., 2013; Ganesh and Gowrishankar, 2011; Venu and Madhavan, 2016; Kannan et al., 2011). Additionally, Potassium additives have been shown to enhance the catalytic effect of other elements during soot oxidation (Pushkin et al., 2013). Of these elements that have been investigated, the most likely to be found in biochars are Ca, K and Mg with smaller amounts of Al, Cu, Fe and Mn.

The most dominant inorganic trace element in most hydrochars, and to a lesser extent biochars, is calcium. Gürü et al. (2002) produced an organometallic additive of calcium abiate and found that an optimal concentration of 50-75 µmol/L could reduce the freezing point of diesel by 8°C. Miyamoto et al. (1987) tested a number of additives including Ca stearate and Ca naphthenate. The Ca and Ba additives were found to reduce smoke emissions the most of the metals tested, and little difference was found between the stearate and naphthenate compounds, suggesting that it is the metal which is the most important factor. The optimum dosage was in the range of 10-20µmol/L. NO_x was reported to slightly increase at low loads and decrease at high loads. CO and HC were both slightly reduced also. The smoke reducing effect was attributed to a catalytic effect in both soot oxidation and suppressing soot formation.

Husnawan et al. (2009) added an MgO-polyol additive mix to diesel and biodiesel mixtures for emissions improvement. The additive was in relatively large concentrations (2%) and the actual amount of Mg present is not mentioned. The largest improvement was a reduction in HC by over 50%. HC and NO_x also decreased. Keskin et al. (2008) produced an organic Mg additive which improved the pour point, viscosity and flash point of a B60 diesel blend. The performance of an engine in testing did not alter significantly with the additive fuel blends but emissions were improved. The additive in concentrations in the range of 8-12 µmol/L reduced engine smoke particularly at high engine speeds and reduced NO_x and CO at low engine

speeds. The effect on NO_x and CO was little at high speeds. The mechanism for this is that metal additives can react with water to produce OH radicals, which enhances soot oxidation or by direct reaction with soot (Keskin et al., 2008).

Pushkin et al. (2013) investigated using additives to improve the rate of soot oxidation. The additives were mixed oxide systems containing Ca, Co, Cu and Mg which were shown to reduce the temperature at which soot oxidation occurred from 480-500°C to 360-420°C and increased the reaction rate. Potassium carbonate was also added to the mixed oxide systems and was shown to make further improvements in all instances. A large difference between hydrochar and biochar is that much of the potassium is removed during hydrothermal carbonisation and so this effect would be reduced.

2.12 Conclusions

The entire process of producing a slurry fuel was reviewed. Pyrolysis is currently the most appropriate route at this time because the technology is used throughout many developing countries, whereas HTC is currently limited. Not all charcoal kilns, however, are suitable for the production of a fuel for slurry engines. The amount of oxygen which enters the pyrolysis chamber must be minimised to reduce the percent ash in the product. It means that metal barrel retorts are potentially the most appropriate design as oxygen is prevented from entering the kiln section. Hydrothermal reactors could be used in the future.

Low temperature thermal conversion is the most suitable condition for making char for slurring because the solid char yield is higher and the material more volatile. The temperature of thermal conversion should still be high enough to make the material brittle enough to grind down. The temperature needed for HTC is lower than pyrolysis, thus hydrochar contains more volatile matter than pyrochar. The desired initial material for pyrolysis should be low in cellulose as only a small proportion converts to a solid char residue and prevents polymerisation of lignin.

There is a consensus in the literature regarding the milling of char material for slurring. Most studies concluded that a wet stirred milling procedure is required to achieve a mean particle size of less than 20µm. A study on attrition via jet milling showed that it could be a more energy efficient process, but as a new method is less suitable for developing countries where equipment is limited.

The liquid media and surfactants are key to ensuring the slurry burns well inside a diesel engine and that it remains stable enough, so it can be stored easily. Using water as the media produces the most stable slurries because the density is closer to that of chars. It is, however, the hardest to burn because the liquid does not aid the combustion of the char. Char-ethanol

slurries, on the other hand, are unstable but will burn better than char water slurries because the ethanol will burn and raise the temperature of the combustion chamber. As the autoignition temperature of ethanol is low, a cetane improver is likely needed. Adding char to ethanol can be used to raise the calorific value on both a volume and mass basis. The simplest slurry to use is a char-diesel slurry because the liquid begins to burn at a lower temperature than ethanol, but compromises on stability between that of ethanol and water slurries. There are currently few studies regarding surfactants to improve the stability of char-diesel slurries, as most work has focused on coal-water slurries, which requires different kinds of surfactants.

The process of burning a liquid fuel in a diesel engine is different to solids. The size of liquid droplets can be altered through injector hole size and injection pressure, whereas the size of solid particles is fixed. Solid chars also burn in two distinct stages, beginning with the burning of volatiles, and finally fixed carbon. In an engine, where the heating rates are high, it is predicted that some of the solid char will break down into gaseous compounds such as hydrogen and carbon monoxide. As the particles in the slurry are very small the rate of combustion is limited by chemical reactions rather than diffusion of reactant gas. Mixing of fuel with air on the macroscale is an important consideration to the overall combustion rate, thus the rheology is important.

2.13 References

- Abdullah, H. and Wu, H. 2009. Biochar as a Fuel: 1. Properties and Grindability of Biochars Produced from the Pyrolysis of Mallee Wood under Slow-Heating Conditions. *Energy & Fuels*. **23**(8), pp.4174-4181.
- Abelha, P.Gulyurtlu, I. and Cabrita, I. 2008. Release Of Nitrogen Precursors From Coal And Biomass Residues in a Bubbling Fluidized Bed. *Energy & Fuels*. **22**(1), pp.363-371.
- Adam, J.C. 2009. Improved and more environmentally friendly charcoal production system using a low-cost retort–kiln (Eco-charcoal). *Renewable Energy*. **34**(8), pp.1923-1925.
- Ahmed, I.I. and Gupta, A.K. 2011. Particle size, porosity and temperature effects on char conversion. *Applied Energy*. **88**, pp.4667-4677.
- Alghoul, Z.M.Ogden, P.B. and Dorsey, J.G. 2017. Characterization of the polarity of subcritical water. *Journal of Chromatography A*. **1486**, pp.42-49.
- Altun, O.Benzer, H. and Enderle, U. 2013. Effects of operating parameters on the efficiency of dry stirred milling. *Minerals Engineering*. **43**(Supplement C), pp.58-66.
- Ambedkar, B.Chintala, T.N.Nagarajan, R. and Jayanti, S. 2011. Feasibility of using ultrasound-assisted process for sulfur and ash removal from coal. *Chemical Engineering and Processing: Process Intensification*. **50**(3), pp.236-246.
- Amin, A.Gadallah, A.El Morsi, A.K.El-Ibiari, N.N. and El-Diwani, G.I. 2016. Experimental and empirical study of diesel and castor biodiesel blending effect, on kinematic viscosity, density and calorific value. *Egyptian Journal of Petroleum*. **25**(4), pp.509-514.
- An, H.Yang, W.M.Li, J. and Zhou, D.Z. 2015. Modeling study of oxygenated fuels on diesel combustion: Effects of oxygen concentration, cetane number and C/H ratio. *Energy Conversion and Management*. **90**(Supplement C), pp.261-271.
- Anca-Couce, A. 2016. Reaction mechanisms and multi-scale modelling of lignocellulosic biomass pyrolysis. *Progress in Energy and Combustion Science*. **53**, pp.41-79.

- Antal, M.J. 1985. Biomass Pyrolysis: A Review of the Literature Part 1—Carbohydrate Pyrolysis. In: Böer, K.W. and Duffie, J.A. eds. *Advances in Solar Energy: An Annual Review of Research and Development, Volume 1 · 1982*. Boston, MA: Springer New York, pp.61-111.
- Armstrong Energy. 2017. ARMSTRONG ENERGY ANNOUNCES JOINT VENTURE TO RECYCLE WASTE PLASTICS. [Online]. [Accessed 23/07/2018]. Available from: ARMSTRONG ENERGY ANNOUNCES JOINT VENTURE TO RECYCLE WASTE PLASTICS.
- Arthur D. Little INC. . 1995. *Coal Fueled Diesel System for Stationary Power Applications-Technology Development*. Morgantown, USA: U.S. Department of Energy.
- Aveyard, R. and Haydon, D.A. 1973. *An Introduction to the principles of surface chemistry*. Cambridge, UK: University Press.
- Aysu, T. and Küçük, M.M. 2014. Biomass pyrolysis in a fixed-bed reactor: Effects of pyrolysis parameters on product yields and characterization of products. *Energy*. **64**(0), pp.1002-1025.
- Bach, Q.-V. and Chen, W.-H. 2017. A comprehensive study on pyrolysis kinetics of microalgal biomass. *Energy Conversion and Management*. **131**, pp.109-116.
- Basu, P. 2010. *Biomass Gasification and Pyrolysis: Practical Design and Theory*. Elsevier Science.
- Bennadji, H.Khachatryan, L. and Lomnicki, S.M. 2018. Kinetic Modeling of Cellulose Fractional Pyrolysis. *Energy & Fuels*. **32**(3), pp.3436-3446.
- Berge, N.Ro, K.Mao, J.Floria, J.Chappell, M. and Bae, S. 2011. Hydrothermal Carbonization of Municipal Waste Streams. *Environ. Sci. Technol.* **45**(13), pp.5696-5703.
- Binder, K.B. 2010. Diesel Engine Combustion. In: Mollenhauer, K. and Tschöke, H. eds. *Handbook of Diesel Engines*. Berlin: Springer.
- Blocquet, M.Schoemaeker, C.Amedro, D.Herbinet, O.Battin-Leclerc, F. and Fittschen, C. 2013. Quantification of OH and HO₂ radicals during the low-temperature oxidation of hydrocarbons by Fluorescence Assay by Gas Expansion technique. *Proceedings of the National Academy of Sciences*. **110**(50), pp.20014-20017.
- Bradbury, A.G.W.Sakai, Y. and Shafizadeh, F. 1979. A kinetic model for pyrolysis of cellulose. *Journal of Applied Polymer Science*. **23**(11), pp.3271-3280.
- Bragadeshwaran, A.Kasianantham, N.Balusamy, S.Muniappan, S.Reddy, D.M.S.Subhash, R.V.Pravin, N.A. and Subbarao, R. 2018. Mitigation of NO_x and smoke emissions in a diesel engine using novel emulsified lemon peel oil biofuel. *Environmental Science and Pollution Research*. **25**(25), pp.25098-25114.
- British Standards Institution. 2013. 2013. *BS EN 590:2013+A1:2017 Automotive fuels. Diesel. Requirements and test methods*. London UK: British Standards Institution.
- Broseghini, M.Gelasio, L.D'Incau, M.Azanza Ricardo, C.L.Pugno, N.M. and Scardi, P. 2016. Modeling of the planetary ball-milling process: The case study of ceramic powders. *Journal of the European Ceramic Society*. **36**(9), pp.2205-2212.
- Bustamante-García, V.Carrillo-Parra, A.González-Rodríguez, H.Ramírez-Lozano, R.G.Corrall-Rivas, J.J. and Garza-Ocañas, F. 2013. Evaluation of a charcoal production process from forest residues of *Quercus sideroxylla* Humb., & Bonpl. in a Brazilian beehive kiln. *Industrial Crops and Products*. **42**(Supplement C), pp.169-174.
- Çelik, M.Solmaz, H. and Serdar Yücesu, H. 2015. Examination of the effects of organic based manganese fuel additive on combustion and engine performance. *Fuel Processing Technology*. **139**(Supplement C), pp.100-107.
- Chang, H.Jia, Z.Zhang, P.Li, X.Gao, W. and Wei, W. 2015. Interaction between quaternary ammonium surfactants with coal pitch and analysis surfactants effects on preparing coal pitch water slurry. *Colloids and Surfaces A: Physicochemical and Engineering Aspects*. **471**, pp.101-107.
- Chen, R.Wilson, M.Leong, Y.K.Bryant, P.Yang, H. and Zhang, D.K. 2011. Preparation and rheology of biochar, lignite char and coal slurry fuels. *Fuel*. **90**(4), pp.1689-1695.

- Chia, M.A.Lombardi, A.T. and Gama Melão, M.d.G. 2013. Calorific values of *Chlorella vulgaris* (Trebouxiophyceae) as a function of different phosphorus concentrations. *Phycological Research*. **61**(4), pp.286-291.
- Choi, H.Lee, W.Kim, D.U.Kumar, S.Kim, S.S.Chung, H.S.Kim, J.H. and Ahn, Y.C. 2010. Effect of grinding aids on the grinding energy consumed during grinding of calcite in a stirred ball mill. *Minerals Engineering*. **23**(1), pp.54-57.
- Churkunti, P.R.Mattson, J.Depcik, C. and Devlin, G. 2016. Combustion analysis of pyrolysis end of life plastic fuel blended with ultra low sulfur diesel. *Fuel Processing Technology*. **142**(Supplement C), pp.212-218.
- Clery, D.S.Mason, P.E.Rayner, C.M. and Jones, J.M. 2018. The effects of an additive on the release of potassium in biomass combustion. *Fuel*. **214**, pp.647-655.
- Cui, L.An, L.Gong, W. and Jiang, H. 2007. A novel process for preparation of ultra-clean micronized coal by high pressure water jet comminution technique. *Fuel*. **86**(5), pp.750-757.
- Cui, L.An, L. and Jiang, H. 2008. A novel process for preparation of an ultra-clean superfine coal–oil slurry. *Fuel*. **87**(10), pp.2296-2303.
- Das, D.Dutta, A.K. and Ray, K.K. 2010. Sub-zero treatments of AISI D2 steel: Part I. Microstructure and hardness. *Materials Science and Engineering: A*. **527**(9), pp.2182-2193.
- de Aguiar, H.B.Strader, M.L.de Beer, A.G.F. and Roke, S. 2011. Surface Structure of Sodium Dodecyl Sulfate Surfactant and Oil at the Oil-in-Water Droplet Liquid/Liquid Interface: A Manifestation of a Nonequilibrium Surface State. *The Journal of Physical Chemistry B*. **115**(12), pp.2970-2978.
- De Bhowmick, G.Sarmah, A.K. and Sen, R. 2018. Production and characterization of a value added biochar mix using seaweed, rice husk and pine sawdust: A parametric study. *Journal of Cleaner Production*. **200**, pp.641-656.
- Demirbas, A. 2009. Pyrolysis Mechanisms of Biomass Materials. *Energy Sources, Part A: Recovery, Utilization, and Environmental Effects*. **31**(13), pp.1186-1193.
- Di Blasi, C. 2008. Modeling chemical and physical processes of wood and biomass pyrolysis. *Progress in Energy and Combustion Science*. **34**(1), pp.47-90.
- Dieguez-Alonso, A.Funke, A.Anca-Couce, A.Rombolà, A.Ojeda, G.Bachmann, J. and Behrendt, F. 2018. Towards Biochar and Hydrochar Engineering—Influence of Process Conditions on Surface Physical and Chemical Properties, Thermal Stability, Nutrient Availability, Toxicity and Wettability. *Energies*. **11**(3), p496.
- Diesel, R. 1898. *Internal-combustion engine*. Google Patents. Available from: <https://www.google.co.uk/patents/US608845>.
- Dobiáš, B. and Rybinski, W.v. 1999. Stability of Dispersions. In: Dobiáš, B., et al. eds. *Solid-Liquid Dispersions*. New York, USA: Marcel Dekker, pp.244-279.
- Donar, Y.O.Çağlar, E. and Sınağ, A. 2016. Preparation and characterization of agricultural waste biomass based hydrochars. *Fuel*. **183**, pp.366-372.
- Downie, R.J. and Bandothayay, P.C. 1988. AUSTRALIAN BROWN COAL/OIL MIXTURES AS A FUEL FOR DIESEL ENGINES; ENGINE PERFORMANCE AND ECONOMIC VIABILITY. *Fuel Science and Technology International*. **6**(4), pp.415-447.
- Du, Z.Hu, B.Ma, X.Cheng, Y.Liu, Y.Lin, X.Wan, Y.Lei, H.Chen, P. and Ruan, R. 2013. Catalytic pyrolysis of microalgae and their three major components: Carbohydrates, proteins, and lipids. *Bioresource Technology*. **130**, pp.777-782.
- Dunn-Rankin, D.Hoornstra, J.Gruelich, F.A. and Holve, D.J. 1987. Combustion of coal—water slurries: Evolution of particle size distribution for coals of different rank. *Fuel*. **66**(8), pp.1139-1145.
- Emiroğlu, A.O. and Şen, M. 2018. Combustion, performance and emission characteristics of various alcohol blends in a single cylinder diesel engine. *Fuel*. **212**, pp.34-40.
- Fares, M.M.Maayta, A.K. and Al-Qudah, M.A. 2013. Polysorbate20 adsorption layers below and above the critical micelle concentration over aluminum; cloud point and inhibitory role

- investigations at the solid/liquid interface. *Surface and Interface Analysis*. **45**(5), pp.906-912.
- Feng, P.Lin, W.Jensen, P.A.Song, W.Hao, L.Raffelt, K. and Dam-Johansen, K. 2016. Entrained flow gasification of coal/bio-oil slurries. *Energy*. **111**, pp.793-802.
- Fisher, T.Hajaligol, M.Waymack, B. and Kellogg, D. 2002. Pyrolysis behavior and kinetics of biomass derived materials. *Journal of Analytical and Applied Pyrolysis*. **62**(2), pp.331-349.
- Food and Agricultural Organization of the United Nations. 1983. *Simple technologies for charcoal making*. Rome: Food and Agricultural Organization of the United Nations,.
- Fu, J. and Wang, J. 2014. Enhanced slurryability and rheological behaviors of two low-rank coals by thermal and hydrothermal pretreatments. *Powder Technology*. **266**(0), pp.183-190.
- Funke, A. and Ziegler, F. 2010. Hydrothermal carbonization of biomass: A summary and discussion of chemical mechanisms for process engineering. *Biofuels, Bioproducts and Biorefining*. **4**(2), pp.160-177.
- Ganesh, D. and Gowrishankar, G. 2011. Effect of nano-fuel additive on emission reduction in a biodiesel fuelled CI engine. In: *International Conference on Electrical and Control Engineering, Yichang, China*. IEEE.
- Ghanooni, N.Leong, Y.-K. and Zhang, D. 2013. Mixing narrow coarse and fine coal fractions – The maximum volume fraction of suspensions. *Advanced Powder Technology*. **24**(4), pp.764-770.
- Grieshaber, H. and Raatz, T. 2014. Basic principles of the diesel engine. In: Reif, K. ed. *Fundamentals of Automotive and Engine Technology: Standard Drives, Hybrid Drives, Brakes, Safety Systems*. Wiesbaden: Springer Fachmedien Wiesbaden, pp.22-39.
- Gu, T.-y.Wu, G.-g.Li, Q.-h.Sun, Z.-q.Zeng, F.Wang, G.-y. and Meng, X.-l. 2008. Blended coals for improved coal water slurries. *Journal of China University of Mining and Technology*. **18**(1), pp.50-54.
- Guiotoku, M.Hansel, F.A.Novotny, E.H. and Maia, C.M.B.d.F. 2012. Molecular and morphological characterization of hydrochar produced by microwave-assisted hydrothermal carbonization of cellulose. *Pesquisa Agropecuária Brasileira*. **47**, pp.687-692.
- Guo, H.Liu, S. and He, J. 2016. Performances and Emissions of New Glycol Ether Blends in Diesel Fuel Used As Oxygenated Fuel for Diesel Engines. *Journal of Energy Engineering*. **142**(1), p04015003.
- Gurney, M. 1984. A combustion and wear analysis of a compression ignition engine using coal slurry fuels. *Am. Soc. Mech. Eng., (Pap.)*. **84-DGP-8**, p84.
- Gürü, M.Karakaya, U.Altıparmak, D. and Alicilar, A. 2002. Improvement of Diesel fuel properties by using additives. *Energy Conversion and Management*. **43**(8), pp.1021-1025.
- Harvey, O.R.Herbert, B.E.Kuo, L.-J. and Louchouart, P. 2012a. Generalized Two-Dimensional Perturbation Correlation Infrared Spectroscopy Reveals Mechanisms for the Development of Surface Charge and Recalcitrance in Plant-Derived Biochars. *Environmental Science & Technology*. **46**(19), pp.10641-10650.
- Harvey, O.R.Kuo, L.-J.Zimmerman, A.R.Louchouart, P.Amonette, J.E. and Herbert, B.E. 2012b. An Index-Based Approach to Assessing Recalcitrance and Soil Carbon Sequestration Potential of Engineered Black Carbons (Biochars). *Environmental Science & Technology*. **46**(3), pp.1415-1421.
- Herman, M.C. and Papadopoulos, K.D. 1990. Effects of asperities on the van der Waals and electric double-layer interactions of two parallel flat plates. *Journal of Colloid and Interface Science*. **136**(2), pp.385-392.
- Heywood, J.B. 1988. *Internal Combustion Engine Fundamentals*. New York: McGraw-Hill.
- Hoekman, S.Broch, A. and Robbins, C. 2011. *Hydrothermal Carbonization (HTC) of Lignocellulosic Biomass*.

- Hoekman, S.K.Broch, A.Felix, L. and Farthing, W. 2017. Hydrothermal carbonization (HTC) of loblolly pine using a continuous, reactive twin-screw extruder. *Energy Conversion and Management*. **134**, pp.247-259.
- Hoekman, S.K.Broch, A.Robbins, C.Purcell, R.Zielinska, B.Felix, L. and Irvin, J. 2014. Process Development Unit (PDU) for Hydrothermal Carbonization (HTC) of Lignocellulosic Biomass. *Waste and Biomass Valorization*. **5**(4), pp.669-678.
- Howard, J.B. and Essenhigh, R.H. 1967. Mechanism of solid-particle combustion with simultaneous gas-phase volatiles combustion. *Symposium (International) on Combustion*. **11**(1), pp.399-408.
- Husnawan, M.Masjuki, H.H.Mahlia, T.M.T.Mekhilef, S. and Saifullah, M.G. 2009. Use of post flame metal-based and oxygenated additive combination for biodiesel-diesel blends. *Journal of Scientific and Industrial Research*. **68**(12), pp.1049-1052.
- Iannuzzi, S.E.Barro, C.Boulouchos, K. and Burger, J. 2016. Combustion behavior and soot formation/oxidation of oxygenated fuels in a cylindrical constant volume chamber. *Fuel*. **167**, pp.49-59.
- Ikegami, M. and Kamimoto, T. 2009. Conventional Diesel Combustion. In: Arcoumanis, C. and Kamimoto, T. eds. *Flow and combustion in reciprocating engines*. Berlin: Springer.
- Ishigaki, H. and Buckley, D.H. 1981. *Effects of Environment on Microhardness of Magnesium Oxide*. Cleveland, OH: NASA.
- Iyogun, K.Lateef, S.A. and Ana, G.R.E.E. 2018. Lung Function of Grain Millers Exposed to Grain Dust and Diesel Exhaust in Two Food Markets in Ibadan Metropolis, Nigeria. *Safety and Health at Work*.
- Janot, R. and Guérard, D. 2005. Ball-milling in liquid media: Applications to the preparation of anodic materials for lithium-ion batteries. *Progress in Materials Science*. **50**(1), pp.1-92.
- Jensen, M.F.Bøttiger, J.Reitz, H.H. and Benzon, M.E. 2002. Simulation of wear characteristics of engine cylinders. *Wear*. **253**(9), pp.1044-1056.
- Jian, X.Zhuang, X.Li, B.Xu, X.Weil, Z.Song, Y. and Jiang, E. 2018. Comparison of characterization and adsorption of biochars produced from hydrothermal carbonization and pyrolysis. *Environmental Technology & Innovation*. **10**, pp.27-35.
- Kalpesh, V. and Dabhi, S. 2014. Investigation of Performance and Air Pollution of Charcoal Blended Diesel on CI Engine. *International Journal of Research and Scientific Innovation*. **1**(7), pp.205-208.
- Kambo, H.S. and Dutta, A. 2015a. Comparative evaluation of torrefaction and hydrothermal carbonization of lignocellulosic biomass for the production of solid biofuel. *Energy Conversion and Management*. **105**, pp.746-755.
- Kambo, H.S. and Dutta, A. 2015b. A comparative review of biochar and hydrochar in terms of production, physico-chemical properties and applications. *Renewable and Sustainable Energy Reviews*. **45**(Supplement C), pp.359-378.
- Kan, T.Strezov, V. and Evans, T.J. 2016. Lignocellulosic biomass pyrolysis: A review of product properties and effects of pyrolysis parameters. *Renewable and Sustainable Energy Reviews*. **57**, pp.1126-1140.
- Kandpal, J.B.Maheshwari, R.C. and Kandpal, T.C. 1995. Indoor air pollution from combustion of wood and dung cake and their processed fuels in domestic cookstoves. *Energy Conversion and Management*. **36**(11), pp.1073-1079.
- Kang, S.Li, X.Fan, J. and Chang, J. 2012. Characterization of Hydrochars Produced by Hydrothermal Carbonization of Lignin, Cellulose, d-Xylose, and Wood Meal. *Industrial & Engineering Chemistry Research*. **51**(26), pp.9023-9031.
- Kannan, G.R.Karvembu, R. and Anand, R. 2011. Effect of metal based additive on performance emission and combustion characteristics of diesel engine fuelled with biodiesel. *Applied Energy*. **88**(11), pp.3694-3703.
- Kashcheev, V.N. and Yampolsky, G. 1981. Abrasive Wear. In: Kragelsky, I.V. and Alisin, V.V. eds. *Tribology - Lubrication, Friction, and Wear*. Moscow: Mir Publishers.

- Katubilwa, F.M.Moys, M.H.Glasser, D. and Hildebrandt, D. 2011. An attainable region analysis of the effect of ball size on milling. *Powder Technology*. **210**(1), pp.36-46.
- Keiluweit, M.Nico, P.S.Johnson, M.G. and Kleber, M. 2010. Dynamic Molecular Structure of Plant Biomass-Derived Black Carbon (Biochar). *Environmental Science & Technology*. **44**(4), pp.1247-1253.
- Keskin, A.Gürü, M. and Altıparmak, D. 2008. Influence of tall oil biodiesel with Mg and Mo based fuel additives on diesel engine performance and emission. *Bioresource Technology*. **99**(14), pp.6434-6438.
- Kilau, H.W. 1990. *The influence of sulfate ion on the coal-wetting performance of anionic surfactants*. Washington DC, USA: U.S. Dept. of the Interior, Bureau of Mines.
- Kim, S.Hyun, K.Moon, J.Y.Clasen, C. and Ahn, K.H. 2015. Depletion Stabilization in Nanoparticle–Polymer Suspensions: Multi-Length-Scale Analysis of Microstructure. *Langmuir*. **31**(6), pp.1892-1900.
- Klein, I. 1928. Engine is run 12 years using pulverised coal as only fuel. *The Southeast Missourian*.
- Lacey, J.A.Emerson, R.M.Thompson, D.N. and Westover, T.L. 2016. Ash reduction strategies in corn stover facilitated by anatomical and size fractionation. *Biomass and Bioenergy*. **90**, pp.173-180.
- Leach, S.V.Ellzey, J.L. and Ezekoye, O.A. 1998. Convection, pyrolysis, and Damköhler number effects on extinction of reverse smoldering combustion. *Symposium (International) on Combustion*. **27**(2), pp.2873-2880.
- Lee, Y.-J.Choi, J.-W.Park, J.-H.Namkung, H.Song, G.-S.Park, S.-J.Lee, D.-W.Kim, J.-G.Jeon, C.-H. and Choi, Y.-C. 2018. Techno-Economical Method for the Removal of Alkali Metals from Agricultural Residue and Herbaceous Biomass and Its Effect on Slagging and Fouling Behavior. *ACS Sustainable Chemistry & Engineering*.
- Lei, Y.Su, H. and Tian, R. 2016. Morphology evolution, formation mechanism and adsorption properties of hydrochars prepared by hydrothermal carbonization of corn stalk. *RSC Advances*. **6**(109), pp.107829-107835.
- Levine, R.B.Sierra, C.O.S.Hockstad, R.Obeid, W.Hatcher, P.G. and Savage, P.E. 2013. The use of hydrothermal carbonization to recycle nutrients in algal biofuel production. *Environmental Progress & Sustainable Energy*. **32**(4), pp.962-975.
- Li, Q.Liu, J.Fu, J.Zhou, X. and Liao, C. 2018. Comparative study on the pumping losses between continuous variable valve lift (CVVL) engine and variable valve timing (VVT) engine. *Applied Thermal Engineering*. **137**, pp.710-720.
- Liaw, S.B. and Wu, H. 2013. Leaching Characteristics of Organic and Inorganic Matter from Biomass by Water: Differences between Batch and Semi-continuous Operations. *Industrial & Engineering Chemistry Research*. **52**(11), pp.4280-4289.
- Libra, J.A.Ro, K.S.Kammann, C.Funke, A.Berge, N.D.Neubauer, Y.Titirici, M.-M.Fühner, C.Bens, O.Kern, J. and Emmerich, K.-H. 2011. Hydrothermal carbonization of biomass residuals: a comparative review of the chemistry, processes and applications of wet and dry pyrolysis. *Biofuels*. **2**(1), pp.71-106.
- Lif, A. and Holmberg, K. 2006. Water-in-diesel emulsions and related systems. *Advances in Colloid and Interface Science*. **123**, pp.231-239.
- McAllister, S.Chen, J.Y. and Fernandez-Pello, A.C. 2011. *Fundamentals of Combustion Processes*. Springer New York.
- McHale, E.T.Scheffee, R.S. and Rossmeissl, N.P. 1982. Combustion of coalwater slurry. *Combustion and Flame*. **45**(0), pp.121-135.
- Mishra, S.K.Senapati, P.K. and Panda, D. 2002. Rheological Behavior of Coal-Water Slurry. *Energy Sources*. **24**(2), pp.159-167.
- Miyamoto, N.Hou, Z.Harada, A.Ogawa, H. and Murayama, T. 1987. Characteristics of Diesel Soot Suppression with Soluble Fuel Additives. In. SAE International.
- Mock, C.Lee, H.Choi, S. and Manovic, V. 2016. Combustion Behavior of Relatively Large Pulverized Biomass Particles at Rapid Heating Rates. *Energy & Fuels*. **30**(12).

- Mohan, D.Pittman, C.U. and Steele, P.H. 2006. Pyrolysis of Wood/Biomass for Bio-oil: A Critical Review. *Energy & Fuels*. **20**(3), pp.848-889.
- Morales, S.Miranda, R.Bustos, D.Cazares, T. and Tran, H. 2014. Solar biomass pyrolysis for the production of bio-fuels and chemical commodities. *Journal of Analytical and Applied Pyrolysis*. **109**, pp.65-78.
- Mori, S.Hara, T.Aso, K. and Okamoto, H. 1984. Zeta potential of coal fine-particles in aqueous suspension. *Powder Technology*. **40**(1-3), pp.161-165.
- Mu, W.Ben, H.Ragauskas, A. and Deng, Y. 2013. Lignin Pyrolysis Components and Upgrading—Technology Review. *BioEnergy Research*. **6**(4), pp.1183-1204.
- Mukherjee, A.Rozelle, P. and Pisupati, S.V. 2015. Effect of hydrophobicity on viscosity of carbonaceous solid–water slurry. *Fuel Processing Technology*. **137**, pp.124-130.
- N'Kpomin, A.Boni, A.Antonini, G. and François, O. 1995. The deashed charcoal—oil—water mixture: a liquid fuel for biomass energetical valorization. *The Chemical Engineering Journal and the Biochemical Engineering Journal*. **60**(1), pp.49-54.
- Negin, C.Ali, S. and Xie, Q. 2017. Most common surfactants employed in chemical enhanced oil recovery. *Petroleum*. **3**(2), pp.197-211.
- Nickel, E.H. and Nichols, M.C. 1991. *Mineral Reference manual*. New York, US: Van Nostrand Reinhold.
- Nicol, K. 2014. *The direct injection carbon engine*. London, UK: IEA Clean Coal Centre.
- Nizamuddin, S.Baloch, H.A.Griffin, G.J.Mubarak, N.M.Bhutto, A.W.Abro, R.Mazari, S.A. and Ali, B.S. 2017. An overview of effect of process parameters on hydrothermal carbonization of biomass. *Renewable and Sustainable Energy Reviews*. **73**(Supplement C), pp.1289-1299.
- Ozyuguran, A.Akturk, A. and Yaman, S. 2018. Optimal use of condensed parameters of ultimate analysis to predict the calorific value of biomass. *Fuel*. **214**, pp.640-646.
- Papachristodoulou, G. and Trass, O. 1984. Rheological Properties of Coal-Oil Mixture Fuels. *Powder Technology*. **40**, pp.353-362.
- Park, W.Park, S.Reitz, R.D. and Kurtz, E. 2017. The effect of oxygenated fuel properties on diesel spray combustion and soot formation. *Combustion and Flame*. **180**, pp.276-283.
- Patton, R.Steele, P. and Yu, F. 2009. Coal vs. Charcoal-fueled Diesel Engines: A Review. *Energy Sources, Part A: Recovery, Utilization, and Environmental Effects*. **32**(4), pp.315-322.
- Patwardhan, P.R.Brown, R.C. and Shanks, B.H. 2011. Product Distribution from the Fast Pyrolysis of Hemicellulose. *ChemSusChem*. **4**(5), pp.636-643.
- Pawlikowski, R. 1924. *Process and apparatus for driving internal combustion engines with solid pulverised fuel*.
- Pehan, S.Jerman, M.S.Kegl, M. and Kegl, B. 2009. Biodiesel influence on tribology characteristics of a diesel engine. *Fuel*. **88**(6), pp.970-979.
- Pérez, L.Pinazo, A.Pons, R. and Infante, M. 2014. Gemini surfactants from natural amino acids. *Advances in Colloid and Interface Science*. **205**, pp.134-155.
- Piriou, B.Vaitilingom, G.Veyssière, B.Cuq, B. and Rouau, X. 2013. Potential direct use of solid biomass in internal combustion engines. *Progress in Energy and Combustion Science*. **39**(1), pp.169-188.
- Pushkin, A.N.Gulish, O.K.Koshcheeva, D.A. and Shebanov, M.S. 2013. Catalytic activity of Cu-containing oxide systems with K₂CO₃ additives in the oxidation of diesel soot by oxygen. *Russian Journal of Physical Chemistry A*. **87**(1), pp.23-27.
- Railsback, B. 2012. *An Earth Scientist's Periodic Table of the Elements and Their Ions*.
- Räisänen, U.Pitkänen, I.Halttunen, H. and Hurta, M. 2003. Formation of the main degradation compounds from arabinose, xylose, mannose and arabinitol during pyrolysis. *Journal of Thermal Analysis and Calorimetry*. **72**(2), pp.481-488.
- Ren, Q.Zhao, C.Chen, X.Duan, L.Li, Y. and Ma, C. 2011. NO_x and N₂O precursors (NH₃ and HCN) from biomass pyrolysis: Co-pyrolysis of amino acids and cellulose, hemicellulose and lignin. *Proceedings of the Combustion Institute*. **33**(2), pp.1715-1722.

- Reza, M.T.Uddin, M.H.Lynam, J.G.Hoekman, S.K. and Coronella, C.J. 2014. Hydrothermal carbonization of loblolly pine: reaction chemistry and water balance. *Biomass Conversion and Biorefinery*. **4**(4), pp.311-321.
- Rodríguez-Cruz, M.S.Sánchez-Martin, M.J. and Sanchez-Camazano, M. 2005. A comparative study of adsorption of an anionic and a non-ionic surfactant by soils based on physicochemical and mineralogical properties of soils. *Chemosphere*. **61**(1), pp.56-64.
- Ross, A. 2016. Five west African countries ban 'dirty diesel' from Europe. *The Guardian*.
- Ryan, I.T.W. 1994. Coal-Fueled Diesel Development: A Technical Review. *Journal of Engineering for Gas Turbines and Power*. **116**(4), pp.740-748.
- Ryan, T.W.Callahan, T.J.Dodge, L.G. and Moses, C.A. 1982. Injection, Atomization and Combustion of Carbon Slurry Fuels. In. SAE International.
- Ryan, T.W.Likos, W.E. and Moses, C.A. 1980. The Use of Hybrid Fuel in a Single-Cylinder Diesel Engine. In. SAE International.
- Sajith, V.Sobhan, C.B. and Peterson, G.P. 2010. Experimental Investigations on the Effects of Cerium Oxide Nanoparticle Fuel Additives on Biodiesel. *Advances in Mechanical Engineering*.
Biot number. 2014. s.v.
- Schläpfer, H.W.Barbezat, G. and Borel, M.O. 1990. Reducing Wear in a coal slurry fired large-bore diesel engine by material modelling. *Materialwissenschaft und Werkstofftechnik*. **21**(6), pp.221-229.
- Schnatz, R. 2004. Optimization of continuous ball mills used for finish-grinding of cement by varying the L/D ratio, ball charge filling ratio, ball size and residence time. *International Journal of Mineral Processing*. **74**(Supplement), pp.S55-S63.
- Schwalb, J.A.Ryan, T.W.Kakwani, R.M. and Winsor, R.E. 1994. Coal-Water-Slurry Autoignition in a High-Speed Detroit Diesel Engine. In. SAE International.
- Semenov, A.N. and Shvets, A.A. 2015. Theory of colloid depletion stabilization by unattached and adsorbed polymers. *Soft Matter*. **11**(45), pp.8863-8878.
- Sengupta, A.N. 2002. An assessment of grindability index of coal. *Fuel Processing Technology*. **76**(1), pp.1-10.
- Shackelford, J. and Alexander, W. 2001. Mechanical Properties of Materials. In: Shackelford, J. and Alexander, W. eds. *CRC Materials Science and Engineering Handbook*. Third ed. Boca Raton, US: CRC.
- Shivaram, P.Leong, Y.K.Yang, H. and Zhang, D.K. 2013. Flow and yield stress behaviour of ultrafine Mallee biochar slurry fuels: The effect of particle size distribution and additives. *Fuel*. **104**(Supplement C), pp.326-332.
- Smart, J.P. and Riley, G.S. 2011. On the effects of firing semi-anthracite and bituminous coal under oxy-fuel firing conditions. *Fuel*. **90**(8), pp.2812-2816.
- Smebye, A.B.Sparrevik, M.Schmidt, H.P. and Cornelissen, G. 2017. Life-cycle assessment of biochar production systems in tropical rural areas: Comparing flame curtain kilns to other production methods. *Biomass and Bioenergy*. **101**(Supplement C), pp.35-43.
- Soehngen, E.E.Research, U.S.E.Administration, D.Soehngren, E. and Associates. 1976. *The development of coal-burning diesel engines in Germany: a state-of-the-art review*. Energy Research and Development Administration.
- Soloiu, V.Lewis, J.Yoshihara, Y. and Nishiwaki, K. 2011. Combustion characteristics of a charcoal slurry in a direct injection diesel engine and the impact on the injection system performance. *Energy*. **36**(7), pp.4353-4371.
- Somerville, M. and Jahanshahi, S. 2015. The effect of temperature and compression during pyrolysis on the density of charcoal made from Australian eucalypt wood. *Renewable Energy*. **80**, pp.471-478.
- Song, E.Schneider, J.G.Anderson, S.H.Goyne, K.W. and Xiong, X. 2014. Wetting Agent Influence on Water Infiltration into Hydrophobic Sand: II. Physical Properties. *Agronomy Journal*. **106**(5), pp.1879-1885.

- Soukht Saraee, H.Jafarmadar, S.Taghavifar, H. and Ashrafi, S.J. 2015. Reduction of emissions and fuel consumption in a compression ignition engine using nanoparticles. *International Journal of Environmental Science and Technology*. **12**(7), pp.2245-2252.
- Sparrevik, M.Adam, C.Martinsen, V.Jubaedah and Cornelissen, G. 2015. Emissions of gases and particles from charcoal/biochar production in rural areas using medium-sized traditional and improved "retort" kilns. *Biomass and Bioenergy*. **72**(Supplement C), pp.65-73.
- Stone, R. 1992. Compression Ignition Engines. *Introduction to Internal Combustion Engines*. London, UK: Palgrave.
- Strugała, A. 2000. Empirical relationships for the determination of true density of coal chars. *Fuel*. **79**(7), pp.743-753.
- Tadros, T.F. 2014. *Introduction to Surfactants*. De Gruyter. Available from: <http://app.knovel.com/hotlink/toc/id:kpIS000035/introduction-surfactants/introduction-surfactants>.
- Takaya, C.A.Fletcher, L.A.Singh, S.Anyikude, K.U. and Ross, A.B. 2016. Phosphate and ammonium sorption capacity of biochar and hydrochar from different wastes. *Chemosphere*. **145**, pp.518-527.
- Takeda, M.Onishi, T.Nakakubo, S. and Fujimoto, S. 2009. Physical Properties of Iron-Oxide Scales on Si-Containing Steels at High Temperature. *Materials Transactions*. **50**(9), pp.2242-2246.
- Tangsathikulchai, C. 2002. Acceleration of particle breakage rates in wet batch ball milling. *Powder Technology*. **124**(1), pp.67-75.
- Taulbee, D.Poe, S.H.Robl, T. and Keogh, B. 1989. Density gradient centrifugation separation and characterization of maceral groups from a mixed maceral bituminous coal. *Energy & Fuels*. **3**(6), pp.662-670.
- Trazzi, P.A.Leahy, J.J.Hayes, M.H.B. and Kwapinski, W. 2016. Adsorption and desorption of phosphate on biochars. *Journal of Environmental Chemical Engineering*. **4**(1), pp.37-46.
- Ugwu, K.E.Ofomatah, A.C. and Exe, S.I. 2013. Influence of solid concentration on the flow characteristics and settling rate of coal-water slurries. *Journal of Energy and Natural Resources*. **2**(3), pp.21-24.
- Vahrman, M. 1987. Charcoal made in the pit-tumulus type of earth-kiln. *International Journal of Energy Research*. **11**(1), pp.133-143.
- Venu, H. and Madhavan, V. 2016. Effect of nano additives (titanium and zirconium oxides) and diethyl ether on biodiesel-ethanol fuelled CI engine. *Journal of Mechanical Science and Technology*. **30**(5), pp.2361-2368.
- Vorobiev, N.Geier, M.Schiemann, M. and Scherer, V. 2016. Experimentation for char combustion kinetics measurements: Bias from char preparation. *Fuel Processing Technology*. **151**, pp.155-165.
- Vuthaluru, H.B.Brooke, R.J.Zhang, D.K. and Yan, H.M. 2003. Effects of moisture and coal blending on Hardgrove Grindability Index of Western Australian coal. *Fuel Processing Technology*. **81**(1), pp.67-76.
- Wang, R.Liu, J.Yu, Y.Zhou, J. and Cen, K. 2013a. Effects of calcium oxide on the surface properties of municipal wastewater sludge and its co-slurrying ability with coal. *Science of The Total Environment*. **456-457**(0), pp.9-16.
- Wang, S.Dai, G.Yang, H. and Luo, Z. 2017. Lignocellulosic biomass pyrolysis mechanism: A state-of-the-art review. *Progress in Energy and Combustion Science*. **62**, pp.33-86.
- Wang, S.Ru, B.Lin, H. and Luo, Z. 2013b. Degradation mechanism of monosaccharides and xylan under pyrolytic conditions with theoretic modeling on the energy profiles. *Bioresource Technology*. **143**(Supplement C), pp.378-383.
- Wang, S.Ru, B.Lin, H. and Sun, W. 2015. Pyrolysis behaviors of four O-acetyl-preserved hemicelluloses isolated from hardwoods and softwoods. *Fuel*. **150**(Supplement C), pp.243-251.

- Wang, S.Wang, K.Liu, Q.Gu, Y.Luo, Z.Cen, K. and Fransson, T. 2009. Comparison of the pyrolysis behavior of lignins from different tree species. *Biotechnology Advances*. **27**(5), pp.562-567.
- Wang, S.Zhou, Y.Liang, T. and Guo, X. 2013c. Catalytic pyrolysis of mannose as a model compound of hemicellulose over zeolites. *Biomass and Bioenergy*. **57**(Supplement C), pp.106-112.
- Wanignon Ferdinand, F.Van de Steene, L.Kamenan Blaise, K. and Siaka, T. 2012. Prediction of pyrolysis oils higher heating value with gas chromatography–mass spectrometry. *Fuel*. **96**, pp.141-145.
- Watanabe, H. 1999. Critical rotation speed for ball-milling. *Powder Technology*. **104**(1), pp.95-99.
- Wibberley, L. 2014. *DICE- THE BEST OPTION FOR COAL?* Melbourne, Australia.
- Wibberley, L. 2015. *Micronised Refined Carbons and the Direct Injection Carbon Engine*. [Presentation]. [Accessed 18.08.17]. Available from: <http://www.jamesoncell.com/EN/Downloads/technical%20papers/Sedgman%20lecture%2010%20June%202015.pdf>.
- Wibberley, L. and Osborne, D. 2015. Premium coal fuels with advanced coal beneficiation. [Online]. Available from: [http://www.jamesoncell.com/EN/Downloads/technical%20papers/Premium%20fuels%20Clearwater%20\(final%20paper\).pdf](http://www.jamesoncell.com/EN/Downloads/technical%20papers/Premium%20fuels%20Clearwater%20(final%20paper).pdf).
- Williams, R.A. 1992. Characterization of process dispersions. In: Williams, R.A. ed. *Colloid and Surface Engineering: Applications in the Process Industries*. Oxford: Butterworth-Heinemann.
- Wilson, R. 2007. *Clean coal diesel demonstration project: Final report*. Cambridge, USA: TIAX.
- Wu, H.Yip, K.Kong, Z.Li, C.-Z.Liu, D.Yu, Y. and Gao, X. 2011. Removal and Recycling of Inherent Inorganic Nutrient Species in Mallee Biomass and Derived Biochars by Water Leaching. *Industrial & Engineering Chemistry Research*. **50**(21), pp.12143-12151.
- Wu, Z.Liang, Y.Fu, E.Du, J.Wang, P.Fan, Y. and Zhao, Y. 2018. Effect of Ball Milling Parameters on the Refinement of Tungsten Powder. *Metals*. **8**(4), p281.
- Wynter, C.I.May, L.Oliver, F.W.Hall, J.A.Hoffman, E.J.Kumar, A. and Christopher, L. 2004. Correlation of Coal Calorific Value and Sulphur Content with 57Fe Mössbauer Spectral Absorption. *Hyperfine Interactions*. **153**(1), pp.147-152.
- Yan, B.Cheng, Y.Jin, Y. and Guo, C.Y. 2012. Analysis of particle heating and devolatilization during rapid coal pyrolysis in a thermal plasma reactor. *Fuel Processing Technology*. **100**(Supplement C), pp.1-10.
- Yan, W.Hoekman, S.K.Broch, A. and Coronella, C.J. 2014. Effect of hydrothermal carbonization reaction parameters on the properties of hydrochar and pellets. *Environmental Progress & Sustainable Energy*. **33**(3), pp.676-680.
- Yang, H.Yan, R.Chen, H.Lee, D.H. and Zheng, C. 2007. Characteristics of hemicellulose, cellulose and lignin pyrolysis. *Fuel*. **86**(12), pp.1781-1788.
- Yang, W.M.An, H.Chou, S.K.Vedharaji, S.Vallinagam, R.Balaji, M.Mohammad, F.E.A. and Chua, K.J.E. 2013. Emulsion fuel with novel nano-organic additives for diesel engine application. *Fuel*. **104**(0), pp.726-731.
- Yu, K.L.Lau, B.F.Show, P.L.Ong, H.C.Ling, T.C.Chen, W.-H.Ng, E.P. and Chang, J.-S. 2017. Recent developments on algal biochar production and characterization. *Bioresource Technology*. **246**, pp.2-11.
- Yu, Y.Lou, X. and Wu, H. 2008. Some Recent Advances in Hydrolysis of Biomass in Hot-Compressed Water and Its Comparisons with Other Hydrolysis Methods. *Energy & Fuels*. **22**(1), pp.46-60.
- Yuchi, W.Li, B.Li, W. and Chen, H. 2005. Effects of Coal Characteristics on the Properties of Coal Water Slurry. *International Journal of Coal Preparation and Utilization*. **25**(4), pp.239-249.

- Zhang, X., Yang, W. and Dong, C. 2013. Levoglucosan formation mechanisms during cellulose pyrolysis. *Journal of Analytical and Applied Pyrolysis*. **104**, pp.19-27.
- Zhao, J., Wang, D., Yan, P. and Li, W. 2016. Comparison of Grinding Characteristics of Converter Steel Slag with and without Pretreatment and Grinding Aids. *Applied Sciences*. **6**(11), p237.
- Zhao, K., Li, Y., Zhou, Y., Guo, W., Jiang, H. and Xu, Q. 2018. Characterization of hydrothermal carbonization products (hydrochars and spent liquor) and their biomethane production performance. *Bioresource Technology*. **267**, pp.9-16.
- Zheng, M., Reader, G.T. and Hawley, J.G. 2004. Diesel engine exhaust gas recirculation—a review on advanced and novel concepts. *Energy Conversion and Management*. **45**(6), pp.883-900.
- Zhu, X., Liu, Y., Qian, F., Lei, Z., Zhang, Z., Zhang, S., Chen, J. and Ren, Z.J. 2017. Demethanation Trend of Hydrochar Induced by Organic Solvent Washing and Its Influence on Hydrochar Activation. *Environmental Science & Technology*. **51**(18), pp.10756-10764.

Chapter 3: Materials and methods

3.1 Introduction

The scope of the project covers the entire slurry fuel process, from choosing the right biomass materials to processing, and finally using the fuel in a diesel engine. The chapter is split into sections based on the stage in the lifecycle of the fuel. The method section follows the order of research, as well as the order of the fuel-making process. The first part states how biomass materials were chosen, collected and processed before conversion to char. The next section covers the thermal conversion methods and determination of the chemical properties of the materials. The methods include analysis of the carbon structure and trace element content. The third part details how the milling and stability tests were performed on the slurry fuels. The final section covers the engine testing beginning with the designing of the test rig itself, objective 5 of the thesis. It covers the selection of engine generator which was used for the tests, engine performance measurement and development of a computer program to log the data. The choice of emissions monitoring equipment is also covered. Images of the equipment used can be found in Appendix 1.

During all experiments, the likelihood of unrepresentative results was minimised by performing each test in duplicate. In the results, the error margin is given when appropriate.

3.2 Selection criteria for slurry fuel feedstocks

3.2.1 Scoping potential feedstocks from a range of materials

A number of feedstocks were selected as potentially being suitable for conversion to a slurry fuel. A range of materials was chosen covering both terrestrial and aquatic biomass. Six were initially chosen: *Rhododendron ponticum* (rhododendron), *Miscanthus spp.* (miscanthus), *Quercus spp.* (oak), *Chlorella vulgaris* (chlorella), *Laminaria digitata* (laminaria) and *Ascophylum nodosum* (ascophylum). Rhododendron is a species of woody biomass which is considered invasive to the UK and other countries in Europe (Stout, 2007). The sample collected was whole branches, roughly 5cm in diameter. Miscanthus is a grassy biomass commonly used as an energy crop (Arnoult and Brancourt-Hulmel, 2015). The part sampled was the stem of the plant which had been air dried to straw. Oak is a group of hardwood trees with species native to several countries throughout the world. Cubes of roughly 5cm of oak were used for the tests.

The first of the aquatic biomass, chlorella, is microalgae and the type used was grown autotrophically, producing energy by photosynthesis, and was freeze-dried for storage. It is a fast-growing organism, high in lipids compared to terrestrial biomass. Laminaria and ascomycota are types of macroalgae harvested from the sea around the UK. The macroalgae samples that were tested were cut and freeze-dried.

3.2.2 Sampling of an important agricultural residue in developing countries

Residue from the traditional extraction of shea butter from *Vitellaria paradoxa* (shea nut) was also included because it is a waste produced in developing countries in west and central Africa with a high calorific value (Adazabra et al., 2016; Elias, 2013). To extract the shea butter, the shea fruits are de-pulped, the nuts dried, deshelled and crushed to a coarse powder (Adazabra et al., 2016). The powder is then mixed with hot water and thoroughly mixed. The crude butter rises to the surface and is removed. The remainder is the waste which was used for thermal conversion. In Africa, there is approximately 1,000,000 metric tons of this waste generated annually (Adazabra et al., 2017).

3.2.3 Assessment of potential feedstocks in Nepal, a developing country

Potential feedstocks were also selected from Nepal, a developing country which could be suitable for electricity generation from slurry fuels. Currently, the nation is plagued by power shortages and electricity produced by petroleum products is unsustainable as they are heavily subsidised (Gautam et al., 2015; Sharma, 2015). Despite having a high potential for other renewable technologies, particularly hydropower, progress has been slow to exploit these (Nepal, 2012).

In total, 27 common types of biomass were chosen for analysis, 12 tree species, 4 shrubs, 4 herbaceous plants and 7 agricultural residues. The tree species were: *Alnus nepalensis* (Nepalese alder), *Castanopsis indica* (chinkapin), *Choerospondias axillaris* (Nepali hog plum), *Ficus semicordata* (drooping fig), *Lagerstroemia parviflora* (crepe myrtle), *Melia azedarach* (chinaberry), *Myrica esculenta* (box myrtle) *Pinus roxburghii* (pine), *Shorea robusta* (sal), *Quercus semecarpifolia* (oak), *Rhododendron arboreum* (rhododendron) and *Schima wallichii* (schima). The shrubs were: *Gaultheria fragrantissima* (fragrant wintergreen), the invasive *Lantana camara* (wild sage), *Lyonia ovalifolia* (angeri), *Woodfordia fruticosa* (fire flame bush) and *Zanthoxylum armatum* (winged prickly ash). The herbaceous plants were: *Artemisia indica* (oriental mugwort) the invasive *Eupatorium adenphorum* (crofton weed), and *Thysanolaena maxima* (Nepalese broom grass). The agricultural residues were: *Brassica campestris* (rapeseed

mustard), *Eleusine coracana* (finger millet straw), *Oryza sativa* (rice husk), *Saccharum officinarum* (sugarcane bagasse) and *Zea mays* (maize cob, stover and shell).

Samples from each of the forestry plants were obtained from the primary branch of mature specimens. The circumference of the primary branch of specimens sampled was less than 25cm. The reason for this is that branches with larger circumferences are often used instead for timber.

3.3 Preparation of char and samples

Table 3-1 summarises the chars made from each set of materials outlined in the previous section. The samples in 3.2.1 were treated across the whole range of temperatures. The results of the analysis of these chars determined which thermal conversion processes were best for the other sets of samples. Shea residue, described in 3.2.2 was converted using both types of thermal process (pyrolysis and HTC), but at one temperature each, because it had been determined that chars produced under these conditions were to be used for slurry engine testing. The samples collected from Nepal in section 3.2.3 were converted using two pyrolysis temperatures. Currently, HTC is not used in developing countries and is therefore considered a future conversion technology to produce char slurries. The two temperatures were chosen as they are representative of typical kiln conditions used for producing charcoal in developing countries.

Table 3-1 Temperatures and thermal conversion method used for each set of samples.

	Pyrolysis				HTC	
	200°C	400°C	600°C	800°C	200°C	250°C
<i>Samples 3.2.1</i>	✓	✓	✓	✓	✓	✓
<i>Sample 3.2.2 (shea)</i>		✓				✓
<i>Samples 3.2.3</i>		✓	✓			

3.3.1 Preparation of samples for analysis and processing

The biomass feedstocks were prepared and homogenised prior to thermal treatment apart from Shea nut residue and freeze-dried *Chlorella vulgaris* as they were already in the form of a coarse powder. Woody biomass was prepared using an SM300 cutting mill (Retsch, Germany). Blocks and branches of the feedstocks were fed into the machine and cut to pass a 10mm square sieve. Grassy biomasses such as *Miscanthus* were prepared using a grinder to reduce the particle size. Samples were further milled in a grinder or cryomill (Retsch, Germany) to a powder below 105µm for analysis.

3.3.2 Pyrolysis

Pyrolysis was performed in the reactor shown in schematic form in figure 3-1 and as an image in figure 3-2. There were two configurations used: the first used an insert into the mesh basket onto which up to 18, 25ml nickel crucibles could be placed allowing for several materials to be pyrolysed at once. Approximately 3g of sample was added to the nickel crucibles when used. This was the format used for producing charcoal from the samples collected from Nepal, detailed in 3.2.3.

The second configuration was without the insert so that a large volume of a single material could be processed at once. Between 100 and 300 g was added each time depending on the density. This configuration was used for samples in 3.2.1 and 3.2.2.

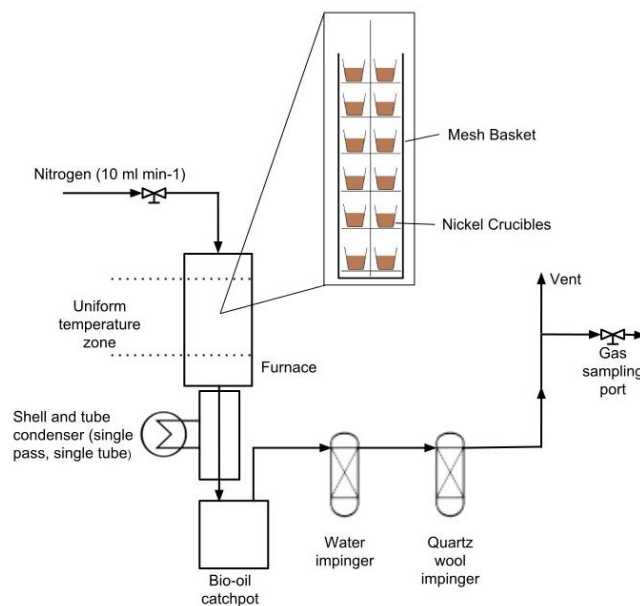


Figure 3-1 Schematic of the pyrolysis reactor used. Showing insert, containing nickel crucibles, used for some tests (top middle).

The pyrolysis reactor consisted of a sealed tube furnace above a condenser set to 4°C, which cooled the hot gases from the furnace to remove the tars which are then collected in a catchpot below. The furnace bore was 95mm x 820mm and had a mesh basket hung at the centre for the samples 82mm I.D. and 355mm deep. Nitrogen was fed through the top of the furnace at a rate of 130ml/min to remove volatile compounds and create an inert atmosphere. The exhaust gases passed through two impingers- the first containing water and the second quartz wool to remove any further liquid or solid residue in the exhaust stream. The heating rate of the furnace was set to between 4.5 and 7.2 °C/min. The reactor is held at the pyrolysis temperature for 1 hour under a constant flow of nitrogen. After this period the heater is switched off and is cooled at a rate of 0.4-1.4°C/min. A number of pyrolysis temperatures were used. The amount of sample which was used was weighed, as was the weight of the charcoal product and was used to calculate the mass yield. Each char was produced at least twice to

confirm the mass yield and is reported as an average. The pyrolysis oils from the catchpot were weighed and stored in glass bottles. The chars once weighed were kept in airtight containers.

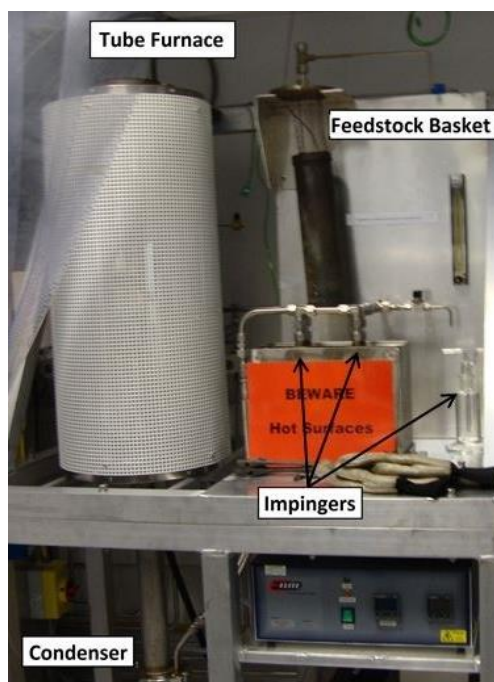


Figure 3-2 Pyrolysis reactor used for producing pyrochar.

3.3.3 Hydrothermal carbonisation (HTC)

HTC was performed at 200 and 250°C using two different reactors, a 600ml and a 2000ml pressure vessel (Parr Instrument Company, USA) (figure 3-3). The smaller reactor was used to create chars for characterisation and the larger was used to produce large amounts of material for producing slurries at 1%wt. and above. When using the 600ml reactor, which is shown in figure 3-4, 24g of sample and 220ml of deionised (D.I.) water (i.e. 10%wt. solids) was added to the cylinder of the reactor. It was then sealed by a split ring held by 6 bolts and placed in a heating mantle. The temperature was controlled by a thermocouple against the inside wall of the cylinder.

The process was similar for the 2000ml reactor except 96g of sample and 880ml of D.I. water was placed inside a glass liner which was then inserted into the cylinder of the reactor. It also contained a pressure transducer which could be used to better determine the average temperature in the reactor than the thermocouple.

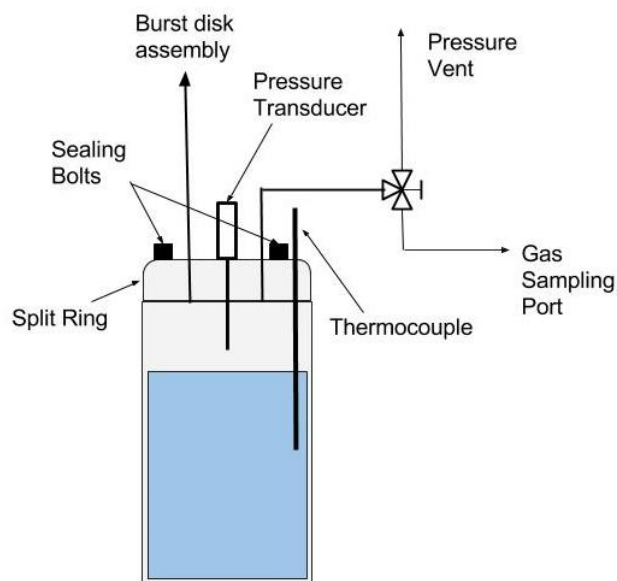


Figure 3-3 Schematic of the HTC reactors used.

The heating rate for the 600ml and 2000ml reactors was approximately $10^{\circ}\text{C}/\text{min}$ and $5^{\circ}\text{C}/\text{min}$ respectively. The cooling rate for the 600ml and 2000ml reactors was approximately $10^{\circ}\text{C}/\text{min}$ and $1^{\circ}\text{C}/\text{min}$ respectively. Once cooled, the reactor was weighed to determine the gaseous loss, and the solid product was separated from the aqueous phase using a filter paper and Buchner funnel. The aqueous phase was disposed of and the hydrochar was further dried in a drying oven for a further 24 hours. Each test was performed twice and the yield values are averaged.

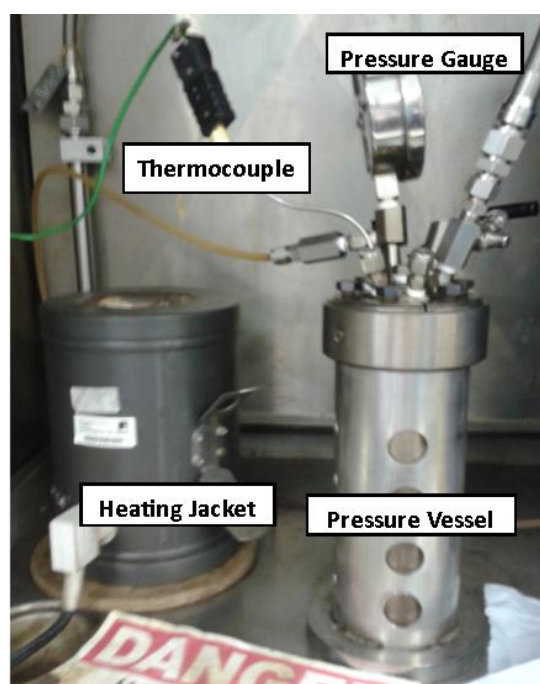


Figure 3-4 600ml hydrothermal reactor.

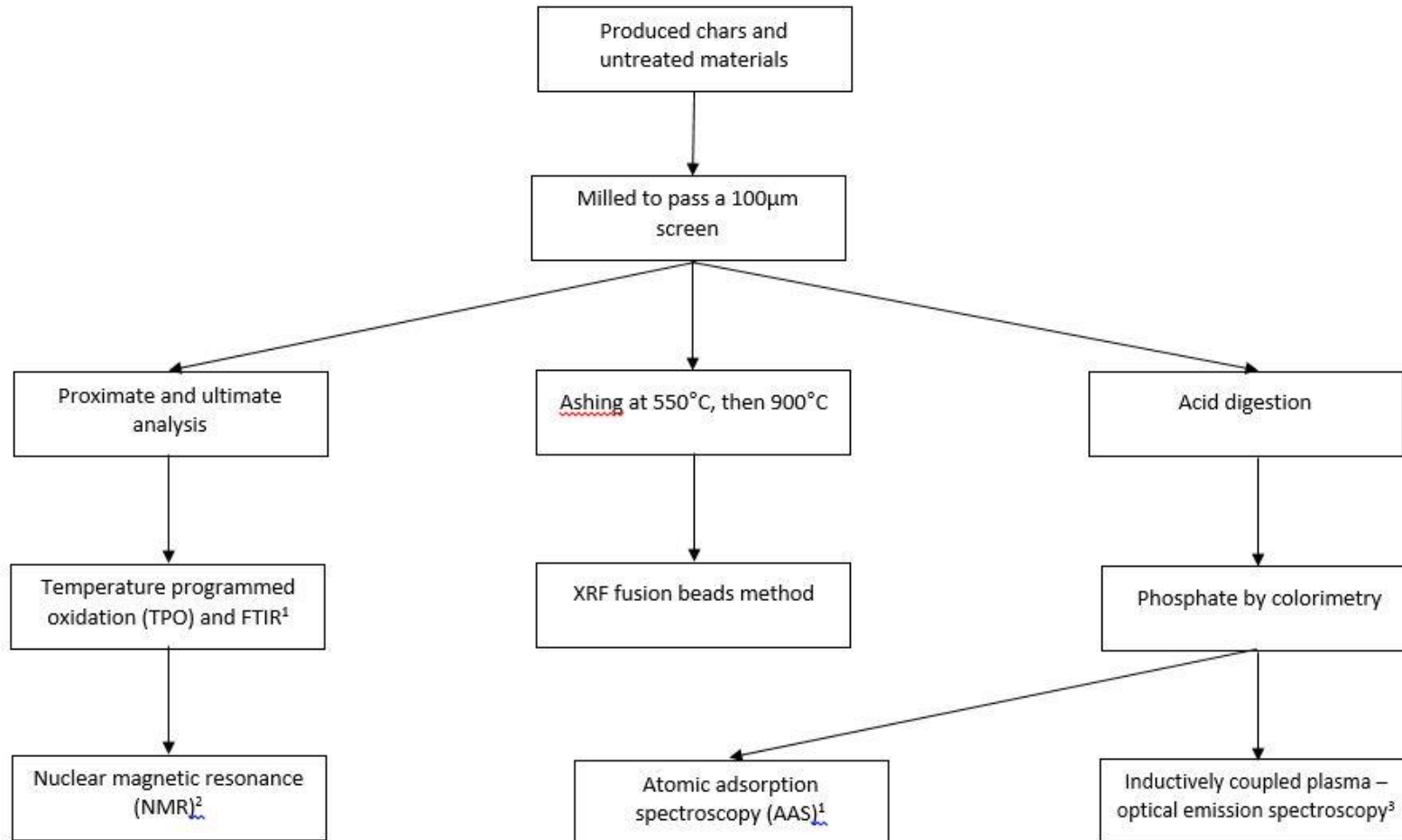


Figure 3-5 Flow diagram of analysis performed on char and feedstock samples. ¹Performed on samples from section 3.2.1 and 3.2.2. ² Performed on samples for chlorella and rhododendron. ³ Used for samples in 3.2.3.

3.4 Char and feedstock analysis

Figure 3-5 shows a flow diagram of the analysis process used for the chars and untreated initial materials. Prior to analysis, all samples were milled to pass a 100µm sieve to improve homogenisation. Some materials were not analysed by all methods. Superscripts denote which methods were used with each set of materials.

3.4.1 Proximate analysis

The proximate values for the feedstocks and chars were determined using a TGA/DSC 1 (Mettler-Toledo, USA) Thermo-Gravimetric Analyser (TGA). Approximately 10mg of sample was first heated to 105°C in an inert atmosphere. The associated weight loss represented the percent moisture content. The sample was then heated to 900°C to determine the volatile content. The atmosphere was then changed to air to burn the fixed carbon and determine the fixed carbon and ash. Figure 3-6 shows a typical curve produced on a TGA programmed to measure proximate values. Each section of the curve represents a different proximate value, leveling out by maintaining the temperature in the program to separate the types of compound in the sample.

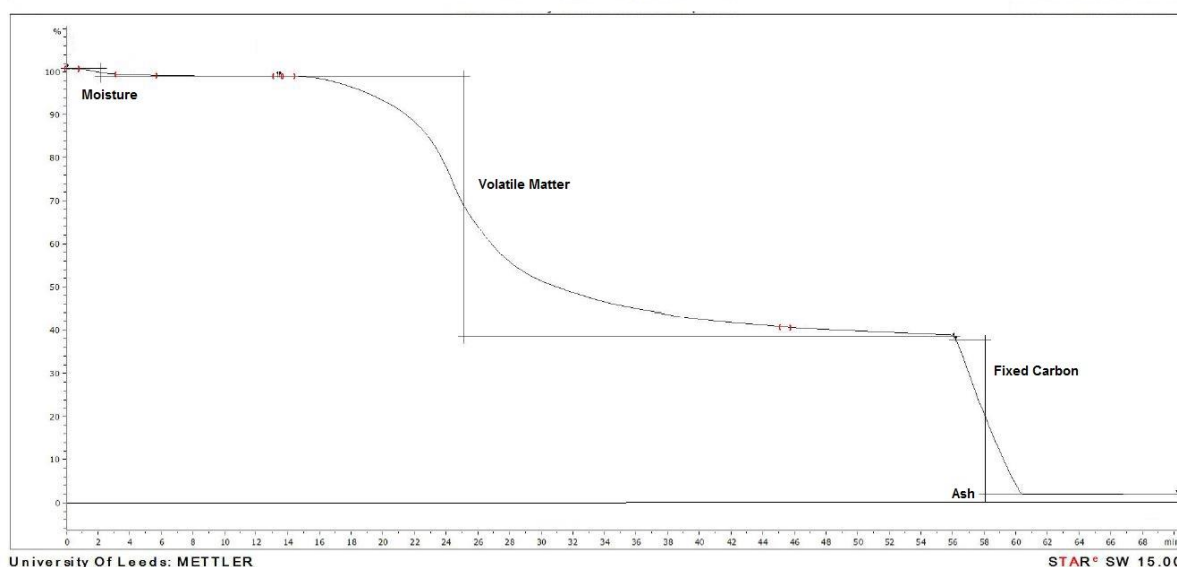


Figure 3-6 An example of a proximate analysis curve produced using a TGA. Marked is what each section of the curve represents in the analysis.

3.4.2 Ultimate analysis

The ultimate analysis was determined using an EA112 Flash Analyser (Thermo-Scientific, USA). Oxygen was determined in two ways. First, by the difference of the sum of carbon, hydrogen, nitrogen, sulphur and ash from the total. Second, by measurement using the same instrument. Which method used is stated in the figure or table. The values for carbon, hydrogen, nitrogen, sulphur and oxygen are given on a dry basis. They are corrected to subtract the moisture measured

in the proximate analysis. Upper calorific value is approximated using Dulong's formula (eqn. 1) on a dry basis (Wanignon Ferdinand et al., 2012).

$$CV \text{ (MJ/kg)} = 0.3386 \times C + 1.444 \times (H - \frac{O}{8}) + 0.09428 \times S \quad (1)$$

The energy recovery (E.R.) is determined by:

$$E.R. (\%) = \frac{\text{mass yield} \times \text{charcoal gross calorific value}}{\text{raw sample gross calorific value}} \quad (2)$$

Energy recovery quantifies how much of the original energy from the sample is retained in the charcoal made.

3.4.3 Preparation for inorganic analysis

Two methods were used for acid digestion of samples for analysis. In the first method, approximately 0.2g of sample was microwave digested in a Multiwave 3000 (Anton Parr, USA) using 10ml of 69% nitric acid. The power of the microwave ramps evenly to 700 W over a 15 minute period. The digested sample was then diluted up to 50ml using ultrapure deionised water and then filtered to remove any remaining solid material.

The second method used was an open vessel method. 0.2g of sample was added to a 50ml conical flask with 10ml of 69% nitric acid. A reflux funnel was inserted into the flask and placed on a hot plate at 250°C for 1 hour. The funnel was then removed to evaporate the remaining mixture to dryness. The process of adding nitric acid to the sample was repeated until it was fully digested. The digested sample was fully removed from the conical flask using ultrapure deionised water and a rubber policeman. The solution was poured into a 100ml volumetric flask and diluted to the mark. This method was used for the samples collected from Nepal (3.2.3). The method was not used for the other set of samples including chars because the tougher carbon structures break down poorly.

3.4.4 Atomic adsorption spectroscopy (AAS)

The digested samples from materials in 3.2.1 and 3.2.2 were analysed by AAS. In the first, aluminium, calcium, iron, magnesium, manganese, potassium and sodium were determined by AAS using a 240FS (Varian, USA). Analysis of iron, magnesium, manganese, potassium and sodium was performed under an acetylene/air flame. Aluminium and calcium were analysed in an acetylene/nitrous oxide flame. This was performed on all samples collected and generated excluding those collected from Nepal. The instrument was calibrated by an external standard. Bulk standard solutions were made which were diluted by the instrument to produce a 5 point calibration curve. AAS was used for these materials because it has good accuracy for relatively high concentrations of elements, compared to inductively coupled plasma – optical emission spectroscopy (ICP-OES). Chars contain concentrated amounts of inorganic elements compared to untreated biomass.

3.4.5 Inductively coupled plasma – optical emission spectroscopy (ICP-OES)

ICP-OES was used to determine the trace elements in the biomass samples collected from Nepal. ICP-OES was used for these samples as it is more accurate for analytes containing low concentrations of the measured element. The method was used to determine Ca, K, Na, Mg, Cr, Cu, Fe, Li, Mn, Ni, Sr, Zn, Mo, V, Ba, Sn and S. The instrument used was an iCAP7600 (Thermo-Scientific, USA). The instrument was calibrated using external standard solutions.

3.4.6 Determination of phosphorous by colorimetry

Phosphorus was determined by colorimetry using ammonium molybdovanadate as the chromogen. Absorbance was measured at a wavelength of 430nm (Smith and Ross, 2016). Measurements were made using a Multiskan GO (Thermo-Scientific, USA), which was calibrated using standard solutions made from monopotassium phosphate. The method was used because phosphorus is unresponsive to ICP-OES and AAS at the concentrations present in the samples.

3.4.7 X-ray fluorescence (XRF)

X-ray fluorescence (XRF) was also used to determine elements less soluble after nitric acid digestion such as aluminium and silicon. The method of analysis used was the fused bead technique. The method was chosen because it removes inhomogeneity in powders caused by mineralogical and grain size effects, which can lead to inaccuracy (Watanabe et al., 2013). The char and untreated biomass samples were prepared by calcining the samples at 550°C for two hours and then a further two hours at 900°C. The ash was collected and mixed with a lithium borate flux. The ratio of which was determined by the highest amount of ash that could be added without cracking the fusion disc as it cooled. The mix was added to a platinum crucible and fused at 1050°C using a Katanax K1 Prime. The fused beads were then analysed on a Primus WDXRF 1 (Rigaku, Japan).

3.4.8 Temperature programmed oxidation (TPO)

TPO was performed using a Mettler Toledo TGA/DSC 1. Approximately 10mg of sample was weighed into crucibles which were inserted into the instrument. The samples were heated from room temperature to 800°C at a rate of 10°C/min in an air atmosphere. Figure 3-7 shows a typical TPO curve showing the mass of the sample as a percentage of the original. From the plots obtained, the recalcitrance index was calculated as the point at which half the total mass loss during the experiment occurred. The first derivative of the mass loss with respect to time was also calculated and plotted against temperature.

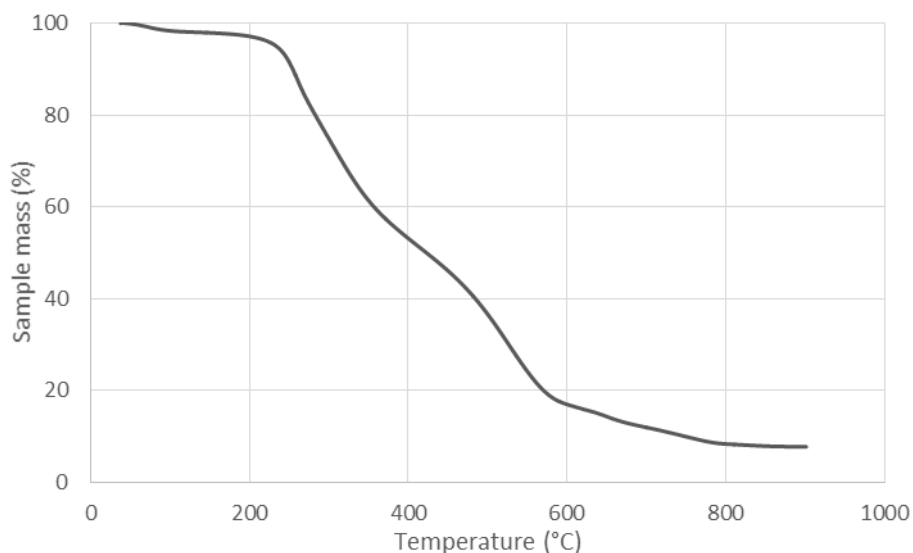


Figure 3-7 Typical TPO curve of biomass material.

3.4.9 Solid state C^{13} nuclear magnetic resonance (NMR)

All C^{13} NMR tests were conducted on a Unity INOVA spectrometer (Varian, USA) at the SCS NMR facility located in the University of Illinois at Urbana-Champaign. It was operated at 75.4 MHz at room temperature. The samples were ground to a fine powder to ensure homogeneity and packed into 4mm O.D. zirconia rotors. Between 30 and 60 mg of powder could be loaded into the rotor each time. The C^{13} NMR spectra for all samples was determined using a 4mm APEX HX Chemagnetics probe under a magic-angle spinning rate of 10 kHz and proton decoupling. The chemical shifts were referenced to a hexamethylbenzene sample ($\delta = 17.3$ ppm for the methyl peak relative to TMS at 0 ppm). Both Direct Polarisation Magic Angle Spinning (DPMAS) and Cross Polarisation Magic Angle Spinning (CPMAS) were conducted on the samples. For DPMAS, the C^{13} 90-degree pulse length was $2.5\mu s$, recycle delay was 30s and 1500 scans were collected. For CPMAS, the H-1 selective 90-degree pulse length determined was $2.25\mu s$. A recycle delay of 1s was used with between 10000-18000 scans acquired for each sample. 1ms and 4ms contact times were used for comparison.

For measuring the degree of aromatic condensation a method was adapted from McBeath and Smernik (2009). Samples were spiked with between 50 and 200 $\mu l/g$ of methanol containing a carbon-13 atom. A higher dose was required for samples which contained carbon with a similar chemical shift to methanol to ensure the right peak was found. The samples were shaken and left for at least 24 hours before analysis. CPMAS was used with 1ms contact time and 4000 scans to determine the location of the sorbed methanol peak. The shift was subtracted from the position of non-sorbed methanol ($\delta = 49.1$ ppm). The raw free induction decay was processed using 40Hz of line broadening and 8192 zero filling before Fourier transform.

3.5 Milling of chars and stability of slurries

3.5.1 Grindability of chars

The chars deemed the most suited for use as a slurry fuel were tested for grindability using a Mixer Mill MM200 (Retsch, Germany). A 10ml stainless steel grinding jar was the container chosen and a 12mm or 10mm stainless steel ball was used as the grinding media. The process was optimised by altering the amount of sample added and shaking frequency of the machine from 10-25Hz and grinding time. The grinding was performed dry, in water or in diesel at sample:dispersant ratios of 2:1, 1:1 and 1:2 by weight. The micronised powders and slurries were analysed using a Mastersizer 2000E (Malvern, UK) laser diffraction particle size analyser. Dry powders were analysed in a wet cell with water as the dispersant. Igepal CA-130 surfactant was added to the water dispersed systems to improve wettability. Samples micronised in diesel were dispersed in the wet cell with diesel.

3.5.2 Processing of chars for slurring

A larger scale process was created and optimised for producing large amounts of slurry for engine tests. The milling process consisted of two stages. In the first stage, approximately 60g of char was milled using a Vibratory Disc Mill RS 200 (Retsch, Germany) in a stainless steel grinding set. The material was milled for 2 ½ minutes at 700rpm. The particle size distribution after the first step was measured using a Malvern Mastersizer 2000E.

In the second stage, a Tencan JM-3L stirred media ball mill was used. The mill consisted of a vertically aligned rotor with paddles driven by an electric motor to stir the media inside a large steel jar. 35g of char was added to the 2L milling container, along with 315g of the liquid media that the slurry was to be composed of. The slurry mixture was therefore 10%wt. solid loading. The material was milled with a charge of 1500 g of 1mm steel balls for 5-30 minutes at 300-750 rpm. The final particle size was measured using a Malvern Mastersizer 2000E. The power consumption for the full process was measured and reported. After milling, the slurry was diluted if necessary to other concentrations and surfactants were added.

3.5.3 Stability analysis and surfactants

Different surfactant mixes and concentrations were tested to gauge their effect on the stability of slurries. A range of surfactants were chosen that were low enough in price to be suitable for this purpose. They also had a wide range of hydrophilic-lipophilic balances (HLB) and there was one of each type i.e. non-ionic, cationic, etc. The surfactants used are shown in table 3-2.

Firstly, different concentrations of a single surfactant were added to slurries and thoroughly mixed. A LUMiSizer (LUM, Germany) was used to assess the stability of the slurries. Rectangular

polyacrylamide cells with a path length of 2mm were filled with the slurry to be tested. The instrument consists of a centrifuge with a light source and detector which measures the transmittance along the height of the cell. Each mix was measured in duplicate.

Table 3-2 Properties of the surfactants used.

<i>Surfactant</i>	<i>HLB</i>	<i>Type</i>	<i>Molecular Weight</i>
<i>Palmitic Acid</i>	2.0	Non-Ionic	256.43
<i>Lecithin (Soybean-derived)</i>	7.0 ± 1.0	Amphoteric	Average 644
<i>Sodium Lignosulfonate</i>	Unknown	Anionic	Average 52000
<i>Sodium Stearate</i>	18.0	Anionic	306.47
<i>Carboxymethyl Cellulose, Sodium Salt</i>	10.5	Anionic	Average 250000
<i>Benzethonium Chloride</i>	14.0 ± 1.0	Cationic	448.08
<i>Span 20</i>	8.6 ± 1.0	Non-Ionic	346.46
<i>Polyethylene Glycol 6000</i>	19.1 ± 0.5	Non-Ionic	Average 6000
<i>Ethanol</i>	7.9	Non-Ionic	46

3.5.4 Measuring char density through pycnometry

The density of chars used for blending with surfactants and diesel tests. The density of chars is inevitably going to affect how quickly the particles settle out. It also affects how much char can be added to diesel fuel. The density of the chars was measured using a Pycnomatic ATC (Thermo-Scientific, USA) helium pycnometer. The instrument measuring density by the displacement of helium in a chamber containing a known mass of the sample being measured.

3.6 Analysis of liquid fuels

3.6.1 Elemental analysis

The elemental analysis of the liquid fuels used was a similar technique to the biomass and char analysis in 3.4.2, except Chemsorb, an inert absorbent, was added to prevent liquid loss from the capsule. The capsules were analysed as soon as they were made to minimise evaporation of the sample from the capsule.

3.6.2 Gas chromatography-flame ionisation detection (GC-FID)

GC-FID was used to measure the length of hydrocarbon chains in the fuels. A Perkin Elmer Clarus 500 On-Col was used for the analysis. The testing of samples was performed in accordance with ASTM D2887.

3.6.3 FAME analysis by GC-MS

The speciation of fatty acid methyl esters (FAME) within the biodiesel samples was performed using GC-MS. The samples were diluted in hexane and 1 μ l was injected at 250°C onto the column of a Shimadzu GCMS-QP2010 SE. A split ratio of 10:1 was used and the carrier gas was helium. The column flow rate was 1.27 ml/min. An RTx-Wax column was used and the column temperature was increased throughout the test time of 35 minutes from 50°C to 230°C.

3.7 Engine test facility

3.7.1 Selection of diesel engine

Table 3-3 gives a prediction of the suitability of several types of engine for using slurry fuels. The least suitable are spark ignition engines which rely on a spark to ignite the fuel as the compression ratio is not high enough to cause autoignition of most fuels. The flash point of char is significantly higher than the autoignition temperature and would thus not combust. Furthermore, most spark ignition engines use a carburettor or a port injector which is unsuitable. Common rail type injection systems are also unsuitable because they are very susceptible to particulates and must be protected with paper fuel filters. The smallest engines which are potentially suitable are high-speed direct injection diesel. High-speed engines run at approximately 1500rpm and above. The potential issue with these engines is that the high engine speed reduces the time available for combustion. The most suitable engines are low-speed types which run at less than 350rpm. This gives the slurry a long time to burn, but are very large and heavier for the given power output. Other potentially suitable engines are ones which are designed to use viscous fuels such as heavy oil. Another option and one that has not been investigated in detail is to use an indirect injection engine which uses simpler, lower pressure injectors that are less prone to blockage.



Figure 3-8 Engine generator setup used for char-slurry tests

An MG6000 SSY (MHM plant, UK) diesel generator was selected for slurry fuel testing and is shown in figure 3-8. It consists of a Yanmar L100N series, single cylinder, naturally aspirated, direct injection 435 cc engine. It is designed to produce single phase electricity at 50Hz (British standard) when the engine operates at 3000rpm. The nameplate output of the engine is 6.5 kW at 3000 rpm. The maximum fuel consumption is 1.7 litres/hour of diesel. The engine is air cooled and is fitted with an electric start motor. The engine was chosen for its low fuel consumption meaning that less fuel had to be produced to complete a full test. A disadvantage of a small cylinder diesel engine is that the rpm is high and is above that of most work with slurry fuels in the literature survey. The exhaust contains a silencer and no after-treatment systems. The generator has several electrical sockets including a single phase 230V, 32A which was used to connect the load bank.

Table 3-3 Prediction of the suitability of different types of diesel engine.

<i>Suitability of engine</i>	<i>Types of engine</i>
Most suitable	Indirect injection diesel. Low to medium RPM diesel. Two-stroke marine. Heavy fuel oil.
Moderately suitable	High-speed direct injection diesel
Unsuitable	Common rail diesel. Spark ignition.

The engine features an inline distributor pump system with two pumps. The first is an electrical low-pressure pump which distributes fuel around the system. The second is a plunger type high-pressure pump running off the crankshaft.

The injector is a simple mechanical type with no solenoid valve to control injection times. This is done by the needle lifting at the point at which the high-pressure pump delivers sufficient pressure. Fuel is sprayed into the engine through four holes in the nozzle equidistant around the circumference. The holes are 230 μ m in diameter and the injection angle is 150° from the centreline. Figure 3-9 shows the injector used and comprising parts. Regulating the injection pressure is a spring (figure 3-9b) which forces down on the injector needle, closing the nozzle. The force of this spring and hence the injector pressure can be altered by adding or removing shims which create pretension. The spacers act to prevent the spring from being tensed when the securing nut is tightened during assembly. The injector needle has an angled lip toward the centre of the length which, when pressure from the fuel from the pump is applied, creates an upward force to counteract the spring. The larger top section of the injector needle is close in diameter to the inner diameter of the injector nozzle so to maintain the injection pressure in the lower cavity of the nozzle. The difference in diameter is just enough to allow the needle to move up and down freely. The bottom of the injector needle is pointed to create a seal around the injector holes when forced down.

Fuel flows through the large hole in the injector body from the high-pressure fuel pump and through a small hole drilled in the body. The fuel enters the cavity in the injector nozzle through one of the holes on the top face that is not occupied by the spacers. Excess fuel supplied by the pump to the injector flows back to the fuel tank via the copper tube on the injector body. The fuel itself is used by the injector to lubricate all parts.



Figure 3-9 Injector used in the diesel engine selected. a) Assembled injector, and b) disassembled injector. Note- an extra nozzle is shown in b) for views at two angles.

Some modifications were made before testing. Firstly, the fuel tank was removed and replaced by a system which allows for specially made tanks to be switched out when changing fuels. There are two filters in the fuel line which were also removed as they prevented the passing of the slurry. The first filter was an inline paper type and the second was a fuel filter/water separator. It was replaced with a single mesh type inline filter with an orifice size of 75 microns. Thermocouples were also added at points (shown in figure 3-10). One was added at the air inlet to the engine after the filter, one in the exhaust manifold approximately 15cm from the exhaust valve and one in the lube oil sump.

The ignition was removed, and a new switch was connected in the control room adjacent to the lab in which the engine was in, so it could be turned on and off remotely. To compensate for the voltage drop within the long cable between the engine and ignition key, a larger battery was connected.

3.7.2 Test bed monitoring

Figure 3-10 shows a schematic of the engine generator and peripherals used for testing based figure 3-8. The exhaust of the engine generator was extended to create locations for sampling ports. The extension was made with a 2 ½ inch OD stainless steel tube. It extended horizontally for the sampling ports then vertically into the ventilation system. A thermocouple was placed into the tube within the horizontal part containing the sampling ports. Three sampling ports were made with ¼ inch Swagelok connectors. The ports were made so that they measured from the centre of the exhaust gas stream and far apart enough as to not interfere with each other. Another port was made to accommodate a zirconia sensor.

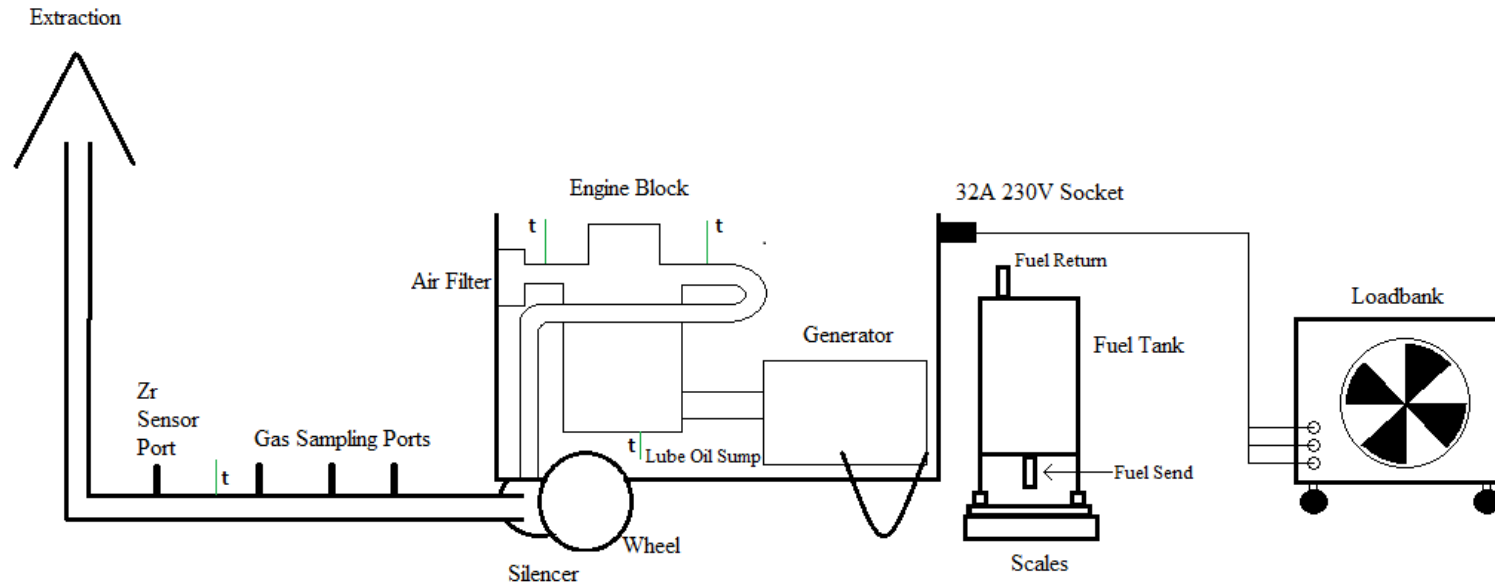


Figure 3-10 Schematic of engine generator and peripherals. Location of thermocouples given in green and labelled with the letter "t".

The electrical socket of the engine generator was connected to a Hillstone HAC240-10 resistive loadbank. The resistors within the loadbank were cooled with a fan at the front of the unit. The purpose of the loadbank was to create a sink for the electricity produced by the generator and alter the load on the engine. The resistance of the loadbank was controlled by a remote in the adjacent control room (figure 3-12). The resistance of the loadbank could be changed in 1kW steps. Software was supplied with the loadbank which logged the voltage, current and frequency at 1 second intervals. It was connected to a computer through the laboratory's internal network via an Ethernet connection.

3.7.3 Andersen cascade impactor

Particulate emissions below 10 μ m were measured using an Andersen impactor for baselining the generator on diesel and biodiesel. The instrument is shown in figure 3-11. The method was also used for measuring soot from the engine when 10%wt. slurries were used. Before each test, 8 GF/A (Whatman Glass fibre "A" grade) and 1 GF/F filter were prepared by placing in a desiccator for 24 hours then weighed on a microbalance. The GF/F was placed at the bottom of the impactor and the exhaust air passed directly through it. Above this, a GF/A filter was placed on each of the plates to capture particles by impaction. Each level captures particles of different size by aerodynamic separation, the holes in the disks between each level gradually become smaller to increase particle velocity. Exhaust air was drawn through the top of the impactor by a fixed displacement pump drawing air at 28 L/min connected to below the final filter. The impactor was covered in an electrical blanket to keep the temperature at 55°C. A thermocouple was also fitted to the top to monitor the inlet exhaust temperature. Each test was performed for between 30 minutes to an hour to ensure enough particles were captured to be accurately measured. The total flow through the impactor during the test was logged. After the test, the filters were removed and placed in a desiccator for 24 hours to remove any residual moisture and then weighed to get the mass of particles.



Figure 3-11 Andersen cascade impactor (cylinder on the left) and single stage filter (smaller cylinder right)

3.7.4 Single stage filter for PM₁₀

PM₁₀ was measured using a single stage filter, shown in figure 3-10, at full load during each test. A GF/F filter was prepared by desiccation for 24 hours and weighed prior to use. The filter was placed in a holder after a PM₁₀ pre-separator to remove any soot material larger than 10µm. A fixed displacement pump was used to draw the exhaust gas through at a rate of 17.5 L/min. Each test was performed over a period of 12 minutes. The filters were removed, desiccated for 24 hours, and then weighed. Both the single stage filter and Andersen cascade impactor instruments were designed in-house.

3.7.5 Horiba stack gas analyser

Dry, non-condensable exhaust gas was analysed using a Horiba MEXA-7100D stack analyser. Carbon dioxide and carbon monoxide were quantified using non-dispersive infrared (NDIR), and oxygen by paramagnetic susceptibility, NO_x and NO by chemiluminescence, and total hydrocarbon (THC) by flame ionisation detection (FID). THC was expressed in terms of parts per million of methane (ppmC). A single-point calibration using a gas mixture of known composition was made prior to tests.

3.7.6 Zirconia sensor

Oxygen and NO_x were further measured using a Horiba 720-NO_x zirconia sensor. The sensor voltage output was calibrated to an external calibration standard. This was connected to the NI datalogging hardware.

3.7.7 Particle size distribution

Real time particulate emissions were measured using a Cambustion DMS500 Fast Particle Analyzer. The instrument was capable of measuring particle size between 5 and 1000nm. Particles were classified by electrical mobility, the process of charging the particles which then deflect at different angles depending on their momentum and therefore size. The sampled exhaust stream first entered a remote cyclone at 8 L/min which removed particles above 1000nm. The gas stream passed through a heated line set at 55°C between the exhaust and the instrument. The stream was diluted within the heated line by a ratio of 8 parts sampling air to 6 parts dilution air. The sampling gas then passed through another cyclone to ensure larger particles are removed before further dilution by a factor of 20:1 in a rotating disk diluter. It then passed through the classifier section for particle size separation. The number of particles detected per cubic centimetre of air and their size distribution was measured in real time at a frequency of one second.

3.7.8 Engine speed

Engine speed was set to 3000 rpm \pm 50 rpm and was measured using a laser tachometer reading from a reflective strip placed on the flywheel. This was remeasured when the load was changed and the speed governor was reset accordingly. Furthermore, the engine speed could be approximated by the frequency of alternating current logged by the load bank.

3.7.9 Fuel consumption

The presence of particles in the fuel made it unviable to measure the fuel consumption by most flow rate means. The fuel consumption was instead measured by using a set of electronic scales beneath the fuel tank. The scales were capable of reading in 10g increments. The data from the scales was logged to the datalogging software developed. The electrical generation efficiency was determined against the higher heating value (HHV) of the fuel as follows:

$$\text{Generation efficiency (\%)} = \frac{\text{Electrical output (kW)}}{\text{Flow rate of fuel } \left(\frac{\text{kg}}{\text{s}}\right) \times \text{Fuel HHV } \left(\frac{\text{MJ}}{\text{kg}}\right)} \times 10 \quad (1)$$

3.7.10 Air-fuel ratio

The air-fuel ratio was determined from the elemental analysis of the fuels used and the composition of the exhaust gas. The Brettschneider/Spindt method was used to determine the amount of water in the exhaust by estimating a value for the equilibrium constant of the water/gas reaction as 3.8 (Silvis, 1997). The gross molecular weight of air was approximated as 28.968 and the composition of air as 20.95% O₂ and 79.05% N₂.

3.7.11 Development of software

Data from the DMS500 and loadbank were logged in their own proprietary software, and values from the Horiba stack analyser were logged manually. Figure 3-12 shows the electrical connections between the datalogging hardware, instruments and computers. Data from the zirconia sensor, thermocouples and fuel consumption measuring scales were all recorded in a program created using LabView loaded onto an 8-slot CompactRio chassis (National Instruments, USA) (appendix 2). This was, in turn, connected to a PC via Ethernet port for visualising and controlling datalogging. The DMS500 was connected to a separate computer via an RS485. The chassis was fitted with an 8-channel 100 samples per second thermocouple reader and an 8-channel \pm 10 V analog-in capable of measuring 500k samples per second. The analog in was used to measure the two voltage outputs from the zirconia sensor, one for oxygen, the other for NO_x. A total of 5 thermocouples were connected to the thermocouple reader.

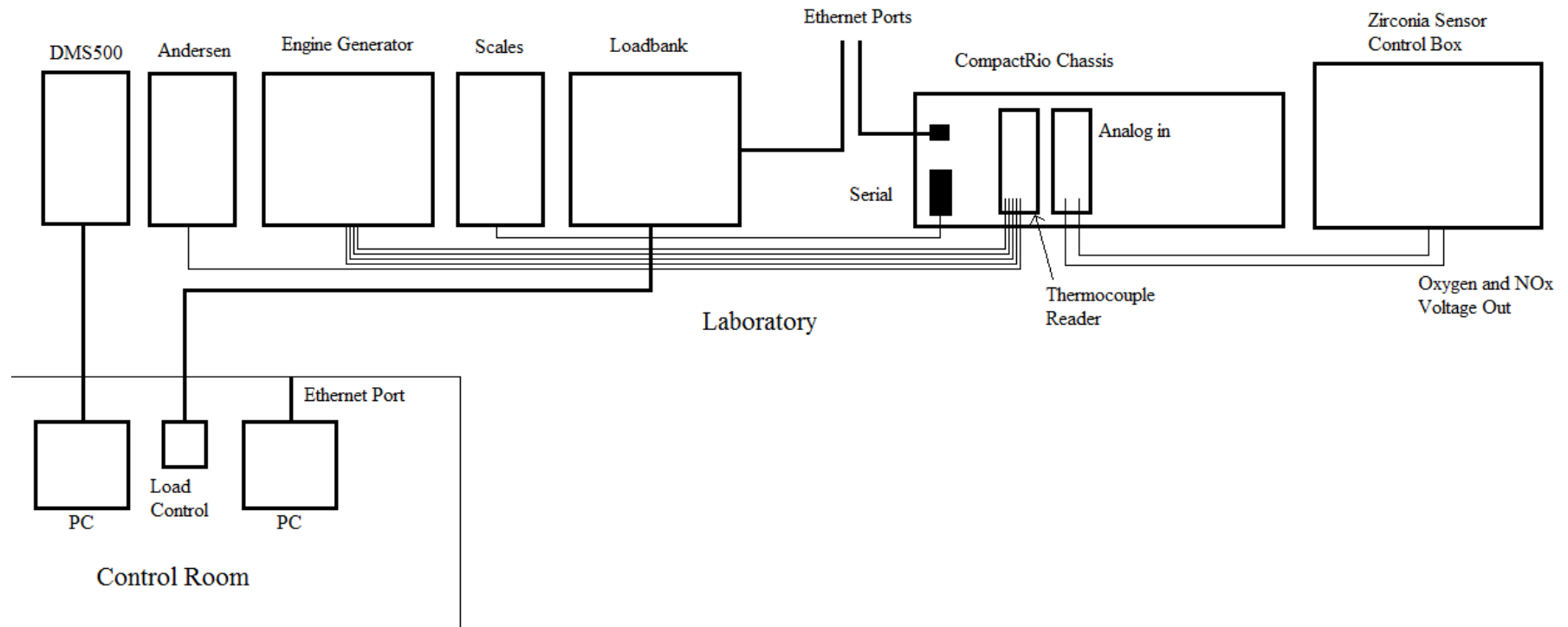


Figure 3-12 Data and control connections on the engine rig

Figure 3-13 shows a process diagram of how each section of data was handled. Voltage inputs to the NI were converted in the CompactRio software to actual values through manufacturer's calibration for thermocouples, and for the zirconia sensor, calibration with the Horiba stack analyser. The scales transmit a string of data every second via a serial connection, from which the mass reading was taken. This was compared to the previous value and saved if different. This means the mass value of the scale is only saved when the value changed. Hence by only logging changes, graphs are smoother and less memory is used. Data measured is stored on a graph in the user interface. Data can be written to a file when a button was pressed. A name for the file was inputted as was the time to write the file for. At this point, data flowing from the sensors was written into a text file until the writing time had passed.

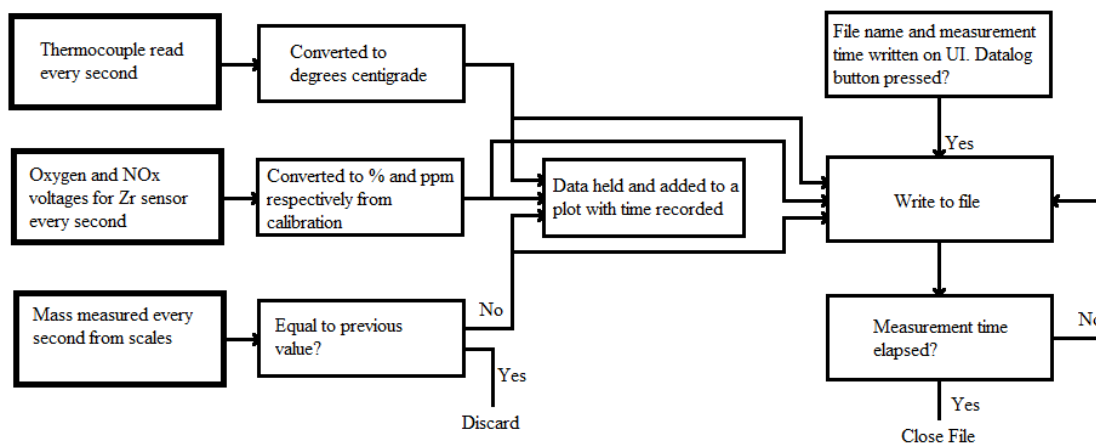


Figure 3-13 Schematic of the data handling process in the software

3.7.12 Engine test procedure

Before testing began, the engine was warmed up using standard diesel fuel at 75-100% load. During this time the engine oil temperature is monitored until it reached 50°C. The fuel was then switched by disconnecting the diesel fuel tank and a new tank containing the fuel to be tested was connected. The tanks for the test fuel were 2.5L square plastic bottles with quick fit connectors on the lid. The bottles were used to prevent contamination from other fuels. Prior to testing, the fuel lines were purged with the fuel that was to be tested for 40 seconds.

The engine was turned on and allowed to reach a condition at which the temperatures being monitored were stable. Before each load condition, the engine speed was recorded with a laser tachometer to ensure the speed is 3000 ± 50 rpm.

The first condition tested was at idle and was measured for 6 minutes once the engine temperatures had settled. The process was repeated with load steps of approximately 1kW up to the maximum load output of roughly 4.4 kW depending on the fuel. For the final full load

condition, the single stage particulate filter was used. To ensure enough soot was collected for accurate measurement, the test is performed for 12minutes.

3.7.13 Offline analysis

Single stage particulate filters collected during the tests were analysed by SEM/EDX. Samples were prepared by first cutting part of the filter paper off and placing in methanol before ultrasonication for 5 minutes. The liquid was then pipetted onto a silicon wafer and dried to remove methanol. It was then analysed with a Hitachi SU8230 SEM.

Deposits on injectors were analysed using a Carl Zeiss EVO MA15 SEM. Injectors were prepared for analysis by using electrical discharge machining to expose the internal surface of the nozzle body.

Lubrication oil was analysed at different points during the testing. It was sampled whilst still hot from the oil sump. The sampled oil was sent for commercial analysis for contamination and viscosity. Oil was also analysed by XRF in-house. Firstly, the oil was ashed at 775°C in a furnace and the percent ash was calculated. The collected ash was prepared into fused beads and analysed following the method in 3.4.7.

3.8 Conclusions

The method chapter has detailed techniques for not only analysing the properties of the fuel but also measures of the practicality of using slurry fuels, such as the energy cost of micronisation and the consumption of fuel per kWh of electricity produced. The structure of the char was studied using several methods, which is important because this could create a catalytic effect and will also affect the amount of emissions from the burning in a diesel engine. Previous studies of carbon structure of chars used in slurry fuels in literature are also limited and so further investigation would be valuable.

Another key area is emissions measurements. A particle number analyser was used as this and particle size instead of mass is increasingly becoming recognised as the important relationship between soot emissions and health risk. A literature review has not found an instance of research investigating the effect of using slurry fuels on particle size. All the key gas pollutants are also measured as is soot on a mass basis.

3.9 References

- Adazabra, A.N. Viruthagiri, G. and Ravisankar, R. 2016. Cleaner production in the Shea industry via the recovery of Spent Shea Waste for reuse in the construction sector. *Journal of Cleaner Production*. **122**(Supplement C), pp.335-344.
- Adazabra, A.N. Viruthagiri, G. and Shanmugam, N. 2017. Management of spent shea waste: An instrumental characterization and valorization in clay bricks construction. *Waste Management*. **64**(Supplement C), pp.286-304.
- Arnoult, S. and Brancourt-Hulmel, M. 2015. A Review on Miscanthus Biomass Production and Composition for Bioenergy Use: Genotypic and Environmental Variability and Implications for Breeding. *BioEnergy Research*. **8**(2), pp.502-526.
- Elias, M. 2013. Influence of agroforestry practices on the structure and spatiality of shea trees (*Vitellaria paradoxa* C.F. Gaertn.) in central-west Burkina Faso. *Agroforestry Systems*. **87**(1), pp.203-216.
- Gautam, B.R. Li, F. and Ru, G. 2015. Assessment of urban roof top solar photovoltaic potential to solve power shortage problem in Nepal. *Energy and Buildings*. **86**(Supplement C), pp.735-744.
- McBeath, A.V. and Smernik, R.J. 2009. Variation in the degree of aromatic condensation of chars. *Organic Geochemistry*. **40**(12), pp.1161-1168.
- Nepal, R. 2012. Roles and potentials of renewable energy in less-developed economies: The case of Nepal. *Renewable and Sustainable Energy Reviews*. **16**(4), pp.2200-2206.
- Sharma, K. 2015. Trade Policymaking in a Land-locked Developing Country: The WTO Review of Nepal. *The World Economy*. **38**(9), pp.1335-1349.
- Silvis, W.M. 1997. An Algorithm for Calculating the Air/Fuel Ratio from Exhaust Emissions. In. SAE International.
- Smith, A.M. and Ross, A.B. 2016. Production of bio-coal, bio-methane and fertilizer from seaweed via hydrothermal carbonisation. *Algal Research*. **16**, pp.1-11.
- Stout, J.C. 2007. Reproductive biology of the invasive exotic shrub, *Rhododendron ponticum* L. (Ericaceae). *Botanical Journal of the Linnean Society*. **155**(3), pp.373-381.
- Wanignon Ferdinand, F. Van de Steene, L. Kamenan Blaise, K. and Siaka, T. 2012. Prediction of pyrolysis oils higher heating value with gas chromatography–mass spectrometry. *Fuel*. **96**, pp.141-145.
- Watanabe, M. Inoue, H. Yamada, Y. Feeney, M. Oelofse, L. and Kataoka, Y. 2013. XRF analysis of high gain-on-ignition samples by fusion method using fundamental-parameter method. *Powder Diffraction*. **28**(2), pp.132-136.

Chapter 4: Feedstock and char properties

4.1 Introduction

Specific physicochemical properties of char are required for producing a slurry fuel. The most critical issue with using slurry fuels in diesel engines is the presence of hard elements that are associated with mechanical wear (Soehngen et al., 1976; Soloiu et al., 2011; Wibberley and Osborne, 2015). The elements identified in the literature review as the most problematic are aluminium and silicon, which are present in both coal and charcoal, but are usually found in considerably lower concentrations in the latter. Using charcoal instead of types of coal high in silicon which cause wear is a key advantage in the concept of char slurries as a fuel for developing countries.

Another issue is the late combustion of slurry fuel compared to traditional liquid fuels used in diesel engines. In previous studies, late combustion of solid particles has continued within the exhaust system, igniting the filtration system (Wilson, 2007). Producing a char that achieves good grindability yet burns at a low temperature and maximises the amount of volatile matter, the faster burning carbonaceous component, is therefore beneficial.

Many of the properties of the char can be predicted from the properties of the original material (McBeath et al., 2014; Li et al., 2018; Lu and Berge, 2014; Zhang et al., 2017). Predicting the properties based on the type of feedstock is particularly useful in areas where access to analytical technology is limited such as in developing countries. Furthermore, it would be impractical to test every feedstock being used if the supply comes from diverse natural forests or subsistence agriculture where many types of biomass are produced. Limiting the required tests or forecasting the properties based on the type of material would be useful.

There has been a concerted effort in recent years to reduce sulphur in fuels, a key source of acid rain (Muñoz et al., 2011). Hence, there is a need to minimise the sulphur in the char created. Another potential source of emissions is the nitrogen content in char which will also add to NO_x tailpipe emissions. Ash is not only important for wear reasons but will also contribute to particulate emission, so even relatively non-abrasive and non-corrosive inorganic material is still potentially an issue.

The first aim of this chapter is to assess the viability of producing slurry fuel from six different feedstocks discussed in 3.2.1, covering a range of types: two are woody, one is a grass used as an energy crop, one is microalgae and two are macroalgae. The six materials are converted into pyrolysis char (pyrochar) at four temperatures (200, 400, 600 and 800°C), and hydrothermal carbonisation (HTC) char (hydrochar) at two temperatures (200 and 250°C).

Each char is appraised for their suitability for slurry fuels through a number of parameters. The structure of the carbon inside the char is assessed by proximate and ultimate analysis, solid-state C^{13} nuclear magnetic resonance (NMR), and temperature programmed oxidation (TPO). The composition of the ash is investigated by atomic absorption spectroscopy (AAS) and x-ray fluorescence (XRF).

Another aim of the chapter is to investigate suitable feedstocks and total availability in developing countries. Information on the selection and collection process is contained in 3.2. Shea nut residue is a high calorie, common waste to tropical regions in Africa which is currently underutilised. Nepal is also investigated as a potential country which could benefit from the technology, as it contains lots of forest and agricultural land. A selection of different feedstocks are analysed and charcoal produced from each.

This chapter focuses on objective 2- to investigate suitable feedstocks and thermal conversion routes for producing charcoal for slurry fuels. The first section of the chapter investigates Nepal as a case study country for producing charcoal for slurry fuels. The total suitable feedstock for slurry fuels is calculated by creating charcoal from a selection of commonly available biomass. The next section focusses on shea residue which is a waste from producing shea butter used in cosmetics. It is a common agricultural waste in tropical regions of Africa and has a high calorific value. Finally, chars made from six feedstocks covering a range of plant biomass were analysed.

4.2 Biomass availability in a case study country: Nepal

Forests in Nepal are diverse owing to the range of climates occurring from the large variation in altitude. In the more tropical Terai (lowlands) region along the south of the country, the dominant species is *Shorea robusta*, known locally as sal (Paudel and Sah, 2015). In the hills, which covers 58% of the nation, the forests are diverse containing pine and broadleaf species such as *Schima wallichii*, *Alnus nepalensis*, *Pinus roxburghii* and *Rhododendron spp.* (Pandey et al., 2014). Forests in the mountain region mostly consist of conifers, oak and *Rhododendron spp.* (Rana et al., 2016).

Table 4-1 shows the total growing stock of some of the most important tree species in Nepal. Within the lowest region, the Terai, located along the southern border with India, the forests are dominated by *Shorea robusta*. Of the "Other" category, roughly half of the total is *Terminalia alata*. Within the Mid-hills, the main species are *Shorea robusta*, *Quercus spp.* and *Pinus spp.*. The most common species in the Mountains region are *Quercus spp.* and *Rhododendron spp.*. Other species found are birch and conifers, such as fir and *Tsuga dumosa*.

Many trees are grown on agricultural land for shade, firewood and food, but there is little information regarding the total quantity of each species. 30-40% of firewood is collected from private land meaning that it contributes to a significant part of the total (Bhattarai, 2013; Shrestha, 2007). Common trees found on agricultural land are *Ficus semicordata*, *Choerospondias axillaris* and *Alnus nepalensis* (Dhakal et al., 2015; Pandit and Paudel, 2013; Zomer and Menke, 1993). Other smaller plants like shrubs which can be used as a source of firewood are not well documented.

Table 4-1 Total forestry above-ground growing stocks of common species by region. Units are $\times 10^6$ tonnes. Dash represents where data is not available (Department for Forest Research and Survey, 2015).

<i>Species</i>	<i>Terai</i>	<i>Mid-hills</i>	<i>Mountains</i>
<i>Shorea robusta</i>	128.8	60.9	-
<i>Quercus spp.</i>	-	69.9	206.7
<i>Rhododendron spp.</i>	-	20.6	51.5
<i>Pinus spp.</i>	4.6	52.9	25.2
<i>Castanopsis spp.</i>	-	15.6	7.0
<i>Schima wallachii</i>	2.0	19.1	3.6
<i>Alnus spp.</i>	-	11.7	-
<i>Lyonia spp.</i>	-	9.9	-
<i>Lagerstroemia parviflora</i>	7.0	4.4	-
<i>Other</i>	89.0	68.0	224.0
<i>Total</i>	231.5	333.1	518.0

Nepal is a nation in which many people still rely on subsistence agriculture for their livelihoods (Shrestha and Nepal, 2016). The largest agricultural area is the Terai as the climate is more favourable, and the mountains the smallest because of the low temperatures and small populations (Ministry of Agricultural Development 2014). Table 4-2 shows the yearly production of agricultural residues from some of the most commonly cultivated crops. The main sources are from rice and maize harvests. The Terai produces large amounts of residues from sugarcane, which does not grow well in the other two regions because of the climate. Wheat is another common residue source found throughout the country.

Approximately 1.1% of the total forestry growing stock can be sustainably harvested each year, meaning that with the exception of the mountains, agricultural residues is the larger source of the two for plant-based biomass (Ministry of Forests and Soil Conservation, 2009). Furthermore, agricultural residues are more accessible as they are produced in areas where people live as opposed to forestry stocks which may be hard to access if not close to settlements or roads. For the purpose of charcoal slurry fuels, the utilisation of agricultural residues would be advantageous as less transportation from the production site to a diesel generator would be needed. Also, agricultural residues are currently underutilised in Nepal,

with just 6% used for energy (Webb and Dhakal, 2011). One of the main reasons is the increased levels of smoke produced by residues compared to firewood (Das et al., 2017b).

Table 4-2 Yearly production of residues from some common crops. Units are $\times 10^6$ tonnes.

Residue	Terai	Mid-hills	Mountains
Rice	8.85	3.27	0.37
Maize	1.24	4.29	0.52
Millet	0.01	0.36	0.09
Mustard	0.20	0.07	<0.01
Sugarcane	1.90	0.01	0.01
Wheat	1.69	0.81	0.14
Potato	0.28	0.40	0.17
Total	14.19	9.22	1.30

Table 4-3 shows the proximate and ultimate analysis of pyrolysis chars produced at 400°C for 27 types of biomass common in Nepal. Appendix 3 contains additional analysis which was also carried out on the untreated samples and pyrolysis chars produced from them at 600°C. In terms of ash content, the two most favourable chars are *Pinus roxburghii* and *Shorea robusta*. The energy recovery, the amount of energy retained in the solid char is also high for both too. Table 4-1 also shows that both species are common in Nepal. There is little difference between the volatile matter of the woody biomass investigated, something which is desirable to be present in slurry fuels. *Eupatorium adenphorum* is another low ash and high calorific value char which could be suitable. The species is invasive to the country and so conversion to slurry fuels could be a suitable way of disposal.

Most of the non-agricultural chars tested have good properties for the purpose of producing slurry fuels. However, *Ficus semicordata*, *Zanthoxylum armatum*, *Artemisia indica* and *Lantana camara* have high ash quantities which make them unlikely to be suitable. *Quercus semecarpifolia*, *Rhododendron arboreum* and *Schima wallichii* which, along with *Shorea robusta* and *Pinus roxburghii*, are species which are part of the five most common genus of trees in Nepal, can be converted in the chars which are potentially suitable. *Quercus semecarpifolia* and *Rhododendron arboreum* also have high energy recoveries.

The tests on agricultural residues showed only two were potentially suitable, *Saccharum officinarum* bagasse and maize cob because the ash levels are high in the others. They both, however, contain less volatile matter than wood chars and so would likely burn slower in a diesel engine. These two types represent just 12% of the total yearly production (3×10^6 tonnes) of residues in table 4-2.

Table 4-3 Proximate and ultimate analysis of pyrolysis chars produced at 400°C from types of biomass commonly found in Nepal.

Sample	Char yield (%)	Moisture (% as received)	Volatile matter (% dry basis d.b.)	Fixed carbon (% d.b.)	Ash (% d.b.)	Carbon (% d.b.) ^b	Hydrogen (% d.b.) ^b	Nitrogen (% d.b.) ^b	Sulphur (% d.b.) ^b	Oxygen (% d.b.) ^c	HHV (MJ/kg d.b.) ^d	Energy recovery (%)
Trees												
<i>Alnus nepalensis</i>	30.3	3.08	28.05	63.21	8.74	69.85	3.42	0.76	N.D.	15.23	26.24	45.78
<i>Castanopsis inidica</i>	33.1	4.49	30.46	62.40	7.14	74.47	3.49	0.71	N.D.	11.02	28.93	57.22
<i>Choerospondias axillaris</i>	27.9	3.89	30.09	63.29	6.62	75.52	3.73	0.28	N.D.	11.08	29.55	51.02
<i>Ficus semicordata</i>	33.6	4.01	32.36	55.40	12.24	67.42	3.43	0.42	N.D.	13.98	25.75	52.38
<i>Lagerstroemia parviflora</i>	34.2	3.84	32.4	59.61	8.00	69.83	3.23	0.70	N.D.	15.74	25.96	54.34
<i>Melia azedarach</i>	32.2	3.71	29.00	63.88	7.12	72.90	3.61	0.72	N.D.	13.11	28.06	48.57
<i>Myrica esculenta</i>	33.3	3.93	28.87	63.07	8.05	73.27	3.29	0.81	N.D.	11.87	27.97	55.73
<i>Quercus semecarpifolia</i>	34.4	3.93	29.52	61.64	8.84	71.22	3.40	0.66	N.D.	13.07	27.14	57.00
<i>Pinus roxburghii</i>	32.6	3.28	28.60	67.53	3.88	76.31	3.80	0.20	N.D.	13.48	29.41	52.21
<i>Rhododendron arboreum</i>	33.8	3.35	29.21	61.96	8.83	76.25	3.66	0.51	N.D.	8.36	30.12	57.08
<i>Schima wallichii</i>	32.5	3.32	26.97	65.11	7.92	72.07	3.37	0.28	N.D.	14.15	27.16	49.19
<i>Shorea robusta</i>	37.3	1.26	29.28	66.23	4.49	76.13	3.53	0.37	N.D.	15.48	28.08	59.77
Shrubs												
<i>Gaultheria fragrantissima</i>	28.9	3.48	26.83	67.40	5.78	76.08	3.58	0.37	N.D.	11.72	29.34	50.24
<i>Lantana camara</i>	29.5	3.80	23.91	65.83	10.26	68.38	3.04	0.77	N.D.	15.15	25.26	44.73
<i>Lyonia ovalifolia</i>	32.1	3.36	26.67	66.47	6.85	74.44	3.54	0.52	N.D.	12.31	28.59	48.03
<i>Woodfordia fruticosa</i>	33.9	4.05	30.19	61.52	8.29	69.29	3.26	0.41	N.D.	16.15	25.77	49.61
<i>Zanthoxylum armatum</i>	29.4	3.84	29.43	60.39	10.18	72.94	3.49	0.73	N.D.	10.04	28.46	49.15
Herbaceous												
<i>Artemisia indica</i>	30.5	4.45	28.22	62.25	9.53	74.40	3.61	1.06	N.D.	8.23	29.59	52.49
<i>Eupatorium adenphorum</i>	28.0	3.24	27.34	66.39	6.26	76.97	3.67	0.62	N.D.	10.13	30.04	50.47
<i>Thysanolaena maxima</i>	32.4	3.95	24.24	60.46	15.30	70.02	3.43	0.28	0.04	8.38	27.66	56.07
Agricultural residues												
<i>Brassica campestris</i>	36.9	6.58	38.19	40.82	21.00	52.05	2.78	1.93	0.10	18.95	18.59	44.99
<i>Finger millet</i>	36.6	5.52	28.64	43.70	27.66	53.93	3.08	1.69	0.04	10.82	21.14	50.06
<i>Maize cob</i>	27.8	2.88	22.46	69.98	7.56	75.89	3.68	0.44	N.D.	10.39	29.58	49.30
<i>Maize stem</i>	32.8	4.27	26.35	58.35	15.29	69.25	3.40	0.35	N.D.	8.96	27.29	51.63
<i>Maize cover</i>	29.1	3.79	26.71	61.74	11.55	73.78	3.66	0.35	N.D.	8.05	29.37	52.61
<i>Rice husk</i>	42.3	3.69	19.20	32.08	48.72	42.96	2.46	1.22	N.D.	3.29	17.58	55.65
<i>Saccharum officinarum bagasse</i>	30.1	2.28	24.05	69.46	6.49	76.21	3.65	0.20	N.D.	11.84	29.29	54.38

The trace element analysis of the untreated feedstocks used to make the chars in table 4-3 is shown in table 4-4. *Melia azedarach* and *Rhododendron arboreum* contain the largest quantities of aluminium in the tree samples, making them less suitable for use as a slurry fuel. They both also contain large amounts of silicon, another highly abrasive element. *Pinus roxburghii* has comparatively large amounts of silicon and aluminium also but does contain the lowest amount of calcium another abrasive element. *Shorea robusta* has the lowest levels of abrasives making it a very suitable fuel. *Ficus semicordata* and *Lagerstroemia parviflora* contain significantly more calcium than the other tree samples tested which makes them less

favourable. *Quercus semecarpifolia*, one of the most common species to Nepal, especially in the Mountains region, has suitable trace element properties to be suitable for slurring.

The shrubs tested generally have low levels of abrasives except for *Woodfordia fruticosa*, which has comparatively high silicon, aluminium and calcium. *Lantana camara* has high potassium content which will potentially cause corrosion within the engine cylinder. The herbaceous plant *Artemisia indica* also has a high level of potassium. Following from the high ash result for the char produced from *Thysanolaena maxima*, the inorganic component is largely silicon which means it is certainly not a viable feedstock.

The main concern in the agricultural residues tested is the high amount of silicon present which is an order of magnitude higher, apart from *Saccharum officinarum* bagasse, than the majority of tree species. Whilst maize cob is relatively low ash, the trace element analysis shows that most of this is silicon making it less desirable. Of the residues tested, only the *Saccharum officinarum* bagasse is of similar suitability as the tree samples for creating a char slurry.

The removal of bark prior to carbonisation is a potential route to remove abrasive elements from the charcoal produced. The percentage of ash in the bark is higher than within the wood and so removal prior to carbonisation will lead to a lower ash char (Almeida et al., 2010; Deka et al., 2014; Filbakk et al., 2011). Abdullah et al. (2010) produced chars from the leaf, wood and bark from Mallee trees finding that the chars from wood contained the lowest ash. Additionally, the silicon and aluminium content was much lower than within the bark. The wood chars had low Si/K and Ca/K ratios meaning that they may have a high slagging propensity, the effect of which on a slurry engine is not well understood. Deka et al. (2014) studied the bark and wood from six trees in north-east India finding that silicon and calcium in wood ash are less as a proportion of the total ash than in the bark. Saarela et al. (2005) also found that calcium was more abundant in the ash of bark from three Scots pine samples than the wood ash. The removed bark can still be used to make char for purposes where the ash content is less critical- as a cooking fuel for example. As there is a larger portion of silicon, the slagging propensity will be lower (Abdullah et al., 2010). The removal of bark potentially increases the number of suitable materials but adds an extra level of complexity in producing a slurry fuel.

Table 4-4 Trace element analysis of untreated samples collected from Nepal. All measured using ICP-OES except P by colorimetry and Si and Al by XRF.

Sample	Na (mg/kg as received)	Mg (mg/kg a.r.)	K (mg/kg a.r.)	Ca (mg/kg a.r.)	P (mg/kg a.r.)	Si (mg/kg a.r.)	Al (mg/kg a.r.)
Trees							
<i>Alnus nepalensis</i>	486	607	2348	6429	1275	288	201
<i>Castanopsis Indica</i>	537	783	5132	3807	1288	1552	N.D.
<i>Choerospondias axillaris</i>	435	1042	1702	5677	218	1141	515
<i>Ficus semicordata</i>	542	899	4411	11555	1289	3270	110
<i>Lagerstroemia parviflora</i>	485	1311	2976	11575	923	1776	1463
<i>Melia azedarach</i>	416	319	1488	5096	773	7944	3602
<i>Myrica esculenta</i>	478	870	3612	5045	1273	2562	1002
<i>Pinus roxburghii</i>	470	217	550	1223	N.D.	2644	1714
<i>Quercus semecarpifolia</i>	461	845	4526	6187	1123	1677	830
<i>Rhododendron arboreum</i>	476	545	2348	4181	563	9656	4689
<i>Schima wallichii</i>	487	325	5980	5301	1019	840	N.D.
<i>Shorea robusta</i>	78	500	52	2439	503	603	345
Shrubs							
<i>Gaultheria fragrantissima</i>	441	325	2612	1336	588	2676	N.D.
<i>Lantana camara</i>	517	647	11205	2205	2193	1314	527
<i>Lyonia ovalifolia</i>	362	354	4176	1313	553	1850	N.D.
<i>Woodfordia fruticosa</i>	542	530	3588	9731	233	3885	1611
<i>Zanthoxylum armatum</i>	481	416	4677	5217	1092	1762	754
Herbaceous							
<i>Artemisia indica</i>	424	483	11376	3216	2242	1658	159
<i>Eupatorium adenophorum</i>	576	708	3553	2172	1231	1234	N.D.
<i>Thysanolaena maxima</i>	522	623	16311	623	2342	21187	159
Agricultural residues							
<i>Brassica campestris</i>	749	3154	22095	15999	3220	13014	3339
<i>Finger millet</i>	1303	1757	31213	5988	4913	42783	5580
<i>Maize cob</i>	451	262	4792	680	N.D.	17071	522
<i>Maize stem</i>	547	2002	8268	2232	2834	11926	247
<i>Maize cover</i>	509	1209	7244	1474	931	14490	2387
<i>Rice husk</i>	583	1148	6303	2638	2787	97509	43
<i>Saccharum officinarum bagasse</i>	456	275	3984	577	1342	4630	N.D.

The amount of agricultural residues which could be converted into electricity via char slurries in Nepal is limited. *Saccharum officinarum* bagasse has been identified as a potentially viable fuel. The amount available is 0.95×10^6 tonnes per year and is nearly entirely located in the Terai area of the country. For the region this is a significant amount as 1.42×10^6 tonnes per year can be sustainably sourced from *Shorea robusta*, the most abundant forestry biomass. Within the Mid-hills are several species which could be used. It is unclear how many of the *Rhododendron spp.* could be used as the specific species sampled from Nepal was unsuitable. The most suitable and abundant species in the region are likely *Shorea robusta*, *Pinus spp.*, *Schima wallichii* and *Quercus spp.*. In the Mountains, there is far less demand for electricity as

the population is small. There exists a large pool of forestry resources which could be used. As the region is the least accessible and furthest away from fuel imports, which pass through the border with India, it would perhaps benefit the most from producing an alternative to conventional hydrocarbon fuel via char slurrying. Also, the cold climate makes it difficult to create energy through the alternative of anaerobic digestion (Almeida et al., 2010).

The data also shows which common species used in agroforestry could be cultivated further to produce suitable feedstocks for the process. *Schima wallichii* is a species that is common in natural forests but is also cultivated as a shade tree and for fodder, and has good properties for converting to a slurry fuel (Orwa et al., 2009). *Choerospondias axillaris*, a fruit-bearing tree, and *Alnus nepalensis* are two other species that could be used for agroforestry purposes, as well as fuel for char slurry engines.

The removal of invasive species is another source of feedstock for slurry fuels. *Lantana camara* is less suited as the char produced is comparatively high in ash. However, a large proportion of this is potassium which can be removed by water leaching prior to carbonisation (Das et al., 2004). *Eupatorium adenophorum* is very suitable for use as a char for slurrying because the levels of abrasive ash are low, and the calorific value of the char is high.

4.3 Shea as a feedstock for char in African developing countries

Shea residue from the production of shea butter was another material selected for tests as it is a common agricultural residue in African countries. The residue remains high in oil after the extraction of the butter therefore potentially making it a good fuel. The use of woody biomass from forests can lead to deforestation- using agricultural residues such as shea is considered to be more sustainable.

Table 4-5 shows the ultimate analysis for shea residue and the chars produced from it. The material contains nitrogen, in similar quantities to macroalgae, analysed in table 4-6, leading to increased NO_x emissions. The H/C and O/C ratios are low and fixed carbon high, suggesting that the raw material contains a high quantity of polycyclic aromatic hydrocarbons. From an initial material with a low H/C ratio, the char produced at 400°C was comparatively high, more than the other terrestrial (grown on land) biomass tested in this section, despite the loss of high H/C lipids. As a result, the material should be less recalcitrant and burn at a lower temperature. The oxygen content of this char is low and so is less likely to reduce soot from diesel when used in an engine as part of a slurry.

Table 4-5 Ultimate analysis of shea chars produced and feedstock used.

Sample	Carbon (% d.b.)	Hydrogen (% d.b.)	Nitrogen (% d.b.)	Sulphur (% d.b.)	Oxygen (% d.b.)	H/C ratio (molar)	O/C ratio (molar)
Shea	55.28	5.23	3.26	N.D.	31.43 ¹	1.14	0.43
Shea 400°C	71.86	3.76	4.03	N.D.	5.23 ¹	0.63	0.05
Shea HTC 250°C	62.46	6.65	2.20	0.10	23.54 ¹	1.28	0.28

N.D. Not detected

¹Calculated by difference from the sum of the other elements plus ash

Figure 4-1 shows the proximate analysis of shea residue and chars. The volatile matter content in the raw shea residue is low because it has undergone a lipid extraction to remove shea butter. Despite the removal of these lipids, the calorific value is still comparatively high compared to other feedstocks tested. During pyrolysis at 400°C some of the lipids present, which contribute to the total volatile matter content, were evaporated and condensed, along with bio oil in the catchpot below the reactor. Nevertheless, the shea pyrolysis char at 400°C still has high volatile content. Of the hydrochars produced at 250°C in this section, the one produced from shea has the highest volatile matter content and thus should burn fastest in a diesel engine.

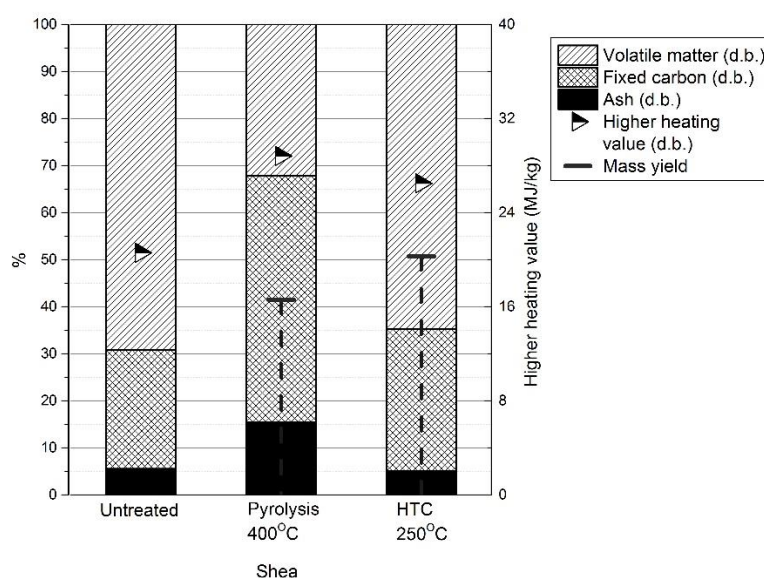


Figure 4-1 Proximate analysis, mass yield and calorific value of shea residue and chars produced using it.

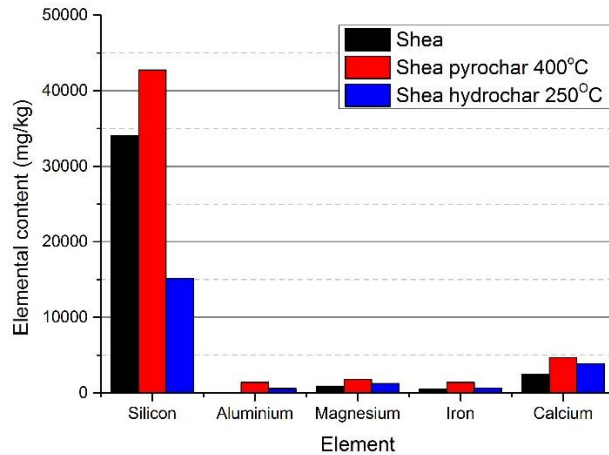


Figure 4-2 Trace element analysis of shea feedstock and the two chars derived from it. Performed by AAS except for aluminium and silicon, which were analysed by XRF.

Figure 4-2 shows the trace element analysis of shea residue and derived chars. The five elements shown are the ones predicted to be most likely to cause issues to the operation of a diesel engine. Silicon, the second most abrasive element after aluminium which is likely to be found in biomass materials, is the trace element in the highest concentration in the shea samples. Pyrolysis at 400°C has further concentrated the silicon present, increasing the likely rate of wear of an engine using a slurry fuel containing it compared to the untreated sample. Hydrothermal carbonisation reduced the concentration of silicon compared to the feed material. The reduction in silicon is over 50% which would likely correspond to a reduction in engine wear rate of a similar level.

Calcium is the next most abundant trace element after silicon in the shea feedstock and derived chars. The less abrasive nature of calcium compared to silicon and the lower concentrations present means that in terms as a factor for engine wear, the presence will have minimal effect.

The shea hydrochar contains less of all five elements shown in figure 4-2 than the pyrochar which is advantageous. The reduction in the concentration of trace elements compared to pyrolysis by the virtue of retaining more carbon in the solid and through the leaching of inorganic elements into the aqueous phase means that a less abrasive product is gained.

4.4 Properties of chars produced from six potential feedstocks for slurry fuels

4.4.1 Proximate and ultimate analysis of preliminary candidates for slurry fuels

Figure 4-3 shows the proximate analysis and calorific values of the chars produced and initial feedstocks used to create them. Of the pyrolysis charcoals produced at 400°C, oak was the most suited as a slurry fuel because it had low ash and had retained the most volatile matter. The presence of volatile matter is beneficial because it burns faster and at a lower temperature than fixed carbon, reducing ignition delay (Roy Choudhury, 1992; Saeed et al., 2016). Ultimately, producing a char with these properties means that the cetane number is higher, a key indicator for the quality of diesel engine fuels. The amount of charcoal yielded at 400°C from oak was higher than the other terrestrial plants: miscanthus and rhododendron. The calorific value, however, was less than rhododendron and miscanthus produced at the same temperature by 9.4 and 9.9% respectively. Miscanthus 400°C pyrolysis char was the highest in ash of the terrestrial plant char samples but was still less than the aquatic alternatives. The rhododendron 400°C pyrolysis char had a calorific value just less than the miscanthus equivalent but had the benefit of less ash and more volatile matter.

The pyrolysis chars produced at 400°C from the two macroalgae samples contained levels of ash unfeasibly high for use in a slurry engine. Furthermore, the calorific value of both is less than a third on a weight basis than diesel which it is replacing. Chlorella pyrolysis char produced at 400°C, when compared to the others made at the same temperature, had high volatile matter content (only oak was higher). The drawbacks were that the calorific value only marginally increased from the raw material, remaining much lower than the terrestrial chars at the same temperature, and the ash was the third highest of all materials tested. Beyond 400°C, the char produced from chlorella becomes less calorific, higher in ash and lower in volatile matter meaning that by all accounts, becomes less suitable as a fuel.

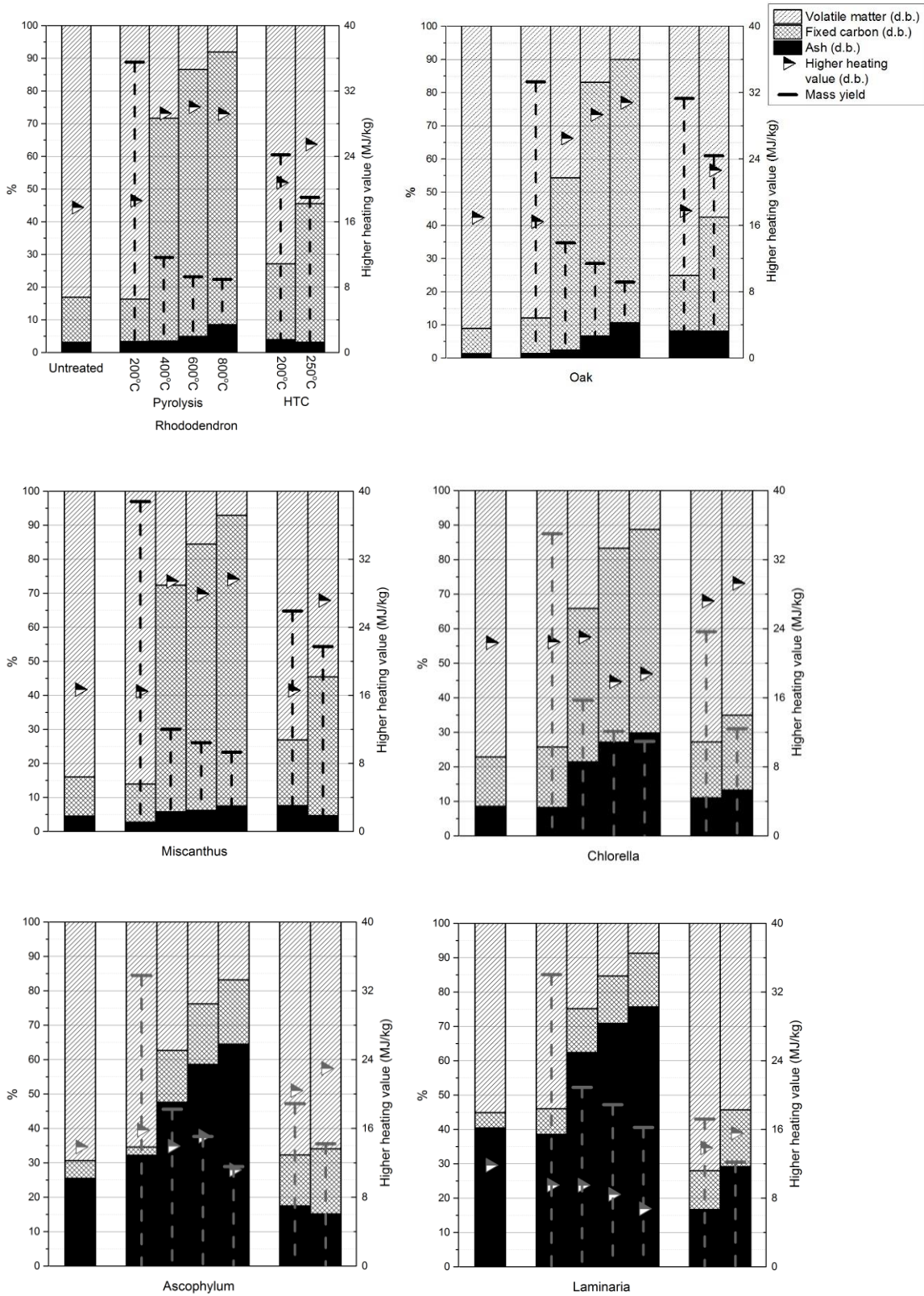


Figure 4-3 Proximate analysis, mass yields and higher heating values of chars produced from the initial biomass types. Each subfigure contains 7 bars. From left, untreated, pyrolysis chars grouped in order: 200°C, 400°C, 600°C and 800°C. The final two are hydrochars produced at 200°C and 250°C. d.b. denotes shown on a dry basis.

At the pyrolysis temperature of 600°C, the mass yield decreases for rhododendron, oak and miscanthus. There is some gain for oak and rhododendron, as the calorific value increases by approximately 3 MJ/kg and 0.8 MJ/kg respectively but reduces by 1.5MJ/kg for miscanthus. Fixed carbon accounts for an even higher proportion which will affect the rate of burn for all terrestrial materials. As a result of the increasing fixed carbon and ash, the main benefit of using a higher temperature char is the improvement in grindability. At the highest pyrolysis temperature, 800°C, there is little gain in terms of calorific value, if at all. At this point, for rhododendron and oak, the ash content is over three and five times higher respectively in the char than the raw material.

The hydrochars produced showed a benefit in calorific value in comparison to the raw material, like pyrolysis, but had some distinct advantages over the other thermal conversion method. The main two being that the mass yield and volatile content were much higher whilst creating a friable product when treated at 250°C. At an HTC temperature of 200°C, the material was still fibrous and not easy to micronise. Rhododendron, for example, produced 60% more char under HTC at 250°C than under pyrolysis at 400°C, and approximately double the amount of volatile matter.

The oak hydrochars are similar to rhododendron hydrochars in terms of volatile content, higher than found in pyrolysis chars. The energy densification caused by the thermal treatment, however, is less effective than during the HTC of rhododendron, as the mass yields were higher, but the calorific value was lower. The reason for this is most likely the composition of the wood in terms of cellulose, hemicellulose and lignin. Kang et al. (2012) produced hydrochars from lignin, cellulose and D-xylose (a substitute for hemicellulose), finding that the mass yield trend was lignin > cellulose > D-xylose, whilst higher heating value (HHV) improvement trend was D-xylose > cellulose > lignin. This would suggest that rhododendron contains more hemicellulose and less lignin than oak. The higher presence of lignin in oak was further supported by the higher char yields during pyrolysis compared to rhododendron, especially at the lower temperatures because lignin is known to yield more char at higher temperatures (Yang et al., 2007).

Miscanthus, a terrestrial raw material containing comparatively high ash, benefits from leaching of inorganic material into the aqueous phase, reducing the ash in the hydrochar product. This effect is most prominent between 200 and 250°C in miscanthus leading to a 3% reduction between the two hydrochars produced.

Unlike the terrestrial biomass, the conversion of algae by HTC was better for increasing calorific value than pyrolysis. The mass yields, however, were much lower and did not exceed

40% at 250°C, compared to 45-65% for terrestrial types. Another advantage over pyrolysis for this feedstock was the lower ash- much of the inorganic material was transferred to the aqueous phase during the process. HTC as a pathway for upgrading macroalgae is more promising than pyrolysis. In the case of *ascophyllum*, the amount of ash is reduced by 8 and 10% at 200 and 250°C respectively from the raw material's value. Furthermore, the calorific value was improved to a level similar to that of oak hydrochar at both temperature conditions. *Laminaria* also reduced in ash during HTC but the calorific value was still low. Whilst possibly the most important consideration for a char for slurring, the ash content, was reduced in macroalgae via HTC, it was still higher than the other fuels tested. It is therefore not an ideal starting material for a slurry fuel. Both *chlorella* and *shea* contain high levels of lipids, a group of volatile compounds, and both yield hydrochars with high volatile matter, which suggests that lipids are retained in the solid during HTC.

Table 4-6 shows the ultimate analysis and energy recovered in the solid product during the different thermal treatments. Although most oxides of nitrogen (NO_x) produced from burning slurry fuels in an internal combustion engine is thermal NO_x, the presence of high concentrations of nitrogen in the algae fuels, in particular, *chlorella*, is a concern (Mushrush et al., 2011). In recent years, the sulphur content in diesel has been reduced to a maximum of 10ppm in the United Kingdom as a result of environmental concerns (British Standards Institution, 2013; Muñoz et al., 2011). In developing countries, however, the use of fuels with sulphur above 1000ppm is common (Mahdi et al., 2017). With the exception of one char, the sulphur content in the fuels produced from the three terrestrial biomass are below 1000ppm, and in most cases, below the detection limit. Macroalgae chars, however, contain 12000-50000ppm of sulphur which is significantly higher than what is found in diesel in both developed and developing countries. Carbonisation of *chlorella* reduces the sulphur content from the raw material by over half, except for pyrolysis at 200°C. The sulphur content of the hydrochars is still high at 1300-2300ppm but is potentially at an acceptable level for some developing countries.

Table 4-6 Ultimate analysis and energy recovery of the chars produced. P denotes that the sample was produced by pyrolysis, and HTC by hydrothermal carbonisation.

Material	Treatment and temperature	Carbon (% dry basis)	Hydrogen (% d.b.)	Nitrogen (% d.b.)	Sulphur (% d.b.)	Oxygen (% d.b.)	Energy Recovery (%)	H/C (molar)
Rhododendron	Untreated	50.33	5.65	0.37	0.24	41.41	N/A	1.35
	P 200°C	51.28	5.75	0.31	0.04	39.25 ¹	93.03	1.35
	P 400°C	78.08	3.21	0.44	0.06	10.05	47.97	0.49
	P 600°C	82.62	2.06	0.35	N.D.	5.13	39.20	0.30
	P 800°C	83.17	0.92	0.33	0.14	1.66	36.81	0.13
	HTC 200°C	53.90	5.68	0.21	N.D.	31.34	70.89	1.26
	HTC 250°C	66.56	4.87	0.28	N.D.	22.75	68.11	0.88
Oak	Untreated	47.45	5.31	0.18	N.D.	37.62	N/A	1.34
	P 200°C	47.68	5.34	0.22	N.D.	40.90	80.99	1.34
	P 400°C	73.07	2.92	0.27	N.D.	13.59	54.43	0.48
	P 600°C	81.87	2.00	0.12	N.D.	6.93	49.40	0.29
	P 800°C	87.93	1.05	0.27	N.D.	2.82	41.66	0.14
	HTC 200°C	49.37	5.33	0.21	N.D.	36.86	82.05	1.30
	HTC 250°C	58.21	4.74	0.27	N.D.	21.52	81.69	0.98
Miscanthus	Untreated	47.14	5.89	0.13	0.04	43.14	N/A	1.50
	P 200°C	47.17	5.85	0.23	N.D.	44.00 ¹	95.80	1.49
	P 400°C	78.97	3.58	0.18	N.D.	13.88	52.92	0.54
	P 600°C	81.10	2.10	0.18	N.D.	14.23	43.69	0.31
	P 800°C	85.48	1.01	0.08	N.D.	4.18	41.37	0.14
	HTC 200°C	49.31	4.71	0.12	N.D.	38.25 ¹	88.47	1.15
	HTC 250°C	70.23	5.08	0.24	N.D.	21.94	64.45	0.87
Chlorella	Untreated	50.69	6.81	8.32	0.70	25.84	N/A	1.61
	P 200°C	51.51	6.55	8.29	0.52	24.87 ¹	87.80	1.53
	P 400°C	57.79	3.71	8.43	0.18	10.66	40.40	0.77
	P 600°C	52.17	1.45	6.75	N.D.	12.44 ¹	23.67	0.33
	P 800°C	57.75	0.57	4.35	0.02	8.87	22.96	0.12
	HTC 200°C	57.50	7.10	8.14	0.23	13.88	71.83	1.48
	HTC 250°C	61.49	7.44	4.95	0.13	12.73	40.58	1.45
Ascophyllum	Untreated	38.51	4.73	1.45	2.31	34.60	N/A	1.48
	P 200°C	39.02	4.38	1.52	1.49	21.35 ¹	96.55	1.35
	P 400°C	42.58	2.33	1.73	3.71	23.14	45.92	0.66
	P 600°C	40.98	0.56	1.18	4.97	0.29	41.11	0.16
	P 800°C	41.03	N.D.	1.34	5.04	14.05	23.38	N/A
	HTC 200°C	52.65	4.51	2.05	3.14	20.14 ¹	69.58	1.03
	HTC 250°C	58.50	5.37	2.07	2.58	23.99	59.06	1.1
Laminaria	Untreated	32.79	4.01	2.77	1.47	28.82	N/A	1.47
	P 200°C	28.62	3.12	1.93	1.20	26.55 ¹	68.43	1.31
	P 400°C	28.63	1.64	1.56	1.33	14.85	42.01	0.69
	P 600°C	28.80	0.51	1.43	1.65	12.16	33.70	0.21
	P 800°C	23.67	N.D.	1.09	1.59	6.40	22.23	N/A
	HTC 200°C	36.90	3.77	3.19	2.02	21.63	50.35	1.23
	HTC 250°C	40.76	4.29	2.65	1.83	23.49	40.49	1.24

¹Calculated by difference from the sum of the other elements plus ash

N/A denotes the field is not applicable

N.D. Not detected

The presence of oxygen in the fuel may influence how emissions form during combustion. It has been found that the increased oxygen content in a fuel reduces the formation of soot precursors (Park et al., 2017). Hydrochars have higher oxygen content than pyrolysis chars produced at 400°C and above, and as a result, should burn with less soot formation. The terrestrial chars produced at 400°C have an oxygen content of between 10-14% which is higher than diesel and in a similar region to biodiesel, which is 11%; the two liquids used to produce slurries. The hydrochars created in some cases contain over double the oxygen value of biodiesel meaning that soot formation may even be reduced in biodiesel with the addition of char by this mechanism. The pyrolysis chars produced at 600°C still contain a level of oxygen which may provide a benefit, except in the case of *ascophyllum*. At 800°C, the three terrestrial samples have a low oxygen content which is unlikely to promote soot reduction.

The hydrogen to carbon ratio of all the materials tested are lower than the diesel fuels (1.85-1.95) that they are to be blended into. This means that without energy efficiency gains, the specific carbon dioxide emission will be greater with the addition of char to the liquid fuel than without. Hydrochars, however, have a significantly higher H/C ratio than pyrolysis chars above 400°C, meaning less specific carbon dioxide emissions. The hydrochar with the highest H/C ratio is made from *chlorella* which also has the highest ratio of all of the raw materials. The hydrochars produced from macroalgae have comparatively high H/C compared to hydrochars from terrestrial biomass, especially at the higher of the two temperatures. Of the hydrochars derived from terrestrial biomass, oak hydrochars have a higher H/C than the other two used, despite the lowest ratio of raw materials.

4.4.2 Trace element analysis of potential feedstocks

Following proximate and ultimate analysis, the chars produced from macroalgae were not considered further because the ash content was high and the calorific value low. Figure 4-4 shows the elemental composition of the ash in each of the terrestrial and *chlorella* pyrolysis chars samples made, and the initial feedstocks for comparison. High silicon content in pyrochars produced from *miscanthus* raises concerns about its feasibility as a source of material for producing slurry fuels. There is also a smaller but significant amount of silicon in the *chlorella* feedstock also. *Rhododendron* and oak chars containing the least silicon, making them more suitable for slurrying in this respect.

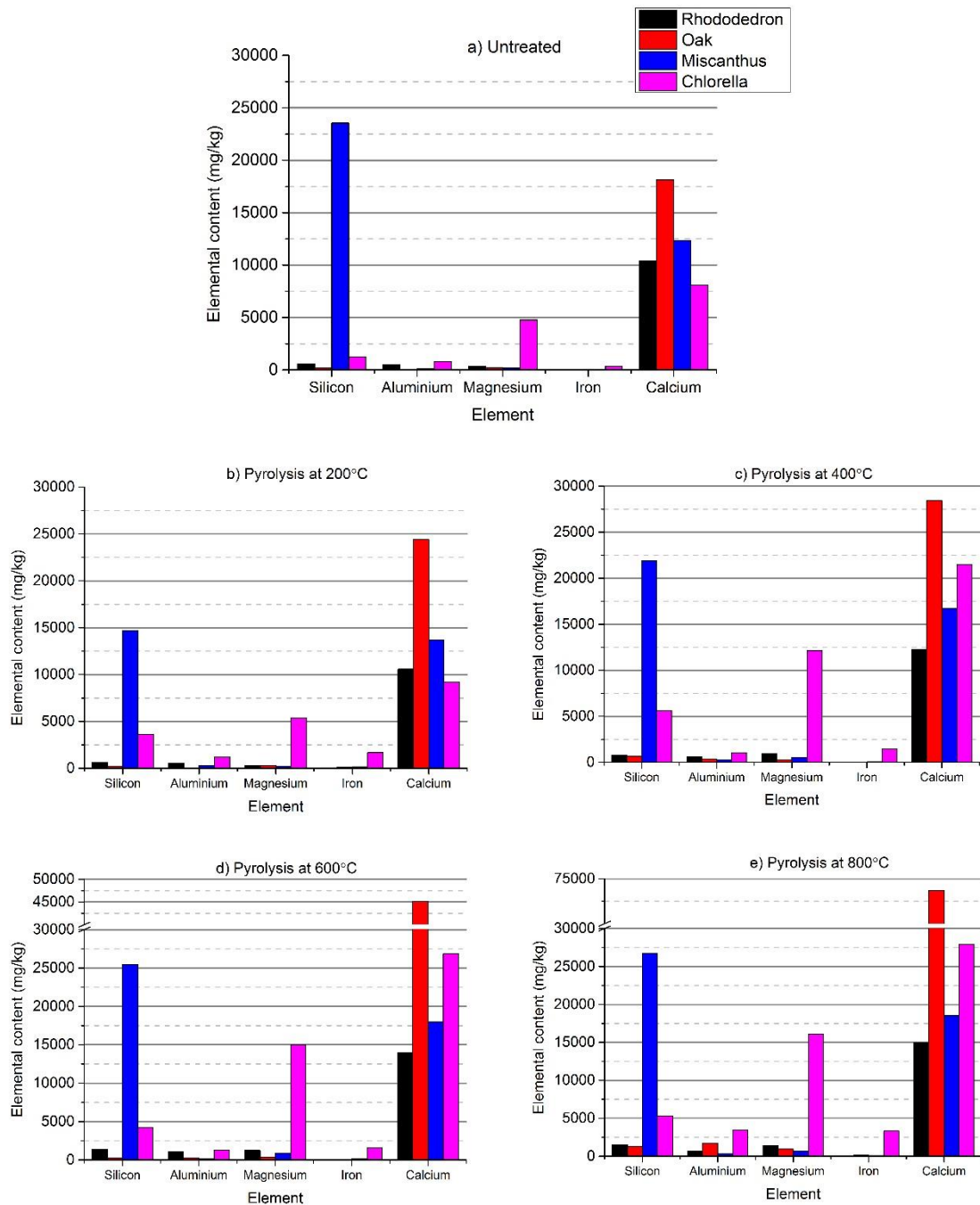


Figure 4-4 Trace element analysis of pyrolysis chars produced from the four most promising initial samples. The five elements highlighted are those most likely to cause abrasion issues within the engine. Aluminium and Silicon performed by XRF, the others- AAS

The amount of aluminium in all the samples is low compared to the other four elements shown in figure 4-4, but it is the most abrasive. The feedstock which contains the most aluminium is chlorella then rhododendron. Oak produced by pyrolysis at 800°C contains over 1500mg/kg of aluminium - only one other pyrochar, made from chlorella at 800°C has more. The concentration of aluminium is low in the pyrochars produced, except for chlorella pyrochars and the oak pyrochar at 800°C, so aluminium is not predicted to cause significant issues to the engine when used as a slurry compared to silicon.

The final three elements shown are much less abrasive than silicon and aluminium but are often more prevalent in plant-based biomass. The sheer quantity of the less abrasive elements can mean that they can be more damaging overall. In the case of magnesium, the hardness of the most common oxide is approximately half of silicon (Ishigaki and Buckley, 1981; Shackelford and Alexander, 2001). Chlorella contains a level of magnesium in the raw material and associated pyrochars which is likely to mean that it is a bigger contributor to abrasion than silicon and aluminium. The presence of iron in the samples, apart from chlorella, will have only a minor effect on abrasion as the concentrations are low and the hardness is less than the other elements shown.

Calcium is common in all four samples shown, the largest amount found in the oak samples. Except for miscanthus, it is the most abundant of the five elements in all the samples. Chlorella has the lowest amount initially but the effect of concentrating the ash during pyrolysis causes the amount to increase significantly- chars at 400°C and higher from the microalgae have the second highest concentrations after oak. Rhododendron chars have comparatively low amounts of calcium under all the carbonisation processes tested. In both rhododendron and oak, calcium is likely to be the main contributor to wear as the amount present is far larger than more abrasive elements measured.

The increasing concentration of the elements in figure 4-4 during carbonisation is inevitably an issue. By pyrolysis at 600°C, the amount of calcium in oak is double the initial value. At 400°C, the concentrations have only just begun to increase but continues through 600 and 800°C. It is therefore advantageous to minimise the pyrolysis temperature so that the material is grindable, unlike the raw feedstock, but less abrasive.

One of the main advantages of HTC is the ability to reduce the inorganic content in the solid char product through leaching of elements into the aqueous phase. The alkaline metals are elements that are generally reduced- sodium and potassium especially, and magnesium, calcium and phosphorus to a lesser extent (Smith et al., 2016). Smith et al. (2016) produced hydrochars from a number of materials such as oak, algae and sewage sludge. With the exception of sewage sludge, over half of all the potassium was leached from the material. In the case of oak and miscanthus, over 69% was removed at 200°C and yet more at 250°C. The removal of calcium was dependent on the initial material- in the case of willow, miscanthus and food waste most was leached but not for algae, sewage sludge and oak. To find a material where the calcium is easily leached or additives that could be added to aid removal would be advantageous in the preparation of char for slurry fuels. In the four feedstock materials shown in figure 4-5, the removal effect on magnesium and calcium at both HTC temperatures is low.

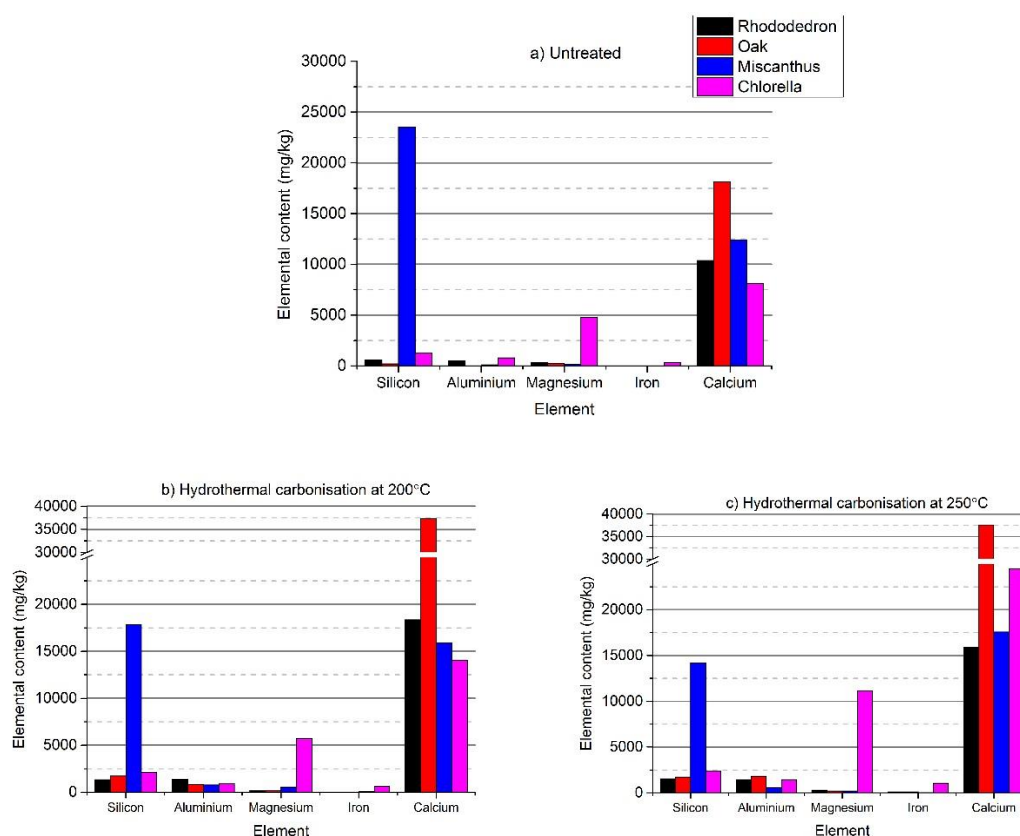


Figure 4-5 Trace elemental analysis of hydrothermal chars produced at two different temperatures.

In figure 4-5, the differences between concentrations of trace elements between the two different process temperatures are small, except for silicon in miscanthus which reduces with temperature, and magnesium and calcium in chlorella which significantly increase. The concentrations of the five elements most likely to cause engine problems in the hydrochars are similar to those produce by pyrolysis at 400°C. The differences are that there is more calcium and aluminium in the hydrochars, but less magnesium.

Combining the proximate and ultimate analysis with the trace element analysis suggests the rhododendron material tested is the best terrestrial biomass as the chars have a good calorific value and low quantities of abrasive trace elements. Of the aquatic types, only chlorella is suitable as the other two tested have too much ash and a low calorific value. It is, however, predicted to be significantly more abrasive the rhododendron and oak chars.

4.4.3 Chars chosen for engine tests

The selection of chars for use as slurry fuels was based on the trace element, proximate and ultimate analysis. The first feedstock chosen was rhododendron because it has low concentrations of ash. Chlorella was selected because it is a third-generation feedstock, representing what could be a future fuel. The other aquatic feedstocks were high in ash and thus unlikely to be suitable. The shea sample was selected because it is a common agricultural

waste in many developing countries in Africa. Using agricultural residues as a fuel would reduce the deforestation issues caused by using woody biomass. The downside of this feedstock, however, is the concentration of silicon.

The pyrolysis temperature chosen for converting untreated biomass to chars for slurring was 400°C because at this temperature there was more volatile matter and less ash compared to higher temperature pyrolysis. For comparison, however, one pyrochar produced at 600°C from rhododendron was selected.

For slurry fuel tests the hydrochar produced at 250°C was selected because more volatile matter is present than in the pyrolysis chars, which should burn better in an engine. The lower hydrochar temperature at 200°C was not chosen as the fuel was not grindable.

Table 4-7 Trace elemental analysis of fuels used for tests.

Sample	P (mg/kg a.r.)	K (mg/kg a.r.)	Na (mg/kg a.r.)	Fe (mg/kg a.r.)	Mg (mg/kg a.r.)	Mn (mg/kg a.r.)	Ca (mg/kg a.r.)	Al (mg/kg a.r.)	Si (mg/kg a.r.)
Rhododendron	1207 ¹	289	176	13	327	28	10384	506 ¹	581 ¹
Rhododendron 400°C	5552 ¹	862	562	36	945	157	12279	607 ¹	778 ¹
Rhododendron 600°C	1559 ¹	1063	627	77	1255	191	14010	1086 ¹	1367 ¹
Rhododendron HTC 250°C	861 ¹	125	75	25	150	22	15895	1440 ¹	1487 ¹
Chlorella	23665 ¹	5096	3152	344	4781	51	8108	795 ¹	1264 ¹
Chlorella 400°C	53603 ¹	13428	8153	1439	12109	142	21492	1021 ¹	5500 ¹
Chlorella HTC 250°C	29765 ¹	713	952	1013	11161	129	24432	1401 ¹	2392 ¹
Shea	2317 ¹	10018	224	526	925	13	2431	N.D.	34101 ¹
Shea 400°C	2820 ¹	25194	255	1410	1812	41	4692	1402 ¹	42757 ¹
Shea HTC 250°C	1766 ¹	2139	238	656	1276	22	3883	605 ¹	15164 ¹

¹Performed by XRF

N.D denotes not detected

Table 4-7 shows the trace element analysis of the most common elements in the chars selected for use as a slurry fuel from the original six starting materials, as well as the shea residue which was also selected. The shea derived fuels contain small concentrations of calcium in comparison to the other fuels but large amounts of silicon which could pose an abrasion issue. The advantages of the shea chars, however, is the high volatile matter and calorific value.

Another potentially important element is potassium which is known to cause corrosion when biomass has been used in boilers (Davidsson et al., 2007). The effect of potassium and alkali

metals in general on corrosion during combustion of slurry fuels in an internal combustion engine, however, is less understood. The presence of potassium in the rhododendron hydrochar is low (less than even the raw material) because of the leaching effect, whereas in the pyrolysis chars, it is high. The low melting point of potassium-based compounds means that droplets could form and solidify onto parts of the engine such as the cylinder head (Nutralapati et al., 2007; Teixeira et al., 2012). On the other hand, as potassium is relatively soft, it may be removed by the vertical action of the piston rings against the surface before deposits can build up. Another possibility is that it solidifies on contact with the engine lube oil film and is eventually washed into the sump.

Compared to coals, which are the typically used solid fuel for slurry engines, the materials chosen have a number of advantages. The main advantage is that aluminium and silicon, which form hard compounds, are present in only small amounts. Spears and Tewalt (2009) found that from 38 samples of bituminous coal extracted from the Parkgate seam, UK, the average aluminium content was 1.15 %wt. and the median was 0.65 %wt.. The mean silicon content was found to be 1.66 %wt. and median 0.96 %wt.. Kubešová et al. (2016) investigated 12 Turkish lignite coals finding the range of aluminium to be 0.41-4.52 %wt. and the mean content was 1.59 %wt.. The silicon content for these 12 samples was found to be in the range of 2.3-14.5 %wt.. Of the biochars selected, the quantity of aluminium is 0.15 %wt. or less. Silicon is also more favourable in most plant biomass chars. Apart from the HTC and pyrolysis chars from shea, containing 1.5 and 4.3 %wt. respectively, the rest favour well in comparison to coal. The chlorella HTC at 250°C and pyrolysis at 400°C char contain 0.55 %wt. and 0.24 %wt. of silicon respectively and the rhododendron chars contain a maximum of 0.15 %wt.. As these are the two most abrasive elements, the lower amounts in biochars represent a significant advantage over coal as a slurry fuel.

4.4.4 Structure and ignition temperature of chars

Table 4-8 shows the recalcitrance of the materials selected for tests, the temperature at which half the mass is removed in an air atmosphere. Untreated rhododendron and shea have a similar recalcitrance index, approximately 325°C, and significantly lower than chlorella, which is 405°C. Figure 4-6 shows the derivative of the mass loss varies significantly between the three materials. Rhododendron begins to slowly devolatilise at approximately 250°C then sees a rapid mass loss as the temperature approaches 326°C. After this, the rate of mass loss reduces and remains steady until 500°C when it is completely burned out. Chlorella also has two distinct combustion regions, but the later char combustion stage is more significant than with rhododendron. Devolatilisation occurs from 200°C at a slower rate than rhododendron and shea, increasing the overall recalcitrance. A second peak occurs later at 575°C which is the

fixed carbon burnout, continuing until 650°C. Shea has more distinct regions of mass loss, possibly for the different types of lipids which remain after the butter extraction process. The onset of the mass loss is slightly earlier than rhododendron and continues slightly longer until 525°C.

The chars produced follow a similar trend to the starting materials in that the ones with the lowest recalcitrance index come from the biomass with the lowest initial value. The pyrolysis char from shea at 400°C has a significantly lower recalcitrance than the ones produced from other materials, shown in table 4-8. Despite untreated rhododendron and shea having almost identical recalcitrance, the chars produced at 400°C vary by nearly 60°C. This means the shea char produced at 400°C consists of smaller aromatic structures which break down at lower temperatures (Ikeya et al., 2011; Wurster et al., 2013). This is a considerable advantage for shea pyrolysis char produced at 400°C compared to the rhododendron equivalent for use as an engine slurry fuel. Figure 4-6c shows that there are two parts to the oxidation of shea char, one that peaks just before 400°C and another after 450°C.

Table 4-8 Recalcitrance of chars and chemical shift of methanol sorbed to char. Dash denotes not determined.

<i>Sample</i>	<i>Recalcitrance (°C)</i>	<i>Methanol peak shift (ppm)</i>
<i>Rhododendron</i>	326	1.18
<i>Rhododendron 400°C</i>	443	0.54
<i>Rhododendron 600°C</i>	487	-4.12
<i>Rhododendron 800°C</i>	561	-8.00
<i>Rhododendron HTC 200°C</i>	345	-
<i>Rhododendron HTC 250°C</i>	368	1.06
<i>Chlorella</i>	405	1.10
<i>Chlorella 400°C</i>	507	0.38
<i>Chlorella 600°C</i>	549	-4.21
<i>Chlorella 800°C</i>	574	-7.45
<i>Chlorella HTC 200°C</i>	404	-
<i>Chlorella HTC 250°C</i>	461	0.94
<i>Shea</i>	323	-
<i>Shea 400°C</i>	387	-
<i>Shea HTC 250°C</i>	375	-

The high volatile matter value for the shea pyrolysis char produced at 400°C is consistent with the low recalcitrance. However, the chlorella char produced under the same conditions has a higher volatile matter content than shea but a higher recalcitrance. The reason for this could be that the compounds break down at a higher temperature in chlorella before releasing of volatile matter. From the ultimate analysis, chlorella contains more nitrogen, suggesting more protein which might increase the recalcitrance index. Knicker (2010) found that N-rich material

produced a char which has greater heat resistance by creating a “black nitrogen” which is incorporated into the large aromatic structures.

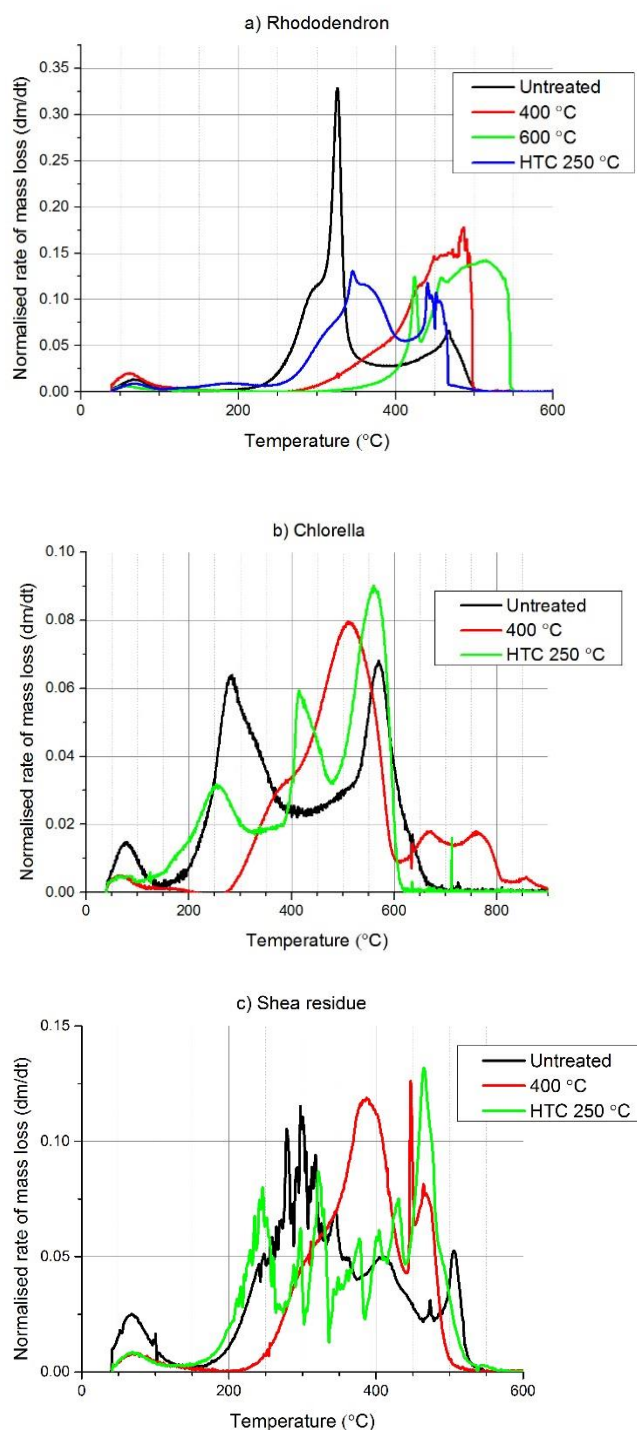


Figure 4-6 Temperature programmed oxidation profiles of solid fuels used in slurry tests.

The oxidation of the two pyrolysis chars from rhododendron against temperature, shown in figure 4-6a, occur in a single broad region which abruptly ends once the fixed carbon has burned. The mass loss of the char produced at 400°C begins at 275°C and ends at 500°C, and 325-550°C for the 600°C pyrochar. At the higher temperature of 600°C, the rhododendron char is still less recalcitrant than the chlorella char at 400°C. The results show that this increase

in pyrolysis temperature affects how easily the char will burn. The difference in the recalcitrance and temperature of complete burnout between the two rhododendron pyrolysis chars is 44°C and 50°C respectively, which is significant but may not prevent the fuel burning in a diesel engine. Therefore, the inclusion of the 600°C pyrolysis char in engine testing is still warranted.

The shea hydrochar produced at 250°C has a higher recalcitrance index than the rhododendron equivalent, despite shea pyrochar made at 400°C having a lower recalcitrance than the rhododendron 400°C pyrochar. An advantage of HTC over pyrolysis for the application of slurry fuels is that a degree of carbonisation occurs but the aromatic structures are smaller and so are less thermally stable (Gronwald et al., 2016). Another advantage, which the oxidation profiles in figure 4-6 show, is that the burnout is complete slightly earlier than compared to the original material in all three instances. One reason might be the change in the ash chemistry occurring from the removal of some elements during the process. However, reduction of ash is usually associated with increasing recalcitrance. Windeatt et al. (2014) found that washing pyrolysis chars increased recalcitrance as potassium removed has a catalytic effect.

Additionally, the shift in the peak of labelled methanol added to the materials produced from rhododendron and chlorella, following the method in 3.4.9 is also shown in table 4-8. The amount the methanol peak shifts in relation to the chemical shift of methanol not adsorbed to the surface of a material gives an indication of the degree of aromatic condensation in the material. In terms of the size of aromatic structures in the pyrochars produced at 400°C, the change in the methanol peak shift from the starting material is small, suggesting the aromatic structures are not much larger than in lignin.

The change in methanol peak shift between pyrochars produced at 400 and 600°C is more pronounced than the change in recalcitrance index. The increasing size of aromatic structures in the char with increased pyrolysis temperature suggests the reactivity of the material is reduced, which is shown by the increased recalcitrance index. Combustion in a diesel engine is more limited by time rather than temperature. The temperature inside a diesel engine cylinder is heterogeneous and the peak mean in-cylinder temperature generally exceeds 1500K even when idling, which is significantly higher than the char burnout temperature (Rahmani et al., 2017; Tan and Azimov, 2017; Wang et al., 2007). As the time in the combustion chamber for the chars is short, the limiting factor is likely the rate of combustion of the char rather than the temperature needed for combustion.

With the pyrolysis temperature further increased to 800°C in table 4-8, the change in methanol peak shift of the rhododendron char further decreases showing that aromatic condensation is still occurring. The rhododendron and chlorella chars show similar values in methanol peak shift. Rhododendron shows more aromatic condensation at 800°C, but chlorella has more at 400 and 600°C.

Another advantage of hydrochars over pyrochars as a fuel for diesel engines is the low aromatic condensation shown by the small change in methanol peak shift from the untreated feedstock. Hence, the char produced by HTC at 250°C from both rhododendron and chlorella should be more reactive than the pyrochars of the same materials.

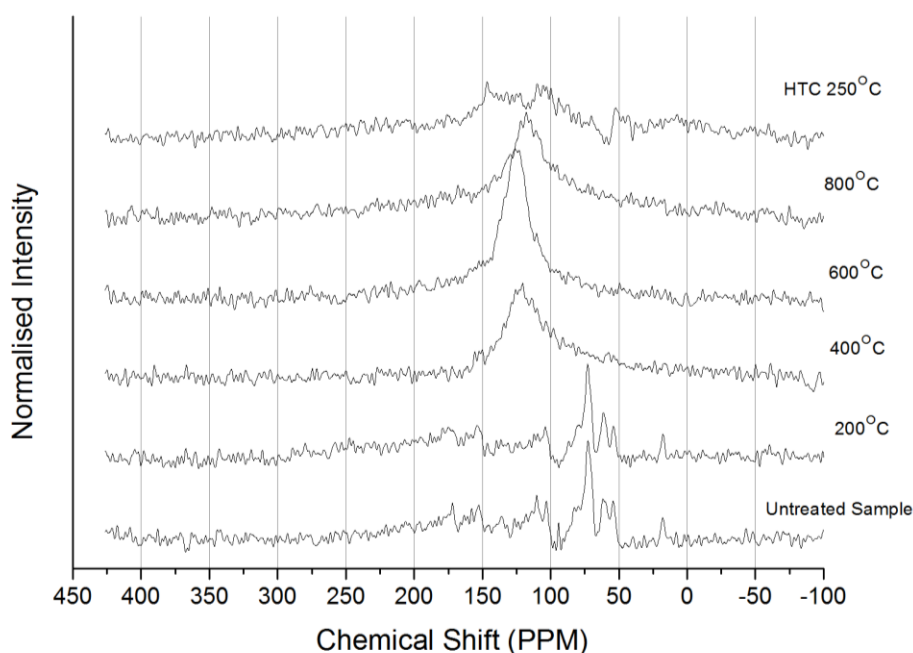


Figure 4-7 Carbon-13 NMR of chars produced from rhododendron.

The structure of carbon in a fuel affects the tendency to soot. In flame and engine studies, the sooting tendency related to the fuel structure is ordered alkanes < cycloalkanes < aromatics (Das et al., 2017a). Soot also increases with the number of C-C bonds (Park et al., 2017). As the H/C ratio is higher for diesel than the chars produced it follows that the number of C-C bonds in the chars are higher when comparing a quantity with the same calorific value. Figure 4-7 shows the solid-state C^{13} NMR for the chars produced from rhododendron. In the untreated rhododendron sample, the presence of lignin is evident from the signal between 100-200 ppm (parts per million), which is the region associated with aromatic carbon. Hemicellulose and cellulose occur at 50-100 ppm in a region of the spectrum which is associated with oxygenated aliphatics, alkenes and cycloalkanes.

At 200°C pyrolysis, the carbon structure remains similar to the untreated rhododendron material and it is not until the 400°C sample that a distinct difference in the carbon structure is detected by NMR. In the signal for the rhododendron pyrolysis char produced at 400°C, a large broad peak occurs in the region associated with aromatic hydrocarbons. For reference, 128 ppm is the chemical shift for benzene, the simplest aromatic compound. The point of maximum signal intensity is to the right of this point suggesting that the level of aromatic condensation is relatively low, and the carbon is still shielded by hydrogen, which has a lower electronegativity. The position of the peak to the right of benzene and an upfield skew suggests the presence of alkenes and cycloalkanes. As aromatic carbon produces the most soot, it is advantageous at the pyrolysis temperature of 400°C that some carbon occurs in other non-aromatic forms. The skew also means that the oxygen atoms are not closely associated or within heterocycles. At a pyrolysis temperature of 400°C, there is no sign of the original cellulose and hemicellulose. During slow pyrolysis cellulose and hemicellulose decompose between 225-325°C and 325-375°C respectively which fits with the absence of signal in figure 4-7 (Di Blasi, 2008). Lignin decomposes over a wider range of 250-500°C, so part of the structure may remain at the pyrolysis temperature of 400°C but is obscured by the aromatic material produced during the process. By comparing with the signal of the original material part appears to have remained between 150-175 ppm.

Carbonisation continues at 600°C and the carbon structure becomes less diverse. The corresponding chemical shift to the most intense peak is now 126ppm, having shifted further into the aromatic region from 400°C. At this point, nearly all the carbon falls within the aromatic region and so it is likely a slurry made with this material will produce more soot. With the molar H/C ratio at 0.3, the aromatic compounds will already contain several rings- coronene (six-ringed) for example, has a ratio of 0.5. It is not clear if the tendency to soot will increase with the size of the aromatic rings because, as liquid and gaseous fuels are almost solely used in internal combustion engines, there has been little investigation. Logic would suggest that the tendency to soot will increase with increasing rings in a structure because they are harder to burn. Oxygen remains which should have an overall benefit in reducing soot.

At 800°C, the peak begins to broaden again, even though the material has become more carbonised and more homogeneous. This has been discussed previously in Freitas et al. (2001) which produced high temperature coconut chars and compared them to graphite. It was found that the peaks broadened with temperature and shifted upfield creating spectra similar to graphite as the carbon becomes more ordered within the basal planes. It is this alignment which causes the unexpected broadening of the peak.

The hydrochar produced from Rhododendron at 250°C has a more diverse carbon structure than the pyrolysis chars. A signal response occurs across the entirety of the aromatic region (100-170ppm) shows this diversity. The broadness of signal in this region shows there are rings containing or linked to electronegative atoms, most likely oxygen from the ultimate analysis. There is no evidence of residual hemicellulose or cellulose as the peak between 50-100ppm is no longer present. There is also more carbon in the region of 0-50ppm than in the original material associated with alkanes and methyl groups. Within the range of 50-100ppm, a signal is present which is associated with oxygenated aliphatics.

Figure 4-8 shows the same selection of chars but made using chlorella. The constituent parts appear in different regions than the rhododendron biomass tested. Between 0-40ppm is non-oxygenated aliphatic carbon related to lipids. From 40-80ppm are oxygenated alkanes related to carbohydrates and esters in triglycerides. The peaks from 100-180ppm could be a number of compounds including alkene groups in lipids and aromatic amino acids (Akhter et al., 2016; Sarpal et al., 2015).

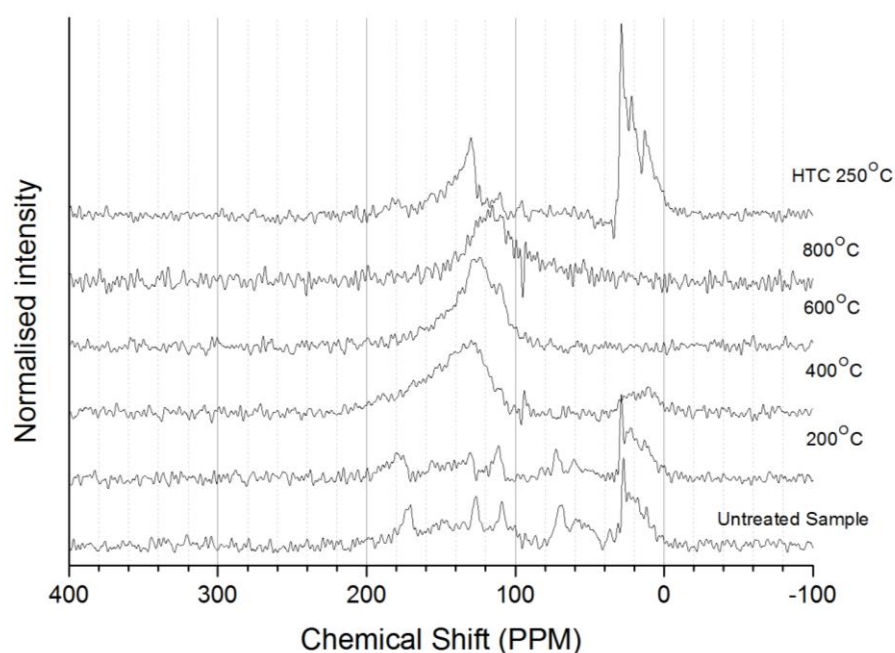


Figure 4-8 Carbon-13 NMR of chars produced from chlorella.

As with rhododendron, chlorella does not carbonise until the 400°C pyrolysis sample. There are differences between the carbon structure of the samples produced at 400°C from rhododendron and chlorella. Fewer alkenes and substituted aliphatics are formed during the carbonisation of chlorella at 400°C than rhododendron, shown by a weaker signal upfield of the main aromatic peak. Nitrogen and oxygen are also substituted or part of the aromatic rings shown by the increased signal downfield of the peak. Some of the aliphatic material from lipids present appears to survive the process. The survival of this aliphatic material suggests that less

soot will be produced. The potential presence of oxygen in aromatic rings has an unknown effect because oxygenated alternatives to conventional diesel are usually straight chained, such as biodiesel.

At 600°C, the aliphatic compounds are lost as are some of the electronegative elements associated with aromatic structures. The peak is, however, broader than the equivalent rhododendron char showing there is still a higher presence of electronegative elements. Further carbonisation at 800°C sees a similar peak broadening as with the woody biomass.

The lipids in chlorella do not appear affected by HTC at 250°C, seen as a similar peak in the 0-40ppm range as observed in the raw material. The remaining lipids are advantageous as the tendency of the fuel to create soot will likely be less than were it to be converted to aromatic hydrocarbons. In the aromatic region, the carbon structure is less diverse than with rhododendron. The electronegative elements are again bonded to aromatic compounds seen in the downfield skew. The C=O bond in the range of 160-180ppm remains after hydrothermal processing.

The most important difference between the structures of the chars made from the two types of material is perhaps how oxygen, which can reduce soot nucleation, is incorporated into the material. Oxygen in chlorella char appears to be part of the aromatic rings or bonded to them, whereas in rhododendron char it is more likely within aliphatic groups. How and when oxygen is released from different compounds will affect how much soot is produced.

4.5 Conclusions

There are many potentially suitable plant derived biomass for conversion to slurry fuel. The majority are in the category of woody biomass. The advantage of this type of biomass is the generally low presence of silicon and aluminium, which are abrasive elements. It is the key benefit of using woody biomass derived materials compared to agricultural residues and the most commonly used fuel for slurring, coal.

Comparison of six different types of biomass samples used to produce six thermally treated chars each showed that *Rhododendron ponticum* was the most suitable of those tested- marginally better than oak because the calcium content was lower. Miscanthus, a species commonly cultivated as an energy crop, is less suitable because the silicon content is high. Macroalgae is not suitable for slurry fuels because, as shown in two samples of this type tested, the ash and sulphur contents are high, and the calorific value is low. Microalgae is potentially suitable but only after HTC which lowers the ash content and produces a char with high calorific value. The two main issues with the microalgae tested, chlorella, was the large quantities of nitrogen and aluminium.

Analysis of char produced from a number of common types of biomass in Nepal found many would be suitable for use as a slurry fuel. One potential feedstock is *Eupatorium adenophorum* which is invasive to Nepal and thus could be cleared and converted to electricity by conversion to slurry fuels. Most woody biomass samples collected and analysed were found to be suitable feedstocks, but the most promising, based on properties and abundance, were *Shorea robusta* and *Pinus spp.*.

A set of agricultural residues were tested, seven from Nepal and one, shea residue, from Ghana. *Saccharum officinarum* bagasse had the lowest calcium content of Nepal biomass tested and medium silicon, so was therefore of similar suitability as the woody biomass species tested. Shea residue is a material made less desirable by high silicon content, but the chars produced are high volatile matter which means they are expected to burn well in an engine. Maize cob is another material which may be suitable for producing slurry fuels.

Preventing wear to the engine caused by char in the slurry is important. In developing countries, one method to reduce wear would be to remove bark which is expected to reduce silicon and calcium, the two elements most likely to cause issues. Having a simple test for silicon and calcium for developing countries using slurry fuel engines would be helpful in selecting appropriate feedstocks.

The thermal conversion route is important when producing a slurry fuel. HTC removed large quantities of potassium from the material processed which will reduce the likelihood of corrosion. The process improves grindability, but more volatile matter is retained than through pyrolysis. Another advantage compared to pyrolysis is more aliphatic material is retained which has a lower tendency to convert to soot during combustion. The H/C ratio of hydrochars produced was higher which means that lower specific CO₂ emissions are predicted than pyrolysis chars. However, pyrolysis produced chars have a higher calorific value than HTC when the initial material is woody biomass. Whilst the results show that HTC is likely the best thermal conversion route of the two, pyrolysis is the only one to be operated in developing countries.

4.6 References

- Abdullah, H. Mediaswanti, K.A. and Wu, H. 2010. Biochar as a Fuel: 2. Significant Differences in Fuel Quality and Ash Properties of Biochars from Various Biomass Components of Mallee Trees. *Energy & Fuels*. **24**(3), pp.1972-1979.
- Akhter, M. Dutta Majumdar, R. Fortier-McGill, B. Soong, R. Liaghati-Mobarhan, Y. Simpson, M. Arhonditsis, G. Schmidt, S. Heumann, H. and Simpson, A.J. 2016. Identification of aquatically available carbon from algae through solution-state NMR of whole ¹³C-labelled cells. *Analytical and Bioanalytical Chemistry*. **408**(16), pp.4357-4370.

- Almeida, G.Brito, J.O. and Perré, P. 2010. Alterations in energy properties of eucalyptus wood and bark subjected to torrefaction: The potential of mass loss as a synthetic indicator. *Bioresource Technology*. **101**(24), pp.9778-9784.
- Bhattarai, L.N. 2013. Exploring the Determinants of Fuel wood Use in Western Hill Nepal: An Econometric Analysis. *J. Econ. Lit.* **11**, pp.26-34.
- British Standards Institution. 2013. *BS EN 590:2013+A1:2017 Automotive fuels. Diesel. Requirements and test methods*. London, UK: British Standards Institution.
- Das, D.D.McEnally, C.S.Kwan, T.A.Zimmerman, J.B.Cannella, W.J.Mueller, C.J. and Pfefferle, L.D. 2017a. Sooting tendencies of diesel fuels, jet fuels, and their surrogates in diffusion flames. *Fuel*. **197**, pp.445-458.
- Das, I.Jagger, P. and Yeatts, K. 2017b. Biomass Cooking Fuels and Health Outcomes for Women in Malawi. *EcoHealth*. **14**(1), pp.7-19.
- Das, P.Ganesh, A. and Wangikar, P. 2004. Influence of pretreatment for deashing of sugarcane bagasse on pyrolysis products. *Biomass and Bioenergy*. **27**(5), pp.445-457.
- Davidsson, K.O.Åmand, L.-E.Leckner, B.Kovacevik, B.Svane, M.Hagström, M.Pettersson, J.B.C.Pettersson, J.Asteman, H.Svensson, J.-E. and Johansson, L.-G. 2007. Potassium, Chlorine, and Sulfur in Ash, Particles, Deposits, and Corrosion during Wood Combustion in a Circulating Fluidized-Bed Boiler. *Energy & Fuels*. **21**(1), pp.71-81.
- Deka, D.Sedai, P. and Chutia, R.S. 2014. Investigating Woods and Barks of Some Indigenous Tree Species in North-East India for Fuel Value Analysis. *Energy Sources, Part A: Recovery, Utilization, and Environmental Effects*. **36**(17), pp.1913-1920.
- Department for Forest Research and Survey. 2015. *State of Nepal's Forests*. Kathmandu, Nepal.
- Dhakal, A.Cockfield, G. and Maraseni, T.N. 2015. Deriving an index of adoption rate and assessing factors affecting adoption of an agroforestry-based farming system in Dhanusha District, Nepal. *Agroforest. Syst.* **89**(4), pp.645-661.
- Di Blasi, C. 2008. Modeling chemical and physical processes of wood and biomass pyrolysis. *Progress in Energy and Combustion Science*. **34**(1), pp.47-90.
- Filbakk, T.Jirjis, R.Nurmi, J. and Høibø, O. 2011. The effect of bark content on quality parameters of Scots pine (*Pinus sylvestris* L.) pellets. *Biomass and Bioenergy*. **35**(8), pp.3342-3349.
- Freitas, J.C.Emmerich, F.G.Cernicchiaro, G.R.Sampaio, L.C. and Bonagamba, T.J. 2001. Magnetic susceptibility effects on ¹³C MAS NMR spectra of carbon materials and graphite. *Solid State Nucl Magn Reson*. **20**(1-2), pp.61-73.
- Gronwald, M.Vos, C.Helfrich, M. and Don, A. 2016. Stability of pyrochar and hydrochar in agricultural soil - a new field incubation method. *Geoderma*. **284**, pp.85-92.
- Ikeya, K.Hikage, T.Arai, S. and Watanabe, A. 2011. Size distribution of condensed aromatic rings in various soil humic acids. *Organic Geochemistry*. **42**(1), pp.55-61.
- Ishigaki, H. and Buckley, D.H. 1981. *Effects of Environment on Microhardness of Magnesium Oxide*. Cleveland, OH: NASA.
- Kang, S.Li, X.Fan, J. and Chang, J. 2012. Characterization of Hydrochars Produced by Hydrothermal Carbonization of Lignin, Cellulose, d-Xylose, and Wood Meal. *Industrial & Engineering Chemistry Research*. **51**(26), pp.9023-9031.
- Knicker, H. 2010. "Black nitrogen" – an important fraction in determining the recalcitrance of charcoal. *Organic Geochemistry*. **41**(9), pp.947-950.
- Kubešová, M.Orucoglu, E.Hacıyakupoglu, S.Erenturk, S.Krausová, I. and Kučera, J. 2016. Elemental characterization of lignite from Afşin-Elbistan in Turkey by k O-NAA. *Journal of Radioanalytical and Nuclear Chemistry*. **308**(3), pp.1055-1062.
- Li, L.Wang, Y.Xu, J.Floras, J.R.V.Hoque, S. and Berge, N.D. 2018. Quantifying the sensitivity of feedstock properties and process conditions on hydrochar yield, carbon content, and energy content. *Bioresource Technology*. **262**, pp.284-293.
- Lu, X. and Berge, N.D. 2014. Influence of feedstock chemical composition on product formation and characteristics derived from the hydrothermal carbonization of mixed feedstocks. *Bioresource Technology*. **166**, pp.120-131.

- Mahdi, D.Vahid, H. and Mohammad Ali, E. 2017. Solid nanoparticle and gaseous emissions of a diesel engine with a diesel particulate filter and use of a high-sulphur diesel fuel and a medium-sulphur diesel fuel. *Proceedings of the Institution of Mechanical Engineers, Part D: Journal of Automobile Engineering*. **231**(7), pp.941-951.
- McBeath, A.V.Smernik, R.J.Krull, E.S. and Lehmann, J. 2014. The influence of feedstock and production temperature on biochar carbon chemistry: A solid-state ¹³C NMR study. *Biomass and Bioenergy*. **60**, pp.121-129.
- Ministry of Agricultural Development 2014. *Statistical Information on Nepalese Agriculture 2013/2014*. Kathmandu.
- Ministry of Forests and Soil Conservation. 2009. *Nepal Forestry Outlook Study*. [Online]. Available from: <http://www.fao.org/docrep/014/am250e/am250e00.pdf>.
- Muñoz, M.Moreno, F.Monné, C.Morea, J. and Terradillos, J. 2011. Biodiesel improves lubricity of new low sulphur diesel fuels. *Renewable Energy*. **36**(11), pp.2918-2924.
- Mushrush, G.W.Quintana, M.A.Bauserman, J.W. and Willauer, H.D. 2011. Post-refining removal of organic nitrogen compounds from diesel fuels to improve environmental quality. *Journal of Environmental Science and Health, Part A*. **46**(2), pp.176-180.
- Nutalapati, D.Gupta, R.Moghtaderi, B. and Wall, T.F. 2007. Assessing slagging and fouling during biomass combustion: A thermodynamic approach allowing for alkali/ash reactions. *Fuel Processing Technology*. **88**(11), pp.1044-1052.
- Agroforestry Database: a tree reference and selection guide version 4.0*. 2009. [Online database].
- Pandey, S.S.Maraseni, T.N.Cockfield, G. and Gerhard, K. 2014. Tree Species Diversity in Community Managed and National Park Forests in the Mid-Hills of Central Nepal. *Journal of Sustainable Forestry*. **33**(8), pp.796-813.
- Pandit, R. and Paudel, K.C. 2013. Introduction of Raikhanim (*Ficus semicordata*) in a Maize and Finger-Millet Cropping System: An Agroforestry Intervention in Mid-Hill Environment of Nepal. *Small-Scale For.* **12**(2), pp.277-287.
- Park, W.Park, S.Reitz, R.D. and Kurtz, E. 2017. The effect of oxygenated fuel properties on diesel spray combustion and soot formation. *Combustion and Flame*. **180**, pp.276-283.
- Paudel, S. and Sah, J.P. 2015. Effects of Different Management Practices on Stand Composition and Species Diversity in Subtropical Forests in Nepal: Implications of Community Participation in Biodiversity Conservation. *Journal of Sustainable Forestry*. **34**(8), pp.738-760.
- Rahmani, R.Rahnejat, H.Fitzsimons, B. and Dowson, D. 2017. The effect of cylinder liner operating temperature on frictional loss and engine emissions in piston ring conjunction. *Applied Energy*. **191**, pp.568-581.
- Rana, E.A.K.Thwaites, R.I.K. and Luck, G. 2016. Trade-offs and synergies between carbon, forest diversity and forest products in Nepal community forests. *Environmental Conservation*. **44**(1), pp.5-13.
- Roy Choudhury, P. 1992. Slurry fuels. *Progress in Energy and Combustion Science*. **18**(5), pp.409-427.
- Saarela, K.E.Harju, L.Rajander, J.Lill, J.O.Heselius, S.J.Lindroos, A. and Mattsson, K. 2005. Elemental analyses of pine bark and wood in an environmental study. *Science of The Total Environment*. **343**(1), pp.231-241.
- Saeed, M.A.Andrews, G.E.Phylaktou, H.N. and Gibbs, B.M. 2016. Global kinetics of the rate of volatile release from biomasses in comparison to coal. *Fuel*. **181**, pp.347-357.
- Sarpal, A.S.Teixeira, C.M.L.L.Silva, P.R.M.Lima, G.M.Silva, S.R.Monteiro, T.V.Cunha, V.S. and Daroda, R.J. 2015. Determination of lipid content of oleaginous microalgal biomass by NMR spectroscopic and GC-MS techniques. *Analytical and Bioanalytical Chemistry*. **407**(13), pp.3799-3816.
- Shackelford, J. and Alexander, W. 2001. Mechanical Properties of Materials. In: Shackelford, J. and Alexander, W. eds. *CRC Materials Science and Engineering Handbook*. Third ed. Boca Raton, US: CRC.

- Shrestha, B.B. 2007. Fuelwood harvest, management and regeneration of two community forests in Central Nepal. *Himalayan Journal of Sciences*. **3**(5).
- Shrestha, R.P. and Nepal, N. 2016. An assessment by subsistence farmers of the risks to food security attributable to climate change in Makwanpur, Nepal. *Food Security*. **8**(2), pp.415-425.
- Smith, A.M.Singh, S. and Ross, A.B. 2016. Fate of inorganic material during hydrothermal carbonisation of biomass: Influence of feedstock on combustion behaviour of hydrochar. *Fuel*. **169**, pp.135-145.
- Soehngen, E.E.Research, U.S.E.Administration, D.Soehngren, E. and Associates. 1976. *The development of coal-burning diesel engines in Germany: a state-of-the-art review*. Energy Research and Development Administration.
- Soloiu, V.Lewis, J.Yoshihara, Y. and Nishiwaki, K. 2011. Combustion characteristics of a charcoal slurry in a direct injection diesel engine and the impact on the injection system performance. *Energy*. **36**(7), pp.4353-4371.
- Spears, D.A. and Tewalt, S.J. 2009. The geochemistry of environmentally important trace elements in UK coals, with special reference to the Parkgate coal in the Yorkshire– Nottinghamshire Coalfield, UK. *International Journal of Coal Geology*. **80**(3), pp.157-166.
- Tan, X. and Azimov, U. 2017. Diesel engine downsizing with application of biofuels. *International Journal of Energy and Environment*. **8**(5), pp.413-426.
- Teixeira, P.Lopes, H.Gulyurtlu, I.Lapa, N. and Abelha, P. 2012. Evaluation of slagging and fouling tendency during biomass co-firing with coal in a fluidized bed. *Biomass and Bioenergy*. **39**, pp.192-203.
- Wang, D.Zhang, C. and Wang, Y. 2007. A Numerical Study of Multiple Fuel Injection Strategies for NO_x Reduction from DI Diesel Engines. *International Journal of Green Energy*. **4**(4), pp.453-470.
- Webb, E.L. and Dhakal, A. 2011. Patterns and drivers of fuelwood collection and tree planting in a Middle Hill watershed of Nepal. *Biomass Bioenerg*. **35**(1), pp.121-132.
- Wibberley, L. and Osborne, D. 2015. Premium coal fuels with advanced coal beneficiation. [Online]. Available from: [http://www.jamesoncell.com/EN/Downloads/technical%20papers/Premium%20fuels%20Clearwater%20\(final%20paper\).pdf](http://www.jamesoncell.com/EN/Downloads/technical%20papers/Premium%20fuels%20Clearwater%20(final%20paper).pdf).
- Wilson, R. 2007. *Clean coal diesel demonstration project: Final report*. Cambridge, USA: TIAX.
- Windeatt, J.H.Ross, A.B.Williams, P.T.Forster, P.M.Nahil, M.A. and Singh, S. 2014. Characteristics of biochars from crop residues: Potential for carbon sequestration and soil amendment. *Journal of Environmental Management*. **146**, pp.189-197.
- Wurster, C.M.Saiz, G.Schneider, M.P.W.Schmidt, M.W.I. and Bird, M.I. 2013. Quantifying pyrogenic carbon from thermosequences of wood and grass using hydrogen pyrolysis. *Organic Geochemistry*. **62**, pp.28-32.
- Yang, H.Yan, R.Chen, H.Lee, D.H. and Zheng, C. 2007. Characteristics of hemicellulose, cellulose and lignin pyrolysis. *Fuel*. **86**(12), pp.1781-1788.
- Zhang, H.Chen, C.Gray, E.M. and Boyd, S.E. 2017. Effect of feedstock and pyrolysis temperature on properties of biochar governing end use efficacy. *Biomass and Bioenergy*. **105**, pp.136-146.
- Zomer, R. and Menke, J. 1993. Site Index and Biomass Productivity Estimates for Himalayan Alder-Large Cardamom Plantations: A Model Agroforestry System of the Middle Hills of Eastern Nepal. *Mt. Res. Dev*. **13**(3), pp.235-255.

Chapter 5: Slurryability of char

5.1 Introduction

Converting char into a liquid slurry is an energy intensive and expensive process, the majority contributing process to the cost of the final fuel (Wilson, 2007). The energy usage is associated with micronisation of the initial material which contributes to the financial cost along with surfactants used to improve stability and flow properties.

This chapter first investigates the milling behaviour of charcoal. Ball milling was chosen as it was the most commonly used in literature. The first study was to optimise the grinding rates in a small single ball mill (3.5.1) using rhododendron pyrolysis char produced at 600°C. The second aspect investigates the influence of the sample being milled and the use of liquid dispersants. Rhododendron, Shea residue and Chlorella chars made via pyrolysis at 400°C and HTC at 250°C were studied.

The second section investigates the scaling up of the process from a single ball shaker mill to a 2L stirred media mill needed for producing enough fuel for engine testing (3.5.2). This type of ball mill was chosen as it had been successfully used in literature and the wet milling in the shaker mill had produced promising results.

The final part studies the use of surfactants for stabilising slurries containing 1% and 10%wt. charcoal (3.5.3). Simple systems containing different concentrations of a single surfactant were first studied before using mixtures in an attempt to further improve stability.

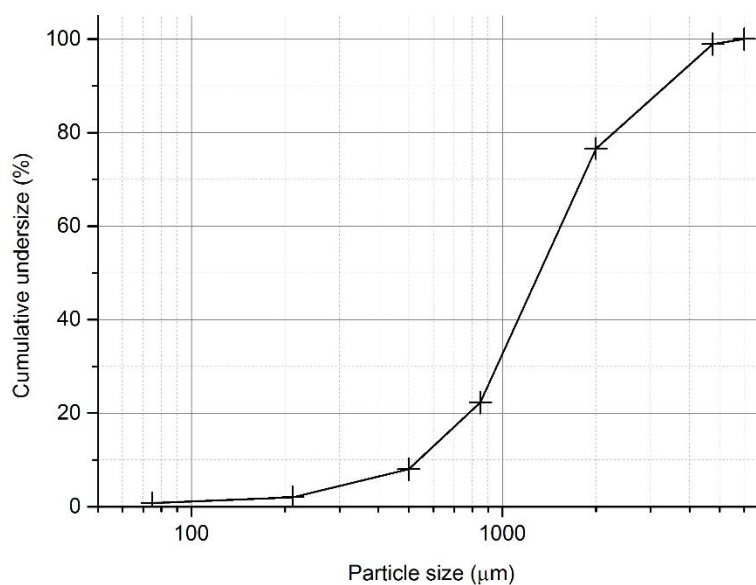
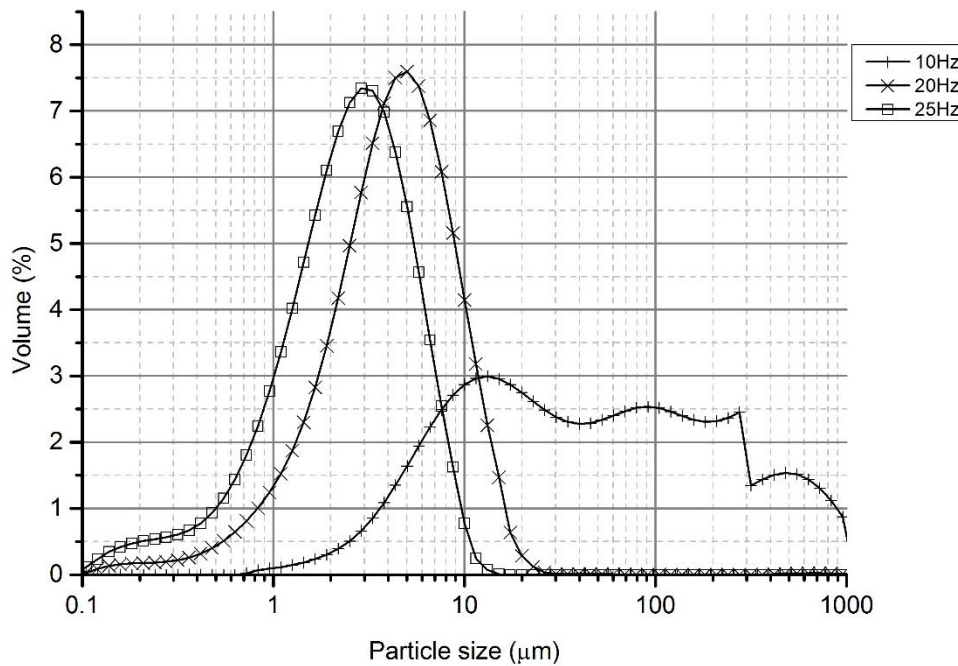


Figure 5-1 Cumulative undersize (weight percent) of Rhododendron chips after pyrolysis at 600°C.

5.2 Effect of milling parameters

The particle size distribution of charcoal chips after pyrolysis was determined by sieving (figure 5-1). Slightly over half of the particles by weight were in the region of 850-2000 μm . Also, the particles in this range represent the median size as roughly the same amount by weight are larger and smaller. Particles out of this range were discarded to reduce the influence of initial particle size.

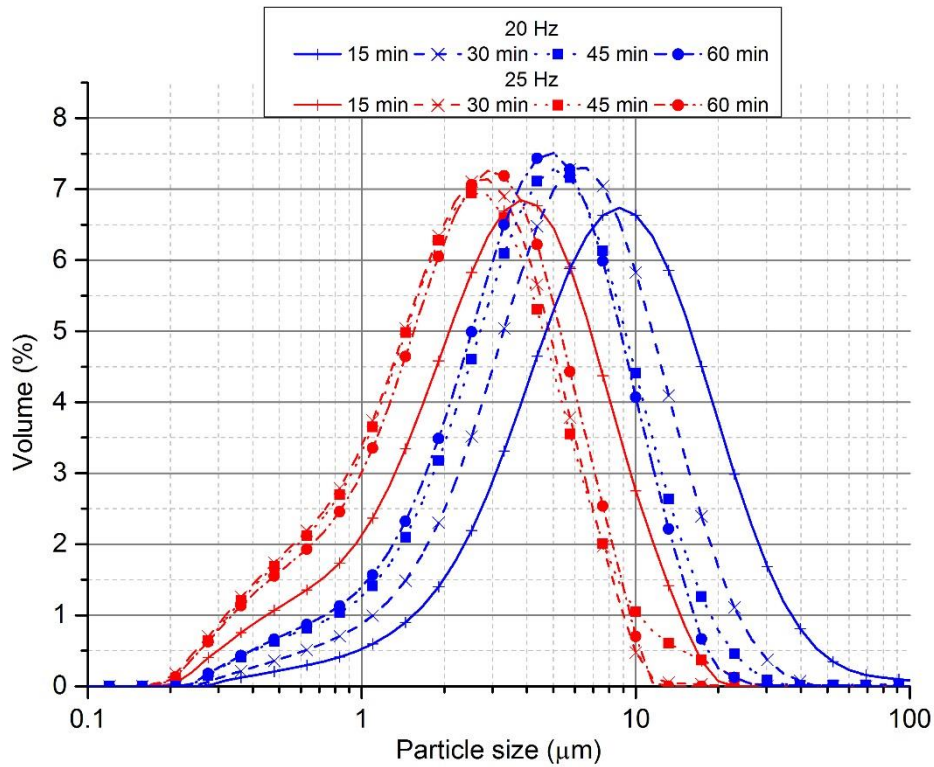


Frequency	$D(0.1)$	$D(0.5)$	$D(0.9)$	Sub 10 μm (%)	Sub 20 μm (%)
10 Hz	6.8	57.9	525.7	19.9	34.4
20 Hz	1.5	4.6	10.8	91.8	99.6
25 Hz	0.8	2.7	6.4	99.7	100

Figure 5-2 Lognormal volume distribution of Rhododendron 600°C pyrolysis char after milling for 1 hour using a single 10mm steel ball at different frequencies.

Figure 5-2 shows the effect of milling frequency on Rhododendron particles produced at 600°C using the Mixer Mill MM200 and the method in 3.5.1. At 10Hz the energy is too low to break particles sufficiently to produce a powder suitable for slurring. The size distribution of particles produced by milling at 20Hz for 1 hour is potentially suitable for slurring because the majority of the material is below 10 μm , a value that has been regarded to be an upper limit for the average size (Nicol, 2014). The wear of the piston rings and cylinder liner is thought to be caused by the incomplete combustion of (char)coal particles due to high viscosity, leading to poor atomization of the slurry and high content of coarse particles larger than 30 μm (Cui et al., 2008; Flynn et al., 1989; Schwalb, 1991). There are no large particles with a diameter similar to the injector orifices (220 μm) remaining which could block the injector holes. Increasing the milling frequency to 25Hz further reduced the average particle size, reducing the largest

particle diameter to below $20\mu\text{m}$. The median particle size was reduced from 4.6 to $2.7\mu\text{m}$ when the frequency was increased from 20 to 25Hz .

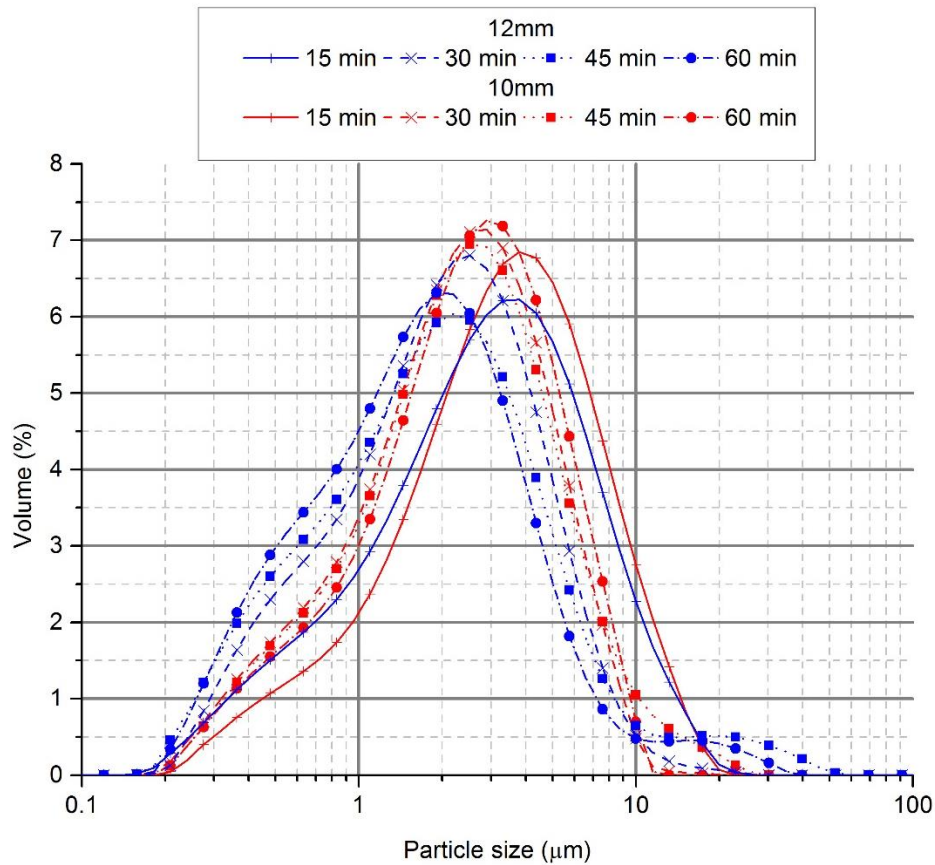


Frequency	Time (min)	D(0.1)	D(0.5)	D(0.9)	Sub $10\mu\text{m}$ (%)	Sub $20\mu\text{m}$ (%)
20 Hz	15	2.71	8.73	24.00	63.2	88.9
	30	1.95	6.10	15.13	80.9	97.3
	45	1.46	4.88	12.13	88.5	98.6
	60	1.38	4.54	10.68	92.0	99.7
25 Hz	15	0.97	3.58	9.20	94.8	99.5
	30	0.68	2.44	5.85	99.8	100
	45	0.70	2.50	6.58	97.3	99.8
	60	0.74	2.65	6.26	99.9	100

Figure 5-3 Comparison of Rhododendron 600°C pyrolysis char milled at two frequencies for different times.

Figure 5-3 investigates the change in distribution with time at the two frequencies which produced potentially viable particle size distribution for slurring in figure 5-2. At 20Hz the particle size distribution characteristics changed throughout the whole hour of testing. However, after 30 minutes, the particle distribution produced is potentially suitable because the majority of particles are below $10\mu\text{m}$ and the maximum size is significantly smaller than the injector holes. From 45 to 60 minutes of milling at 20Hz , the median (D(0.5)) changes little but the larger particles continue to reduce in size.

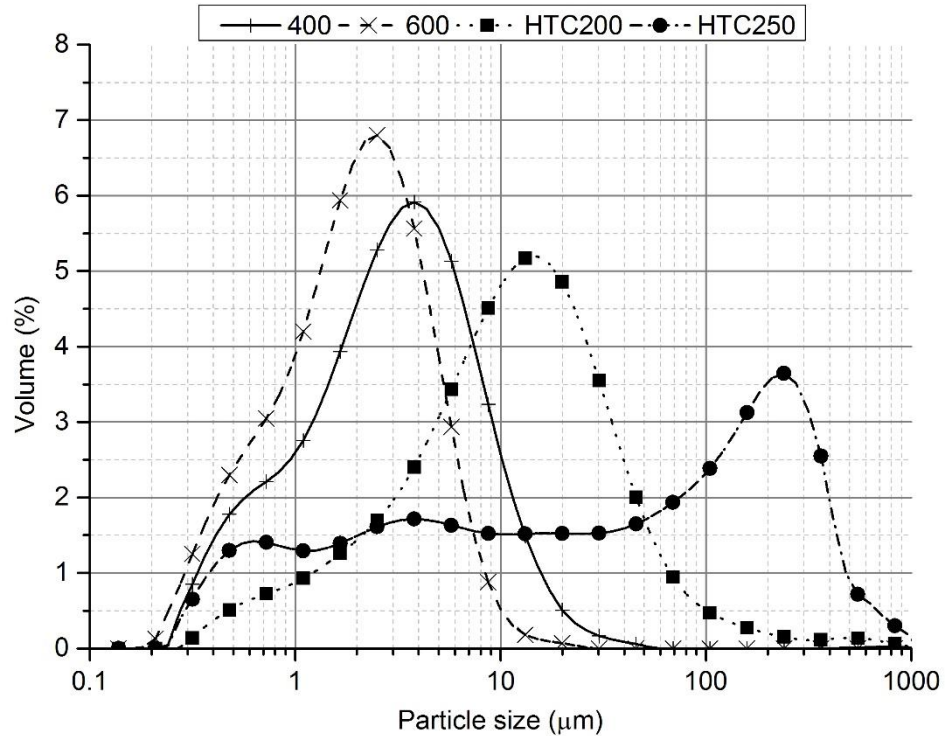
At 25Hz, the particle size distribution changes until 30 minutes is reached, after which the differences are marginal. In 15 minutes, the particle size is smaller than is achieved in an hour at 20Hz. The optimum milling conditions were chosen from the results as 25Hz milling frequency for 30 minutes because shorter times are less energy intensive, which is achieved at this frequency unlike at 20Hz.



Ball Size	Time (min)	D(0.1)	D(0.5)	D(0.9)	Sub 10 micron (%)	Sub 20 micron (%)
10mm	15	0.97	3.58	9.20	94.8	99.5
	30	0.68	2.44	5.85	99.8	100
	45	0.70	2.50	6.58	97.3	99.8
	60	0.74	2.65	6.26	99.9	100
12mm	15	0.73	3.09	8.55	95.7	100
	30	0.59	2.15	5.46	99.2	99.9
	45	0.52	2.00	6.25	95.5	98.0
	60	0.51	1.82	5.36	96.2	98.4

Figure 5-4 Effect of ball size on lognormal volume distribution of Rhododendron 600°C pyrolysis charcoal at 25Hz.

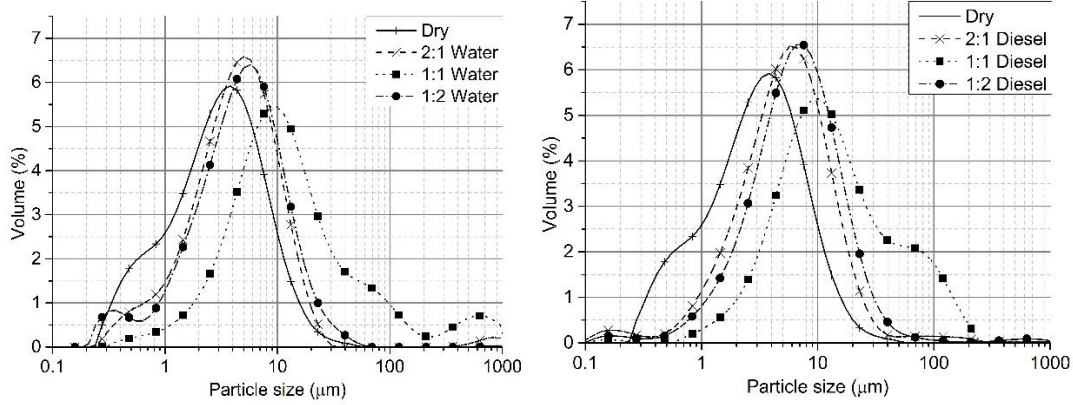
The size of the grinding ball was varied to determine the influence. Figure 5-4 compares the distribution of char milled with a 10 and 12mm steel ball. Using the larger ball produced generally smaller particles shown by D(0.1, 0.5, 0.9) values. However, after 30 minutes the particles begin to agglomerate, causing larger particles to reappear. The optimal test conditions used for further experiments were a 12mm ball milling for 30 minutes at 25Hz.



Char	$D(0.1)$	$D(0.5)$	$D(0.9)$	Sub 10 micron (%)	Sub 20 micron (%)
Pyrolysis 400°C	0.73	3.28	9.79	93.0	98.9
Pyrolysis 600°C	0.59	2.15	5.46	99.2	99.9
HTC 200°C	2.04	12.52	46.21	46.9	72.2
HTC 250°C	4.06	74.18	266.04	37.5	45.1

Figure 5-5 Effect of thermal treatment on Rhododendron char. Particle size distribution under optimised conditions

Figure 5-5 shows the influence of thermal treatment on the grindability of rhododendron chars. The pyrolysis char produced at the higher of the two temperatures, 600°C, had a narrower distribution profile and was easier to micronise. The sample produced by pyrolysis at 400°C, whilst not as grindable as 600°C, still produced a distribution under these conditions which is potentially suitable for slurry fuels because the particles were mostly below 20µm and significantly smaller than the injector hole orifice. The hydrochars did not grind sufficiently under the conditions set. The HTC 200°C sample remained fibrous so the achievable particle size reduction was less. Rhododendron HTC 250°C char was crumbly but the grinding achieved was poor. The wide particle size range and multimodality of the distribution suggests that agglomeration has occurred. Upon removal of the sample from the mill, the powder was visibly sticky, likely as a result of the inherent moisture and volatile matter on the surface of the char particles. The hydrochars, therefore, need a dispersant to prevent agglomeration.

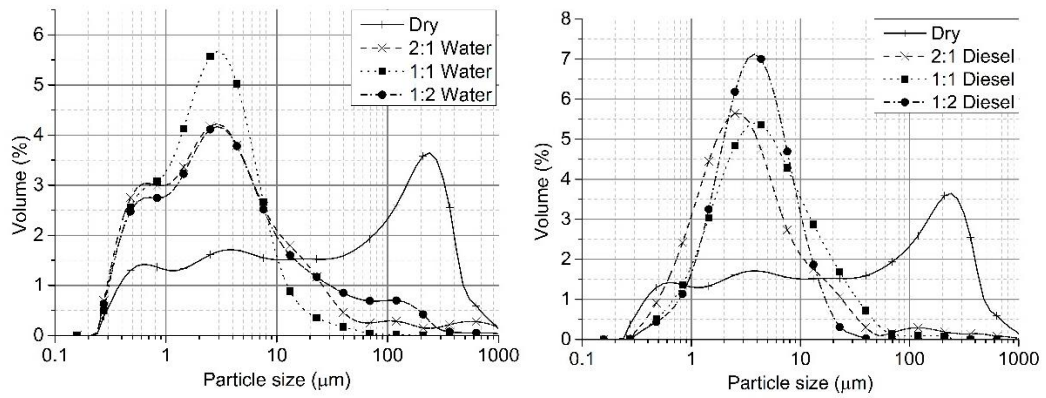


Dispersant	Solid:liquid ratio	D(0.1)	D(0.5)	D(0.9)	Sub 10 micron (%)	Sub 20 micron (%)
Dry	-	0.73	3.28	9.79	93.0	98.9
Water	2:1	1.28	4.70	12.56	87.6	98.3
	1:1	3.14	11.62	98.12	49.6	71.8
	1:2	1.29	5.12	14.38	85.0	97.1
Diesel	2:1	1.61	5.75	16.28	80.3	95.4
	1:1	3.74	13.13	78.86	44.9	67.9
	1:2	2.05	7.00	19.89	72.7	92.7

Figure 5-6 Rhododendron 400°C pyrolysis char milled in various concentrations of dispersants.

Dispersants were tested on the chars selected in chapter 4 for engine testing. Two dispersants were chosen; water and diesel, which are commonly used in the blending of slurry fuels. Water is polar, diesel non-polar which may also influence the particle size distribution and how well they disperse the powder.

Milling tests were performed on the rhododendron pyrochar at 400°C char but with a liquid dispersant added to improve the grindability. The distributions produced in the two dispersants follow a similar trend in respect to the ratio in which they were added. The addition of dispersant to rhododendron 400°C pyrochar, shown in figure 5-6, initially caused the particle size to increase, the largest being under the conditions of 1:1 solid:liquid. The particle size did begin to decrease when the solid:liquid ratio was changed to 1:2 but was not an improvement on the dry milled. The likely reason for the initial deterioration of grindability is that the liquid adsorbing onto the particles causes adhesion with others. The further addition of liquid causes the viscosity to decrease allowing the particles to become more mobile during milling.



Dispersant	Solid:liquid ratio	D(0.1)	D(0.5)	D(0.9)	Sub 10 micron (%)	Sub 20 micron (%)
Dry	-	4.06	74.18	266.04	20.3	28.4
Water	2:1	0.57	2.96	21.99	82.2	90.5
	1:1	0.60	2.56	8.31	94.6	98.3
	1:2	0.60	3.26	42.28	78.6	86.1
Diesel	2:1	0.99	3.22	17.20	84.9	92.9
	1:1	1.33	4.68	19.92	79.2	92.1
	1:2	1.42	3.96	10.49	92.1	99.3

Figure 5-7 Milling Rhododendron 250°C hydrochar at different dispersant ratios. Left) water, and right) diesel

The addition of a dispersant in the case of rhododendron HTC 250°C char did make a significant improvement to the grindability of the char (figure 5-7). Water added at a ratio of 1:1 was the most effective at decreasing particle size achieving a similar distribution to dry milled pyrolysis char produced at 400°C. Adding diesel at a ratio of 1:2 solid:liquid was the next effective regime increasing the amount of sub 20µm material compared to water 1:1 ratio, but less was below 10µm. There is an advantage in producing a size distribution which contains large particles yet still below the upper limit because more char can be added to the slurry because the voids between larger particles are proportionally smaller.

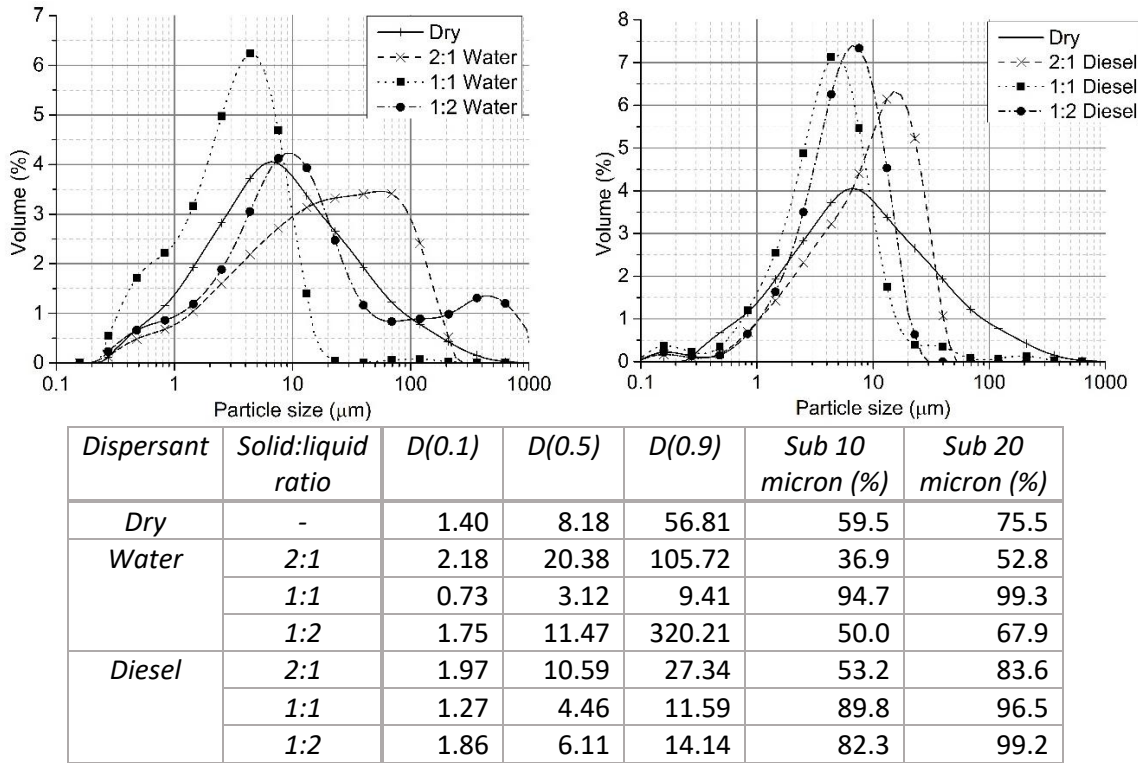
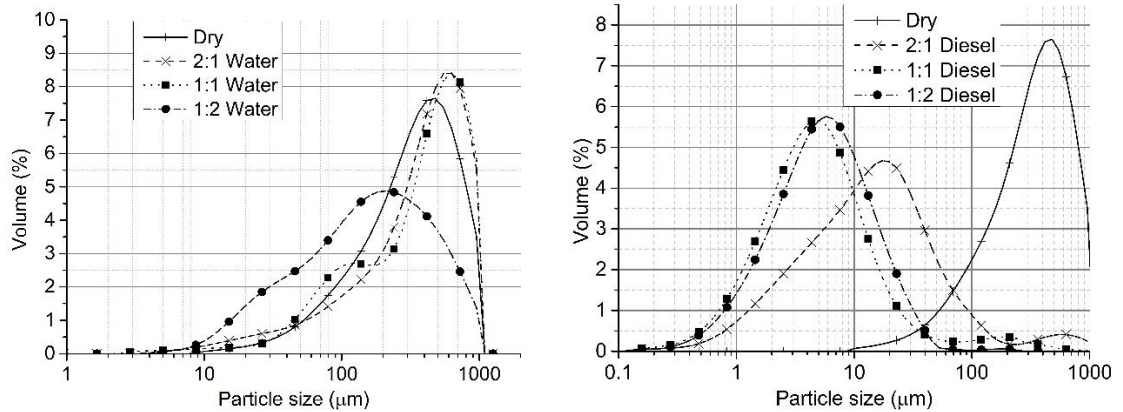


Figure 5-8 Milling behaviour of Shea 400°C pyrolysis char.

Figure 5-8 shows that the milling behaviour of shea pyrochar produced at 400°C is different to that of the rhododendron char. Dry milling the material created a wide distribution with a lot of the powder above the desired upper limit. The dry grindability of the material is better than the rhododendron hydrochar but worse than the rhododendron 400°C pyrochar. The reason is likely the amount of volatile material remaining. The most effective regime was a 1:1 ratio of char to water for creating the finest particles. Diesel added at a ratio of 1:2 solid:liquid created a particle distribution which was larger than the best water test but was within the required upper limit.

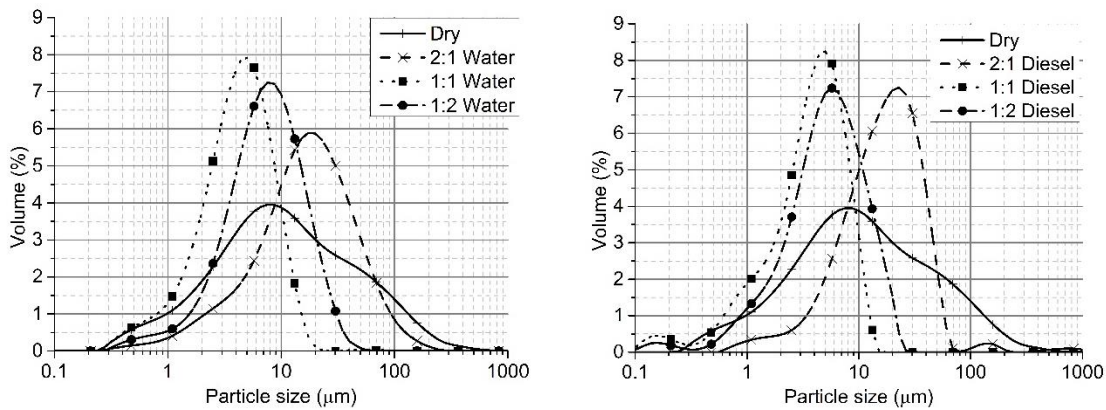
In figure 5-9, the particle size distributions of shea hydrochar samples are shown. The dry milling of shea hydrochar was ineffective yielding a particle size distribution much higher than required. Wet milling in water was also ineffective at all dispersant ratios. The particle size did reduce with increasing amounts of water added. Milling in diesel was more effective, improving with higher concentrations of liquid to solid. At 1:2 solid to diesel, there was still 7% of material above the upper limit of 20µm. Potentially, further addition of diesel would have helped. The shea hydrochar contained the most volatile matter of the chars tested for grindability and milled the poorest in dry conditions. The volatile matter whilst desired to improve combustion, has an adverse effect on milling.



Dispersant	Solid:liquid ratio	D(0.1)	D(0.5)	D(0.9)	Sub 10 micron (%)	Sub 20 micron (%)
Dry	-	96.53	367.44	795.34	0.1	0.8
Water	2:1	76.73	436.88	870.94	1.0	2.9
	1:1	78.31	435.21	879.33	1.0	1.9
	1:2	31.53	173.07	597.86	1.1	6.0
Diesel	2:1	2.39	14.78	76.08	42.4	64.9
	1:1	1.33	4.95	19.73	80.1	91.6
	1:2	1.50	5.80	18.90	76.7	93.3

Figure 5-9 Shea 250°C hydrochar milling behaviour.

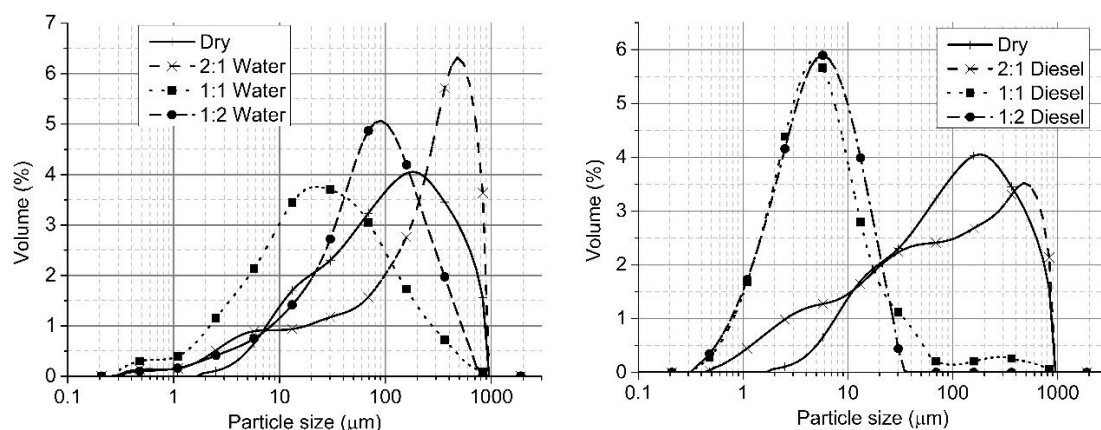
Chlorella 400°C pyrochar was also milled in a selection of dispersants in figure 5-10. Dry milling, once again, was a poor option, with just 70% of material below the upper limit of 20µm. Material remained larger than 100µm which is close to orifice size of injectors. The dry milled particle size distribution was similar for the chlorella and shea pyrochars which contain near identical proportions of volatile matter at 31-33%. Diesel was the more effective dispersant achieving the finest distribution at a ratio of 1:1 diesel to solid material ratio. Water dispersant was also sufficiently effective when added at a ratio above 1:1. The particle size distribution increased again when more dispersant was added to make a 1:2 solid:liquid ratio.



Dispersant	Solid:liquid ratio	D(0.1)	D(0.5)	D(0.9)	Sub 10 micron (%)	Sub 20 micron (%)
Dry	-	1.72	10.67	76.72	52.2	69.1
Water	2:1	3.90	18.03	57.08	32.3	60.2
	1:1	1.47	4.52	10.09	93.6	99.7
	1:2	2.58	7.87	19.57	69.4	93.7
Diesel	2:1	5.60	18.34	42.10	29.3	61.5
	1:1	1.06	4.19	8.79	97.5	100
	1:2	1.63	5.65	13.78	83.8	99.4

Figure 5-10 Chlorella 400°C pyrochar milling behaviour.

In figure 5-11, the milling behaviour of chlorella hydrochar is similar to that of shea hydrochar shown in figure 5-9, both of which have a high lipid content. In both cases, the grindability is poor dry and when using water as a dispersant. The grindability improved with the addition of diesel to help disperse the sticky volatile material on the surface. At a 1:1 ratio of char to diesel, the majority of particles are below 20 μm , but there are remnants of particles over 100 μm , too large for engine injectors. Increasing the ratio to 1:2 char to diesel removed large particles, producing a suitable slurry.

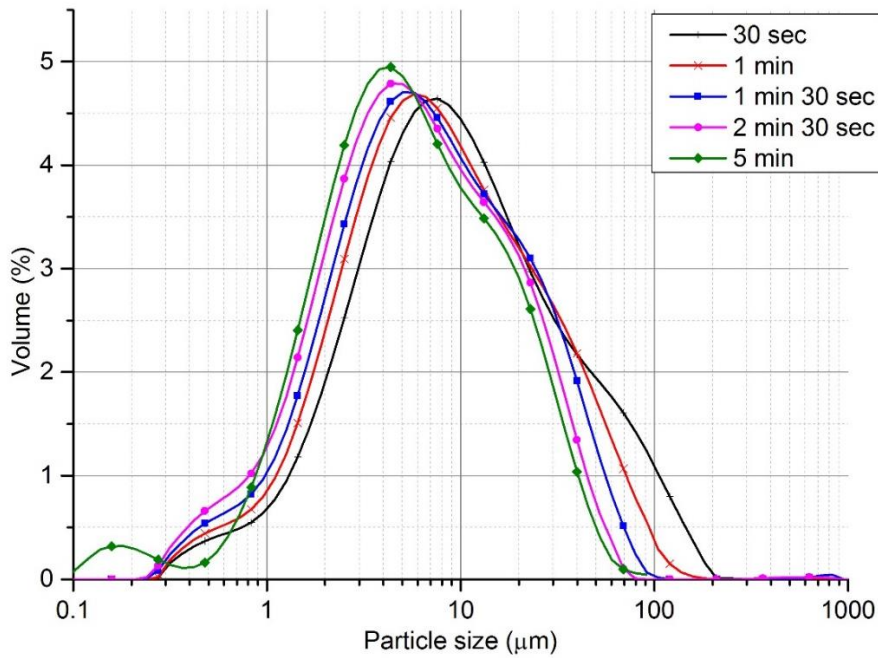


Dispersant	Solid:liquid ratio	D(0.1)	D(0.5)	D(0.9)	Sub 10 micron (%)	Sub 20 micron (%)
Dry	-	15.09	120.23	523.51	6.8	15.8
Water	2:1	9.23	261.25	699.67	11.4	16.3
	1:1	3.66	26.19	160.26	28.6	46.4
	1:2	11.14	80.31	296.66	10.3	18.2
Diesel	2:1	4.60	88.12	588.38	18.8	27.5
	1:1	1.58	5.39	26.18	77.1	89.2
	1:2	1.52	5.48	16.18	79.8	96.8

Figure 5-11 Chlorella 250°C hydrochar milling behaviour.

5.3 Larger scale milling

On scaling up tests to produce an amount of fuel that would be sufficient to conduct engine tests, a two-stage milling process was selected. The reason was so that larger grinding media which are good at reducing the size of larger particles could be used before switching to smaller media which better achieve ultrafine particles. The first stage of the milling process used a dry vibratory disc mill with a large steel ring and cylinder used as the grinding media. The second stage was a wet process which was chosen as it can be optimised to still achieve an acceptable particle size distribution but also reduces the need to handle fine dusts. It was found that without an initial grinding step, the particles were too large for the small grinding balls to disintegrate.



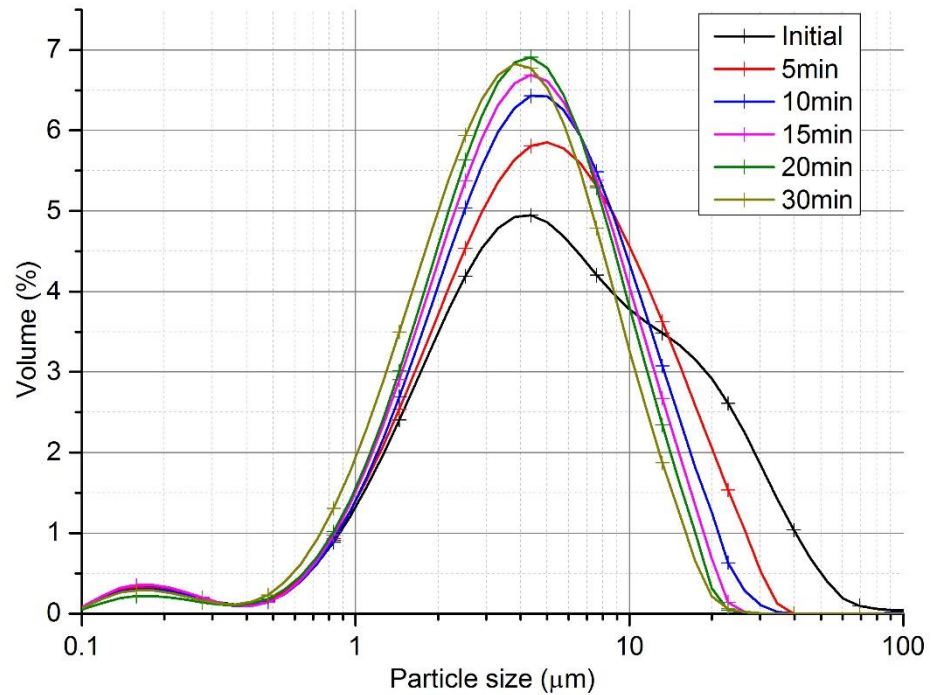
Time	D(0.1)	D(0.5)	D(0.9)	Sub 10 micron (%)	Sub 20 micron (%)
30 sec	2.22	9.67	56.04	55.5	74.3
1 min	1.91	8.06	39.99	61.1	79.0
1 min 30 sec	1.68	7.13	32.23	64.9	82.8
2 min 30 sec	1.44	6.09	26.29	69.7	87.1
5 min	1.50	5.74	25.87	71.2	87.7

Figure 5-12 Disc milling shea 400°C at 1000rpm for different timespans.

Figure 5-12 shows the optimisation of the first section of the micronisation process, dry grinding. Micronisation for 30 seconds yielded a particle size distribution with over 50% of particles by volume under 10µm, but particles were still present which are larger than injector nozzle orifices. Increasing the milling time caused the whole distribution to shift to smaller sizes. After 1 min 30 sec all particles are reduced to below 100µm. The process, whilst fast to begin micronisation, does not reduce the size sufficiently for slurry fuels. Between 2 min 30 sec and 5 min the reduction in particles above 20µm and D(0.1,0.5,0.9) through increased milling time is small. The particle distribution remains too large for the majority of engines. Hence, further milling is required using a mill more suited to achieving the desired distribution.

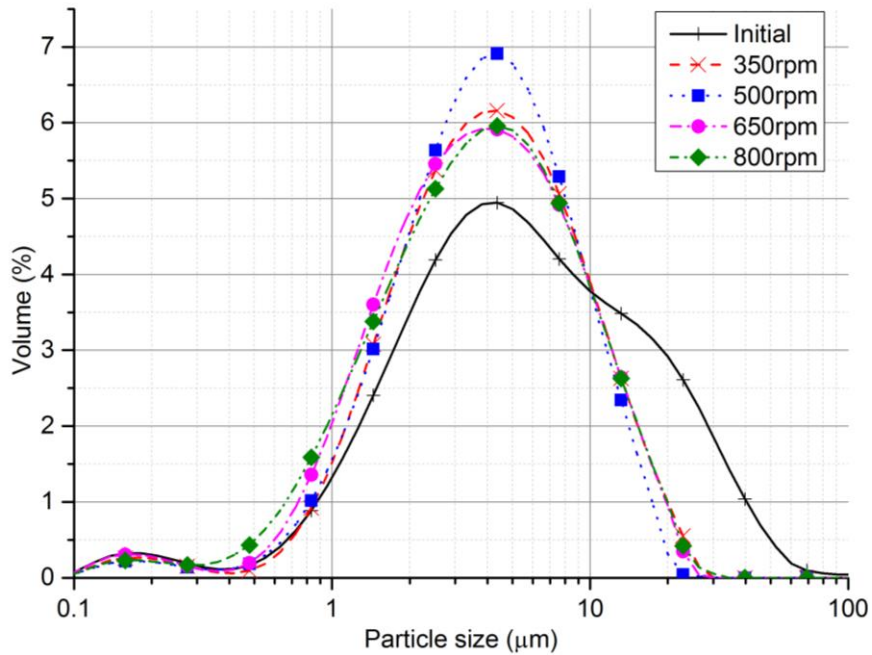
Figure 5-13 shows the particle size distribution achieved by the two-stage process, altering the duration of wet milling. Wet milling for 5 minutes removed the majority of particles likely too large for engine injectors, reducing the size of the biggest particles to 30µm. After approximately 15 minutes of grinding, nearly all the material is smaller than 20µm and hence is likely to pass through the injector orifices without issue. Compared to the results in figure 5-8 using the same material, the two-stage method achieved a smaller average particle and upper size than using the shaker mill with 1:2 sample:dispersant ratio. The two-stage process was also operated for approximately half the time of the shaker mill method. After 15 minutes of

milling, the rate of change of the particle size distribution decreases. The distribution begins to narrow, seen by the increase in maximum peak value, then the modal particle size decreases. In terms of $D(0.1,0.5,0.9)$ the values decreased but only a small amount between 15-30 minutes of milling- in double the grinding time $D(0.9)$ reduced by just $1.54\mu\text{m}$. The small reduction in particle size achieved for longer milling times suggested that the energy consumption is not warranted.



Time (min)	$D(0.1)$	$D(0.5)$	$D(0.9)$	Sub 10 micron (%)	Sub 20 micron (%)
Initial	1.50	5.74	25.87	71.2	87.7
5	1.47	5.11	15.78	81.3	96.8
10	1.48	4.68	13.03	86.6	98.9
15	1.41	4.37	11.58	89.8	99.8
20	1.44	4.25	11.03	91.1	99.4
30	1.28	3.85	10.04	93.2	99.8

Figure 5-13 Shea 400°C pyrolysis char milled in a stirred reactor at 10% wt. solids in diesel at 500 rpm.



Speed rpm	D(0.1)	D(0.5)	D(0.9)	Sub 10 micron (%)	Sub 20 micron (%)
Initial	1.50	5.74	25.87	71.2	87.7
350	1.47	4.48	14.01	88.6	99.3
500	1.44	4.25	11.03	91.1	99.4
650	1.27	4.04	11.83	89.2	99.6
800	1.17	4.12	12.29	89.0	99.4

Figure 5-14 Particle size distribution of shea 400°C pyrolysis char milled in a stirred reactor at 10%wt. solids in diesel with variation of milling speed. Milling was performed for 20 minutes.

The milling speed was altered to gauge the effect on particle size distribution. Figure 5-14 shows the results from using 4 different milling speeds for 20 minutes. All speeds provided sufficient energy to the mill to break down the particles in the char powder added. At the lowest milling speed used, nearly all the material was milled to below 20 μm . The mode of the particle size distribution was 4.1 μm . Increasing the milling speed to 500rpm narrowed the particle size distribution and reduced the number of particles larger than 10 μm . The average particle size reduced in comparison to the particles produced at 350rpm. The particle size distribution widened when the milling speed was increased to 650rpm, producing more ultrafine particles but also more above 10 μm . The effect of widening the distribution is predicted to reduce viscosity, which is beneficial. The extra energy of using a speed over 500rpm may outweigh this benefit. When the milling speed was set at 800rpm, the particle size distribution broadened again.

5.4 Power consumption of milling process

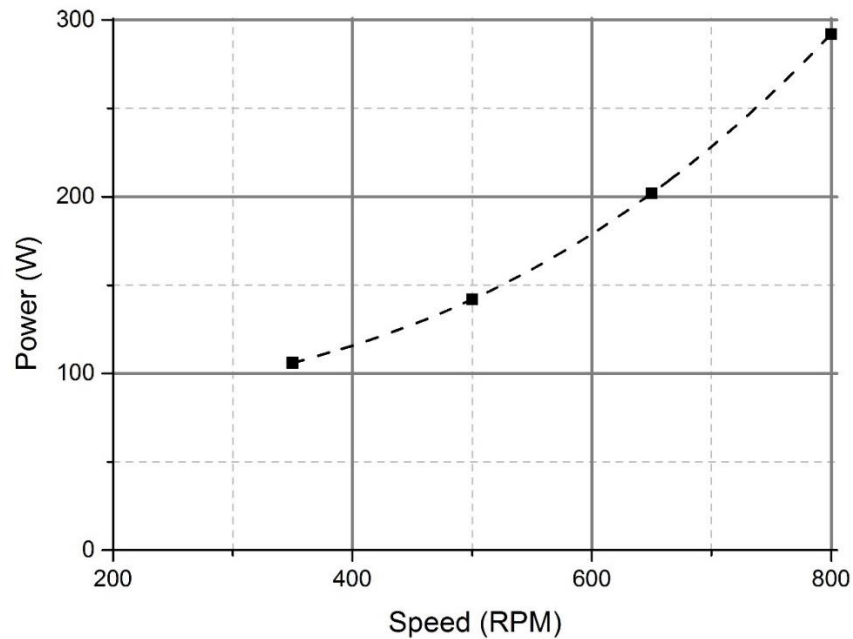


Figure 5-15 Power curve for the stirred media mill used for wet milling experiments.

Figure 5-15 shows the power consumption during the stirred media mill tests. The difference in power consumption between the lowest and highest speed is significant and so will heavily influence the energy balance of the slurry fuel produced. Therefore, slower speeds are recommended to significantly reduce energy consumption. Based on figure 5-14 and 5-15, 500rpm was chosen as the milling speed for 20 minutes was chosen for later processing because the top size particles are reduced compared to 350rpm, but the extra energy consumption is not severe. Reducing the top size particle diameter was prioritised at this point because issues with the engine wanted to be avoided.

The total milling energy consumption when using the parameters for converting the shea 400°C pyrolysis char was 4.85 MJ/kg or 16.8% of the energy within the material. This represents a significant amount of energy consumed. However, reductions could potentially be made by decreasing the milling time by half or more and reducing milling speed if it could be proven that the slightly larger particles would not cause engine operational issues. The upper size of particles milled at 350 rpm for 10 minutes was 35µm which is, potentially sufficient and would reduce energy consumed during milling by nearly a half. The amount of energy used to grind will also decrease with larger volumes of material milled each batch. The current parameters represent a batch of approximately 400 ml of 10%wt. slurry fuel, far less than what would be produced even for small-scale production. The engine used in tests consumes 1.5kg of fuel every hour.

Previous studies focusing on larger scale production of slurries found the energy consumption was much lower than found in the stirred media ball mill tests. Cui et al. (2008) used a high-pressure slurry jet mill technique to reduce a 50%wt. coal-diesel slurry, with a similar initial diameter to the shea tested ($D(0.5)=2.71\mu\text{m}$) micronising almost all the material to below $10\mu\text{m}$ using 0.45 MJ/kg. Using a ball mill on the same coal slurry consumed 1.59 MJ/kg achieving $D(0.5)=3.13\mu\text{m}$. Mankosa et al. (1989) investigated using a stirred ball mill for grinding coal also concluded that using low stirring speeds was the most energy efficient method for micronisation. It was also found that increasing the solid loading from 20 to 50%wt. had no effect on the grinding efficiency. At higher loadings the grinding efficiency reduced. A mean product size of $D(0.5)=6\mu\text{m}$ was achieved with an energy input of 0.23 MJ/kg from an initial feed with $D(0.5)=70\mu\text{m}$.

5.5 Stability

The stability of slurries is defined as the tendency for particles to remain in suspension in a liquid. It is important as good stability reduces sedimentation which can cause blockages and ensures that the fuel remains homogeneous after being stored.

Table 5-1 shows some of the key properties of the fuels used for creating slurries with the micronised particles. Rapeseed methyl ester (RME) contains higher oxygen meaning that molecules present are generally more polar than diesel. The result of this is that RME molecules will be more attracted to the char than diesel the more polar the surface of the particle is, hence improving stability. Comparing to the elemental analysis of chars produced at 400°C and discussed in chapter 4, the carbon and oxygen content of all chars more closely matches that of RME. The hydrochars had an even greater O/C and so still more similar to RME than diesel. The chars produced at 600°C have an O/C more closely matching diesel than RME. Density is another important factor for stability as the closer the values of the char and liquid, the slower they will separate. RME has a higher density than diesel by roughly 3%, meaning that char slurries should be more stable in RME as a result of this property.

Table 5-1 Properties of the two fuels used as a matrix for char particles. All elements were measured directly. Higher heating value was calculated by Dulong's formula.

Fuel	Carbon (%)	Hydrogen (%)	Nitrogen (%)	Sulphur (%)	Oxygen (%)	Higher heating value (MJ/kg)	Density (g/L)
Diesel	82.85	13.12	N.D.	N.D.	3.66	46.33	832
RME	80.99	12.60	N.D.	N.D.	11.56	43.52	856

Table 5-2 shows the stability of chars tested in two different media at 10% wt. solid loading. For all chars tested the stability was higher when using RME. The higher presence of oxygenated chemical groups is the likely reason for improved stability because of the attractions between them and similar groups on the surface of the char. Chars have oxygen containing groups on the surface, such as carboxyl and hydroxyl groups which will cause hydrogen bonding between the solid and biodiesel (Chen et al., 2015). The HTC chars tested were more stable than the pyrolysis 400°C chars made from the same material. The pyrolysis char produced at 600°C, however, was more stable despite being denser. One reason for the improved stability could be that the particle size of the pyrolysis 600°C sample is, on average, slightly smaller and hence more stable (figure 5-5). Another reason could be the increasing hydrophobicity of the char particles with pyrolysis temperature giving them a stronger affinity to diesel dispersal medium.

The chars made from shea were more stable than the comparative rhododendron samples. The reason for the differences between the two samples is not clear from the analysis of the materials in chapter 4. There is also no correlation in the density of the chars which would explain this. The property that is consistently higher for the two shea samples than the rhododendron samples is the amount of volatile matter and H/C ratio. The volatile matter may act as a surfactant between the shea particles and diesel. Upon settling of char within diesel, the liquid becomes discoloured suggesting some of the volatile matter from the char had been dissolved. The higher H/C ratio in the shea samples means that the values are closer to that of diesel than the rhododendron and so have a stronger attraction to diesel.

Table 5-2 Stability of char in diesel and RME at 10%wt. solid loadings.

<i>Material</i>	<i>Char</i>	<i>Density of char (g/cm³)</i>	<i>Stability in Diesel</i>	<i>Stability in RME</i>
<i>10% wt. Rhododendron</i>	<i>Pyrolysis 400°C</i>	1.415	1 hour	9 hours
	<i>Pyrolysis 600°C</i>	1.541	5 hours	-
	<i>HTC 250°C</i>	1.343	1.5 hours	11.5 hours
<i>10% wt. Shea</i>	<i>Pyrolysis 400°C</i>	1.449	4.5 hours	15 hours
	<i>HTC 250°C</i>	1.265	26 hours	55 hours

Table 5-3 shows the stability of slurries with surfactants added to improve stability. Surfactants were chosen across the hydrophilic-lipophilic balance (HLB) range. The most effective surfactant in terms of stability was lecithin, increasing the stability to over a day for all slurries tested and, in some cases, to over a week. Lecithin was significantly more effective at stabilising pyrolysis char slurries than hydrochar, meaning they have a longer shelf life than hydrochar slurries produced from the same material despite the opposite trend in stability true without surfactant. Lecithin was an effective surfactant for both RME and diesel based

slurries. For most of the slurries tested, the addition of the smaller quantity, 0.5%, produced the most stable mixture. This suggests that even more stable slurries could be achieved by adding less than 0.5%wt. surfactant. The reason for this reduction in stability with further addition of surfactant could be depletion flocculation (Semenov and Shvets, 2015).

Table 5-3 Stability observed of surfactant, liquid and char mixtures. All chars added at 10%wt.. "P" preceding a temperature denotes the method used was pyrolysis. Numbers in brackets is the hydrophilic-lipophilic balance (HLB) values of the surfactants. B Cl is benzethonium chloride, Na Lig is sodium lignosulfonate, Na stearate is sodium stearate and CMC is carboxymethyl cellulose, sodium salt. Dash denotes test not performed.

Liquid	Material	Char	Surfactant										
			None	0.5% B Cl (14)	1% B Cl	0.5% Na Lig (-)	1% Na Lig	0.5% Lecithin (7)	1% Lecithin	0.5% Ethanol (7.9)	1% Ethanol	0.5% Na Stearate (18)	1% Na Stearate
Diesel	Rhododendron	P400°C	1 h	1.5h	2h	1.5h	1.5h	5d	4d	1.5h	2h	1h	1h
		HTC250°C	1.5 h	2h	3.5h	<1h	<1h	27h	34h	<1h	3h	4h	15h
	Shea	P400°C	4.5h	9.5h	7.5h	6h	5h	12d	11d	9.5h	1.5h	12h	12h
RME	Rhododendron	P400°C	9h	18h	12h	33h	28h	22d	25d	23h	19h	40h	40h
		HTC250°C	12h	22h	13h	26h	25h	9.5d	9d	19h	18h	23h	21h

Table 5-3 continued

Liquid	Material	Char	Surfactant					
			0.5% Palmitic acid (2)	1% Palmitic acid	0.5% CMC (10.5)	1% CMC	0.5% Span 20 (8.6)	1% span 20
Diesel	Rhododendron	P400°C	1h	2h	1.5h	1.5h	3.5h	5.5h
		HTC250°C	5.5h	5.5h	1.5h	1.5h	5.5h	8.5h
RME		P400°C	29h	28h	-	-	-	-
		HTC250°C	28h	27h	-	-	-	-

The next most effective surfactant was sodium stearate although it failed to stabilise the rhododendron 400°C pyrolysis char in diesel. The surfactant is more hydrophilic than lecithin owing to the carboxylate group at one end of the hydrocarbon chain. The group is attracted to hydrophilic parts of the char which explains why an improvement in stability occurs in the rhododendron 250°C hydrochar in diesel because it is more oxygenated, hence hydrogen bonding can occur. However, Shea 400°C pyrochar slurry stability is improved by the presence of sodium stearate despite containing less electronegative elements than the rhododendron hydrochar used. The hydrophilic head of sodium stearate might instead be attracted to positively charged trace elements on the surface, improving stability. Slurries made in an RME matrix show the opposite trend with sodium stearate stabilising the rhododendron pyrolysis char to a higher degree than the hydrochar.

The addition of palmitic acid produced an improvement in the stability of a slurry produced from rhododendron hydrochar but little in a pyrolysis char slurry. A previous study by Soloiu et

al. (2011) investigated improving the stability of charcoal-diesel slurries using water along with fatty acid, fatty acid soap and alkyl ester surfactants. It was reported that using two different types of fatty acid, which were not specified but a category in which palmitic acid falls, produced a slurry which was stable for one day, much longer than found using palmitic acid in this study. Using a fatty acid soap also improved stability in Soloiu et al. (2011) and when used in conjunction with a fatty acid, increased the stability to 4 days. The fatty acid soap used in this study, sodium stearate, however, was ineffective.

Sodium lignosulfonate and sodium carboxymethyl cellulose, surfactants regularly used in coal-water slurries, did not alter the stability of diesel slurries (Boylu et al., 2005; Savitskii, 2013; Yang et al., 2007). These two surfactants contain hydrophilic groups throughout the structure like lignin and cellulose and thus will have a poor solubility in diesel, preventing the important bridging mechanism occurring. Benzethonium chloride performed slightly better in most slurries tested despite being very hydrophilic. The compound has larger hydrophobic regions which will be stronger attracted to the diesel than sodium lignosulfonate and sodium carboxymethyl cellulose. It was the only cationic surfactant tested which means it will be attracted to negative ions of dipoles on the surface of the char and chemical groups like chlorides and phosphates. Span 20 increased the stability of rhododendron chars in diesel and was the second most effective surfactant for these two.

Table 5-4 Surfactant blends tested in a 10%wt. rhododendron 400°C diesel slurry.

<i>Surfactant 1</i>	<i>Surfactant 2</i>	<i>Stability</i>
0.5 % lecithin	0.5% CMC	9 days
0.5 % lecithin	0.5% Na stearate	10 days
0.5 % lecithin	0.5% Na lig	9 days
0.5 % lecithin	0.5% ethanol	9 days
0.5 % lecithin	0.5% B Cl	4.5 days
0.5% lecithin	0.5% span 20	4 days
0.5% lecithin	0.5% palmitic acid	12.5 days
0.25% lecithin	0.75% palmitic acid	6.5 days
0.75% lecithin	0.25% palmitic acid	6 days

Table 5-4 shows mixtures of surfactants created to further improve the stability. With the exception of benzethonium chloride and span 20, all mixes improved the stability compared to using lecithin alone. Adding a second surfactant that was comparatively poor when used alone also improved the overall stability when used in conjunction with lecithin, such as sodium carboxymethyl cellulose. Using palmitic acid with lecithin produced the most stable slurry. Further tests altering the proportions of each used showed that a 1:1 ratio of lecithin and palmitic acid was the most effective. However, the solubility is poor and requires a long period of shaking to dissolve, which is something for practical consideration.

The next most stable mixture was lecithin and sodium stearate, doubling the time the slurry remains stable. Sodium stearate was the second most effective surfactant when tested individually, although did not improve the stability of the rhododendron 400°C pyrochar diesel slurry. When mixed with lecithin, however, sodium stearate significantly improved the overall stability of the rhododendron 400°C pyrochar diesel slurry. The sodium stearate might be interacting with the lecithin attracted to the surface of char particles in a way which repels other particles surrounded by the surfactant. Another possibility is the sodium stearate forms micelles in the diesel which get between particles, preventing them from agglomerating. Sodium lignosulfonate, sodium carboxymethyl cellulose and ethanol mixed with lecithin also improved stability despite not stabilising the slurry when used as the sole surfactant.

The results in table 5-4 show there is merit using more than one surfactant to improve stability but the cost will increase. Improving stability might not be as important as the extra cost and so it may be preferred to remix before use.

5.6 Conclusions

The milling tests showed that wet milling is the preferred route because particularly high volatile content containing materials, especially hydrochar, respond poorly to dry methods. Diesel was the best dispersant at the ratios tested and assisted in the milling of the samples to a fineness suitable for slurry fuels. It was likely better as a dispersant than water because it is non-polar, like the char it was mixed with. On scaling up the milling process, a stirred media ball mill was used with a diesel dispersant at 10%wt. solid loading of char. The optimum process uses an initial milling stage to make a coarse powder before milling at 500rpm for 15 minutes. 99.8% of material below 20µm was achieved which is sufficient to pass injectors.

Tests milling different types of char material with different quantities of surfactant showed that the degree of micronisation was strongly linked with the amount of volatile matter present. The two materials that contained the highest volatile matter, 250°C hydrochars produced from chlorella and shea, milled poorly when dry and in water. The addition of 1:2 solids:diesel was required to micronise sufficiently for a slurry fuel application. The presence of lipids in the material was also thought to have reduced the ability to micronise dry and in water.

The study of stability of 10%wt. slurry mixtures showed that chars are more stable in RME biodiesel than fossil fuel diesel and hydrochars are more stable than pyrochars. As a result, the use of biodiesel in char-diesel slurries as a stabiliser should be considered. The most efficient stabiliser found was lecithin which worked for all chars in both diesel and biodiesel. It was, however, more effective for stabilising pyrochars than hydrochars.

Adding another surfactant to lecithin further increases stability. The addition of palmitic acid increased stability the most, followed by sodium stearate. Solubility, however, was an issue with palmitic acid, making it hard to mix well into the slurry. As the stability with just lecithin was sufficient as long as the slurry is remixed before use, it may not be cost effective, especially in developing countries, to add an extra surfactant because the cost of the slurry needs to be minimised.

5.7 References

- Boylu, F.Ateşok, G. and Dinçer, H. 2005. The effect of carboxymethyl cellulose (CMC) on the stability of coal-water slurries. *Fuel*. **84**(2), pp.315-319.
- Chen, Z.Xiao, X.Chen, B. and Zhu, L. 2015. Quantification of Chemical States, Dissociation Constants and Contents of Oxygen-containing Groups on the Surface of Biochars Produced at Different Temperatures. *Environmental Science & Technology*. **49**(1), pp.309-317.
- Cui, L.An, L. and Jiang, H. 2008. A novel process for preparation of an ultra-clean superfine coal–oil slurry. *Fuel*. **87**(10), pp.2296-2303.
- Flynn, P.L.Leonard, G.L. and Mehan, R.L. 1989. Component Wear in Coal-Fueled Diesel Engines. *Journal of Engineering for Gas Turbines and Power*. **111**(3), pp.521-529.
- Mankosa, M.J.Adel, G.T. and Yoon, R.H. 1989. Effect of operating parameters in stirred ball mill grinding of coal. *Powder Technology*. **59**(4), pp.255-260.
- Nicol, K. 2014. *The direct injection carbon engine*. London, UK: IEA Clean Coal Centre.
- Savitskii, D.P. 2013. Rheological properties of highly concentrated anthracite coal-water slurries stabilized with sodium carboxymethyl cellulose. *Solid Fuel Chemistry*. **47**(1), pp.39-42.
- Schwalb, J.A. 1991. *Wear Mechanism and Wear Prevention in Coal-Fueled Diesel Engines Task III: Traditional Approaches to Wear Prevention*. San Antonio, Texas, USA: Southwest Research Institute.
- Semenov, A.N. and Shvets, A.A. 2015. Theory of colloid depletion stabilization by unattached and adsorbed polymers. *Soft Matter*. **11**(45), pp.8863-8878.
- Soloiu, V.Lewis, J.Yoshihara, Y. and Nishiwaki, K. 2011. Combustion characteristics of a charcoal slurry in a direct injection diesel engine and the impact on the injection system performance. *Energy*. **36**(7), pp.4353-4371.
- Wilson, R. 2007. *Clean coal diesel demonstration project: Final report*. Cambridge, USA: TIAX.
- Yang, D.Qiu, X.Zhou, M. and Lou, H. 2007. Properties of sodium lignosulfonate as dispersant of coal water slurry. *Energy Conversion and Management*. **48**(9), pp.2433-2438.

Chapter 6: Using char as an additive to conventional fuel

6.1 Introduction

The effect of adding small quantities of char to diesel fuel was investigated to determine if the addition alters the combustion behaviour of the bulk conventional fuel. Char contains a wide range of compounds and elements which, even in small quantities, can significantly alter the emissions produced. Several elements present in char have been used in compounds as additives in fuel to reduce different types of emissions (Ribeiro et al., 2007). The most important emissions to reduce in diesel engines are particulates and oxides of nitrogen, which have come into the public eye because of the deterioration in air quality in cities caused by the switch to diesel cars (Torjesen, 2014).

An important question to answer is the fate of the char added. Despite only a small quantity of char being added, it could have a marked effect on the total particulate emission, as less than 0.1% of diesel ends up as soot. Char has a higher autoignition temperature than diesel thus may not burn fully in the short period of time during the expansion stroke. The other key issue is how ash is removed from the engine; it could leave through the exhaust, or become entrained in the oil sump- both are potentially problematic. Exiting through the exhaust will cause particulate pollution, the damage to the air quality dependent on the particle size of the ash. Accumulation in the oil sump is less problematic in terms of public health but could cause a number of issues. It will likely decrease the interval between oil changes and alter the properties of the oil. It could also result in the abrading of the cylinder as particles will gradually increase in concentration in the oil film between moving parts.

A selection of potentially appropriate fuels was made from the char properties investigated in chapter 4. Included are materials that fall into the categories of second and third generation biofuels. The third-generation feedstock chosen is *Chlorella vulgaris*, a microalgae, which was found to be more suitable than the macroalgae materials tested because chlorella chars contained less ash and had a higher calorific value. *Rhododendron ponticum* and residue of shea nut are the second-generation biomass materials used. The two materials are chosen because they cover two important subcategories in second-generation biomass: woody biomass and agricultural waste.

The chapter firstly investigates some of the chemical properties of the biodiesel and diesel fuels used in testing. Baseline tests using these fuels are completed as a marker of performance for slurry fuels. A total of 13 slurry fuels are tested at 0.1% wt. content- 3

different raw biomass materials (rhododendron, chlorella and shea) are used to make charcoal. The effect of thermal treatment is also investigated, with each of the raw biomass materials converted to a 400°C pyrochar and a 250°C hydrochar, the processes found to be the most suitable for creating a slurry fuel in previous chapters. Each char is mixed with diesel and biodiesel. Another pyrochar is produced at 600°C from rhododendron to investigate how altering the pyrolysis temperature affects the emissions.

The final section investigates further increasing the char solid loadings to 1%wt. in diesel - a concentration in between an additive and a fuel. The practicalities and emissions are studied on a total of four fuels: rhododendron 400°C pyrochar, rhododendron 250°C hydrochar, shea 400°C pyrochar and shea 250°C hydrochar.

The chapter aims to address objective 6 of the thesis- to investigate using char as an additive to conventional fuel. The baseline tests on the engine test bed also pertain to part of objective 5- to design and construct a slurry engine test bed. The methods used in this section can be found in 3.6 and 3.7 of the materials and methods chapter.

6.2 Chemical composition of fuels used

6.2.1 Biodiesel analysis

Table 6-1 shows the composition by carbon number of the two biodiesel fuels used in tests. The majority of both fuels are comprised of C18 (stearic, oleic and linoleic) methyl esters and some C16 (such as hexadecanoic) methyl esters. The biodiesel derived from waste cooking oil (waste cooking oil methyl ester (WCOME)) contains, on average, smaller carbon chains than rapeseed biodiesel. This difference is also reflected in the elemental analysis of waste cooking oil biodiesel containing more hydrogen and oxygen. Rapeseed and other members of the *Brassicaceae* genus generally contain long-chain monosaturated fatty acid methyl esters such as oleic, erucic and eicosenoic acids (Ahmad et al., 2013). Tallow and palm oil-derived biodiesel, however, which are potentially present in the waste cooking oil used to produce WCOME, have smaller C16 chains present (Liu et al., 2011; Montoya et al., 2014).

Table 6-1 Carbon number and elemental analysis of the two biodiesel fuels used.

Fuel	Carbon number (% vol)					Elemental analysis (%wt.)					Dulong's HHV (MJ/kg)
	<C16	C16	C17	C18	>C18	C	H	N	S	O	
Rapeseed biodiesel	1.89	4.00	N.D.	88.71	5.40	80.99	12.60	N.D.	N.D.	11.56	43.52
Waste cooking oil biodiesel	5.48	13.73	0.81	76.52	3.46	79.53	12.87	N.D.	N.D.	11.51	43.43

Figure 6-1 shows the FAME analysis of the two biodiesel fuels used, which further confirms the analysis in table 6-1. WCO biodiesel contains higher concentrations of the shorter chain C16:0 palmitic acid. There are differences between the two biodiesels used in the saturation of C18 fatty acid methyl esters. WCO biodiesel contains more of the saturated stearic acid and the polyunsaturated linoleic acid. Pinzi et al. (2013) found NO_x emissions increase with fatty acid chain length and the degree of unsaturation. Total hydrocarbons, carbon monoxide and soot were also found to increase with chain length. Therefore, the increased concentration of stearic acid in RME than WCOME will reduce the NO_x emission, but linoleic acid will have the opposite effect meaning that the overall difference in the NO_x emission between the two fuels is hard to predict.

For the engine tests waste cooking oil (WCO) biodiesel was selected because it is considered more sustainable. Also, it avoids the fuel vs. food debate that has been argued against certain feedstocks including rapeseed.

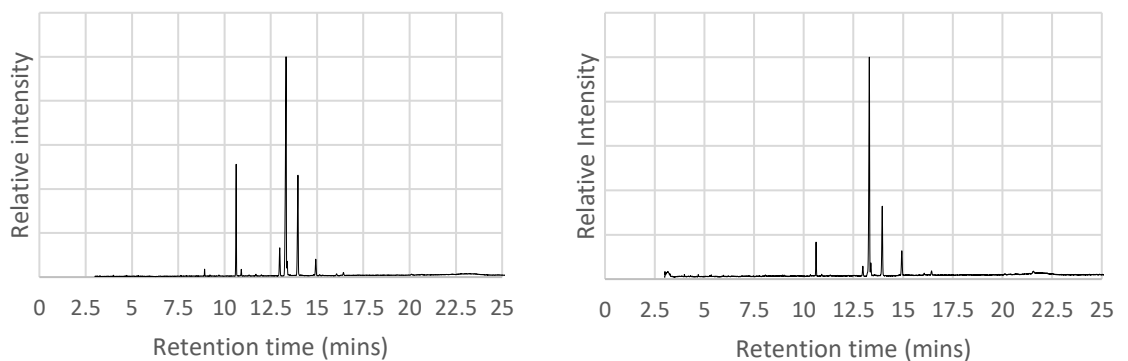


Figure 6-1 FAME analysis of the two biodiesels used. Left: Derived from waste cooking oil, and right: Derived from rapeseed. Methyl ester peaks by retention time are: 8.9mins-Methyl myristate, 10.6mins-Hexadecanoic acid, 10.9mins-Palmitoleic acid, 13mins-Stearic acid, 13.3mins-Oleic acid, 14mins-Linoleic acid, 14.9mins- Linolenic acid, 16.1mins- Arachidic acid, and 16.4mins-Paullinic acid.

6.2.2 Diesel analysis

The carbon number distribution of white and red diesel tested is shown in figure 6-2. The distribution of both the red (tax-free, agricultural diesel) and white (EN590 road diesel) fuels are similar but white contains compounds of, on average, a higher carbon number. The difference between the two might be a case of using a different blend for improved winter operation, rather than an indication of quality. Compared to the biodiesels, the two petroleum diesels tested have a wider distribution and lower average carbon number.

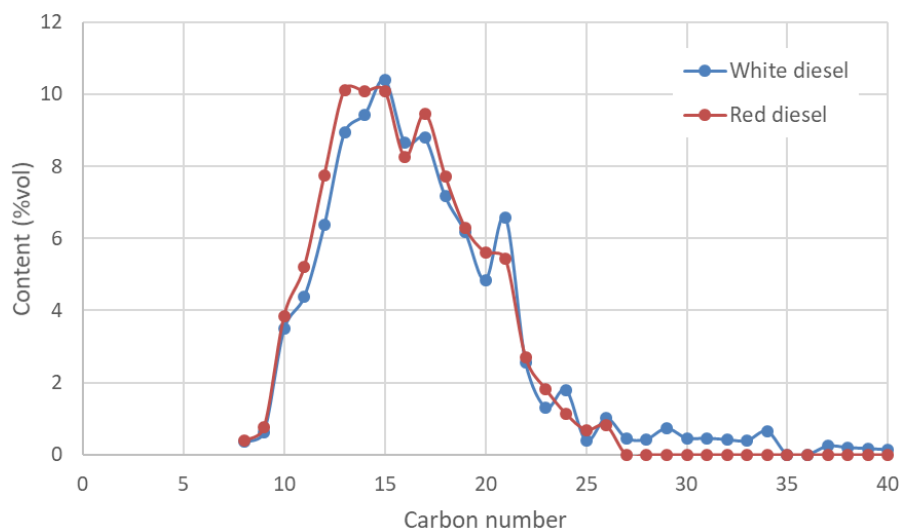


Figure 6-2 Carbon number distribution of compounds in red and white diesel.

Despite a slightly higher average carbon number than red diesel, white diesel has a higher molar H/C ratio (1.90 vs. 1.88). White diesel has a higher calorific value than the red diesel used (table 6-2). Quantification of oxygen in both petroleum fuels yielded values higher than expected because the fuel is non-oxygenated except for the small amount (<8%) of biodiesel present. The reason for the higher percentage than expected could be instrument error or contamination of the samples. Both petroleum diesels have a higher calorific value than biodiesel.

White diesel was used throughout for the mixing of slurry fuels and baselining. Red diesel was used for heating up the engine before tests.

Table 6-2 Elemental analysis of diesel fuels used. All elements measured directly.

Fuel	Elemental analysis (%wt.)					Dulong's HHV (MJ/kg)
	C	H	N	S	O	
White diesel	82.85	13.12	N.D.	N.D.	3.66	46.33
Red diesel	81.51	12.77	N.D.	N.D.	2.97	45.50

6.3 Baseline tests using conventional fuels

A set of baseline tests were performed to ascertain the performance of the engine using diesel and biodiesel without the addition of char. Prior to the baseline tests, the engine was operated for 24 hours to “run-in”. A new engine is known to operate slightly differently during initial operation as surfaces and parts are not yet lubricated and naturally smoothed by the rubbing motion of parts across each other.

6.3.1 Diesel baseline

Figure 6-3 shows the baseline emissions and fuel consumption of the engine generator operating on white diesel. Maximum thermal efficiency occurs between 3.25 and 4.5 kW, peaking at 22.5%. CO₂ emissions normalised to power output (specific emissions) fall in agreement with falling fuel consumption versus power.

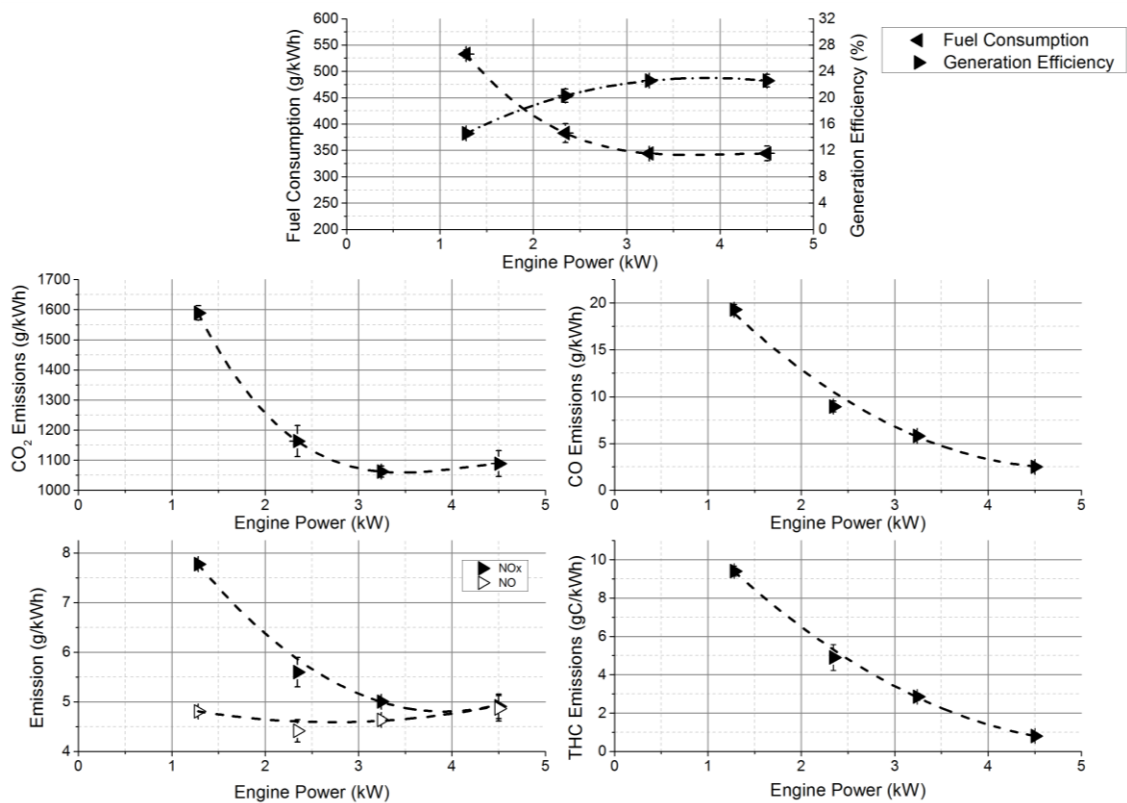


Figure 6-3 Baseline emissions using white diesel fuel. Error bars shown. Top: Fuel consumption and generation efficiency and varying loads. Middle left: CO₂ emissions. Middle right: CO emissions. Bottom left: Oxides of nitrogen emissions. Bottom right: Total hydrocarbon (THC) emissions in terms of grams of methane equivalent.

Carbon monoxide emissions are low and very dependent on engine power- an 85% reduction is achieved from 25% to 100% load. The emission profile of oxides of nitrogen is more complex. Increasing efficiency at higher load causes oxides of nitrogen to decrease but higher cylinder temperatures counteract this, causing more to be produced (Shameer and Ramesh, 2017). The lowest specific emissions of NO_x are achieved at a load of approximately 4kW. Specific emissions of nitric oxide are slightly higher at low and high loads. At high loads, when the air-fuel ratio is lower, the lack of oxygen causes nitric oxide to form instead of nitrogen dioxide (Liu et al., 2012; Wei and Geng, 2016). Total hydrocarbon (THC) specific emissions, like CO, are dependent on the engine load, reducing significantly at higher power

Figure 6-4 shows the particle number size distribution at four points across the total power range of the generator normalised to be expressed as a function of electrical output. The integral on a logarithmic basis of the distributions is equivalent to the total number of particles emitted per kWh. Error bars are also displayed at each point showing the variation between the two tests performed. The repeatability of the results is comparatively low at 1.28 and 2.34kW. The reason for this variation is unclear as the temperature measured in the engine exhaust is similar, ruling out cold start effects. The distribution is bimodal, with one peak at 20nm and another around 100nm. The peak at 20nm reduces rapidly with increasing load and contributes an ever smaller proportion to the overall distribution. The reduction in the height of this 20nm peak from 25% to 100% load is 90%. This reduction in ultrafine particles is especially beneficial for health as these are known to be more harmful (Virtanen et al., 2004). The larger mode in the distribution occurring at roughly 100nm also changes in height at different loads but to a lesser extent than the mode at 20nm. The height varies from 1.5×10^{15} at 3.24kW to 2.6×10^{15} at 1.28kW. The location of the peak gradually shifts toward larger particle size with increasing load- from 83nm to 150nm. The overall particle size therefore gradually increases with load.

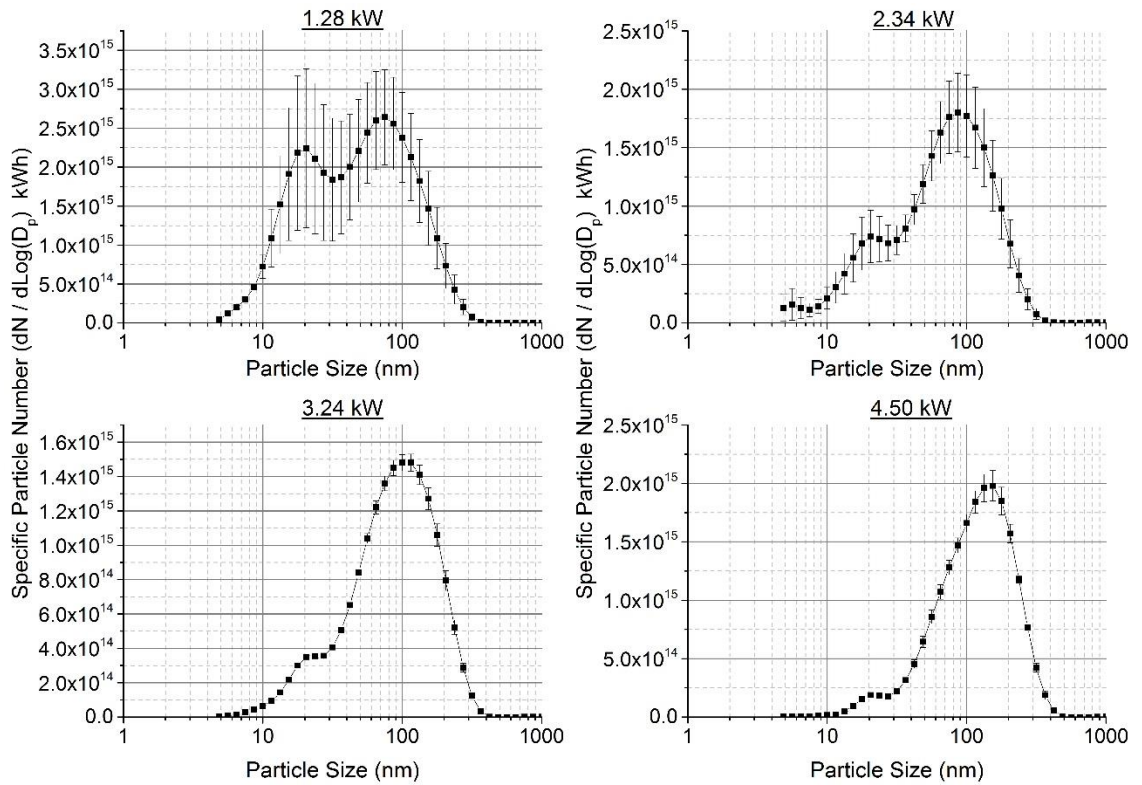


Figure 6-4 Specific exhaust particle size distributions at varying engine load when using white diesel.

Figure 6-5 shows a summary of particle number emissions across the whole working range of the engine generator. The particle number emission is lowest on a per kWh basis at approximately 3.5kW of output. The particle distribution vs. power contour map also shows the gradual shift toward larger particle size with load.

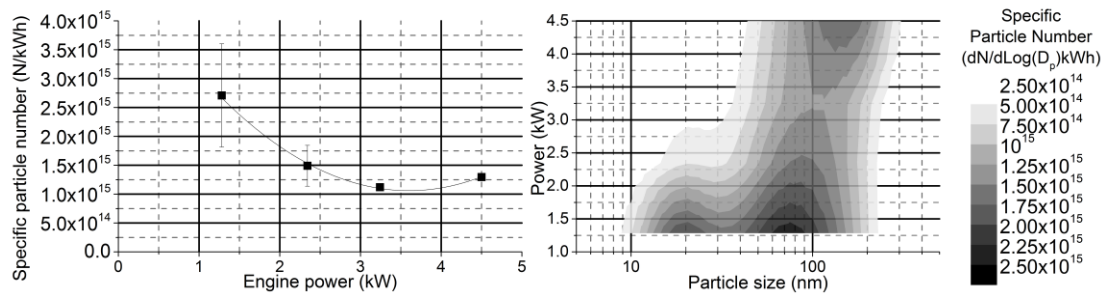


Figure 6-5 Variation in particle emissions with power when using white diesel. Left: Particle emission per kWh hour with respect to engine power. Right: Particle size distribution vs. power map.

6.3.2 Biodiesel from waste cooking oil (WCOME) baseline

Figure 6-6 shows the same parameters for biodiesel as figure 6-3 shows for diesel. The thermal efficiency is lower when using biodiesel with a maximum of 21.5% achieved, a percent less than diesel. The lower efficiency also means that specific CO₂ emissions are higher than diesel despite the higher H/C ratio of biodiesel. The CO emission profile for biodiesel is near identical with that measured using white diesel showing there is no benefit in this criteria to switching

to the low carbon fuel. THC emissions recorded when using biodiesel were higher but are close to convergence with diesel at full load. NO_x and NO reduction is a benefit occurring when using biodiesel compared to diesel using this generator. Reduction in NO_x and NO is most pronounced at medium load- at 50% load, the reduction is 15% and 7% respectively. Despite the heightened concentration of oxygen in biodiesel compared to diesel, NO is reduced by less than NO₂ emissions.

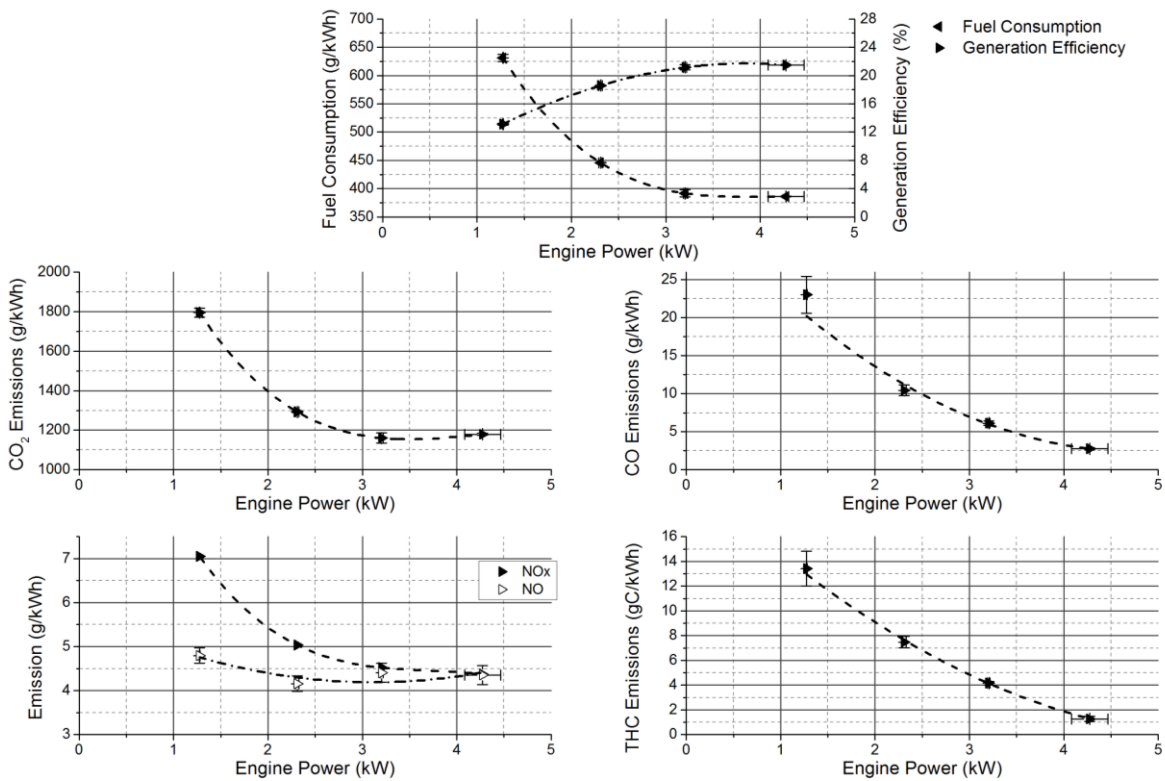


Figure 6-6 Biodiesel from waste cooking oil consumption, generation efficiency and emission characteristics.

The particle size distribution of soot produced from using biodiesel is shown in figure 6-7, displaying some similar trends to diesel. The average particle size increases with load and the distribution is bimodal. The first mode appears at approximately 20nm, as was the case in diesel, and the second at 50nm, which is significantly smaller than diesel. The magnitude of the particle size distribution is consistently higher for biodiesel than diesel, especially at low load. The reason for higher particle emission despite the fuel containing fewer aromatics and other compounds is the increased cetane number. Increased cetane number reduces ignition delay, hence increasing the proportion of diffusion combustion, the stage at which most soot is formed (Tree and Svensson, 2007). The reduction of ignition delay reduces premixed combustion which is responsible for significant NO_x production which also fits with the evidence in figure 6-6 (Yu et al., 2014).

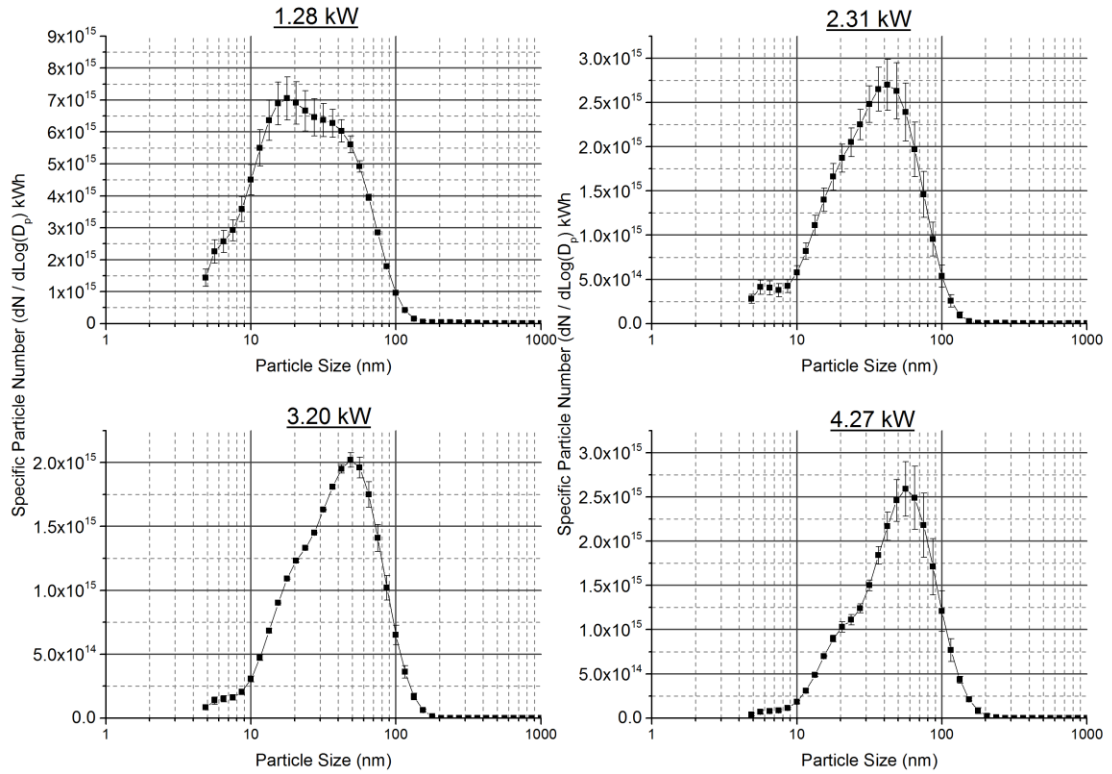


Figure 6-7 Particle size distribution of soot emission from the engine running on biodiesel.

The total number of particles emitted with respect to the amount of electricity produced, shown in figure 6-8, is higher than when using diesel, although the difference reduces to 17% more when at full load. The issue of particle emissions is an issue particularly at low loads with the particle number being over double that of diesel at 25% load.

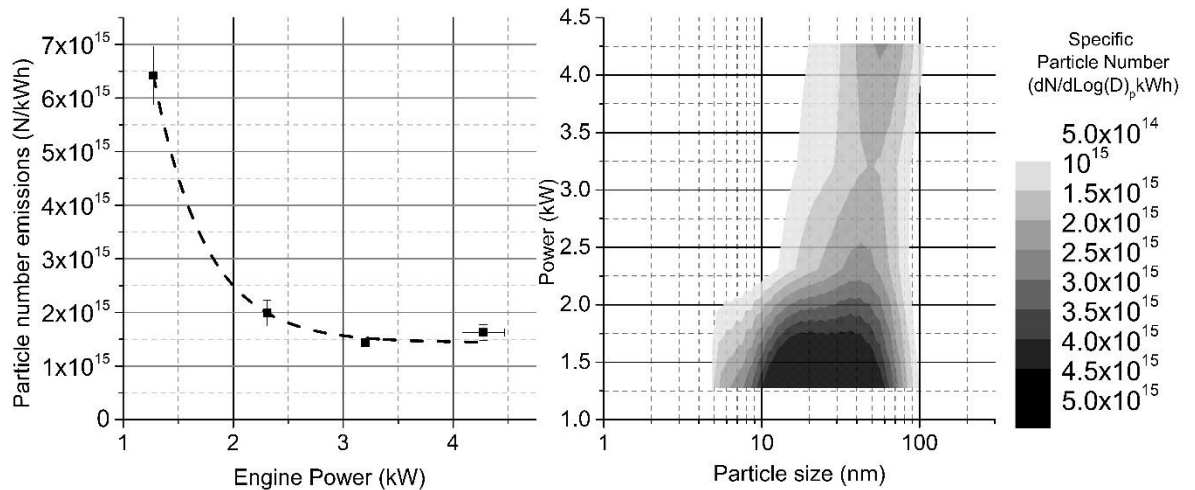


Figure 6-8 Particle emissions from the engine using biodiesel. Left: Particle number emissions as a function of power. Right: Particle number distribution heat map.

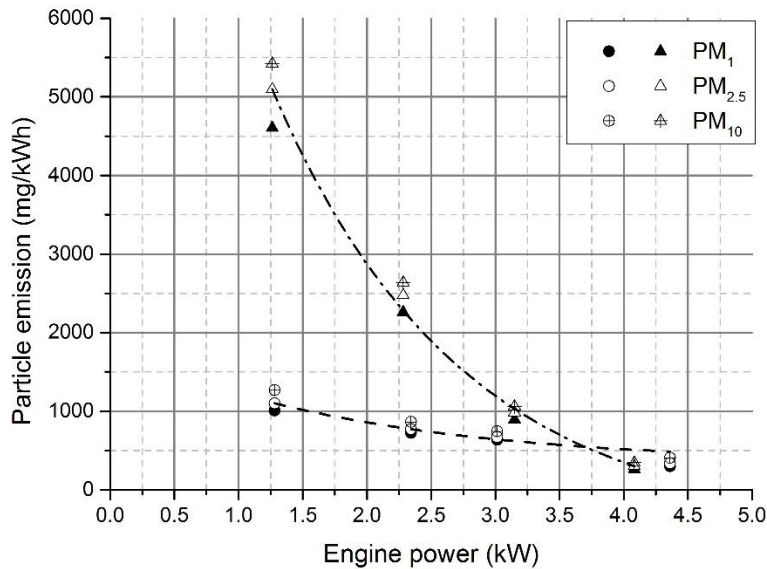


Figure 6-9 Particle emissions on a mass basis. Circles and triangles represent data for diesel and biodiesel respectively. Subscript denotes the maximum size in micrometres of particles. Lines of best fit are for PM_{2.5}.

Emissions were also measured using an Andersen cascade impactor. The particle mass distribution is used to calculate PM₁, PM_{2.5} and PM₁₀ in figure 6-9. The results further confirm that a larger quantity of smoke is produced using biodiesel compared to diesel. The percent change in particle emissions between diesel and biodiesel, however, is different to the percent change in particle number shown in figures 6-5 and 6-8. For example, at 1.25kW PM₁ measured for biodiesel is over 4 times that of diesel whereas the particle number is between 2-3 times higher. It is unclear why this discrepancy exists as the particle size for biodiesel soot was measured to be lower, therefore the percent difference in particle mass between biodiesel and diesel should be less than the percent difference in particle number. Also, at full load, biodiesel produces less soot by mass despite the particle number remaining higher. However, this is potentially explained by the smaller particles present in biodiesel exhaust meaning that by mass the value is lower. The possible reasons for the discrepancy at low load are either an experimental error or a difference in density between the two soot samples generated. An experimental error that could have occurred is that soot may have got trapped in the tubes connecting the instruments to the sampling probe. Density has been previously found to differ between exhaust particles with the same mobility size (Park et al., 2003).

The results are somewhat surprising as the use of biodiesel is generally reported to reduce PM, THC and CO whilst increasing NO_x (Xue et al., 2011). The reason for this can be explained by some properties of the engine and of the fuel. Firstly, the cetane number of biodiesel is usually higher than fossil fuel derived diesel (Bose, 2009). İçingür and Altıparmak (2003) states this

reduces NO_x because ignition delay is decreased. It was also found that, in some cases, this could also increase smoke emissions.

Another property that may cause these results is the higher viscosity of biodiesel which leads to poorer atomisation and therefore more smoke (Geacai et al., 2015). Patel et al. (2016) found the injection spray of biodiesel produced from jatropha had lower spray penetration and cone angle than mineral diesel when using an injector from a 7.4kW, single cylinder engine with near identical injection pressure to the one used in this study. In terms of biodiesel, ones derived from waste cooking oil generally have a higher viscosity because of the nature of the triglycerides present in the feedstock (Valente et al., 2011). Feedstocks for first-generation biodiesel are often selected to obtain low viscosity biodiesel (Bueno et al., 2017). Dias et al. (2008) found biodiesel produced from waste cooking oil had a higher viscosity than those produced from virgin sunflower and soybean oil.

The engine used for testing in this thesis has a relatively low injection pressure at 200 bar. Modern common rail injection systems can achieve pressures of up to 2,500 bar. Therefore, poorer atomisation of more viscous biodiesel may have been achieved compared to higher pressure systems used in literature, creating the difference in the emissions results. Jeon and Park (2018) found that specific soot emissions increased using a 20% biodiesel fuel, compared to pure mineral diesel, especially at the lowest injection pressure tested, which was 500 bar. The difference between soot produced by the two fuels was small when the injection pressure was increased to 1300 bar. The parameters of the engine used by Jeon and Park (2018) were similar to the one used in this study- the cylinder volume was 510 cm³ compared to 436 cm³ used on the current study, both were single cylinder and high speed (2000 vs. 3000rpm used here).

6.4 Char additive tests at 0.1%wt.

The first set of tests explored using 0.1%wt. of char added to diesel and biodiesel (WCOME) to investigate if the char can act as an additive to reduce emissions. The level for the concentration was chosen based on previous studies which have added graphite oxide nanoparticles to fuels (Carroll, 2015; Ooi et al., 2016). For these tests, no modifications were needed except for the removal of paper filters in the fuel line to allow particles to pass through the fuel line.

The effect of adding char at 0.1%wt. to conventional fuels on the overall fuel consumption appears in figure 6-10 to be negligible. The majority of sampling points fall within the error bars of the other fuels tested meaning that any changes in fuel consumption are below the detection limits.

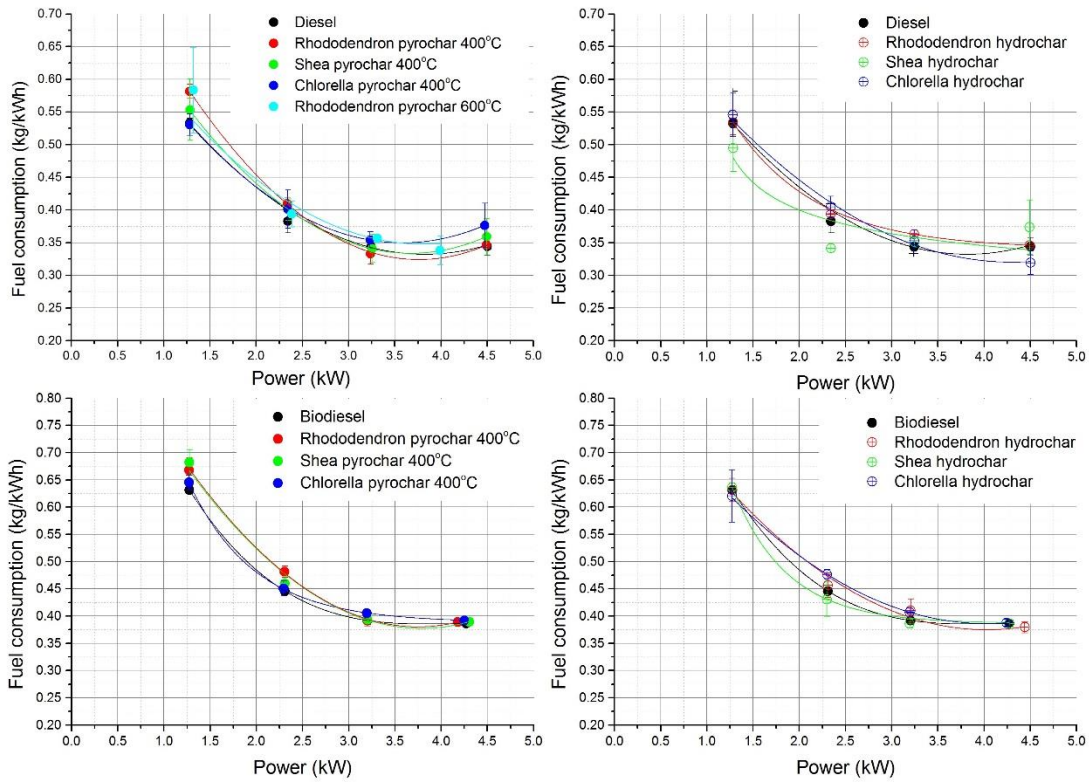


Figure 6-10 Fuel consumption of 0.1% wt. slurries. Top: Char in diesel, Bottom: char in WCO biodiesel.

6.4.1 Gaseous emissions from 0.1%wt. slurries

Figure 6-11 shows the CO₂ concentration in the exhaust with respect to the power output. CO₂ emissions give an indication of the fuel efficiency because the carbon in the exhaust increases with the amount of fuel burned. Each of the slurries show a similar CO₂ concentration to the baseline, except for the rhododendron 600°C pyrochar which is consistently higher across the power range. At high loads, most slurry chars display a small increase in CO₂ concentrations compared to the baseline tests. The difference, however, is potentially a result of reducing CO or THC. Rhododendron hydrochar in biodiesel displays a small CO₂ decrease and pyrochars in biodiesel produced near identical results to the baseline.

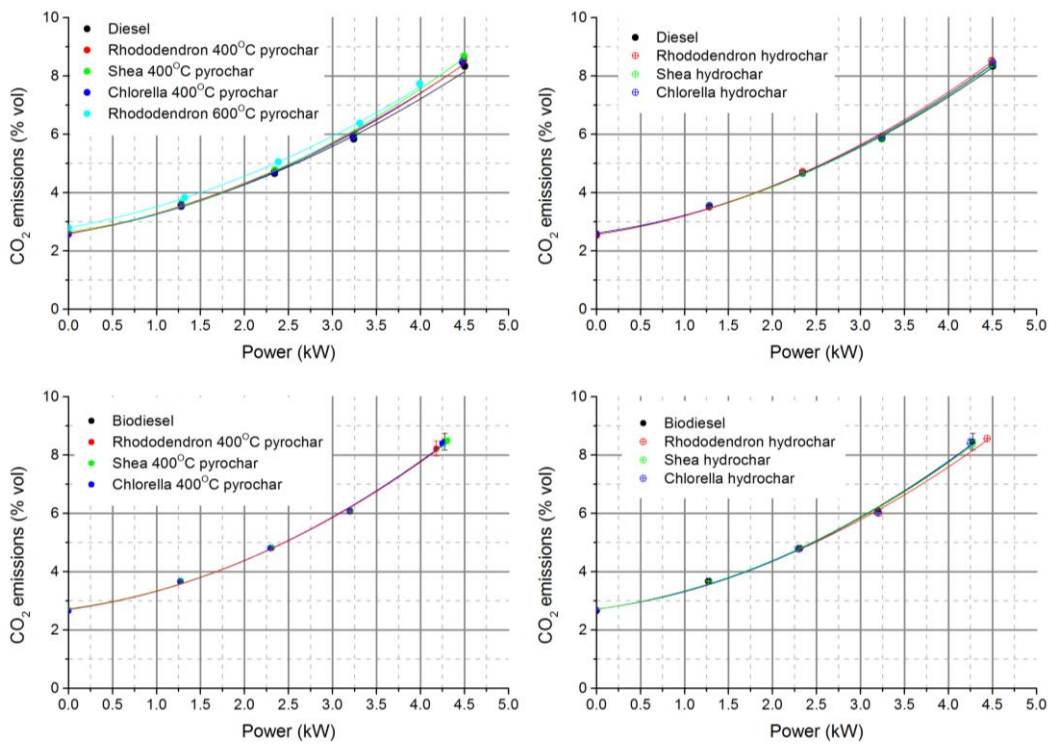


Figure 6-11 CO₂ emissions from 0.1%wt. slurries.

Figure 6-12 shows that adding low concentrations of char affects NO_x emissions. The addition of pyrolysis char alters the NO_x emission from both diesel and WCO biodiesel. Chlorella pyrochar increased NO_x, whereas shea and rhododendron pyrochar decreased it. The difference becomes slightly more pronounced with increasing load. One explanation for the decrease in NO_x is that the pyrochar reduces the premix combustion phase, a period of high NO_x production. Another reason could be the presence of char reducing the peak cylinder temperature. However, there is no correlation between the detected NO_x reduction and measured exhaust temperature, suggesting this is not the mechanism (Liu et al., 2018).

The amount of NO_x emissions created by the pyrochar slurry fuels reduces with nitrogen content of the pyrochars (i.e. shea has the highest, rhododendron the lowest) which might be causing the difference between the slurries. The amount of nitrogen in the rhododendron, shea and chlorella 400°C chars is 0.44%, 4.03% and 8.43% respectively, however, as the amount of char present is low, even at full load the chlorella pyrochar, which contains the highest amount of nitrogen, only produces 0.03 g/kWh, a tiny fraction of the total difference in NO_x emission from the baseline, 4.9 g/kWh.

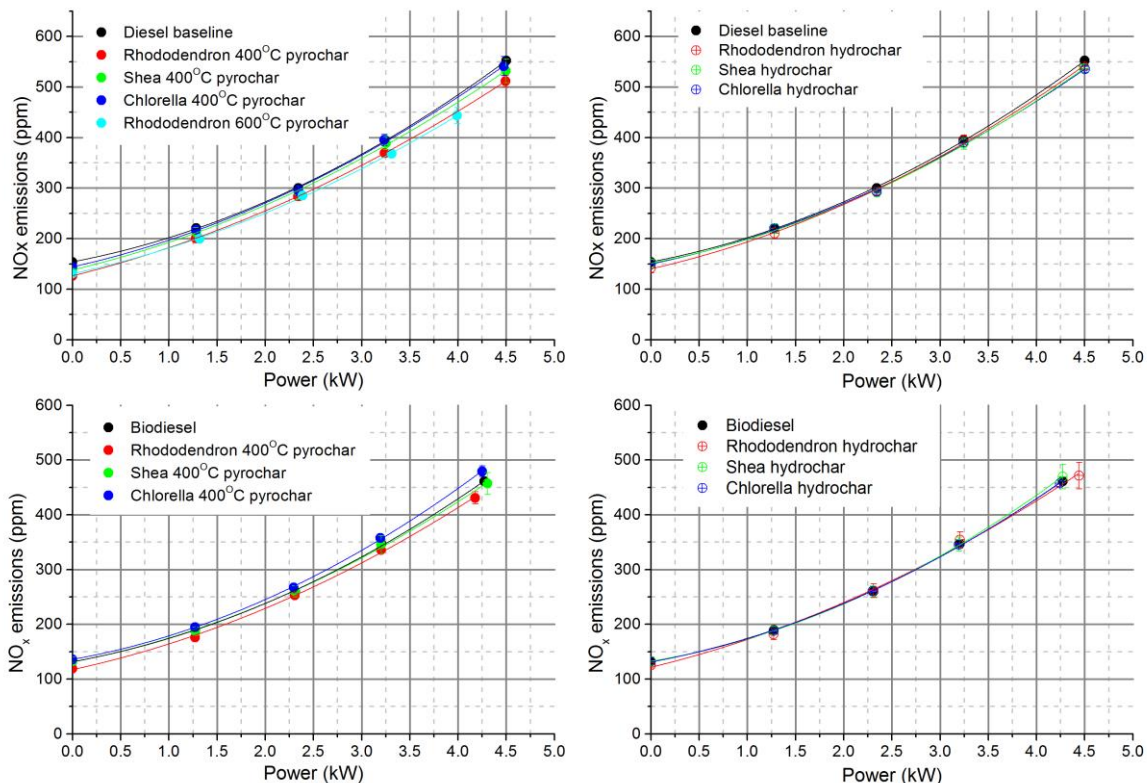


Figure 6-12 NO_x emissions from 0.1%wt. slurries.

The effect of increasing the pyrolysis temperature of rhododendron to 600°C made no difference to the NO_x emissions across the whole power range. As the difference in NO_x emissions is not affected by pyrolysis temperature, the most likely cause for the differences is the trace ash elements associated with the type of feedstock used.

The hydrochars tested did not produce the same effects the pyrochars did. The NO_x emissions of slurries containing this type of char were similar to that of the neat fuel baseline. The key differences between the two types of char are the structure of carbon and the relative absence of alkali elements, especially potassium, in hydrochars (Smith et al., 2016). Nejar and Illán-Gómez (2007) investigated potassium-cobalt and potassium-copper catalysts, finding that both removed soot and NO_x from a simulated diesel exhaust gas. Shangguan et al. (1998) also found that doping a catalyst with potassium further promoted NO_x and soot reduction. However, rhododendron pyrochar at 400°C had the lowest potassium content of the three pyrochars tested, and less than the shea hydrochar tested meaning that this catalytic effect from potassium is not necessarily occurring, or is not the main mechanism. The differences between the slurry fuels in terms of NO_x emission could be a result of the type potassium containing compounds present, each with a different effectiveness in reducing NO_x.

Wang et al. (2016) compared the NO_x emissions of washed and unwashed coals burned in air. It was found that washed coals produced more NO_x because the amount of sodium had been reduced. As with potassium, the majority of sodium is removed through hydrothermal carbonisation but remains after pyrolysis. Chlorella pyrochar contains significantly more sodium than rhododendron and shea, 8153ppm vs. 562 and 255ppm respectively, which does not correlate with the NO_x reductions. In fact, chlorella contains more of nearly all of the trace elements investigated than the other two chars, suggesting it is the carbon structure accounting for the NO_x reductions.

Carbon supported catalysts have previously been used for after treatment removal of NO_x with success (Li et al., 2015; Santillan-Jimenez et al., 2011). Activated carbon has also been used to adsorb NO_x from a gas stream (Davini, 2001). Activated carbons catalyse NO whilst in the presence of oxygen, to NO₂ which is then adsorbed (Rubel and Stencel, 1996). Zawadzki and Wiśniewski (2007) investigated the reduction in NO_x by carbon films made from carbonised cellulose. Various nitrogen species were formed on the carbon surface including C-NO₂, C-ONO and C-NCO. The compounds were then converted to N₂ by outgassing with 80% efficiency. Illán-Gómez et al. (2001) modified a coal-based activated carbon with bimetallic catalysts including KNi, finding that the introduction of inorganic material improved NO_x reduction and reduced carbon consumption. These mechanisms are potentially the same ones

occurring during the combustion of 0.1%wt. pyrochar slurries. As the carbon structure in hydrochar is less graphitic, it would explain why a similar effect is not happening.

As the two rhododendron pyrochars contain the most carbon, shea next, and chlorella the least, the NO_x concentration results correlate. Increasing the pyrolysis temperature alters the carbon structure of rhododendron char but not in a way which affects the interaction of the carbon with NO_x.

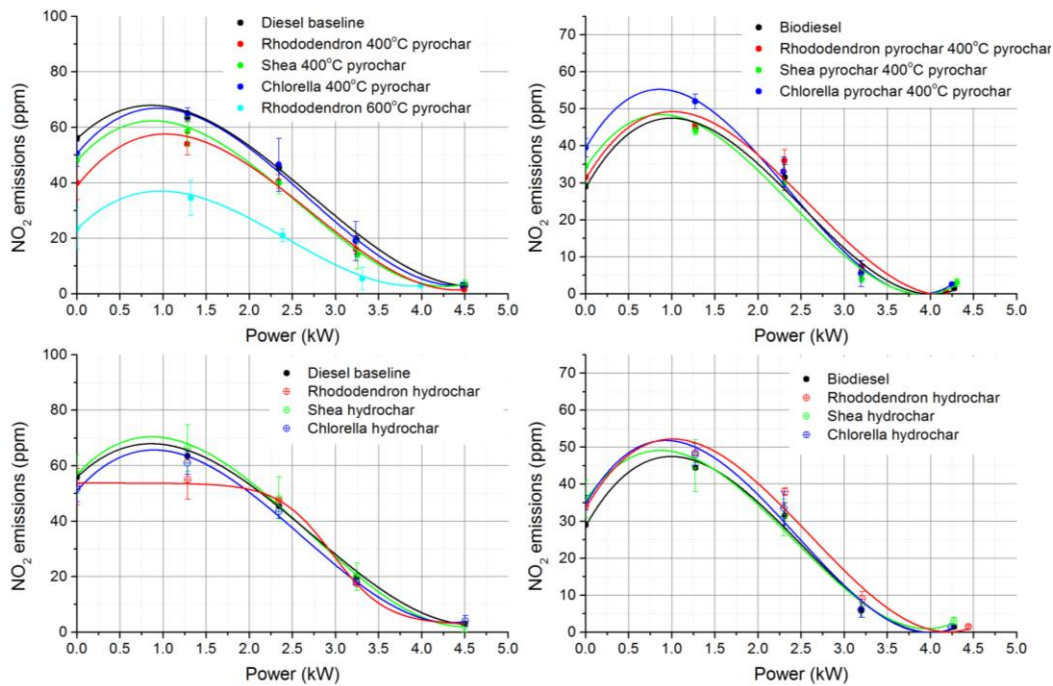


Figure 6-13 NO₂ emissions from 0.1%wt. slurries used in a diesel engine.

Figure 6-13 shows the NO₂ emissions from 0.1%wt. slurries, which is one component of NO_x (the other being nitric oxide (NO)), from the diesel engine when using several 0.1%wt. slurry fuels. The addition of 0.1%wt. of pyrochar appears to show a reduction in NO₂ emissions at all powers compared to the baseline of neat diesel. The largest reduction occurs when rhododendron pyrochar produced at 600°C is added. Shea and rhododendron pyrochar added to diesel also show a reduction in NO₂ emissions. Chlorella 0.1%wt. diesel slurry, however, did not show a reduction in NO₂ emissions.

Adding hydrochar to diesel at 0.1%wt. did not show the same benefit as the pyrochars did. Also, neither the pyrochars nor hydrochars in biodiesel showed the same effect. The lack of reduction in NO₂ is likely why no change in NO_x emissions was detected in any of the 0.1%wt. biodiesel slurries. In most instances, the data points for the 0.1%wt. biodiesel slurries are within the margin of error of the baseline.

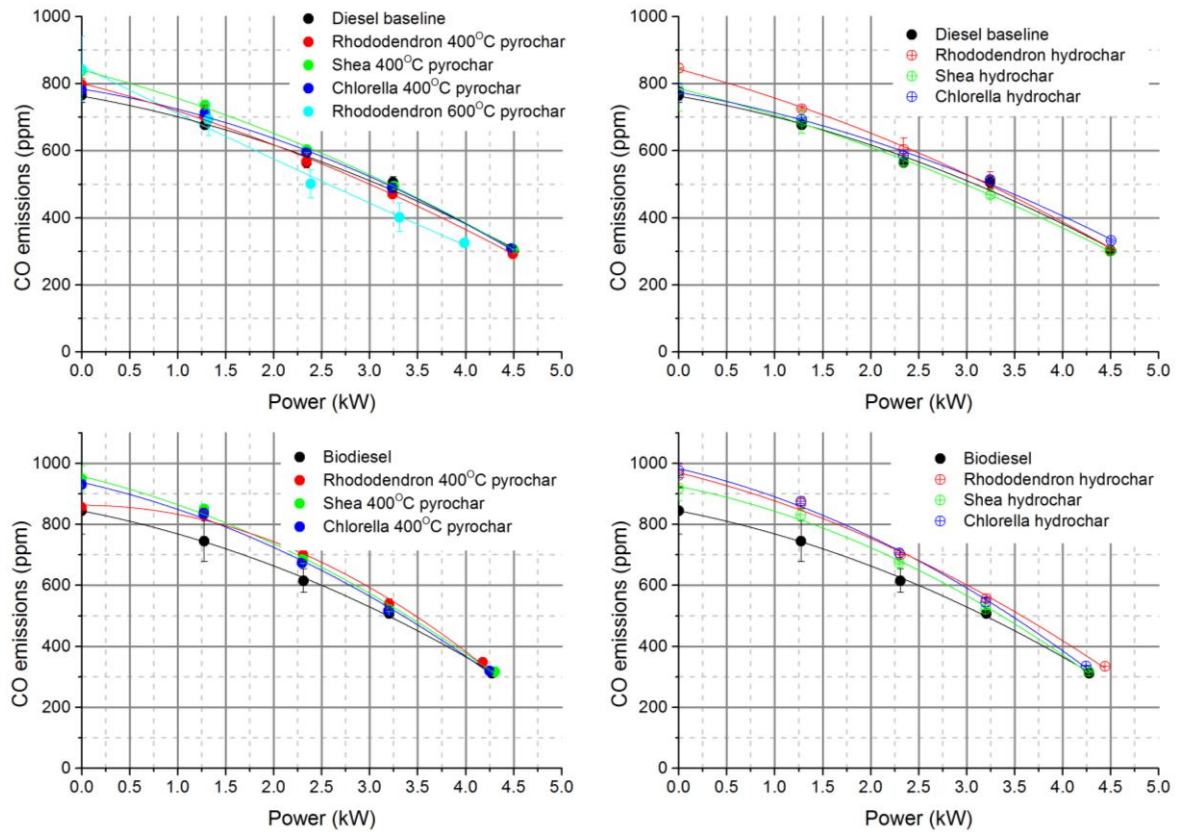


Figure 6-14 CO emissions from slurry fuels containing 0.1%wt. char.

The emission of CO from diesel engines is an indicator of incomplete combustion and is usually highest in terms of exhaust gas concentration and specific emission at low loads. In figure 6-14, the CO emission concentration reduced in relation to the baseline with the addition of 0.1%wt. of rhododendron pyrochar produced at 600°C at high loads. Chlorella and shea pyrochar slurries in diesel produced slightly more CO, and the rhododendron 400°C pyrochar in diesel slurry was similar to the baseline. The reason for the reducing CO emissions from the high-temperature rhododendron pyrochar is catalytic or by improving atomisation. Hydrochars in diesel slurries increased CO across all loads. CO also increased for biodiesel slurries but to a larger extent than diesel. All pyrochar biodiesel slurries displayed a similar increase in CO compared to the baseline and converged at full load. Hydrochar biodiesel slurries display an increase in CO also similar to that of the pyrochar biodiesel slurries.

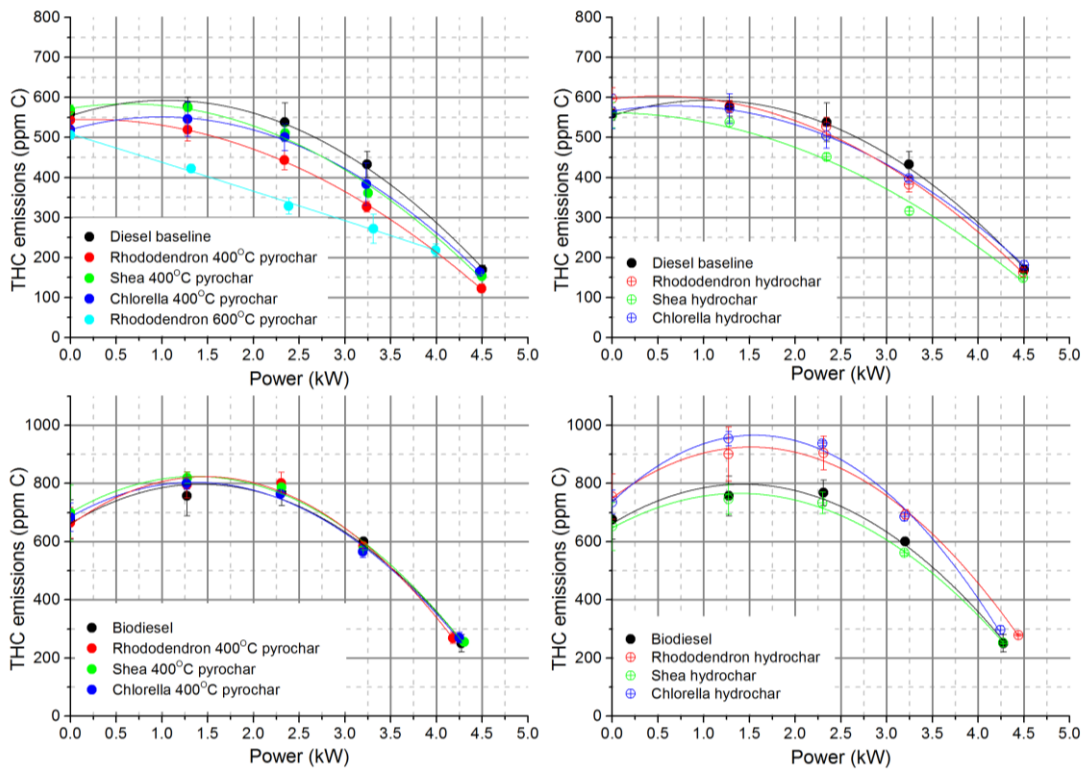


Figure 6-15 THC emissions from 0.1%wt. slurry.

Figure 6-15 illustrates that shea hydrochar reduced THC in regards to the baseline in both diesel and biodiesel. Rhododendron and chlorella hydrochars, however, increased THC emission in both liquid fuels. Pyrochars in diesel affected the THC emissions substantially, with each reducing the amount produced. Rhododendron pyrochar at 600°C produced the greatest benefit, causing a 40% reduction in THC at 50% load from the baseline. Rhododendron pyrochar at 400°C is the next effective at reducing THC, followed by shea and chlorella which have similar values to each other. The THC reduction did not occur when using pyrochars in conjunction with biodiesel.

The change in THC emissions is therefore liquid fuel dependent suggesting that the char might affect the physical properties of the fuel in some way. Increasing viscosity is associated with poorer atomisation and higher fuel spray penetration which, in turn, increases THC and CO emissions (Yang et al., 2007). The presence of char at these concentrations may alter viscosity or improve atomisation, which would reduce THC formation occurring in cooler parts of the engine. If this was the case, then a concurrent CO reduction would be expected, but this did not happen. The concurrent CO emission decrease expected from the hypothesis that viscosity and/or atomisation is improved could be counteracted by another effect, such as CO formation from the char additive itself.

6.4.2 0.1%wt. slurries particle emissions

The particle size distribution for the liquid fuels neat is shown in figure 6-16. For diesel, the mode at full load occurs at roughly 200nm and is 2×10^8 dN/dLogDp cc. The three mid-range sampling points shown on the plot by dotted lines have a mode in the region of 70-100nm of approximately 1×10^8 dN/dLogDp cc. Particles at idle are smaller, the mode is at 20nm and approximately 1×10^8 dN/dLogDp cc. The biodiesel particle emission concentration is higher than diesel. At full load, the mode is 2.8×10^8 dN/dLogDp cc at 60nm. At the other three sampling points in the mid-range, the mode is $1.6 - 2 \times 10^8$ dN/dLogDp cc.

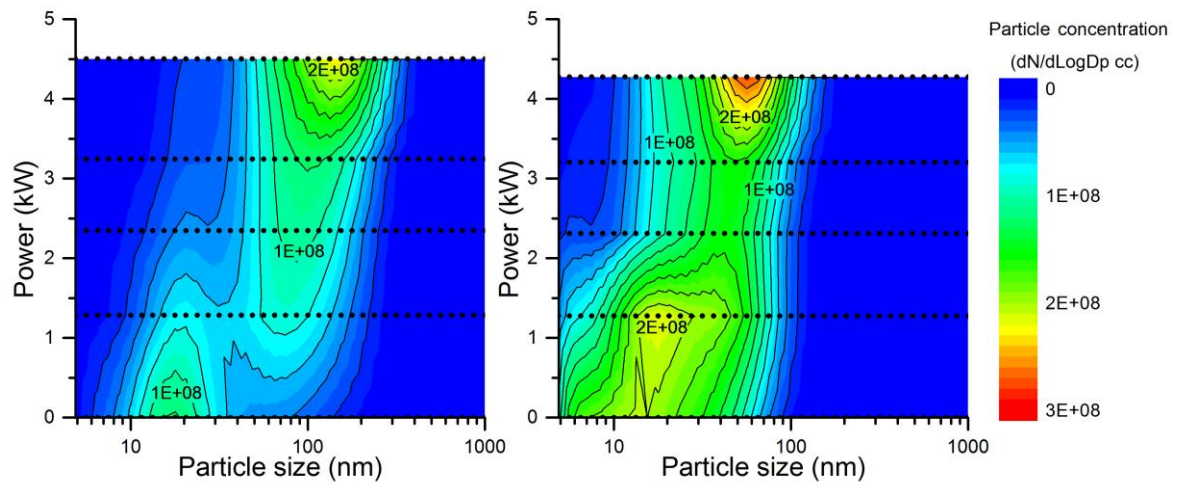


Figure 6-16 Particle size distribution of soot produced at different loads. Left: diesel baseline, and right: biodiesel baseline.

Figure 6-17 shows the change in soot particle distribution of 0.1%wt. slurries compared to the engine baseline operating solely on diesel. At low loads, idle to 1.5kW, particle emissions are significantly higher, especially at 10nm, suggesting that the char particles added are not completely burned. This region of particles is present in emissions from every slurry fuel, but the smallest for rhododendron HTC 250°C char, the material with the lowest recalcitrance index and the lowest complete burnout temperature. The temperature programmed oxidation (TPO) profiles in chapter 4 show that the complete burnout of the rhododendron hydrochar occurs just before 500°C, whereas for the shea and chlorella hydrochar this occurs at 550°C and 625°C respectively.

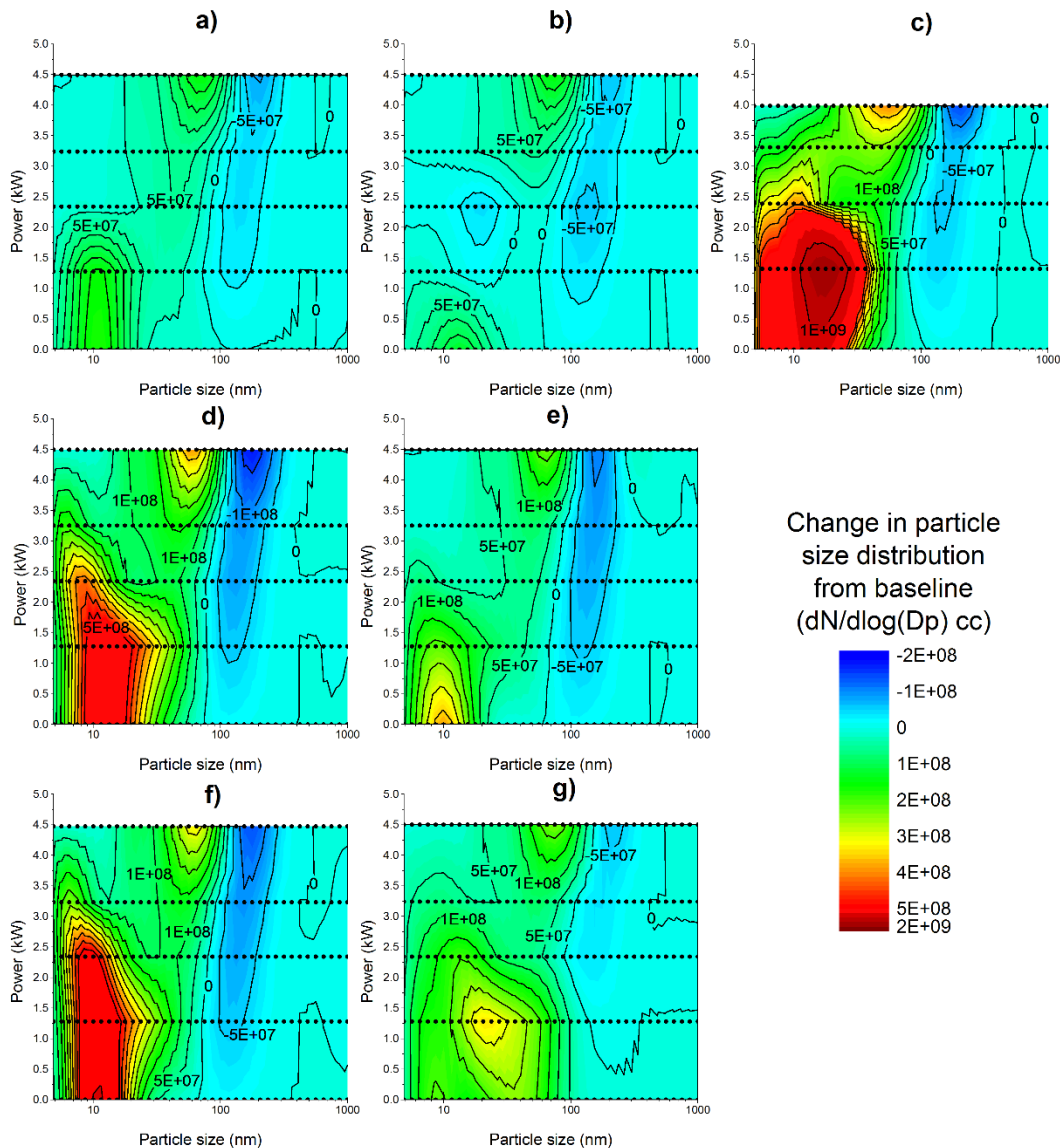


Figure 6-17 Difference in particle size distribution of 0.1%wt. diesel chars from the neat diesel baseline in figure 6-15. a) Rhododendron pyrochar produced 400°C, b) Rhododendron hydrochar, c) Rhododendron pyrochar produced at 600°C, d) Shea 400°C pyrochar, e) Shea 250°C hydrochar, f) Chlorella 400°C pyrochar and, g) Chlorella 250°C hydrochar. Dotted lines represent the sampling points.

The pyrochars tested show a similar pattern, the rhododendron pyrochar had the smallest increase in particle emissions in the region of 10nm at low load. However, in this instance, the shea pyrochar has the lowest recalcitrance index, yet demonstrates a high increase in circa 10nm particles at low load. Shea pyrochar contains significantly more ash than rhododendron (15.49% vs. 3.56%), but the increase in particles is not from ash because the increase does not occur at high load. The heightened presence of ash, however, could affect the combustion chemistry, leading to more ultrafine soot particles. The rhododendron pyrochar produced at the higher temperature of 600°C demonstrates significantly higher ash compared to the baseline and is worse than the other two rhododendron chars which are less recalcitrant. At 1.35kW, the mode of the particle size distribution from using the rhododendron 600°C pyrochar slurry is ten times larger than the baseline test, showing that the pyrolysis temperature has a marked effect on particle emissions. The mode increases in the majority of instances, except for the rhododendron hydrochar at 50% load, with the addition of char particles in relation to the baseline. The particle size distribution shifts to smaller sizes with the addition of char seen by a reduction in particle emission between 100 and 200nm, and an increase in the range 20-80nm.

Chars added to biodiesel behaved similarly to 0.1%wt. diesel slurries. The particle size distribution heat maps shown in figure 6-18 for the change in particle number distribution against load in 0.1%wt. biodiesel slurries demonstrate the same increase in particles of roughly 10nm at low loads, which also occurred with the 0.1%wt. diesel slurries. Whilst there was some reduction in particle emission around 100nm, this was less pronounced than when diesel was used as the liquid fuel. Similarly, the increase in particle size distribution follows a similar pattern with regards to the char used in 0.1% wt. biodiesel slurries as in the diesel equivalent. A large region occurs at around 10-20nm, especially at low loads, increasing the height of the mode. In the case of both chlorella chars and shea pyrochar, the increase in the mode is over 4 times. The material type which affects the particle size distribution most is, in ascending order: chlorella, shea and rhododendron, the same for both types of slurry. One difference that occurs is between the rhododendron hydrochar in the two different fuels tested. When used with diesel, there is no large increase in particles at low loads, whereas, in biodiesel, the amount is significant and more than the rhododendron 400°C pyrochar in diesel.

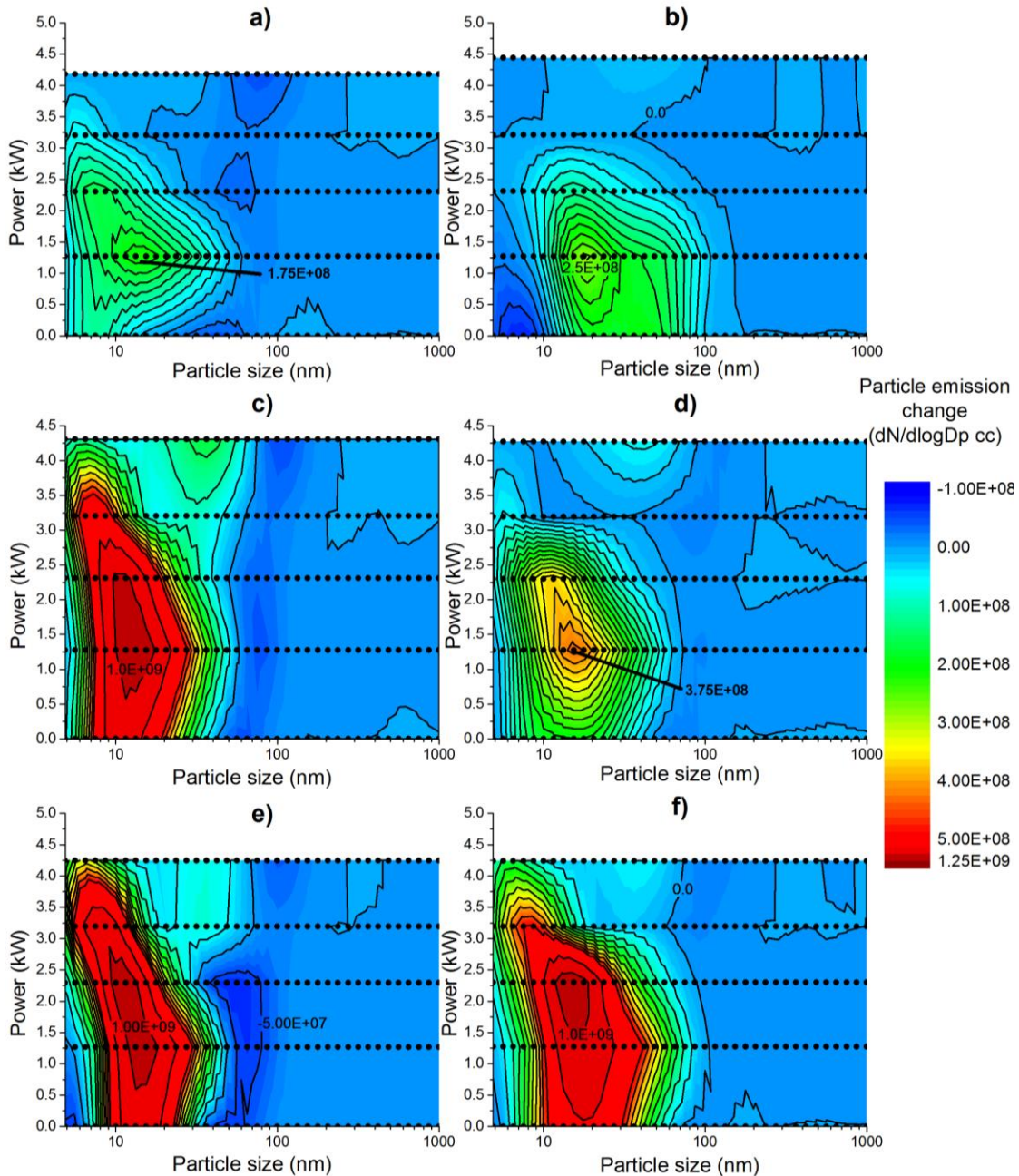


Figure 6-18 Difference in particle size distribution of 0.1%wt. biodiesel chars from the baseline. a) Rhododendron 400°C pyrochar, b) Rhododendron hydrochar, c) Shea 400°C pyrochar, d) Shea hydrochar, e) Chlorella 400°C pyrochar, and f) Chlorella hydrochar. Dotted lines represent the sampling points.

Biodiesel slurries with 0.1%wt. of char show a larger increase in particle emissions at 50% and above loads than the diesel slurries. Considering particle emissions with the CO and THC emissions shown in figures 6-14 and 6-15 respectively, which also showed higher values when using biodiesel slurries compared to pure biodiesel, it suggests more incomplete combustion is occurring with the addition of 0.1%wt. char.

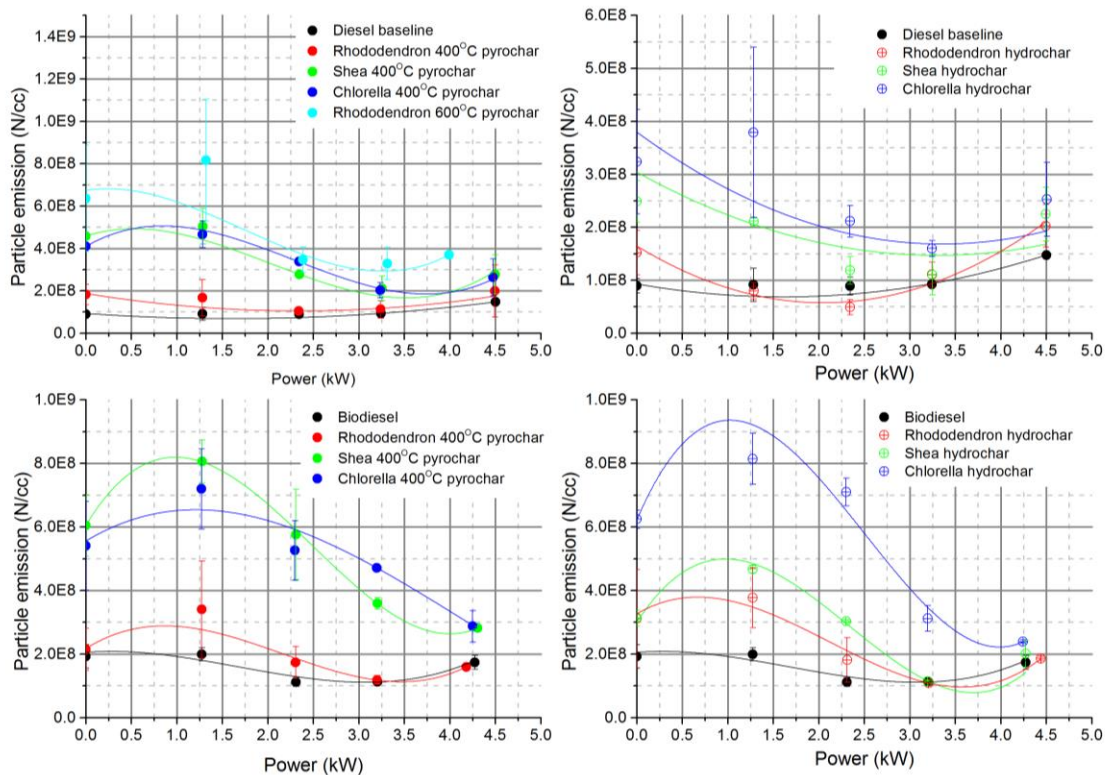


Figure 6-19 Power normalised particle emissions from 0.1%wt. slurries tested.

Figure 6-19 shows the total particle emission over all loads for the 0.1%wt. slurries tested. Similar to the particle size distributions, the total particle emission is highest at around 25% load and tends to converge with the value for the respective baseline at high loads. When diesel is used as the liquid matrix, the rhododendron 600°C slurry performs the worst of all the pyrochars in terms of the particle emission at all loads. The chlorella and shea pyrochar slurries have similar particle emission profiles across all loads. Both of these slurries produce consistently over twice the amount of particles than the pure fuel baseline. The rhododendron 400°C pyrochar-diesel slurry produced the lowest amount in this particular set of fuels, but still produces more particles than the baseline.

Only one slurry gave a lower particle number than the baseline at any point, which was the rhododendron hydrochar in diesel at 50% power (2.25kW). At full power, however, the increase from the baseline in particle emissions was 33% when using rhododendron hydrochar in diesel. The other two hydrochars in diesel produce fewer soot particles than the pyrochar slurries produced from the same materials.

Pyrochar in biodiesel slurries behave similarly as diesel slurries, with rhododendron increasing the particle number emission the least. The pyrochars from chlorella and shea consistently produce more particles across loads than the baseline, ranging from an increase of 50% at full load to 200% under half load.

The particle emission profile of chlorella hydrochar in biodiesel slurry is incongruous with the trend occurring with the other five hydrochar slurries in that materials treated through HTC produce fewer or similar quantities of particles than those treated through pyrolysis.

Rhododendron hydrochar in biodiesel did not yield the same low particle emission at low to medium loads which occurred when the char was used in conjunction with diesel. Figures 6-17, 6-18 and 6-19 show that hydrochars do not burn well when biodiesel is used until higher loads. In figure 6-18 the emission for hydrochar biodiesel slurries, particularly shea, increased significantly in the region of 20nm from idle to 25% load. Chlorella hydrochar in biodiesel slurry continued to produce significantly higher particle number emissions in this area until 3.25kW when it began to decrease. In hydrochar diesel slurries, however, this region of increased particle emissions diminishes earlier, between idle and 25% load.

Table 6-3 Total suspended particles below 10 μ m (PM₁₀) at full load testing. The amount of ash which is created during the tests is also predicted.

<i>Fuel</i>	<i>Char species</i>	<i>Treatment</i>	<i>Ash emission (predicted) (mg/m³)</i>	<i>PM₁₀ (mg/m³)</i>
<i>Diesel</i>	<i>None</i>	-/-	-/-	32.0 \pm 6.8
	<i>Rhododendron</i>	Pyrolysis 400°C	2.3	27.5 \pm 8.3
		Pyrolysis 600°C	2.5	31.8 \pm 0.1
		HTC 250°C	2.0	26.3 \pm 5.9
	<i>Shea</i>	Pyrolysis 400°C	10.6	39.9 \pm 4.1
		HTC 250°C	3.4	31.9 \pm 6.3
	<i>Chlorella</i>	Pyrolysis 400°C	14.6	32.2 \pm 2.7
		HTC 250°C	7.7	31.5 \pm 4.2
<i>Biodiesel</i>	<i>None</i>	-/-	-/-	26.6 \pm 7.5
	<i>Rhododendron</i>	Pyrolysis 400°C	2.5	25.8 \pm 2.9
		HTC 250°C	2.4	28.3 \pm 0.7
	<i>Shea</i>	Pyrolysis 400°C	11.6	26.7 \pm 0.6
		HTC 250°C	3.7	24.2 \pm 0.7
	<i>Chlorella</i>	Pyrolysis 400°C	15.5	27.8 \pm 1.8
		HTC 250°C	9.5	30.4 \pm 2.2

Table 6-3 shows the mass of soot produced at full load per volume of exhaust gas when using 0.1%wt. slurry fuels. Whilst the amount of char added is only small, the amount of ash produced is still significant when compared to the amount of soot. If ash does flow out of the cylinder through the exhaust (the other possibility being that it ends up in the lube oil), then it might be possible to determine even at these low quantities. However, the results in table 6-3 appear to show no firm correlation between ash produced and soot emission. For example, shea hydrochar and chlorella pyrochar in diesel slurries emit similar amounts of PM₁₀ despite the latter producing over 4 times the amount of ash.

There does, however, appear to be a correlation between the degree of carbonisation and soot emissions. The amount of PM₁₀ emissions from rhododendron slurries is highest for the 600°C char, the most carbonised, and the lowest for the hydrochar, which was found to have the lowest degree of carbonisation in chapter 3 of the 3 rhododendron chars tested as fuels. Of the 6 sets of fuels tested, 4 have lower soot emissions when the hydrochar is used compared to the pyrochar.

There is no correlation between feedstock used and total soot emission found at this concentration of char. For example, chlorella and shea hydrochar produce similar levels of soot, but the difference between the soot emissions from the pyrochars is marked. Whilst the shea chars are the worst for soot when mixed with diesel, in biodiesel the hydrochar is the best.

Overall, the levels of PM₁₀ do not vary significantly from the baseline and so it is difficult to see a trend. Combining table 6-3 with figure 6-19 shows little difference at full load for the combustion of slurry fuels compared to the baseline. The key issue is particulate emissions during low load.

6.4.3 Presence of ash in soot samples

Soot samples were analysed using SEM/EDX by transferring particles from the filter papers to a silicon wafer. Analysis by EDX of the 400°C pyrochar showed most of the material by weight was carbon but other elements were present. Calcium, sodium, aluminium and potassium were detected, but in quantities significantly less than the prediction of ash emissions in table 6-3 suggests. Zinc and barium were also detected which is most likely to have been produced from burning engine oil. Sodium and potassium were detected by EDX in the rhododendron hydrochar slurry soot sample, but in smaller quantities than the pyrochar slurry.

Overall, it appears unlikely that all the ash escapes the cylinder via the exhaust because total soot emission on a mass basis, shown in table 6-3, does not increase to the extent that the ash content would suggest. Additionally, although not a precise method for detecting trace levels of elements, EDX analysis of the soot suggests less ash is present than would be expected from the input.

6.5 1%wt. char slurries

The amount of char was further increased by a factor of 10, toward the highest concentration of char which is considered to be an additive rather than a co-fuel. Following the 0.1%wt. slurry tests, the use of chlorella chars was ended as the material behaved similarly to shea. Also, chlorella is the least suitable feedstock for developing countries. Rhododendron pyrochar produced at 600°C was also no longer used because most types of emissions were higher than the pyrochar produced at the lower temperature of 400°C, thus was less desirable. To the 1%wt. slurries, a further 0.1%wt. of lecithin was added to improve the stability of the slurries. A new baseline was performed using diesel containing 0.1%wt. of lecithin to remove the surfactant as a variable in the results and to account for modifications to the engine, and any wear, tear and deposits that had built up over time.

6.5.1 Modifications before tests

During the first tests, it was found that the relatively small addition of 1%wt. char caused issues with the diesel injector mechanism. The problem was that particles entered between the guide section of the injector needle and body, seizing the mechanism. A failed injector was inspected visually and by scanning electron microscopy (SEM) once the internal cavity was exposed, and the needle freed by machining the nozzle body in half by wire electrical discharge machining (EDM) (figure 6-20). Fuel is fed into the pressure chamber from the high-pressure pump and is sprayed into the engine via the injector holes once the needle has lifted. The motion occurs once the pressure inside the chamber can exceed the force of the spring acting onto the pressure pin. The seal in the pressure chamber is maintained by the small gap between the needle guide and nozzle body, (less than 10µm difference in inner diameter of the body and outer of the guide) hence the ability of particles to enter this area as they are still smaller than the gap. As there is no secondary oil port inside the main injector assembly, the gap is required to maintain lubrication by allowing some fuel through. A previous study found that when running 25% wt. charcoal in diesel, the same issue of seizing occurs which was remedied to an extent by machining a channel for high-pressure lubricating oil into the guide area (Soloiu et al., 2011). This idea was rejected in this case because the specific design of the injector made it unrealistic to machine a channel.

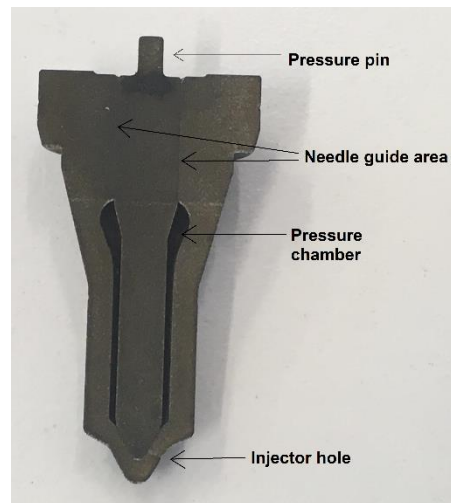


Figure 6-20 Cut through injector nozzle body and needle with key sections labelled.

Figure 6-21, shows SEM images of needle guides confirming the hypothesis that particles are becoming trapped on the surface. The image on the left shows an injector needle prior to use which has a uniform surface with a small number of surface particles. On the right, the seized needle contains significantly more particles on the surface, similar in size to the charcoal slurry particles, but the surface remains undeformed. Particles covered the whole surface, but also had the tendency to agglomerate, further immobilising and preventing the needle from working itself free, such as in the centre of the right-hand image in figure 6-21. Energy dispersive x-ray (EDX) of the deposits, as well as the darker colour in the image, showed that the material is carbonaceous rather than, for example, metallic debris from part wear.

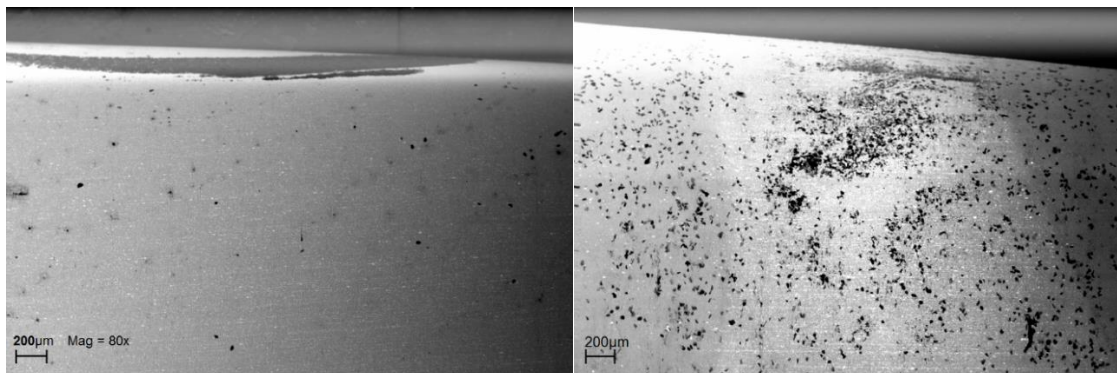


Figure 6-21 SEM images of the needle guide area at 80x magnification. Left: Unused. Right: After seizing.

Attempts were made to reduce injector seizing by adding lubricants to the fuel used. Two different commercial lubricants were used: a two-stroke oil- which was selected because it is designed to be blended with fuels and lubricate parts of a two-stroke engine, and a commercial additive designed to improve lubricating properties of engine oil. Both were tested at 1 part additive to 50 parts 1%wt. slurry fuel, the recommended dosage for two-stroke oil. The addition of either oil did not create a discernible difference in the tendency of the injector needle to stick and so the idea was abandoned.

Two modifications were made to reduce the likelihood of needle seizing. First, the diameter of the needle guide section was reduced to give further clearance for particles to pass freely. The diameter of the needle guide was reduced by 10 μ m. Second, the strength of the spring regulating the injection pressure was decreased so that less force is preventing the needle from lifting. This was done by removing a shim which preloads the spring in the injector casing. Removing the shim reduced injection pressure by approximately 196 bar to 176 bar. This injection pressure is relatively low for diesel engines, especially modern systems. Injection pressures can be in the range of 400-2000 bar (Agarwal et al., 2013; Du et al., 2017; Lee and Park, 2002; Xiang et al., 2013). It should be noted that reducing the engine injection pressure will affect the quality of atomisation and therefore increase soot emissions (Xu et al., 2014). Increasing injection pressure tends to increase NO_x, and CO₂, but reduces CO and HC (Agarwal et al., 2015; Liu et al., 2015a).

6.5.2 1%wt. slurry fuel consumption

The new diesel baseline fuel consumption shown in figure 6-22 remains similar to the original in figure 6-3 but has some differences. The consumption at 1.35 kW is 0.02 kg/kWh higher than the original baseline. The middle two sampling points are within the same range as the equivalent points in the baseline in figure 6-3. The final point at 4kW has a fuel consumption of 0.39 kg/kWh, 0.05 kg/kWh higher than in the original baseline, a significant difference. An increase in fuel consumption of over 10% after the addition of a surfactant is certainly unexpected and unlikely to be a genuine change. There are, inevitably differences in the inlet air temperature, and the lube oil temperature can fluctuate by 5°C whilst testing at full load, but this is unlikely to cause such a marked variation in consumption. Similarly, the 1%wt. slurries also vary drastically in measured fuel consumption. The margin of error is also large, and in many cases over 10%.

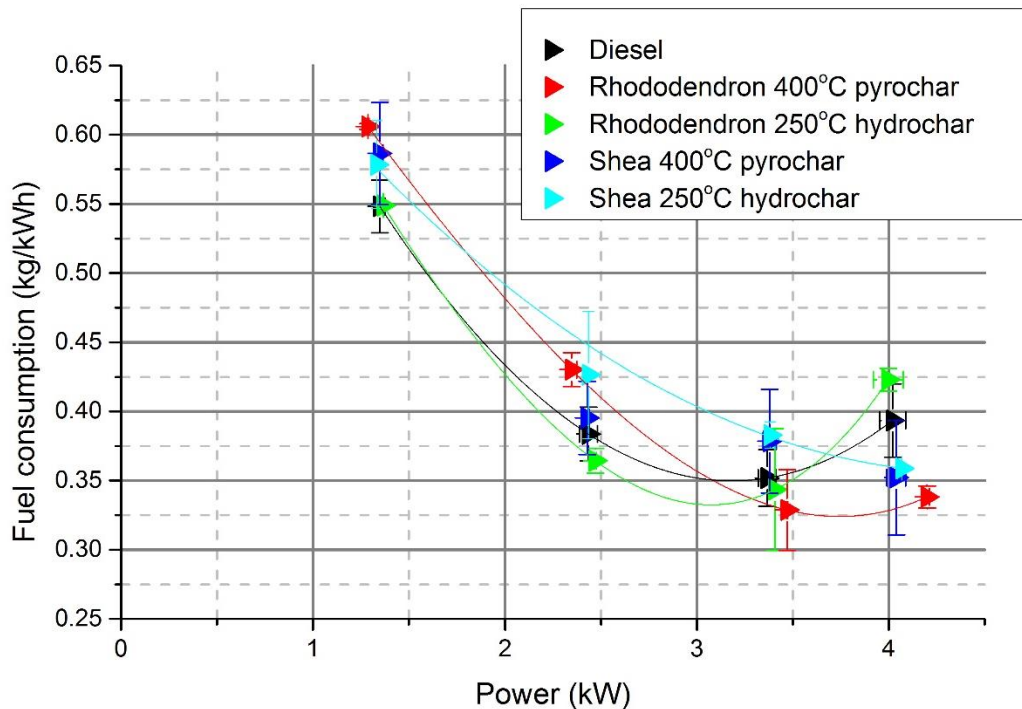


Figure 6-22 Fuel consumption of 1%wt. slurries compared to a diesel baseline containing the lecithin surfactant used.

The other possibilities for the difference are an error in measuring the amount of fuel used or poor repeatability in how the engine operates. The former is more probable and could be caused by a number of reasons. Only the fuel tank is weighed and so there is a length of tubing from it which could act as a reservoir, reducing the accuracy of the response of the balance to the fuel consumption. The change in position and mass of the tubing will affect the centre of mass of the tank being measured on the scales, causing an instrument error known as corner load. Another possibility is the vibration of the engine alters the position of the fuel lines, changing the value of the balance. The problem with inconsistencies in results could be with the mechanism of the balance itself. The readability of the scale is 0.01 kg which is relatively large compared to the difference in fuel consumption expected between fuels used. Figure 6-23 shows the raw data for fuel mass against time at full load. Whilst the correlation is good, the variance throughout is enough to make a real difference to the results. The gradient over the whole test gives a fuel consumption of 1.5 kg/hr, but calculating the gradient of the first and second half separately gives a consumption of 1.67 and 1.41 kg/hr respectively, pointing to a lack of precision.

Variation in the engine operation could exist leading to inconsistent fuel consumption. In the same test shown in figure 6-23, the power output fluctuates by 145W, although most of the effect of this is removed when fuel consumption is normalised. It does, however, show the engine does operate inconsistently, as does the fluctuations in engine speed which also occur. Emission concentrations in the exhaust also vary over time which might be an effect of changing power and speed or could indicate a change in quantity and timing of injection of fuel consumed.

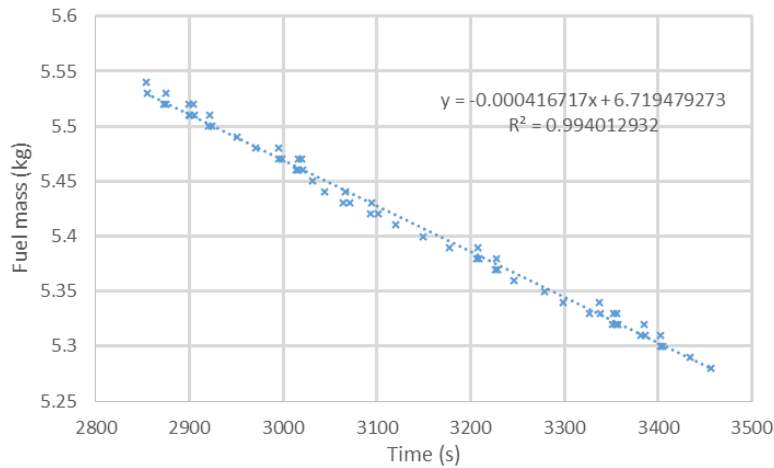


Figure 6-23 Raw data from balance measuring fuel mass change of diesel with 0.1%wt. lecithin at full load.

6.5.3 Gaseous emissions from 1%wt. slurries

The variation in CO₂ emissions between the 1%wt. slurry fuels tested is minimal across the full set of loads except for the rhododendron pyrochar at full load which produces less CO₂. The error bars on the sampling points in figure 6-24 are larger than the variation showing that it is not statistically significant. The new baseline for diesel with 0.1%wt. lecithin added varies slightly to the original baseline which could be caused by a build-up of deposits or the modifications made. The new baseline at 4 kW has increased CO₂ emissions of 0.35% vol..

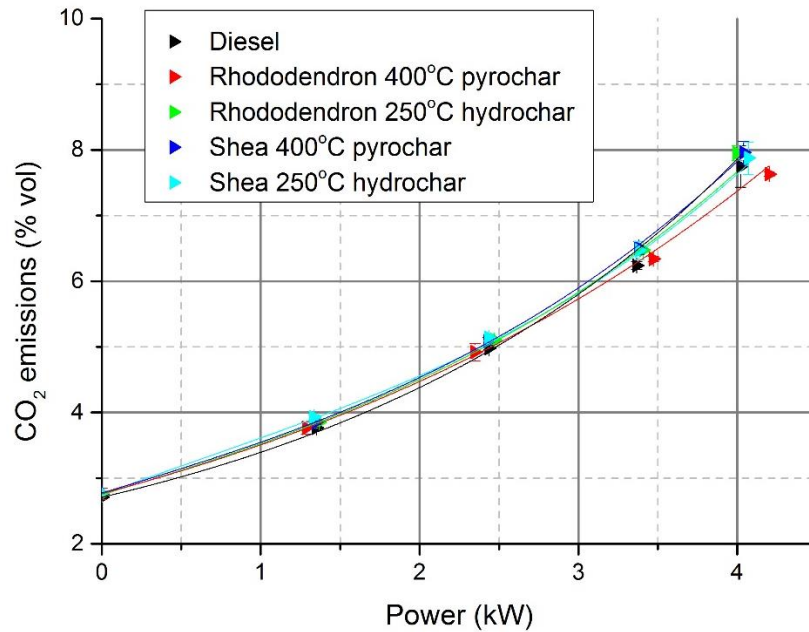


Figure 6-24 CO₂ emissions of 1%wt. slurries.

The CO emissions for the 1%wt. slurries shown in figure 6-25 are lower than the baseline. The new baseline is near identical in terms of CO with the original baseline the 0.1%wt. slurries were compared to. Whereas when only 0.1%wt. of char was added, just rhododendron pyrochar produced at 600°C yielded a clear reduction, at the higher concentration of 1%wt. char the benefit becomes apparent. The most effective char at reducing CO emissions is the rhododendron hydrochar, closely followed by the shea pyrochar, then shea hydrochar.

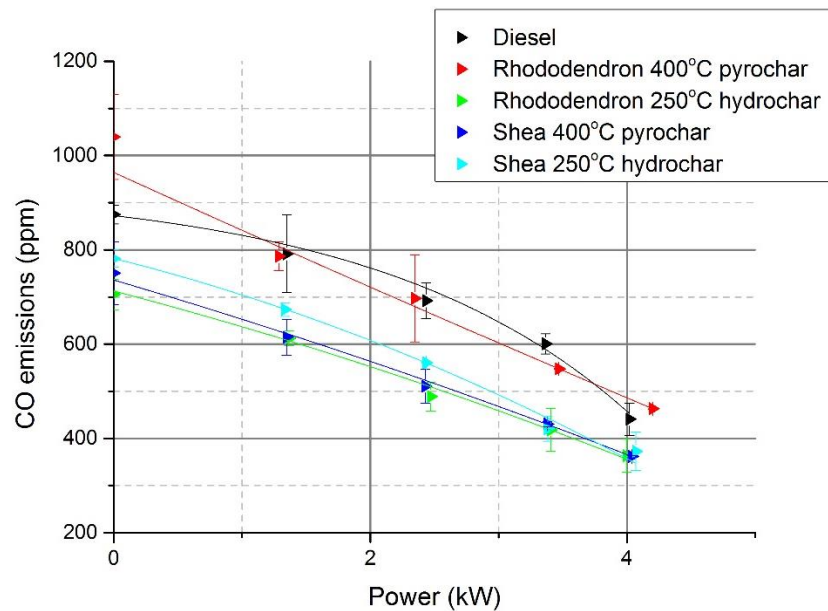


Figure 6-25 CO emissions of 1%wt. slurries.

At full load, the benefit to CO reduction caused by the char diminishes. A reduction in CO did not occur when rhododendron pyrochar was added. Rhododendron pyrochar slurry was also the least reliable to use and caused the injector to stick several times or caused the operation of the engine to be less smooth. Potentially, this sticking and clogging might have caused the CO emissions to increase because of poor fuel injection.

There are several factors that could cause the decrease in CO emissions- the likelihood of formation increases in diesel engines if the droplets of fuel are too large or if there is insufficient turbulence to mix reactants thoroughly (Reşitoğlu et al., 2015). Soloiu et al. (2011) investigated the droplet size of 25%wt. char diesel slurry fuels produced by milling the char for varying lengths of time. It was found that the presence of char increased the average droplet size because the viscosity increased. It is therefore unlikely that a reduction in droplet size has occurred, reducing the CO.

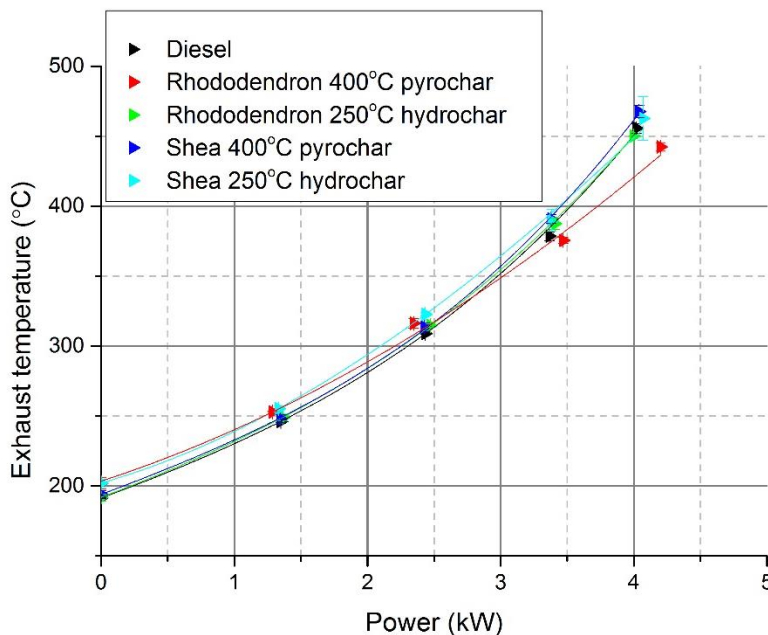


Figure 6-26 Exhaust manifold temperature during the operation of the genset using 1%wt. chars in diesel.

The most likely cause of the reduction is an alteration in the chemical kinetics caused by the presence of char particles. The formation of CO mainly occurs from the burning of soot during the final stage of combustion (Ithnin et al., 2015). As char contains significant quantities of oxygen, it may form compounds which react with the CO formed, producing CO₂.

Increased CO emissions are also related to combustion temperatures, thus if char were to increase the temperature, then it would cause a CO reduction. The study in Soloiu et al. (2011) with a 25%wt. charcoal diesel slurry calculated the maximum instantaneous volume-averaged gas combustion temperature to be 30°C higher compared to diesel. It was also higher for the

rest of the power stroke, suggesting the temperature in the cylinder is at a sufficient level to convert CO to CO₂ for longer. Figure 6-26 shows the exhaust manifold temperature during the tests is hotter when using slurries, except for rhododendron pyrochar above 50% load, which suggests a higher combustion temperature. However, the shea hydrochar has the highest exhaust temperature across all loads yet does not have the lowest CO concentration, suggesting another factor is involved such as a chemical interaction between char and diesel.

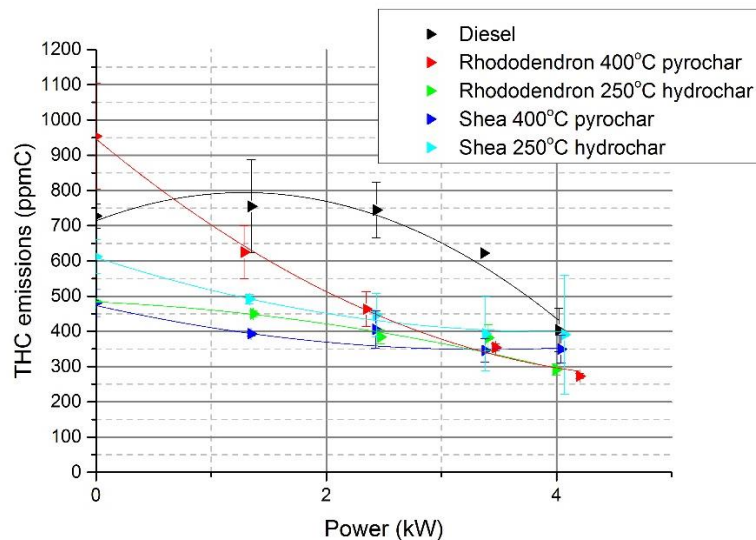


Figure 6-27 Total hydrocarbon emissions versus load when using 1%wt. slurries.

Another indication of incomplete fuel combustion is THC emissions which are caused by hot gases quenching on cool surfaces of the combustion chamber (Ho Choi et al., 2005; Liu et al., 2015b). Generally, trends in CO are mirrored in the THC emissions (Pinzi et al., 2013). Figure 6-27 shows the THC emissions, which further supports the results from CO emissions, that combustion with 1%wt. char decreases incomplete combustion. All the chars produced less THC emissions than the baseline, except rhododendron pyrochar at idle. As with the CO emissions, the difference between the baseline and slurries narrows with higher load. The reason for the rhododendron pyrochar slurry reducing THC but not CO could be that the slow-burning char produces CO, counteracting any improvement from the diesel part of the fuel. The tests performed in chapter 4 showed that the recalcitrance index of the rhododendron 400°C pyrochar was higher than the other three chars used in the 1%wt. tests meaning that it needs higher temperatures to burn.

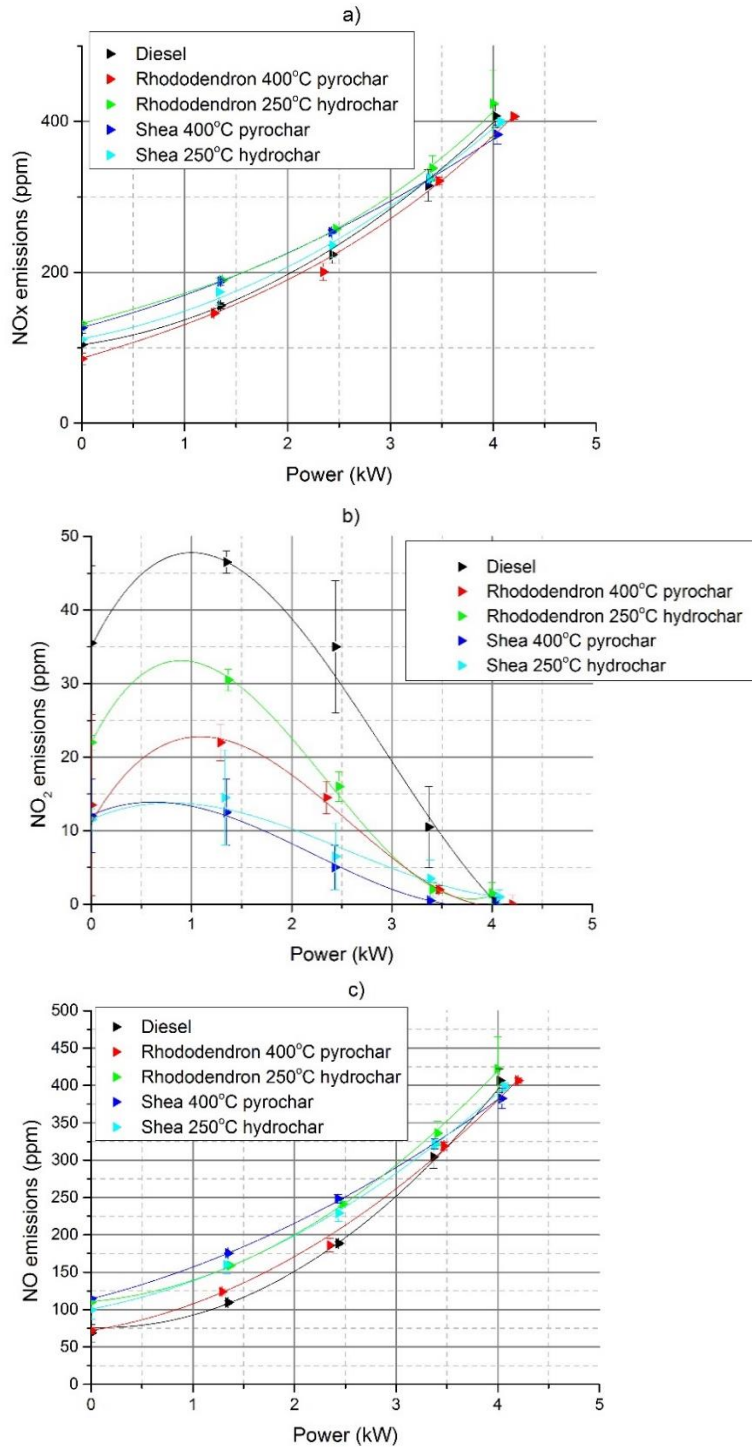


Figure 6-28 Oxides of nitrogen emissions from 1%wt. slurries. a) Total oxides of nitrogen, b) Nitrogen dioxide, and c) Nitric oxide

Figure 6-28 shows the emissions of oxides of nitrogen from 1%wt. slurry fuels. Overall, the variation in NOx emission concentrations from the baseline is small. At full load, the NOx concentration from the two shea slurries is lower than the baseline. Shea hydrochar slurry produces less NOx across all loads than the baseline. The effect of adding rhododendron hydrochar to diesel on NOx emissions is either maintained or marginally increased.

The most notable difference from the baseline occurs with NO₂ emissions at low load. At 1.35 kW, the biggest reduction from the baseline of 65% was achieved with the 1%wt. shea pyrochar slurry. Both shea chars perform similarly in this aspect and better than rhododendron hydrochar suggesting that the inorganic content in shea is responsible rather than the type of hydrocarbon structures. Furthermore, the closeness in values measured indicates similar quantities of the inorganic compound present, therefore not one that is leached in significant quantities during the hydrothermal process. Rhododendron hydrochar also produced an NO₂ reduction effect albeit to a lesser extent.

Zouaoui et al. (2014) performed a kinetic study of diesel soot oxidation by NO₂, O₂ and water. Oxygen reacts with soot only at high temperatures- above 450°C, whereas nitrogen dioxide reacts at 300°C to form nitric oxide and carbon monoxide/dioxide. Figure 6-29b shows a drop in nitrogen dioxide and an increase in nitric oxide in slurry fuels at low load, suggesting that oxidation of soot or char by nitrogen dioxide is occurring, therefore, reducing NO₂ emissions.

6.5.4 Particle emissions from 1%wt. slurries

The alterations, addition of surfactants, and potentially wear and tear change the emissions of the new baseline compared to the previous baseline. In figure 6-29, the modal particle emission is significantly higher than the test in figure 6-16. The new particle size distribution is shifted toward smaller sizes. For example, previously the modal size of soot particles was approximately 120nm, but is now in the region of 60nm. A large spike in emissions appears at roughly 1.5kW at 20nm potentially caused by a combination of low temperature and poor atomisation. The lowering of injection pressure before the 1%wt. tests would have made the atomisation worse. Still, as previous, the particle size distribution shifts to larger diameters with increasing load.

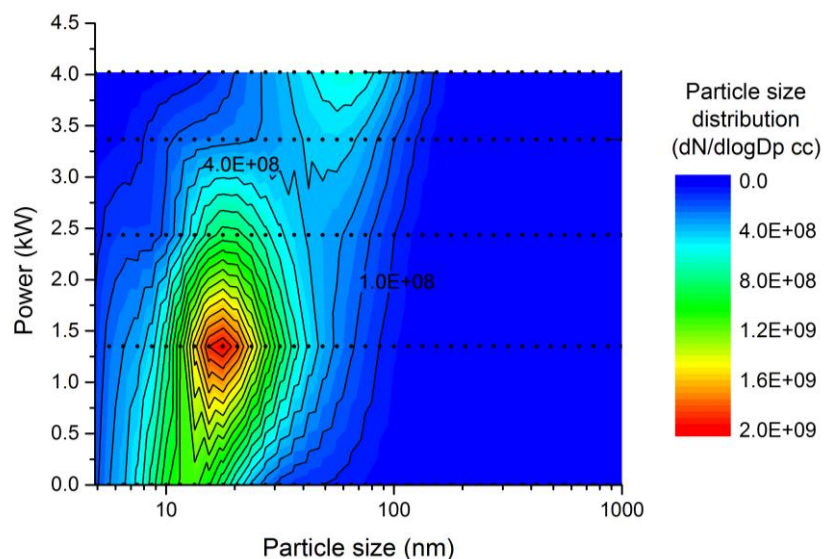


Figure 6-29 Particle emissions from 0.1%wt. lecithin in diesel baseline test.

The addition of char at 1% wt. altered the particle size distribution markedly (figure 6-30). The 1%wt. rhododendron hydrochar slurry showed little sign of incomplete combustion of char particles from the particle size analysis except at idle, with a small increase occurring around 20nm. There are regions of the soot particle size map for the rhododendron hydrochar slurry where the number of particles emitted decreases significantly. Between 25% and 50% load, the particle number reduced in the 10-30nm region. At idle there is a smaller reduction around 7-10nm.

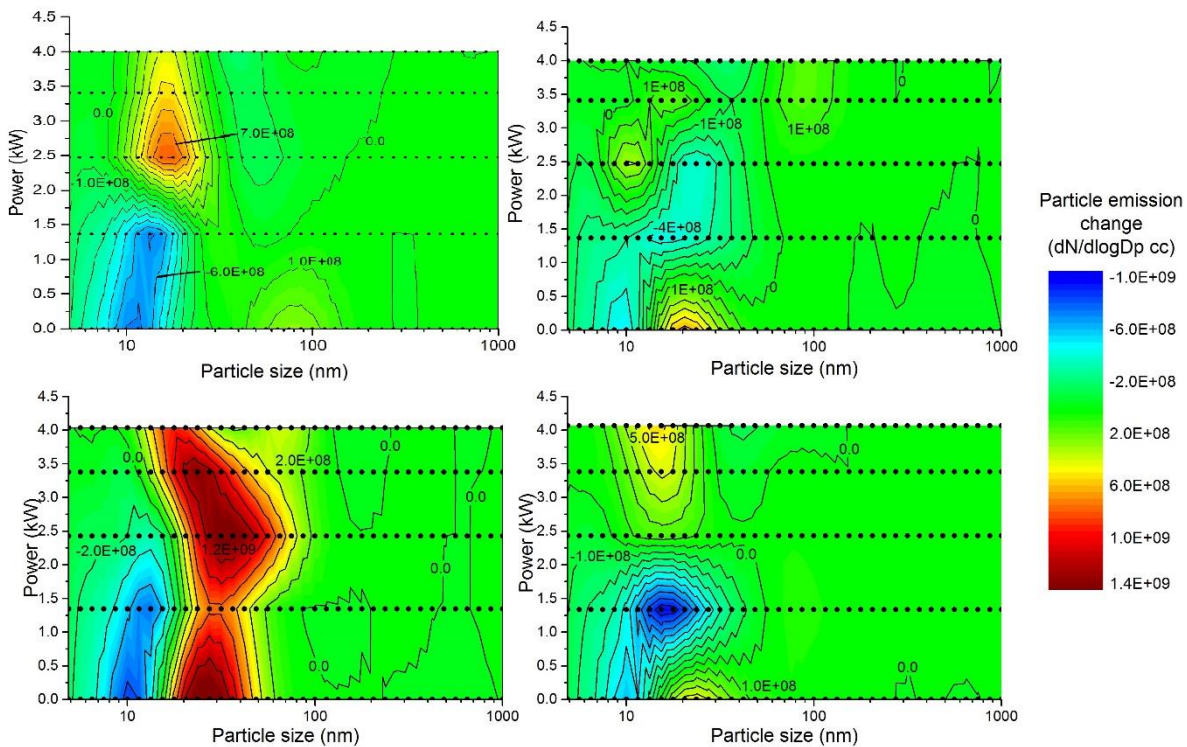


Figure 6-30 Change in particle emissions from the baseline when using 1 %wt. slurries. Top left: Rhododendron 400°C pyrochar, top right: Rhododendron 250°C hydrochar, bottom left: Shea 400°C pyrochar and, bottom right: Shea 250°C hydrochar.

Shea hydrochar behaves similarly as rhododendron hydrochar in terms of particle emission. Both show a small increase in particles produced at idle. A reduction in particle emission occurs at 25% load between 10-30nm, which is similar to rhododendron hydrochar, but greater in intensity. The particle emission in the region of 10-30nm increases with further addition of load, eventually increasing the particle emission to above the baseline test at 3kw. The 1% wt. Rhododendron pyrochar slurry showed a reduction in particles at idle and low load around 10nm. At 50% to full load, at roughly 17nm there is an increase in particles emitted. The rest of the distribution remains similar to the baseline test.

The shea pyrochar slurry caused a significant increase in the intensity of particles emitted in the region of 20-40nm across full loads. The 0.1%wt. tests using shea pyrochar (figure 6-17)

also increased particle emissions in a similar region, but slightly larger diameter in figure 6-31. The difference in diameter is potentially caused by the reduction in injection pressure, leading to larger particles (Labecki et al., 2013). When under 50% load using the 1%wt. shea pyrochar slurry, a sharp decrease in particles of 10nm compared to the baseline occurred, possibly as soot particles were more likely to agglomerate.

Table 6-4 Particle emissions PM₁₀ from 1%wt. slurry fuels in diesel

<i>Char species</i>	<i>Treatment</i>	<i>Ash emission (predicted) (mg/m³)</i>	<i>PM₁₀ (mg/m³)</i>
<i>None</i>	-	-	28.5±1.0
<i>Rhododendron</i>	Pyrolysis 400°C	23.0	45.1±8.2
	HTC 250°C	20.0	47.5±3.4
<i>Shea</i>	Pyrolysis 400°C	106.0	55.1±1.1
	HTC 250°C	34.0	34.2±4.7

Table 6-4 shows the particle emissions on a mass basis. The emissions from 1%wt. slurries were found to be consistently higher than the baseline experiment, but not as high as the ash content would suggest. Rhododendron pyrochar and hydrochar slurry had a soot emission roughly the sum of the baseline plus the amount of ash produced. It is, therefore, possible that the soot emission remains the same as the baseline and the difference in total is caused by the ash. In the case of the shea slurry fuels, the PM₁₀ emission is equal to or less than the amount of ash produced. It is therefore much clearer than with the 0.1%wt. slurry tests that some of the ash produced is unaccounted for. With the shea pyrochar slurry, at least half of the ash is unaccounted for and likely to be much greater as some of the collected particulates will be soot.

The particulate matter data suggests that the ash particles are generally larger than the soot particles because no significant increase in particle number was detected in figure 6-30, meaning that the ash is larger than 1000nm. For the particles to be collected in the oil sump, the momentum of the ash particles must be large enough to prevent entrainment in the gases, and instead contact the cylinder wall and get scraped into the oil sump. Two potential causes for ash having a larger momentum than soot particles are that the ash fragments are either larger or denser. Another possibility is that the ash particles are initially entrained in the exhaust flow but come out when the diameter of the tube increases. Poor entrainment of larger ash particles in the exhaust may also prevent them from being drawn through the sampling probe.

The density of oxides vary from element to element and are different than the density of soot. This could explain why, for example, small quantities of shea ash is collected from the exhaust stream whereas more of the rhododendron hydrochar ash is. The apparent density of diesel

soot is in the range of 0.3-0.9 g/cm³ (Rissler et al., 2013). Oxides have consistently higher densities than this (Railsback, 2006). Oxides from group 1 elements are generally the least dense at roughly 2 g/cm³. Quartz is next between 2-3 g/cm³. Group 2 oxides and aluminium are in the range of 3-4 g/cm³. Transitional metal oxides have densities in the region of 4.5-8 g/cm³. From the analysis in chapter 4, the shea chars are dominated by silicon, but with significant portions of potassium, iron and calcium. Rhododendron ash is dominated by calcium, which forms oxides denser than silicon, and are therefore more likely to leave the exhaust gas stream. However, this is not the case from table 6-4 which suggests a higher proportion of rhododendron ash leaves the engine entrained in the exhaust. The likely reason for the difference in mass of particles collected in the single stage filter used for table 6-4 with respect to the amount of ash in the engine is therefore likely to be the size of inorganic particles in the slurry fuel. In essence, inorganic fragments in shea are larger than in rhododendron.

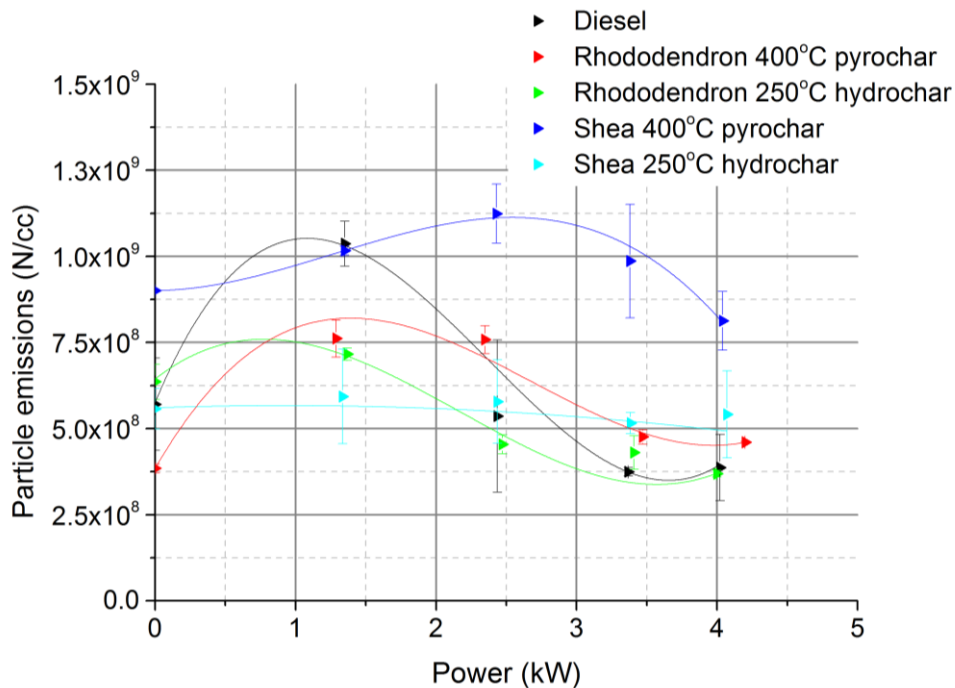


Figure 6-31 Particle number emission from 1%wt. slurries versus load.

Figure 6-31 shows the particle number emission from 1%wt. slurries compared to load. The baseline value is significantly higher than when the 0.1%wt. tests were performed, meaning the effect of reducing the injection pressure to prevent the slurry from sticking the injector causes an issue before the fuel is even switched. Using an unmodified injector previously yielded particle emissions consistently below 1.5x10⁸ N/cc (figure 6-19), whereas the baseline in figure 6-31 is continuously above 3.0x10⁸ N/cc. An alternative to reducing injection pressure at the injector is to boost pressure at the high injection pump but was not done in this instance as the pump could not be modified.

The 1%wt. rhododendron hydrochar slurry emitted fewer particles than the baseline except at idle. This is similar to the 0.1%wt. tests which showed the rhododendron hydrochar did at some loads cause a reduction in particle number emissions. The 1%wt. shea hydrochar was, at under 50% load, the best performer in terms of particle emissions. The shea hydrochar slurry in the previous 0.1%wt. tests did not perform as well compared to the baseline or the rhododendron hydrochar. Rhododendron pyrochar slurry improved on particle number emissions at low load but increased slightly at full compared to the baseline. 1%wt. shea pyrochar slurry was the worst in terms of total number of particles emitted from the 1%wt. slurries tested, as it was in the 0.1%wt. tests. The differences between this slurry and the others is most pronounced at loads over 50%.

6.6 Conclusions

The addition of char even at low concentrations can have an influence on the emissions produced by a diesel engine. THC emissions from diesel were reduced by the introduction of char at 0.1% and 1%wt.. The effect, however, did not occur when char was added to biodiesel. Pyrolysis char was generally more effective at reducing THC emissions, although hydrochar also worked at 1%wt.. Nitrogen dioxide emissions were reduced when 1%wt. of char was added by as much as 65% from the baseline. The most important factor in the char to achieve this reduction was the feedstock used, shea outperformed rhododendron, then thermal treatment - pyrolysis chars were better than hydrochars. This suggests that it is the trace element content which caused this reduction rather than the carbon compounds. The decrease in nitrogen dioxide was concurrent with an increase in nitric oxide which means that there is a reduction reaction occurring in the cylinder as a result of adding char. 0.1%wt. of pyrochar reduced NO_x emissions in both biodiesel and diesel. 1%wt. of char to diesel had the opposite effect, increasing NO_x. CO emissions, in some instances, were reduced by the addition of char to diesel or remained the same. Generally, adding char to biodiesel increased CO.

One of the most important emissions are particulates which were expected to increase as inert ash would have to leave the combustion chamber somehow. The 0.1%wt. tests showed an increase in particle number in nearly all conditions, caused by a shift in particle size distribution to smaller diameters and poor combustion at low loads. The difference between slurries and baseline narrowed at full load. The difference in particle number emissions when using 1%wt. slurries were less. The baseline had increased significantly as atomisation became poorer because the injection pressure was decreased to help the slurry fuels run smoother. With this increase in soot particles in the baseline, the 1%wt. char reduced the formation of soot in some instances. The worst performing char also had the highest amount of ash.

In terms of particulate mass emissions, less was produced from the char slurries than predicted. The 0.1%wt. tests did not produce the mass of particulates the percentage of char in the fuel would suggest. In the 1%wt. tests, the rhododendron char slurries produced the amount of particulate expected, roughly the soot from the baseline plus the ash from the fuel. However, the shea char slurry fuels produced roughly half what was expected. The data shows that, at least in some instances, ash is deposited in the lubrication oil. The implications of this are mixed- fewer particulates emitted is positive as it reduces the impact to air quality caused by the slurry engine, but creates a challenge in ensuring that the contamination to the lubrication oil does not adversely affect the lifespan of the engine.

The effect of pyrolysis temperature on emissions from slurry fuels was investigated when at solid concentrations of 0.1%wt. with rhododendron used as a feedstock. Increasing the pyrolysis temperature from 400 to 600°C increased CO₂ but reduced NO₂, THC and CO. The reason for the reduction in NO₂ is likely that it is consumed as an oxidant with the later burning char. The reason for reducing THC and CO with pyrolysis temperature is less clear but might be related to a catalytic effect with the char. The most significant drawback of increasing the pyrolysis temperature is the increase in particle number emissions which is at least doubled at all powers when the pyrolysis temperature is raised from 400 to 600°C.

Objective 6 was to investigate using char as an additive. The results show that the usefulness, at least at the concentrations tested are limited. Pyrolysis chars are the most effective as an additive in reducing emissions, but the increase in particle number, especially at low loads is concerning. Potentially, this could be reduced by using higher quality low ash biomass, but this could also negate the emissions reductions. The chars were mostly ineffective at reducing emissions from biodiesel.

6.7 References

- Agarwal, A.K.Dhar, A.Gupta, J.G.Kim, W.I.Choi, K.Lee, C.S. and Park, S. 2015. Effect of fuel injection pressure and injection timing of Karanja biodiesel blends on fuel spray, engine performance, emissions and combustion characteristics. *Energy Conversion and Management*. **91**, pp.302-314.
- Agarwal, A.K.Dhar, A.Srivastava, D.K.Maurya, R.K. and Singh, A.P. 2013. Effect of fuel injection pressure on diesel particulate size and number distribution in a CRDI single cylinder research engine. *Fuel*. **107**, pp.84-89.
- Ahmad, M.Zafar, M.Rashid, S.Sultana, S.Sadia, H. and Ajab Khan, M. 2013. Production of Methyl Ester (Biodiesel) From Four Plant Species of Brassicaceae: Optimization of the Transesterification Process. *International Journal of Green Energy*. **10**(4), pp.362-369.
- Bose, P.K. 2009. Empirical approach for predicting the cetane number of biodiesel. *International Journal of Automotive Technology*. **10**(4), pp.421-429.

- Bueno, A.V.Pereira, M.P.B.de Oliveira Pontes, J.V.de Luna, F.M.T. and Cavalcante, C.L. 2017. Performance and emissions characteristics of castor oil biodiesel fuel blends. *Applied Thermal Engineering*. **125**, pp.559-566.
- Carroll, B.O. 2015. *Analysis of graphite oxide and graphene as enhancers for NATO F-76 diesel fuel*. Master of Science in Mechanical Engineering thesis, NAVAL POSTGRADUATE SCHOOL.
- Davini, P. 2001. SO₂ and NO_x adsorption properties of activated carbons obtained from a pitch containing iron derivatives. *Carbon*. **39**(14), pp.2173-2179.
- Dias, J.M.Alvim-Ferraz, M.C.M. and Almeida, M.F. 2008. Comparison of the performance of different homogeneous alkali catalysts during transesterification of waste and virgin oils and evaluation of biodiesel quality. *Fuel*. **87**(17), pp.3572-3578.
- Du, W.Lou, J.Yan, Y.Bao, W. and Liu, F. 2017. Effects of injection pressure on diesel sprays in constant injection mass condition. *Applied Thermal Engineering*. **121**, pp.234-241.
- Geacai, S.Iulian, O. and Nita, I. 2015. Measurement, correlation and prediction of biodiesel blends viscosity. *Fuel*. **143**, pp.268-274.
- Ho Choi, G.Jong Chung, Y. and Han, S.B. 2005. Performance and emissions characteristics of a hydrogen enriched LPG internal combustion engine at 1400rpm. *International Journal of Hydrogen Energy*. **30**(1), pp.77-82.
- İçingür, Y. and Altıparmak, D. 2003. Effect of fuel cetane number and injection pressure on a DI Diesel engine performance and emissions. *Energy Conversion and Management*. **44**(3), pp.389-397.
- Illán-Gómez, M.J.Brandán, S.Salinas-Martínez de Lecea, C. and Linares-Solano, A. 2001. Improvements in NO_x reduction by carbon using bimetallic catalysts. *Fuel*. **80**(14), pp.2001-2005.
- Ithnin, A.M.Ahmad, M.A.Bakar, M.A.A.Rajoo, S. and Yahya, W.J. 2015. Combustion performance and emission analysis of diesel engine fuelled with water-in-diesel emulsion fuel made from low-grade diesel fuel. *Energy Conversion and Management*. **90**, pp.375-382.
- Jeon, J. and Park, S. 2018. Effect of injection pressure on soot formation/oxidation characteristics using a two-color photometric method in a compression-ignition engine fueled with biodiesel blend (B20). *Applied Thermal Engineering*. **131**, pp.284-294.
- Labecki, L.Lindner, A.Winklmayr, W.Uitz, R.Cracknell, R. and Ganippa, L. 2013. Effects of injection parameters and EGR on exhaust soot particle number-size distribution for diesel and RME fuels in HSDI engines. *Fuel*. **112**, pp.224-235.
- Lee, C.S. and Park, S.W. 2002. An experimental and numerical study on fuel atomization characteristics of high-pressure diesel injection sprays. *Fuel*. **81**(18), pp.2417-2423.
- Li, D.Tang, X.Yi, H.Ma, D. and Gao, F. 2015. NO_x Removal over Modified Carbon Molecular Sieve Catalysts Using a Combined Adsorption-Discharge Plasma Catalytic Process. *Industrial & Engineering Chemistry Research*. **54**(37), pp.9097-9103.
- Liu, H.Ma, J.Tong, L.Ma, G.Zheng, Z. and Yao, M. 2018. Investigation on the Potential of High Efficiency for Internal Combustion Engines. *Energies*. **11**(3), p513.
- Liu, J.Yao, A. and Yao, C. 2015a. Effects of diesel injection pressure on the performance and emissions of a HD common-rail diesel engine fueled with diesel/methanol dual fuel. *Fuel*. **140**, pp.192-200.
- Liu, J.Zhang, X.Wang, T.Zhang, J. and Wang, H. 2015b. Experimental and numerical study of the pollution formation in a diesel/CNG dual fuel engine. *Fuel*. **159**, pp.418-429.
- Liu, S.Li, H.Gatts, T.Liew, C.Wayne, S.Thompson, G.Clark, N. and Nuszkowski, J. 2012. An Investigation of NO₂ Emissions from a Heavy-Duty Diesel Engine Fumigated with H₂ and Natural Gas. *Combustion Science and Technology*. **184**(12), pp.2008-2035.
- Liu, S.Wang, Y.Oh, J.-H. and Herring, J.L. 2011. Fast biodiesel production from beef tallow with radio frequency heating. *Renewable Energy*. **36**(3), pp.1003-1007.
- Montoya, C.Cochard, B.Flori, A.Cros, D.Lopes, R.Cuellar, T.Espeout, S.Syaputra, I.Villeneuve, P.Pina, M.Ritter, E.Leroy, T. and Billotte, N. 2014. Genetic Architecture of Palm Oil

- Fatty Acid Composition in Cultivated Oil Palm (*Elaeis guineensis* Jacq.) Compared to Its Wild Relative *E. oleifera* (H.B.K) Cortés. *PLoS ONE*. **9**(5), pe95412.
- Nejar, N. and Illán-Gómez, M.J. 2007. Potassium–copper and potassium–cobalt catalysts supported on alumina for simultaneous NO_x and soot removal from simulated diesel engine exhaust. *Applied Catalysis B: Environmental*. **70**(1), pp.261-268.
- Ooi, J.B.Ismail, H.M.Swamy, V.Wang, X.Swain, A.K. and Rajanren, J.R. 2016. Graphite Oxide Nanoparticle as a Diesel Fuel Additive for Cleaner Emissions and Lower Fuel Consumption. *Energy & Fuels*. **30**(2), pp.1341-1353.
- Park, K.Cao, F.Kittelsson, D.B. and McMurry, P.H. 2003. Relationship between Particle Mass and Mobility for Diesel Exhaust Particles. *Environmental Science & Technology*. **37**(3), pp.577-583.
- Patel, C.Lee, S.Tiwari, N.Agarwal, A.K.Lee, C.S. and Park, S. 2016. Spray characterization, combustion, noise and vibrations investigations of *Jatropha* biodiesel fuelled genset engine. *Fuel*. **185**, pp.410-420.
- Pinzi, S.Rounce, P.Herreros, J.M.Tsolakis, A. and Pilar Dorado, M. 2013. The effect of biodiesel fatty acid composition on combustion and diesel engine exhaust emissions. *Fuel*. **104**, pp.170-182.
- Railsback, L.B. 2006. Density of minerals III: Oxides and stoichiometry. In: Railsback, L.B. ed. *Some Fundamentals of Mineralogy and Geochemistry*. [Online].
- Reşitoğlu, İ.A.Altinişik, K. and Keskin, A. 2015. The pollutant emissions from diesel-engine vehicles and exhaust aftertreatment systems. *Clean Technologies and Environmental Policy*. **17**(1), pp.15-27.
- Ribeiro, N.M.Pinto, A.C.Quintella, C.M.da Rocha, G.O.Teixeira, L.S.G.Guarieiro, L.L.N.do Carmo Rangel, M.Veloso, M.C.C.Rezende, M.J.C.Serpa da Cruz, R.de Oliveira, A.M.Torres, E.A. and de Andrade, J.B. 2007. The Role of Additives for Diesel and Diesel Blended (Ethanol or Biodiesel) Fuels: A Review. *Energy & Fuels*. **21**(4), pp.2433-2445.
- Rissler, J.Messing, M.E.Malik, A.I.Nilsson, P.T.Nordin, E.Z.Bohgard, M.Sanati, M. and Pagels, J. 2013. Effective Density Characterization of Soot Agglomerates from Various Sources and Comparison to Aggregation Theory. *Aerosol Science and Technology*. **47**, pp.792-805.
- Rubel, A.M. and Stencel, J.M. 1996. Effect of Pressure on NO_x Adsorption by Activated Carbons. *Energy & Fuels*. **10**(3), pp.704-708.
- Santillan-Jimenez, E.Miljković-Kocić, V.Crocker, M. and Wilson, K. 2011. Carbon nanotube-supported metal catalysts for NO_x reduction using hydrocarbon reductants. Part 1: Catalyst preparation, characterization and NO_x reduction characteristics. *Applied Catalysis B: Environmental*. **102**(1), pp.1-8.
- Shameer, P.M. and Ramesh, K. 2017. Experimental evaluation on performance, combustion behavior and influence of in-cylinder temperature on NO_x emission in a D.I diesel engine using thermal imager for various alternate fuel blends. *Energy*. **118**, pp.1334-1344.
- Shangguan, W.F.Teraoka, Y. and Kagawa, S. 1998. Promotion effect of potassium on the catalytic property of CuFe₂O₄ for the simultaneous removal of NO_x and diesel soot particulate. *Applied Catalysis B: Environmental*. **16**(2), pp.149-154.
- Smith, A.M.Singh, S. and Ross, A.B. 2016. Fate of inorganic material during hydrothermal carbonisation of biomass: Influence of feedstock on combustion behaviour of hydrochar. *Fuel*. **169**, pp.135-145.
- Soloiu, V.Lewis, J.Yoshihara, Y. and Nishiwaki, K. 2011. Combustion characteristics of a charcoal slurry in a direct injection diesel engine and the impact on the injection system performance. *Energy*. **36**(7), pp.4353-4371.
- Torjesen, I. 2014. Switch to diesel engines is significantly to blame for poor air quality in UK cities, experts say. *BMJ : British Medical Journal*. **348**.
- Tree, D.R. and Svensson, K.I. 2007. Soot processes in compression ignition engines. *Progress in Energy and Combustion Science*. **33**(3), pp.272-309.

- Valente, O.S.Pasa, V.M.D.Belchior, C.R.P. and Sodré, J.R. 2011. Physical–chemical properties of waste cooking oil biodiesel and castor oil biodiesel blends. *Fuel*. **90**(4), pp.1700-1702.
- Virtanen, A.K.K.Ristimäki, J.M.Vaaraslahti, K.M. and Keskinen, J. 2004. Effect of Engine Load on Diesel Soot Particles. *Environmental Science & Technology*. **38**(9), pp.2551-2556.
- Wang, C.a.Liu, Y.Jin, X. and Che, D. 2016. Effect of water washing on reactivities and NOx emission of Zhundong coals. *Journal of the Energy Institute*. **89**(4), pp.636-647.
- Wei, L. and Geng, P. 2016. A review on natural gas/diesel dual fuel combustion, emissions and performance. *Fuel Processing Technology*. **142**, pp.264-278.
- Xiang, W.Guangya, Z. and Ke, L. 2013. A phenomenological bubble number density model developed for simulation of cavitating flows inside high-pressure diesel injection nozzles. *International Journal of Numerical Methods for Heat & Fluid Flow*. **23**(8), pp.1356-1372.
- Xu, Z.Li, X.Guan, C. and Huang, Z. 2014. Effects of Injection Pressure on Diesel Engine Particle Physico-Chemical Properties. *Aerosol Science and Technology*. **48**(2), pp.128-138.
- Xue, J.Griff, T.E. and Hansen, A.C. 2011. Effect of biodiesel on engine performances and emissions. *Renewable and Sustainable Energy Reviews*. **15**(2), pp.1098-1116.
- Yang, H.-H.Chien, S.-M.Lo, M.-Y.Lan, J.C.-W.Lu, W.-C. and Ku, Y.-Y. 2007. Effects of biodiesel on emissions of regulated air pollutants and polycyclic aromatic hydrocarbons under engine durability testing. *Atmospheric Environment*. **41**(34), pp.7232-7240.
- Yu, L.Ge, Y.Tan, J.He, C.Wang, X.Liu, H.Zhao, W.Guo, J.Fu, G.Feng, X. and Wang, X. 2014. Experimental investigation of the impact of biodiesel on the combustion and emission characteristics of a heavy duty diesel engine at various altitudes. *Fuel*. **115**, pp.220-226.
- Zawadzki, J. and Wiśniewski, M. 2007. An infrared study of the behavior of SO₂ and NO_x over carbon and carbon-supported catalysts. *Catalysis Today*. **119**(1), pp.213-218.
- Zouaoui, N.Labaki, M. and Jeguirim, M. 2014. Diesel soot oxidation by nitrogen dioxide, oxygen and water under engine exhaust conditions: Kinetics data related to the reaction mechanism. *Comptes Rendus Chimie*. **17**(7), pp.672-680.

Chapter 7: Testing char-diesel slurry fuels

7.1 Introduction

In many developing countries, grid electricity can be intermittent, or even non-existent in more rural areas. Diesel generators are in many places the main source of electrical energy, despite the high price of diesel (Inyang, 2008). Between 2006 and 2016, the average cost of diesel per litre in the least economically developed countries was US\$0.84-1.25 (The World Bank, 2018b). During the same period, the GDP per capita in these countries was \$490-1010 (The World Bank, 2018a). Considering the large fluctuation between both the cost of fuel to run generators and the limited amount of money people have to spend means that ensuring electricity can always be produced is very difficult. To be able to extend the amount of electricity that can be produced by blending diesel with locally made char could be beneficiary especially when money is scarce, or oil prices are high. Electricity is vital for economic development in rural developing regions allowing people, for example, to operate agricultural machinery or work past daylight hours (Kanagawa and Nakata, 2008).

Previous tests show that modifications are needed even when small quantities of char are added. 1%wt. chars required removal of a small amount of material in the guide area between needle and injector nozzle, as well as a reduction in injection pressure to prevent seizing of the part. During the additive tests, despite the need for modification, no critical failures occurred. However, the quantity of char that is needed to be added to replace an amount of diesel that will make meaningful savings to the fossil fuel consumption of an engine generator during a year of operation is higher than the 1%wt. already tested. Diesel fuel has a calorific value of roughly 46 MJ/kg whereas the chars created for slurring are 23-30 MJ/kg. Hence, the concentrations previously tested replaced just 0.5-0.75% of diesel fuel on an energy basis.

The chapter investigates using char blended with diesel at 10%wt.. The char added contributes roughly 5-7.5% of the total energy of the fuel at this concentration, depending on the material used. One of the reasons for choosing a concentration of 10%wt. was that it had previously been found that adding this much carbon black to diesel did not adversely affect atomisation (Ryan et al., 1980). Pyrochars generally have a higher calorific value than hydrochars (chapter 4) which means a greater contribution to the overall energy content can be made with using pyrochars. On the other hand, hydrochars have more volatile matter and less ash than pyrochars meaning that the hydrochar should burn better and cause less wear. The difference in performance between blending hydrochars and pyrochars into diesel is also investigated.

The chapter aims to complete objective 7- to use a char-diesel slurry as a fuel for a diesel engine. The objective encompasses measuring emissions, efficiency and engine performance. Wear is also investigated as part of the objective to gain an understanding of long-term issues which may occur. Methods used in this chapter are in section 3.7.

7.2 Initial studies

7.2.1. More modifications to the injector

First tests using 10% wt. slurry fuels proved problematic, once again with the injectors becoming stuck. The needles would rarely become fully stuck in the nozzle body by the build-up of solid particles, rather prevent sufficient fuel from entering the engine to maintain turnover. To overcome this, the diameter of the needle in the guide section was further reduced in order to improve the smoothness of operation. Removal of 20 μm from the diameter in total (i.e. 10 μm more removed from the needle used in the 1%wt. slurry tests in chapter 6) reduced the chances of stalling but did not completely remove occurrence, even at low load. Removal of 30 and 40 μm reduced the issue of stalling, yet was still not sufficient. At 60 μm of removal from the needle diameter, the engine would have issues with starting and maintaining pressure in the cavity required to cause the needle to move upwards and allow fuel into the engine. By 100 μm of removal from the diameter, the engine would not start because injection pressure would not build in the injector.

Another issue which occurred was the blocking of the mesh filter used to keep large particles out of the fuel injection system. Over time, particles had agglomerated on the mesh, preventing the passage of fuel to the engine. Whilst by no means a severe issue especially as mesh filters are cheap, it does show the need for a filter which can be dismantled and cleaned to ensure continuous operation can be achieved.

A different approach was taken to improve the operation of the injector. Instead of removing material from the entire diameter, allowing particles to move through the gap without getting stuck, a deep groove was made at the centre of the guide section of the needle. The logic for this alteration was that less surface area on the needle could come into contact with the nozzle body via the agglomeration of char particles. With less surface area, the amount of shear force produced counteracting the lifting force of the needle is lower than without the modification. The small cavity also provides an area for particles to enter without causing a blockage. By retaining part of the material on the guide above and below the cavity, the pressure seal is retained. The cavity was created by spinning the needle and using a grinding tool to remove material.

Figure 7-1, shows the development of the injector needle for using 10%wt. slurries, and figure 7-2 the temperature profiles from the exhaust thermocouple when using the modified needles. Injector 2, which is the same as the original injector 1 except with some material removed reduced the surface area in the guide section in contact with the nozzle body by 40%. Whereas the unmodified injector would operate only for a matter of seconds if the engine even managed to start at all, injector 2 worked for about five minutes. At the end of the test shown in figure 7-2, the temperature dropped and the engine began to stall as the needle would not lift smoothly preventing fuel from entering the combustion chamber. Throughout the test, the engine could not maintain stable operation- some points extra fuel was burning or not at the right time, seen by the increase in temperature, and sometimes the needle would not open causing the exhaust temperature to drop. The changes in temperature were accompanied by a very clear change in noise frequency indicating the engine was not maintaining a constant speed as a result of the poor combustion.

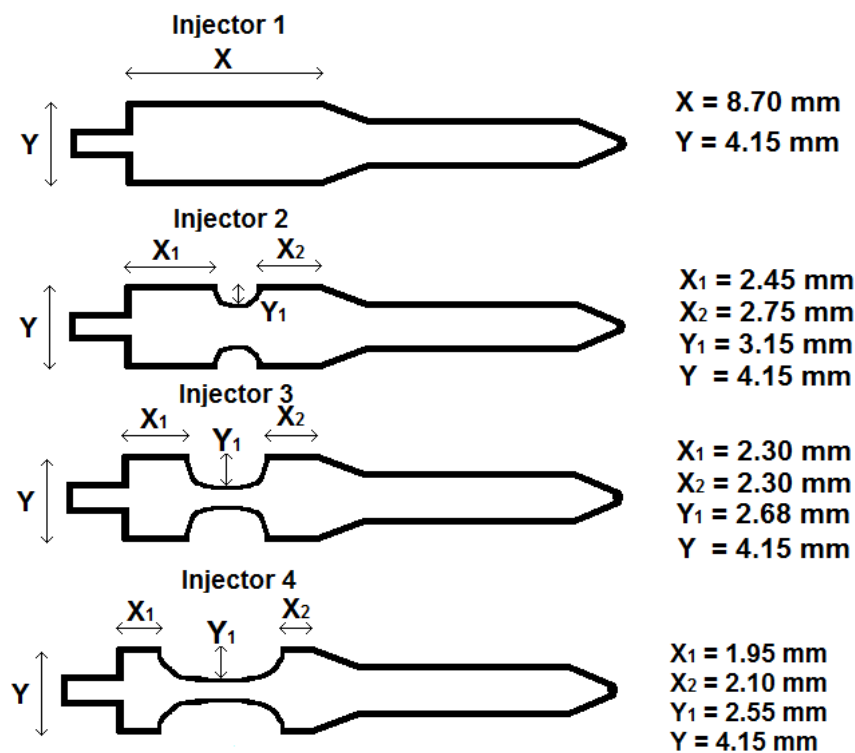


Figure 7-1 Development of injector for 10%wt. slurries.

Further removal of material from the guide improved the smoothness of operation. During idle operation using injector 3, the engine would not begin to stall as happened with injector 2 before. The total variation in exhaust temperature using injector 3 at idle was within 30°C. This modification had removed 48% of the contacting surface of the guide. The engine, however, did not run smooth enough to be considered stable operation, with NO_x emissions varying between 75 and 150ppm throughout the test.

Injector 4 had the most material removed and yielded the best results. A total of 53% of the surface had been removed from the middle of the guide area of the needle. Figure 7-2, shows operation on a 10%wt. char-diesel slurry as smooth as expected when using pure diesel fuel. The variation in exhaust temperature is approximately 6°C during idle. The average exhaust manifold temperature during operation with injector 4 is lower than the other two modified injectors, suggesting fuel is burning more efficiently.

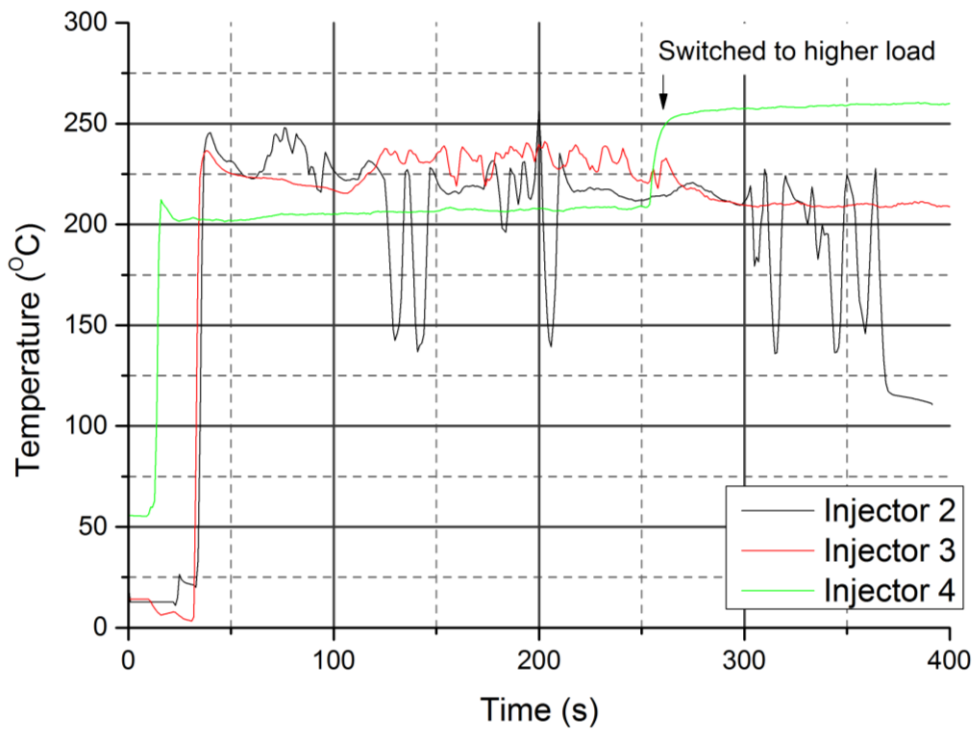


Figure 7-2 Performance of modified injectors from figure 7-1 operating on a 10% wt. shea pyrochar slurry at idle. The temperature was measured at the exhaust manifold, a key indicator of if fuel is burning as intended.

The most effective injector, number 4 was studied further, from idle to full load, which is shown in figure 7-3. The engine ran smoothly up until full load when it began to struggle. At one point, the injector stuck, nearly stalling the engine. Throughout the rest of full load operation, the temperature fluctuated far more than it did during lower loads.

Notwithstanding the dip caused by the engine nearly stalling, the variation in temperature of the manifold during full load was 18°C. At 75% load, the variation was just 7.5°C. In response to the rough running, the guide was further smoothed to remove any remaining rough edges caused by the machining and to reduce the diameter by 10µm to 4.14mm.

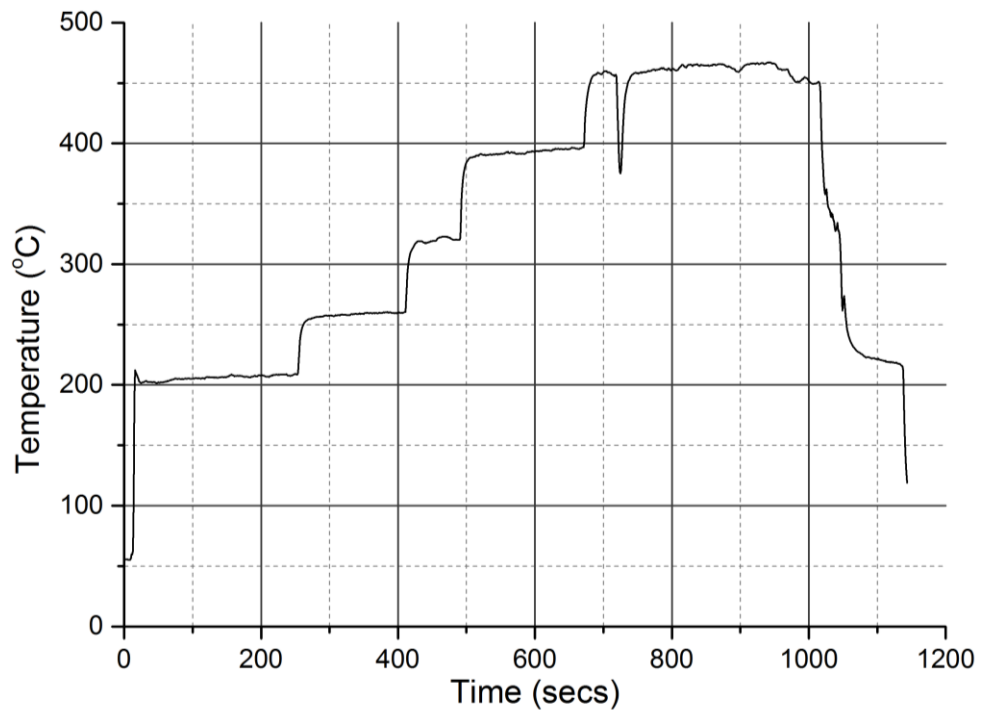


Figure 7-3 Performance of injector 4 across all loads.

7.2.2 Engine cylinder wear

After testing the new injectors using 10%wt. shea pyrochar in diesel slurry, issues occurred operating the engine. Approximately 180 hours of operation had been completed on the engine at this point. The generator would not start cold without the use of high cetane diethyl ether and would only achieve half the previous maximum power output. The requirement for ether to start the engine is indicative of loss of compression ratio caused by a lack of seal in the combustion chamber. Further inspection showed no issues with either the intake or exhaust valve, but wear was noticed across the combustion cylinder surface. Upon removal of the cylinder head, asymmetric wear was found on the surface of the cylinder. In figure 7-4, the surface in the left-hand image shows a smooth, unscratched surface. The right-hand image taken with the cylinder perpendicular to the first shows criss-cross honing marks still present meaning the wear occurring is less in that direction. Wear has been more severe on the surfaces parallel to the crankshaft which are the two sides affected by thrust caused by the rotating motion.

As increased cylinder wear can occur when using 10%wt. slurries, it would be beneficial to choose an engine design which incorporates a separate cylinder liner which can be replaced or made from a harder material to prevent wear. The current design features a cast aluminium engine block with a cast-iron non-removable cylinder liner. The liner is less hard than most ferrous materials (a hardened steel, for example, would be better) and so is more susceptible to wear, especially when using char slurries containing abrasive particles. Flynn et al. (1989) investigated wear on parts in a coal-water slurry engine. It was found that the shortest life component was the fuel injection nozzle, then piston rings and cylinder liners, with little wear occurring on other lubricated parts. Tungsten carbide coatings were found to be the best for liners and rings.



Figure 7-4 Inspection of the internal surfaces of the engine cylinder after failure. O denotes a common point on the surface of the piston to show orientation.

On dismantling the engine, the crankshaft, balancer shaft, camshaft and bearings were found to be in good condition. Also, no issues were found with the high-pressure fuel pump which has to handle the particles in the slurry. There were issues found with the piston and connecting rod. Figure 7-5 shows part of the connecting rod big end, the part which connects the piston to the crankshaft at the end closest to the crankshaft, has asymmetric wear. The surface in the upper half of the image is more worn than the bottom. The upper half appears darker as it has become more scuffed. There are also some areas in the centre showing spot marks of wear. Asymmetric marks on the big end is an indicator of an imbalance of force acting on the surface.

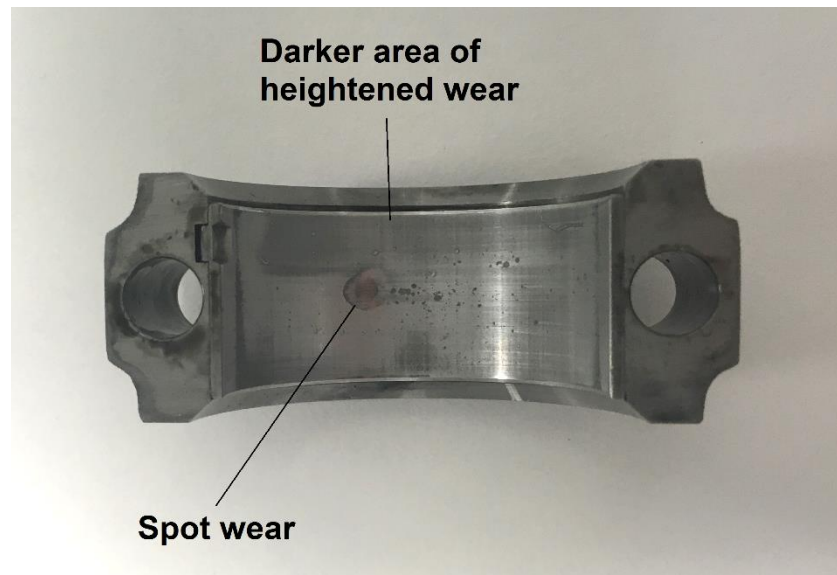


Figure 7-5 Worn big end. Bottom part of the connecting rod removed from the damaged engine.

Asymmetric wear is also seen in figure 7-6 on the skirt and upper edge surface on the thrust sides of the piston. Figure 7-6a shows a single area of wear on the skirt where the dry lubricating Teflon coating has worn away to show the aluminium underneath. In figure 7-6b, there is a section of wear on the skirt, in the same area as a). On the same side at the upper edge of the piston, above the first compression ring, the surface is darker from wear, whereas in figure 7-6b the surface is lighter like the original colour of the piston.

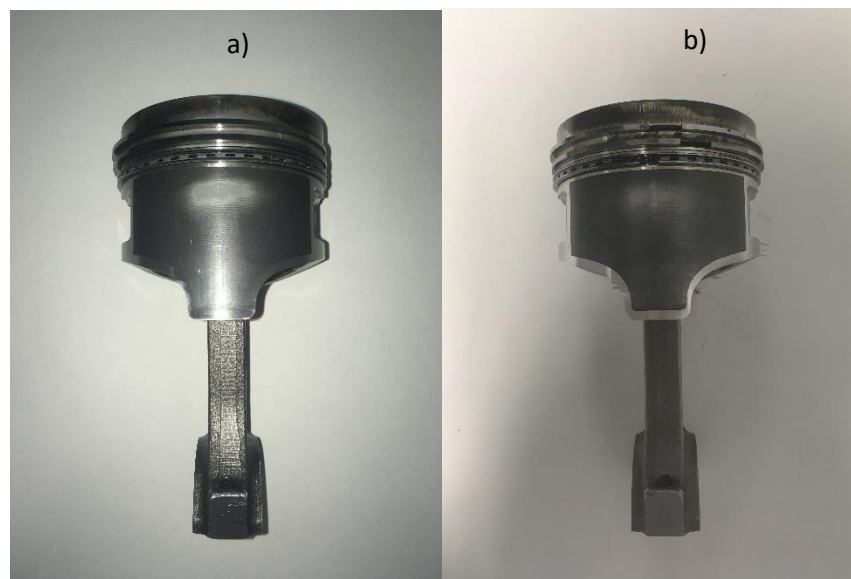


Figure 7-6 Worn piston imaged from: a) major, and b) minor thrust side.

The cause of asymmetric wear on the connecting rod was potentially caused by a slight warping of the connecting rod. This was possibly a pre-existing fault causing the maximum achievable power of the engine to be less than the design specifications. Another cause of the warping of the connecting rod could have been an overpressure occurring on the piston, potentially from hydrostatic lock. This issue occurs when liquid is present in the engine, which

is virtually incompressible, unlike gas, causing a reaction force which can cause the connecting rod to bend. Another sign was found which points to this as a cause- when the engine is turned over by hand, with the cylinder head off so that there is no resistance caused by the build-up of pressure in the combustion chamber, the rotation is not smooth and sticks at certain points. The bend in the connecting rod causes heightened wear on the cylinder bore, possibly exacerbated by the presence of solid char particles, eventually leading to the loss of compression.

7.2.3 Analysis of lubrication oil after engine failure

Lubrication oil from the failed engine was analysed, as well as a sample of the unused oil. Schwalb (1991) tested wear rates in the cylinder using clean engine oil and oil contaminated with coal ash. It was found that contamination significantly increases wear. The addition of detergent to the contaminated oil reduced wear rate to a level similar as the clean oil. Contamination is, therefore, a useful assessment for determining which elements present in the biomass char cause the most damage.

Table 7-1 shows the inorganic analysis of the remaining residue in the lubrication oil after ignition at 775°C, in accordance with ASTM D2482-03. Both new and used oil had a similar amount of ash, 1.04% for each. The analysis of used engine oil further confirms wear has occurred as the amount of iron is over 20 times higher than in the unused oil. This could have come from wear on the cylinder liner, valves, balancer shaft, bearings, crankshaft or camshaft which are all made from ferrous materials. Trace amounts of copper, chromium and molybdenum were also found in the used oil and could also have occurred from the wear of ferrous surfaces. Increased aluminium in the used oil is most likely occurring from wearing of the engine block but is also present in the range of 600-1500ppm in the chars used (see table 4-7).

Some elements have decreased after use for 180 hours, these are: phosphorous, calcium, zinc and barium. Barium was detected during SEM/EDX of exhaust soot samples. Calcium is a major constituent of ash in rhododendron and chlorella chars, so it is somewhat surprising that the amount present in the oil has reduced. As calcium is present in a comparatively high concentration, it could be that more calcium is lost through the burning of engine oil than is replaced by the char ash.

The increase in sodium, magnesium and potassium are all likely to have occurred from the presence of these elements in the ash of char used. Oxides of group 1 and 2 metals are relatively soft, with magnesium the hardest of the three (Mg, K and Na) that have increased in concentration in the engine oil after tests (Shackelford and Alexander, 2001). The chlorella

chars contain the most magnesium at approximately ten times the value per kilogram than rhododendron and shea chars. Chlorella chars also contain the most sodium. The concentration of potassium in the chlorella and shea pyrochars was high and the most likely to have caused the increase in the used engine oil. The presence of potassium and sodium in fuel produced by gasification is known to cause corrosion in engines using the syngas (Brown et al., 2009).

Table 7-1 Inorganic analysis by XRF of engine oil before and after testing for 180 hours. During the operating time, 0.1% and 1%wt. slurries of all chars were used, and 10%wt. of shea pyrochar.

<i>Oxide (mass % in ash)</i>	<i>Unused engine oil</i>	<i>Engine oil sampled after engine failure</i>
<i>Na₂O⁴</i>	0.51	1.09
<i>MgO^{4,5}</i>	0.26	1.22
<i>Al₂O₃</i>	0.52	0.87
<i>SiO₂^{4,6,7}</i>	1.31	4.10
<i>P₂O₅^{1,4,5}</i>	39.11	34.26
<i>SO₃</i>	0.79	2.11
<i>Cl</i>	0.05	0.09
<i>K₂O^{4,6}</i>	0.04	0.46
<i>CaO^{1,2,3,4,5}</i>	34.87	33.75
<i>Fe₂O₃</i>	0.09	1.92
<i>ZnO</i>	21.99	19.24
<i>SrO</i>	0.02	0.02
<i>BaO</i>	0.44	~
<i>Cr₂O₃</i>	~	0.56
<i>MnO</i>	~	0.04
<i>NiO</i>	~	0.04
<i>CuO</i>	~	0.13
<i>As₂O₃</i>	~	0.01
<i>MoO₃</i>	~	0.09

Superscript numbers denote which chars used contained more than 5000ppm of the element in question. 1) Rhododendron 400 °C pyrochar, 2) Rhododendron 600 °C pyrochar, 3) Rhododendron hydrochar, 4) Chlorella 400 °C pyrochar, 5) Chlorella hydrochar, 6) Shea 400 °C pyrochar, and 7) Shea hydrochar.

The amount of silicon in the used engine oil has significantly increased and is known to accelerate wear (Needelman and Madhavan, 1988; Sendilvelan and Anandanatarajan, 2016). The increased concentration of silicon has occurred either from dust entering the air intake or, more likely, from the slurry fuel burned. Shea chars contain the most silicon and at least ten times as much as the rhododendron chars. Chlorella chars also contain significant amounts of silicon accounting for 0.24 and 0.55% of the total mass in hydrochar and pyrochar respectively. The increasing concentration of silicon in the lubrication oil is likely the largest contributing

factor to wear caused by the oil during operation of the engine. It is therefore even more important to choose materials that are low in silicon.

Sulphur also increased in the engine oil during operation on slurry fuels. Increases in sulphur in engine lubrication oil when using conventional fuels like diesel is usually attributed to the presence of trace amounts within the fuel contaminating the oil (Motamen Salehi et al., 2017). The chars tested as slurries contained a maximum of 1800ppm of sulphur (chlorella pyrochar) down to levels which are not detectable by the elemental analyser. The fuels used were EN590 ultra-low sulphur diesel, red diesel and biodiesel from waste cooking oil which must contain less than 10ppm of sulphur (British Standards Institution, 2013; British Standards Institution, 2014). Even at 0.1%wt. of chlorella char in a diesel slurry, the amount of sulphur per kilogram of fuel will be at least double of that of the diesel fuel by itself. Using this slurry fuel will, therefore, increase the rate at which sulphur levels in the engine oil increase. Lubrication oil contains alkaline compounds which neutralise sulphuric acid formed during the combustion of sulphur containing fuel (Sautermeister, 2012). Thus, the faster accumulation of sulphur from the use of char slurries shortens the lifespan of the lubrication oil.

Table 7-2 Commercial analysis of lubrication oil from the test engine.

	<i>Unused oil</i>	<i>Oil after 0.1% tests and 125 hours</i>	<i>Oil after 180 hours. Point of failure</i>
<i>Aluminium (ppm in oil)</i>	1	10	30
<i>Chromium (ppm in oil)</i>	0	7	40
<i>Iron (ppm in oil)</i>	1	42	152
<i>Silicon (ppm in oil)</i>	0	29	73
<i>Calcium (ppm in oil)</i>	2538	2700	2506
<i>Magnesium (ppm in oil)</i>	12	35	84
<i>Phosphorus (ppm in oil)</i>	1766	1710	1592
<i>Zinc (ppm in oil)</i>	1948	1927	1797
<i>Copper (ppm in oil)</i>	0	5	13
<i>Viscosity at 40°C (centistokes)</i>	98.5	91	93.20

A standard lubrication oil analysis from a commercial laboratory was also performed on the original oil, the oil collected after the engine failed at 180 hours and oil after the 0.1%wt. slurry tests at 125 hours of operation. Table 7-2 shows the results of the analysis displaying a similar trend as the XRF analysis in table 7-1 of an increase in silicon indicative of contamination from the slurry and a rise in iron from wear. In terms of lubrication oil chemistry, the samples have remained in good condition throughout the tests. The levels of calcium, phosphorus and zinc which are additives to prevent wear, corrosion and oxidation have remained at similar values throughout. The viscosity also remains similar. Nitration, sulfation and oxidation tests were all

within allowable limits meaning that the slurries, which contain heightened sulphur and nitrogen, do not cause issues in these respects. The water content in the lubrication oil also showed negligible change. The extra commercial analysis further confirms the main issue which has arisen from using slurry fuels is the contamination of silicon, leading to part wear.

7.2.4 Replacement engine and recommissioning

The original engine was replaced by another of the same model, but with slightly different specifications. The new unit had a different speed governor, a device which limits the high-pressure fuel pump so that a steady engine speed is achieved. The speed device does not affect the performance of the engine but does change how the speed of the engine is altered by the operator. The new engine could achieve a higher output, operating at a maximum of 5.5kW, over a kilowatt more than was achieved on the previous engine, suggesting that damage may have occurred before or during baseline testing. The warping of the connecting rod in 7.2.2 may have caused this power loss.

7.3 Testing 10%wt. slurries

7.3.1 Properties of fuels tested

Table 7-3 shows the properties of the four fuels tested in this section. Diesel was again tested because the injector was altered and a new engine (although the same model as previous) was used. The addition of surfactant does alter some of the properties significantly. The addition of the surfactant reduced the calorific value by approximately 1% on a mass basis and increased oxygen by 20%.

The addition of 10%wt. pyrochar further increased the oxygen content and decreased calorific value on a mass basis. However, on a volume basis, the calorific value is higher than diesel which is a benefit for issues such as transportation and storage in developing countries. The hydrochar slurry contains the most oxygen, which may help to reduce emissions such as CO, and also has a higher volumetric calorific value than diesel.

Table 7-3 Properties of fuels tested.

	Carbon (%)	Hydrogen (%)	Nitrogen (%)	Sulphur (%)	Oxygen (%)	Density (g/L)	Higher Calorific Value (MJ/kg)	Higher Calorific Value (MJ/L)
Diesel	83.16	13.17	N.D.	N.D.	3.68	845	46.33	39.15
Diesel and surfactant	82.37	13.07	0.12	N.D.	4.45	853	45.80	39.07
10% rhododendron pyrochar 400°C	81.86	12.07	0.16	0.01	5.08	910	44.09	40.12
10% rhododendron hydrochar 250°C	80.71	12.24	0.15	N.D.	6.35	903	43.71	39.47

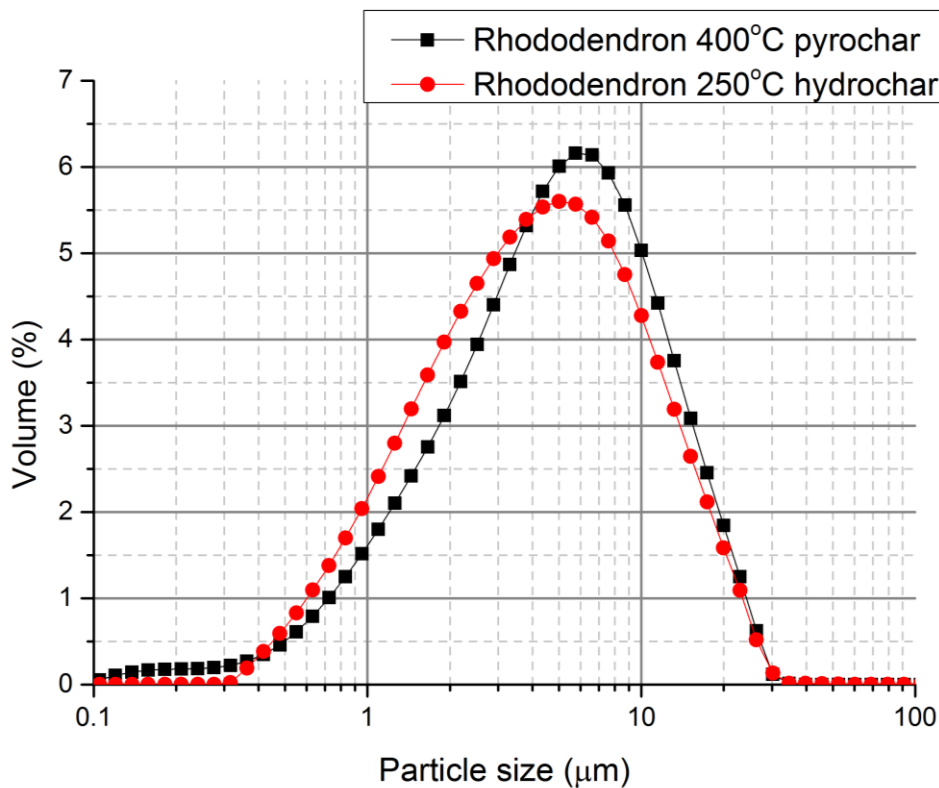


Figure 7-7 Particle size distribution of char used in the 10%wt. char-slurry diesel tests.

Figure 7-7 shows the particle size distribution of the two chars used for the 10%wt. slurry tests. The distributions of both the rhododendron pyrochar and hydrochar have no particles above 32µm and so should not cause problems with blocking injector hole orifices. On average, the hydrochar particles were smaller than the pyrochar particles. As the particles are so small anyway, the rate of combustion is unlikely to change significantly.

7.3.2 Particulate emission baseline

Before testing the slurry fuels, the engine was baselined using diesel and the fuel containing diesel and 0.5%wt. lecithin which was used as the surfactant to improve stability. Figure 7-8 shows the particle number distribution when using diesel solely. Compared to previous

baseline tests using the same fuel but original engine and injector, the distribution has changed significantly. The nucleation mode which occurs at approximately 20nm in figure 7-8 and the previous baseline in 6.3.1, is now less pronounced. The accumulation size mode occurs at 70nm to 100nm in the old and new baseline respectively.

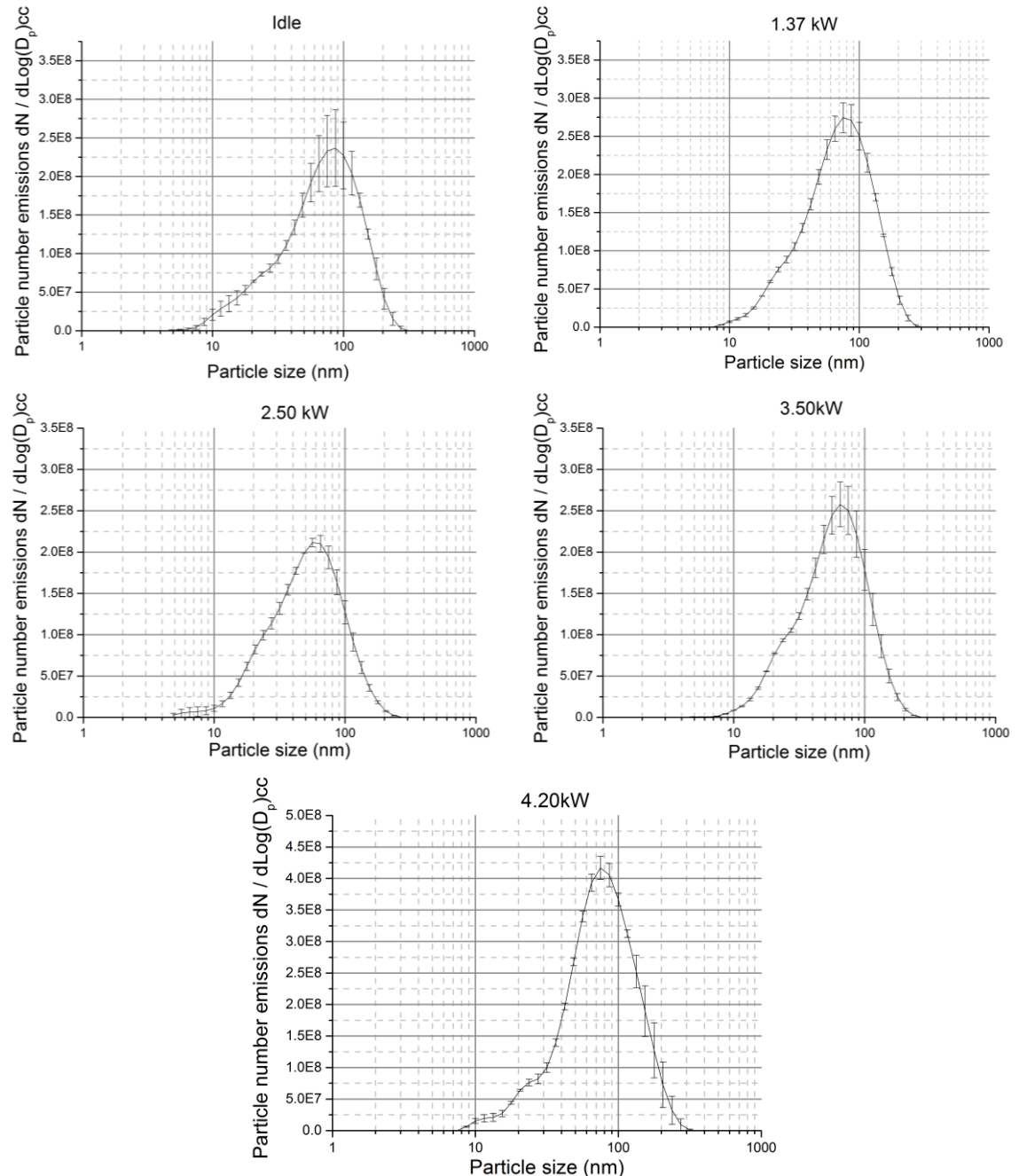


Figure 7-8 Particle number emission distribution using pure diesel. Error bars showing the difference between test repeats.

The addition of 0.5%wt. lecithin changes the particle number distribution of diesel. Figure 7-9 shows the distribution across the full load range of the engine. More soot is produced at smaller particle sizes around 20nm with the addition of lecithin. This region in the particle size distribution, known as the nucleation mode is primarily caused by volatiles cooling in the exhaust, which can be caused by the incomplete combustion of high viscosity impurities

(Rahman et al., 2014). In the case of the diesel-surfactant mix, the lecithin is potentially burning poorly, creating volatiles in the exhaust. The overall intensity of the particle number peaks is also higher with the addition of the surfactant meaning that the overall number of particles released in the exhaust is greater. The results show that the choice and concentration of surfactant is also important from an emissions perspective, as well as a rheological one.

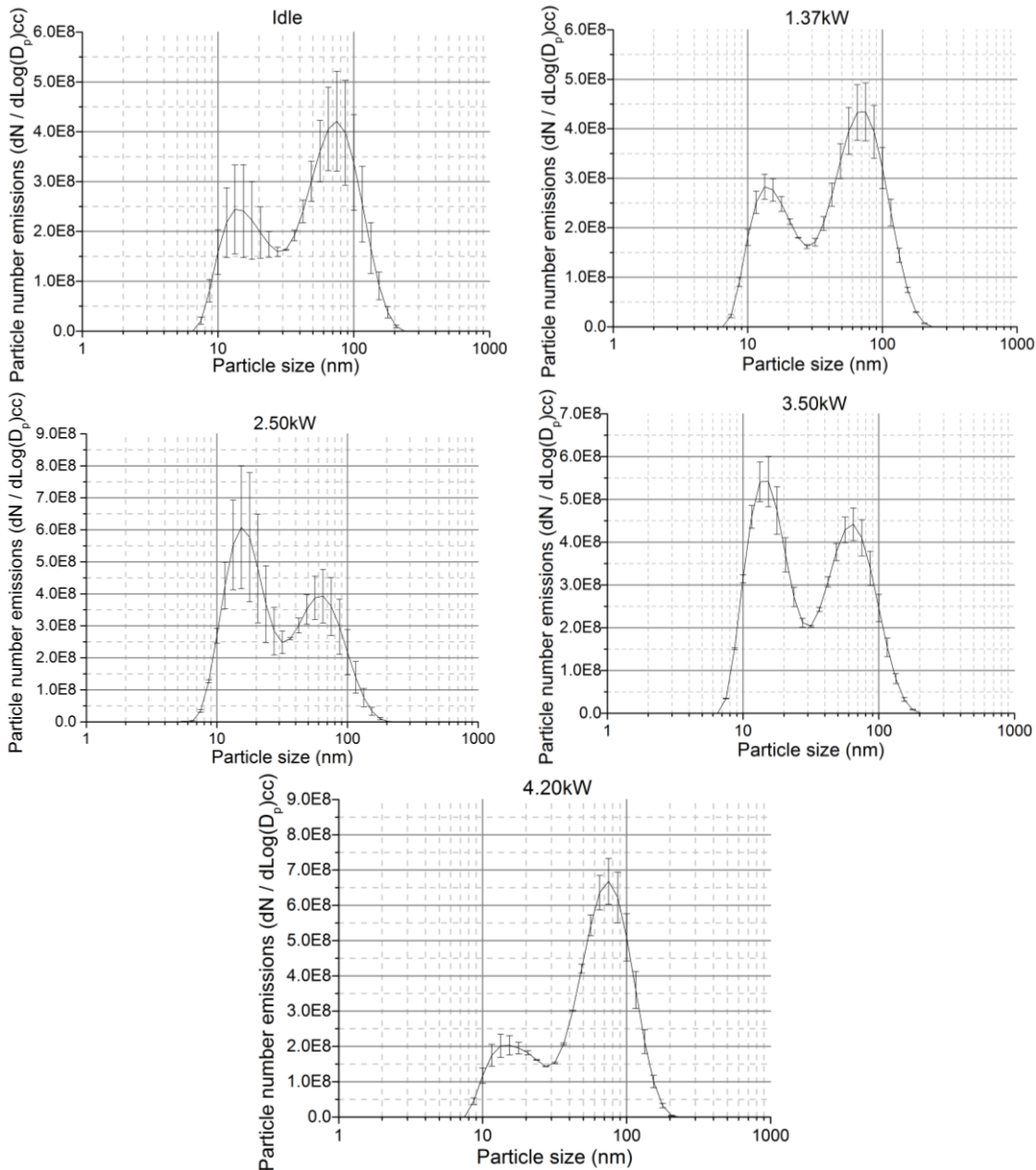


Figure 7-9 Particle number emission distribution using diesel containing the surfactant dosage used in 10%wt. slurries- 0.5% lecithin.

The difference between the duplicated baseline tests with regards to the particulate emission distribution is small in most instances, shown by the error bars on graphs in figure 7-8 and 7-9. The pure diesel tests in figure 7-8 show more consistent distributions than the diesel-surfactant mix in figure 7-9. The particle size distribution in figure 7-9 shows some

considerable error at idle and 2.50 kW. The reason could be differences in engine temperature or differences in the fuel mixture.

7.3.3 Effect of using 10%wt. slurries on engine generation efficiency

Issues occurred during the tests of 10%wt. slurries regarding the injection of the fuel. Maintaining consistent injection was difficult above 4kW, with the engine failing to remain at a constant speed. Later inspection appeared to show that the injector holes would get blocked and the particles would also stop the injector needle seating properly which is required to stop and start the fuel flow. The spray pattern was also affected by the char deposits in the injector which required cleaning out. For this reason, data was not recorded for above 4kW. Similar issues would also occur at approximately 3kW, but these were intermittent.

The effect of adding 0.5%wt. lecithin to diesel on efficiency is too small, if there is any difference, to detect with the accuracy of the instruments measuring fuel flow and power output. In figure 7-10, the difference in data points between diesel and the diesel-surfactant mix are within the error bars suggesting the differences are insignificant. The 10%wt. slurries tested were worse than diesel and the surfactant mix in terms of efficiency. At loads below 2.75kW, the reduction in generation efficiency from using 10% slurries is over 2%, meaning that adding char to the diesel actually burns more diesel than using diesel in pure form. The disparity in efficiency between the slurries and diesel baseline reduced at higher load. At roughly 3.5kW, 10%wt. rhododendron pyrochar slurry burned with similar efficiency to pure diesel. Continuing the trend line suggests that the generation efficiency would have levelled around the same level as pure diesel were it not for difficulties with the injection at full load.

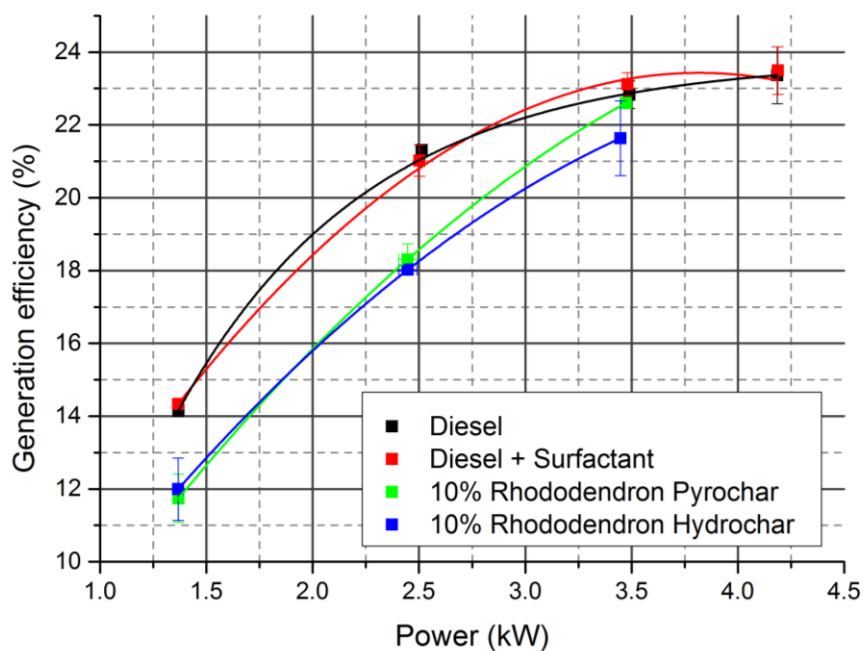


Figure 7-10 Electrical generation efficiency of the engine using diesel and 10%wt. slurry fuels.

The efficiency of the 10%wt. hydrochar slurry was similar to the pyrochar slurry (figure 7-10). It was predicted that, because of the lower recalcitrance, hydrochar slurries would burn better, especially at the low temperatures occurring at lower loads, resulting in higher efficiency. This, however, did not happen. At the highest load tested, the hydrochar slurry had a lower efficiency than the pyrochar. One of the hydrochar slurry tests performed, ran less smoothly than the replicate test, likely as a result of particle build-up in the injector, which reduced the average efficiency. One of the tests using the hydrochar slurry did produce the same efficiency at approximately 3kW as the pyrochar slurries.

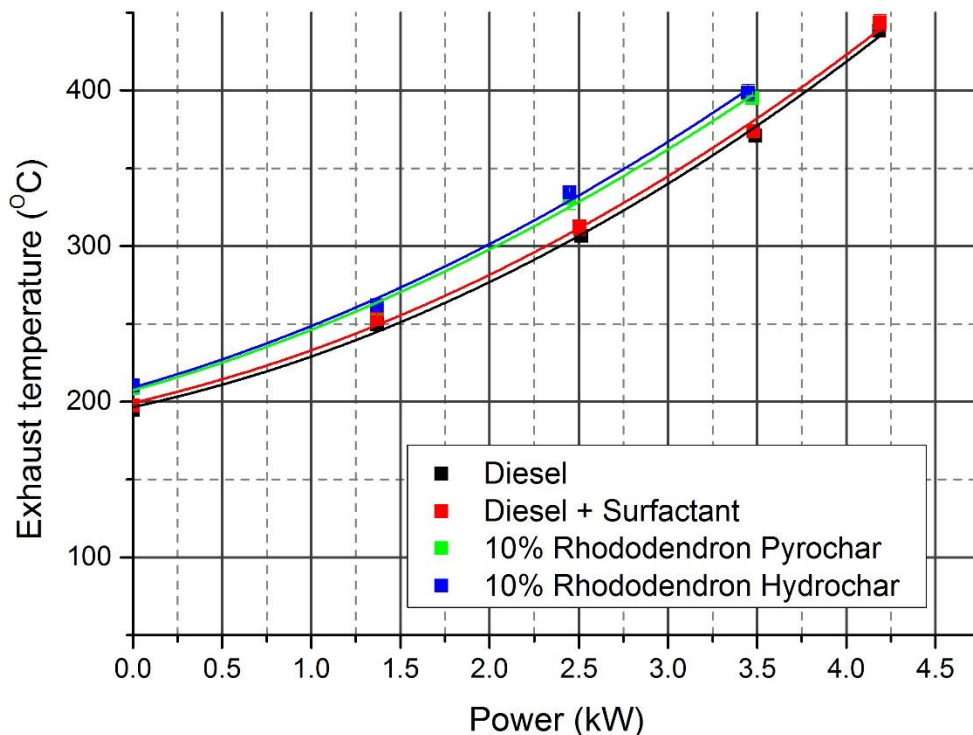


Figure 7-11 Exhaust temperature occurring at different loads using different fuels.

Figure 7-11 shows that significantly more heat was wasted via the exhaust when using 10%wt. char slurries compared to neat diesel. The higher exhaust temperature was indicative of slower combustion which could be caused by, but not limited to: high viscosity, low heat release rate and high double bonds (Shehata and Razeq, 2011). The difference between the two char slurries in terms of the exhaust temperature was small despite the differences in carbon structure suggesting that the cause of the increase against neat diesel is associated with the rheological properties. The addition of 0.5% lecithin to diesel caused a small increase from the neat diesel baseline in the exhaust temperature also.

Combining the exhaust temperature measurements and generation efficiency data shows that, at least at loads over 75%, 10%wt. slurry fuels can achieve similar efficiencies as pure diesel, thus saving fossil fuel. Modifying the engine by changing the injection timings and reducing the

engine speed would likely further improve the efficiency of the slurry fuel engine as the exhaust temperature data shows the onset of combustion is retarded. Choosing a surfactant that reduces viscosity would also be beneficial to reduce waste heat from the exhaust.

7.3.4 Effect of using 10%wt. slurries on engine gaseous emissions

CO₂ emissions when using 10%wt. slurry fuels were consistently higher than when using diesel (figure 7-12). Increased CO₂ emissions is another indicator of less efficient combustion as it shows more carbon is burned. Another cause was that the calorific value of the char slurry fuels was lower and hence more carbon has to be burned to input the same amount of energy into the engine. The presence of the surfactant does not increase the CO₂ emission concentration, despite the calorific value being reduced. The reason was that the carbon content of diesel with surfactant added was approximately 1% less- the same as the percentage reduction in calorific value on a mass basis.

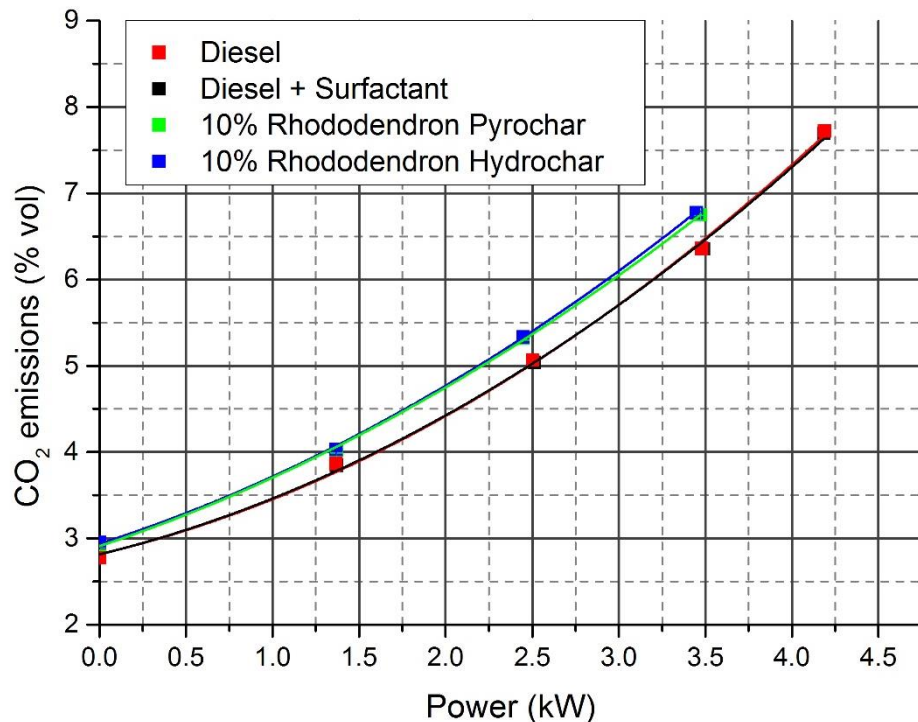


Figure 7-12 CO₂ emissions using 10%wt. slurries.

Carbon monoxide (CO) emissions were increased by the addition of surfactant and char particles. Figure 7-13 shows the carbon monoxide concentration in the exhaust gas during the tests. Adding 0.5%wt of lecithin to diesel raised the CO emissions by approximately 50ppm across the full load range. 10%wt. of char added to the diesel-surfactant mixture further increased CO, especially at low loads. For example, at idle, CO was at least 200ppm higher than the baseline by adding char. The difference in CO emissions between the slurries and diesel decreased with increasing load, to a similar value as the diesel-surfactant mixture at 3.5kW. The heightened CO emission at low loads from slurries suggests more incomplete combustion

is occurring compared to the baseline. This is because the cylinder temperature is lower at low loads.

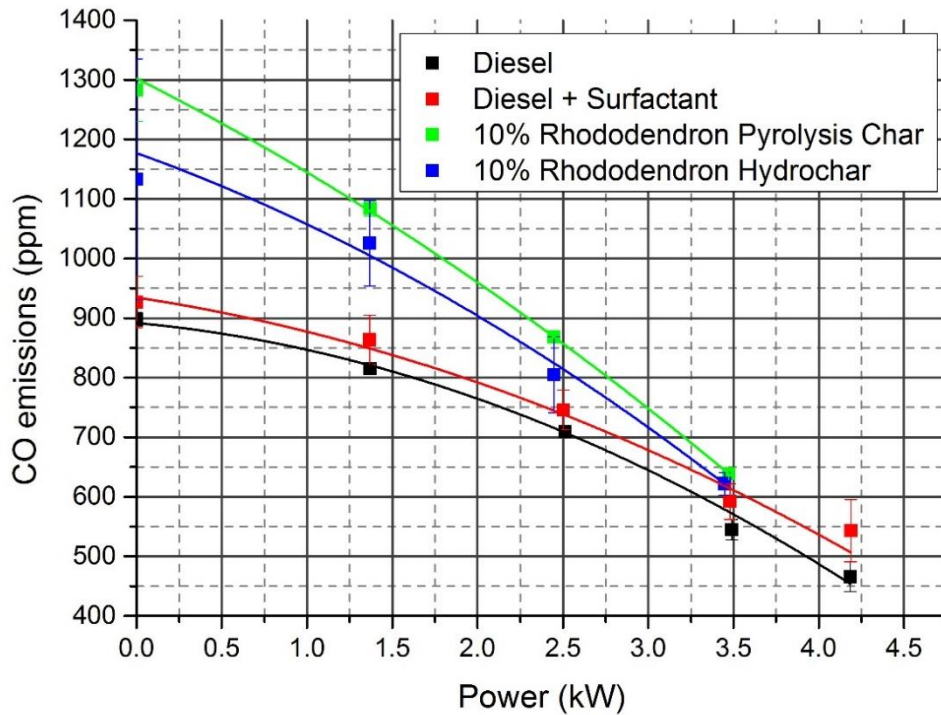


Figure 7-13 Carbon monoxide emissions produced by the engine when using 10%wt. slurries.

Comparing the two char slurries together, the one containing hydrochar, the less recalcitrant of the two fuels, produces less CO. This shows that the recalcitrance of the fuel is important in ensuring that the fuel burns fully, reducing harmful CO emissions. However, once the engine cylinder is at higher temperatures and load, both char slurries burn equally well.

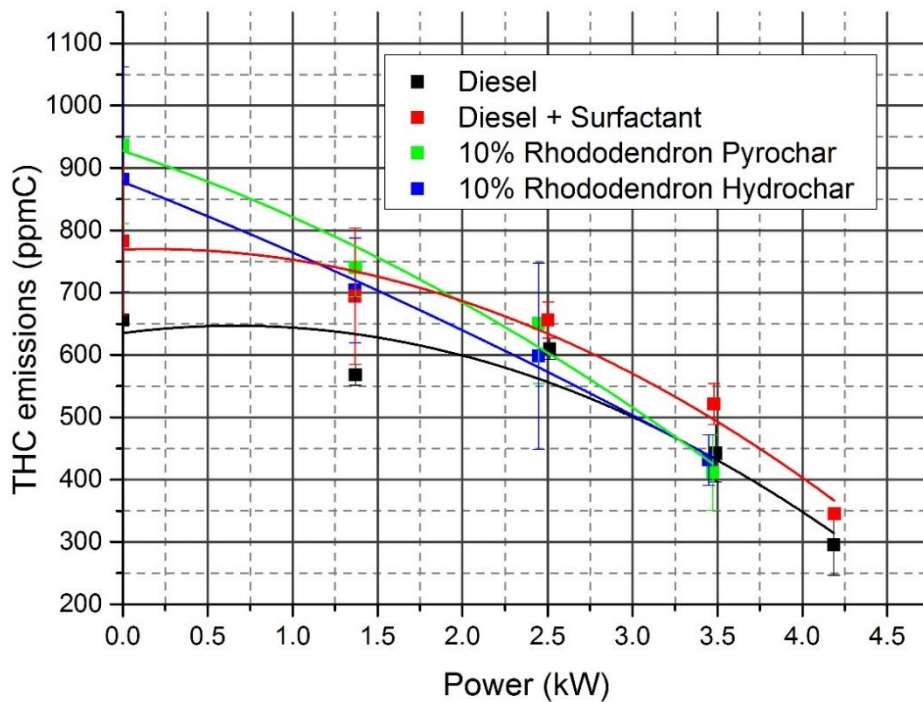


Figure 7-14 Total hydrocarbon emissions (THC) from using 10%wt. slurries.

Total hydrocarbon emissions (THC) are shown in figure 7-14. The addition of surfactant raised THC emissions compared to pure diesel operation across all loads. Unlike the previous tests with 0.1%wt. and 1%wt. of char added, the 10%wt. slurry fuels had higher THC emissions than pure diesel. As the load approaches 3.5kW load, THC emissions from the 10%wt. slurry fuel decrease and are equal to the diesel baseline. THC emissions were lower using hydrochar particles than pyrochar, with the difference reducing with load, which was a similar pattern to CO emissions in figure 7-13. The reason for this is the same as with CO emissions, combustion completeness increases as the combustion chamber becomes hotter with increasing load. The addition of char reduces THC emissions above 50% load compared to the diesel and surfactant mix, suggesting that the char addition counteracts the increase in THC caused by the surfactant. Therefore, there is still potentially some catalytic benefit which was seen in the earlier 0.1% and 1%wt. slurry tests in chapter 6. The improvement in THC emissions due to the addition of char likely decreases with increasing char concentrations because the relatively poor combustion of char becomes the dominant factor compared to the catalytic benefit.

The THC and CO emissions results, measures of how complete combustion is in a diesel engine, show that at low load, 10%wt. slurries burn worse than neat diesel. Combining this information with electrical generation efficiency results suggests that, for this type of diesel engine, slurry fuels are inappropriate for partial load operation. The results also show a significant negative impact of the surfactant on CO and THC emissions. The addition of lecithin may increase the viscosity of diesel, reducing atomisation, leading to poorer combustion.

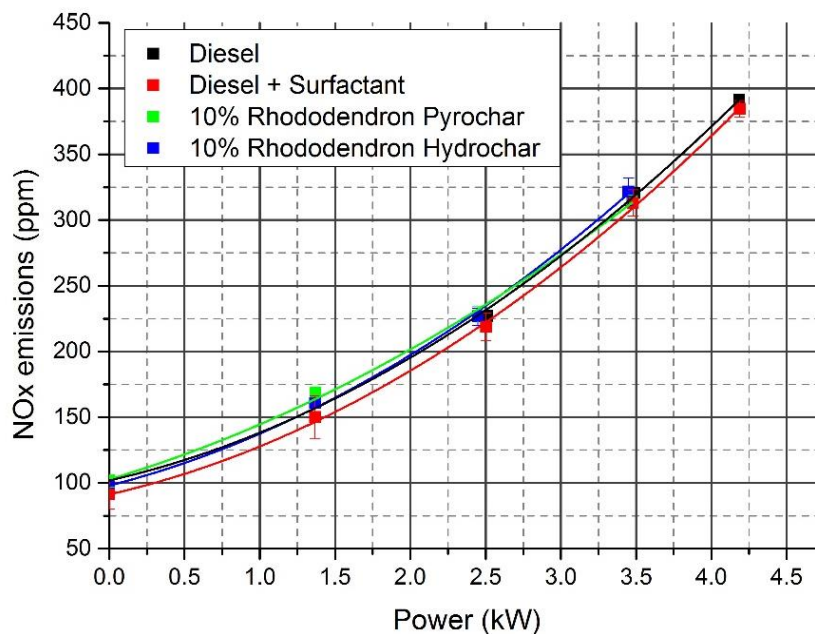


Figure 7-15 NO_x emission concentration in the exhaust of the engine generator when using 10%wt. slurries.

Figure 7-15 shows the NO_x emissions from the two liquid fuels used as a baseline for performance and the two 10%wt. slurries. Adding surfactant to diesel decreased NO_x emissions compared to pure diesel by approximately 10-20ppm at all loads. This was likely caused by the reduction in the quality of atomisation caused by the surfactant. The addition of 10%wt. of char to the diesel-surfactant mix caused an increase in NO_x emissions. The values for NO_x emissions of pyrochar and hydrochar slurries also show differences between each other. The pyrochar slurry produced more NO_x than the hydrochar slurry at loads below 2.5kW. The results from the measurements of CO and THC emissions showed incomplete combustion due to the higher recalcitrance, hence later onset of combustion, of rhododendron 400°C pyrochar than diesel. An increase in ignition delay caused by the higher recalcitrance of the fuel would lead to more NO_x being produced. The higher exhaust temperature from using 10%wt. pyrochar slurry shown in figure 7-11 means the peak cylinder temperature was higher, which is positively correlated with NO_x production (Shameer and Ramesh, 2017).

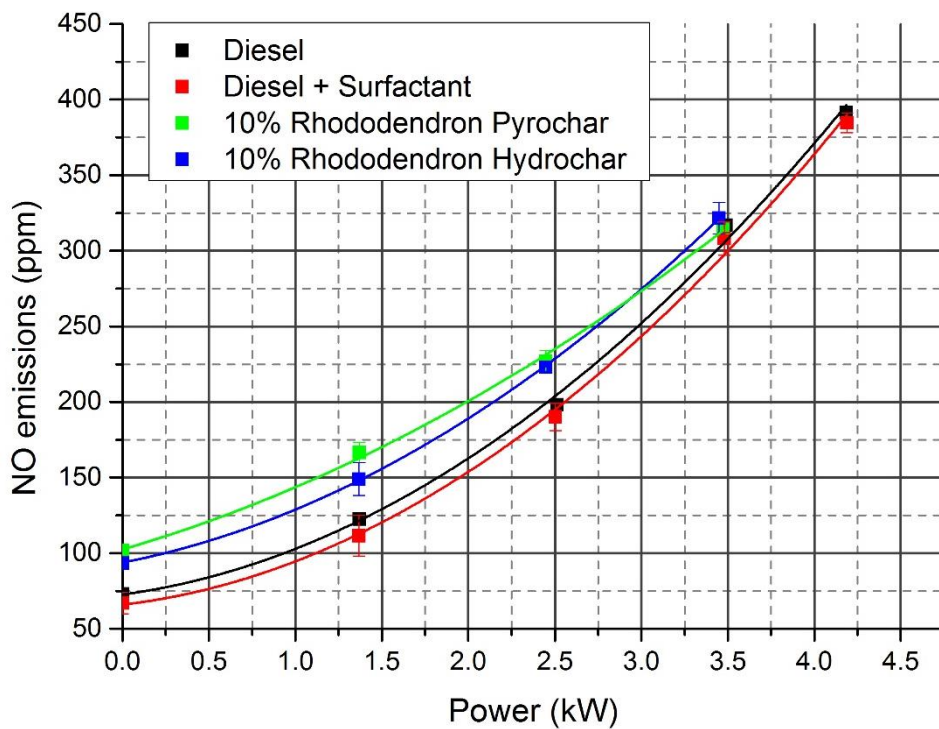


Figure 7-16 Nitric oxide emissions when using 10%wt. slurry fuels.

The previous 0.1% and 1%wt. tests of rhododendron 250°C hydrochar in diesel showed unchanged and increased NO_x emissions respectively compared to the baseline. Therefore, a NO_x reduction was not expected using the 10%wt. hydrochar slurry fuel. The reason for lower NO_x emissions from the hydrochar than the pyrochar slurry is likely the lower recalcitrance of the hydrochar which becomes an increasingly important factor as solid loading increases. Combining the results for 0.1%, 1% and 10%wt. rhododendron pyrochar diesel slurries showed that there is an initial NO_x reduction at low concentrations which diminishes with increasing solid loading.

The surfactant addition reduces NO emissions with respect to neat diesel across all loads, which is shown in figure 7-16. The NO emissions from rhododendron slurries significantly increased compared to both the baseline and the diesel-surfactant mix. At idle, for example, adding 10%wt. char approximately doubled NO emissions. The disparity between the baseline and slurry fuels reduced as load increased. The rhododendron pyrochar slurry tested produced more NO than the hydrochar slurry. Combined with the higher exhaust temperature data, the extra NO produced using the 10%wt. slurries is further evidence that the peak cylinder temperature has increased.

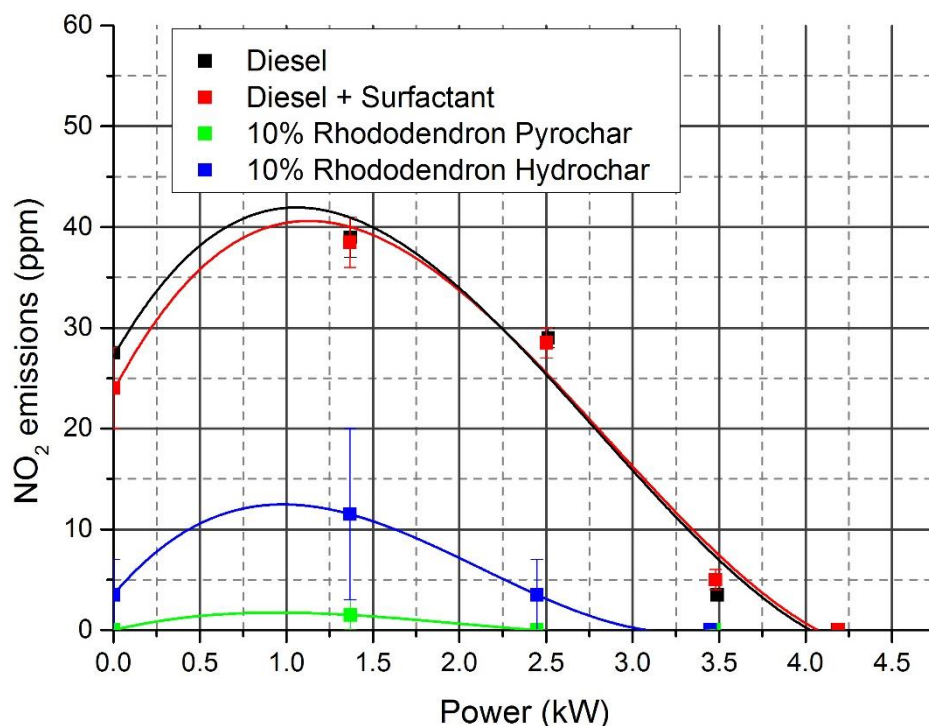


Figure 7-17 Nitrogen dioxide emissions from 10%wt. slurries.

The effect of the surfactant added to stabilise the slurry on NO₂ emissions was minimal as shown in figure 7-17. Significant reductions, however, were made with the addition of 10%wt. char. At idling conditions, the reduction in NO₂ was at least 80%, depending on the type of char added. The rhododendron pyrochar slurry reduced NO₂ emissions the most from the baseline.

At loads above 2.5kW, the level of NO₂ in the exhaust when the pyrochar slurry was used was undetectable. Rhododendron hydrochar slurry reduced NO₂ at all loads compared to the baseline. The reason was previously discussed in 6.5.3, that NO₂ acts as an oxidant reducing the temperature that soot oxidises at, and in this case, remaining char also (Matyshak et al., 2006). NO₂ was therefore consumed by late char combustion.

The results in chapter 6 regarding NO₂ emissions of 1%wt. slurries showed a similar pattern regarding the type of char used- the 1%wt. hydrochar reduced NO₂ with regards to the baseline, but not as dramatically as the pyrochar. The effect on NO₂ emissions of slurries amplifies with increasing solid loading. Beginning at 0.1%wt. char to fuel, a small reduction was found and the maximum difference at 10%wt. in the NO₂ emission concentration.

7.3.5 Particle emissions from using 10%wt. slurries

One of the most important areas regarding using slurry fuels is the number of soot particles produced by the engine. Figure 7-18 shows the particle number emissions of the four fuels tested. The diesel-surfactant mix produced more particles than the neat diesel tested. The increase in particle concentration in the exhaust is between 50 and 170%, depending on the load.

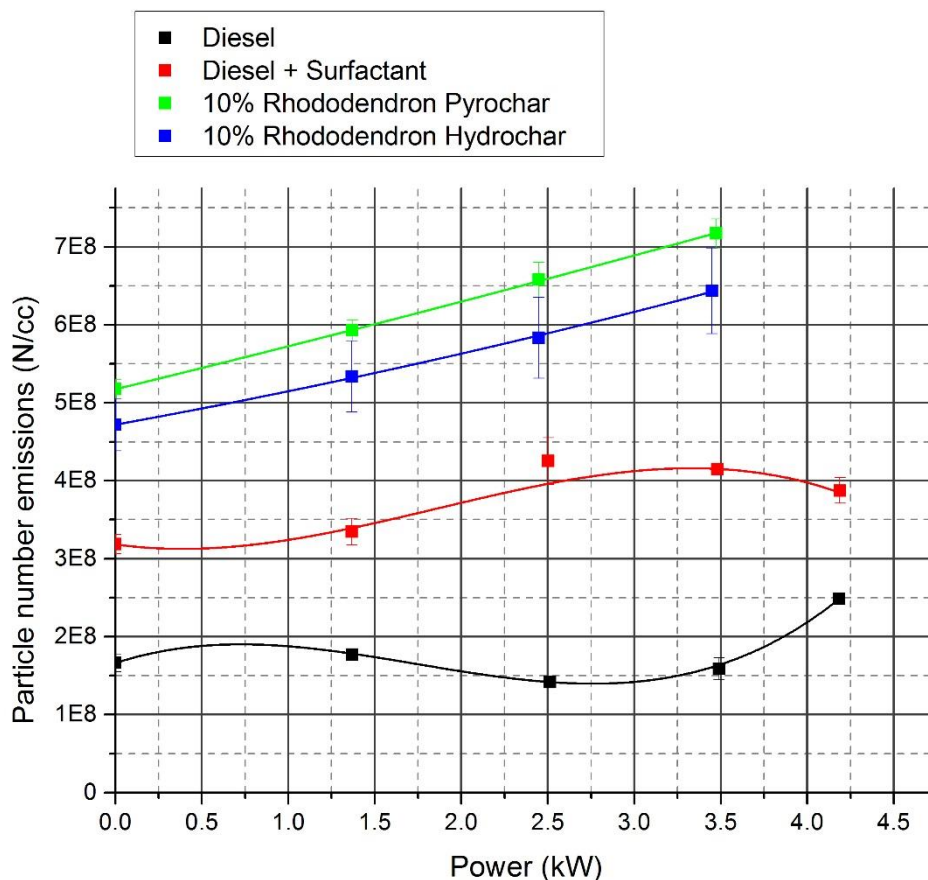


Figure 7-18 Particle number emission concentration in the exhaust when using 10%wt. slurries.

Particle emission concentration further increases with the addition of 10%wt. char to the diesel-surfactant mixture. Unlike with the two non-slurry fuels in figure 7-18, the particle number emissions grow linearly with load. This was possibly related to the increasing rate of ash produced as more fuel is used, thus leading to more particles emitted from the exhaust. The pyrochar slurry emitted more particles than the hydrochar slurry which could be for two reasons. First, is that the char burns worse if it is more recalcitrant pyrochar which is evidenced by the THC and CO emission data. Second is that the ash content in the pyrochar is higher.

Comparing the data at idle, the increase in particle emissions from the neat fuel to 10%wt. rhododendron hydrochar fuel is roughly half caused by the surfactant used and half caused by the char. At other loads, the proportion of particle number emissions caused by the two additions to diesel are roughly the same. The choice of surfactant is therefore important in reducing the overall particulate pollution caused by the fuel, which would be harmful to communities living near a slurry engine site. The results show that finding a surfactant which can stabilise the fuel as well as lecithin but produce less particulate emissions would be a major benefit. It also raises the question if it is more favourable to sacrifice the stability of the fuel for I emissions. Reducing the amount of lecithin would achieve this and save money in fuel formulation which might be a better overall option.

Figure 7-19 summarises the particle size distributions shown in figure 7-8 and 7-9 as an engine map for comparison with the slurry fuels tested. Figure 7-19a shows the mode of the distribution is approximately 80nm across all loads. The intensity of the mode increases between 3.5kW and 4.2kW, which is also reflected in the particle number shown in figure 7-18. The same mode exists in approximately the same region when using the diesel and surfactant mixture in figure 7-19b. The mode at 80nm also increases between 3.5 to 4.2kW. The mode is also least intense during both tests at 2.5kW. The difference between the two fuels is the nucleation mode which appears at 15nm in figure 7-19b. This is most intense at 2.5kW which causes a rise in the particle number which does not occur in neat diesel.

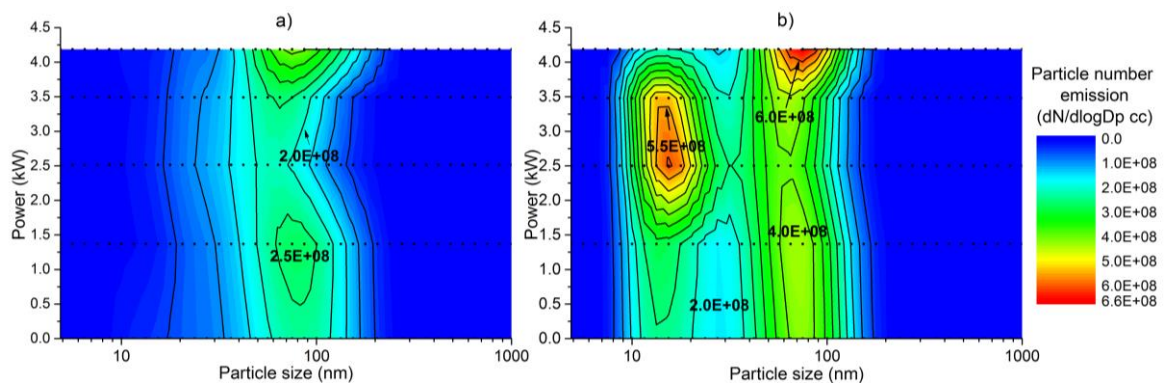


Figure 7-19 Particle number distribution map across the full load range. a) Neat diesel fuel, and b) diesel and 0.5%wt. lecithin.

The particle number distribution of the 10%wt. slurries shown in figure 7-20 are monomodal except for the rhododendron pyrochar slurry when idling. The mode for both slurries is at approximately 22nm, shifting toward 35nm with increasing load. The peak intensity increases as load increases. Excluding the overall intensity of particle emission, the region of the particle size distribution of soot is similar for both slurries tested.

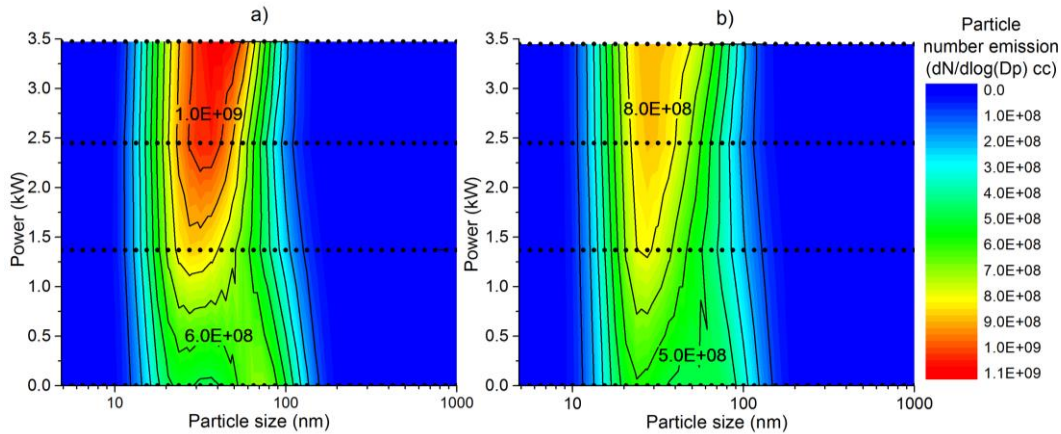


Figure 7-20 Particle number distribution of soot in the exhaust gas. a) 10%wt. rhododendron pyrochar slurry, and b) 10%wt. rhododendron hydrochar slurry.

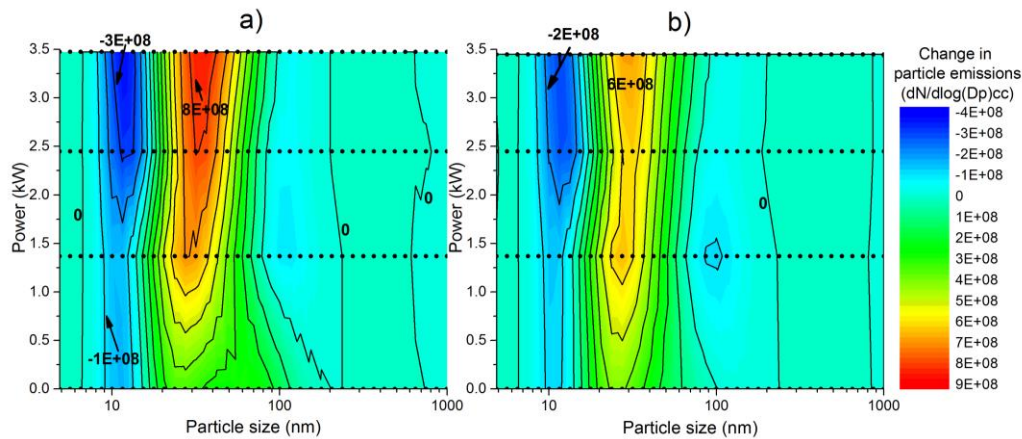


Figure 7-21 Change in particle size distribution of soot compared to the tests using the diesel and surfactant mixture. a) 10%wt. rhododendron pyrochar in diesel, and b) 10%wt. rhododendron hydrochar in diesel.

Figure 7-21 shows the change in particle emission distribution caused by the addition of char into the diesel and surfactant mixture. Both types of char have affected the distribution similarly. The distribution narrows seen by a negative change in particle emissions from 6-17nm and 100-200nm. The reduction in the finest particles around 10nm is greater in the pyrochar slurry than the hydrochar slurry. A similar reduction in particles around 10nm occurred when 1%wt. of char was added. The largest reduction in the finest 10nm particles occurs at the highest loads.

Table 7-4 Particle mass emission from the combustion of 10%wt. slurries in an engine generator.

<i>Fuel</i>	<i>Ash in fuel burned (mg/m³)</i>	<i>Total particulate mass (mg/m³)</i>
<i>Neat Diesel</i>	-	27.9 ± 0.8
<i>Diesel + Surfactant</i>	-	38.6 ± 3.0
<i>10%wt. Rhododendron Pyrochar</i>	230	78.0*
<i>10%wt. Rhododendron Hydrochar</i>	200	42.7 ± 4.4

* Denotes test only performed once

Table 7-4 shows the measured soot emissions from the engine at 3.5kW load. The particulate mass emissions measured using a single stage filter follow a similar trend to particulate number- that neat diesel produces the least soot and 10%wt. rhododendron pyrochar slurry the most. As was found during the 0.1% and 1%wt. tests, the particulate mass emissions from 10%wt. slurries were significantly less than the ash expected to be emitted. In the case of the 10%wt. pyrochar slurry the amount of particulate mass was approximately a third of what would be expected, and a fifth in the case of hydrochar. This further shows that the ash is likely entering the oil sump. Soloiu et al. (2011) found smoke measured by a Bosch smoke meter (which is an optical measurement of a soot collecting filter paper) was lower than diesel at all loads when a 25%wt. charcoal-diesel slurry was used. The 1.77% ash content of the charcoal used in this previous study should have considerably raised the value of particulate matter on the filter if it had exited through the exhaust. The evidence from the tests in chapter 6 and 7, as well as in literature point to the majority of ash being deposited in the lubrication oil or somewhere else.

The addition of surfactant increases the concentration of particulates in the exhaust by 40%. The extra particulates caused by the addition of 10%wt. of char is dependent on the type of thermal treatment used in its production. The hydrochar slurry produced 45% less soot on a mass basis than the pyrochar slurry. The hydrochar added made only a small difference to particulate emissions compared to the diesel-surfactant mix. The difference in particulate emissions between hydrochar and pyrochar slurries is potentially a result of the lower recalcitrance of hydrochar, meaning more burns fully in the engine. The structure of the carbon may also be the cause, the lower degree of aromatisation of hydrochar would make it less susceptible to forming soot (Das et al., 2017). The additional oxygen in hydrochar could also help reduce soot formation.

7.3.6 Lubrication oil analysis

The lubrication oil in the engine generator was analysed after the 10%wt. slurry tests were completed and shown in table 7-5. Significant levels of wear have occurred during the use of the two 10%wt. rhododendron slurries shown by increased levels of iron, chromium and aluminium. The level of iron in the lubrication oil is higher than was found when the engine failed (table 7-2). Silicon content is also comparatively high for lubrication oil and would significantly increase the wear rate. The most abundant trace elements in the char used were calcium and phosphorus, which are difficult to assess in terms of ash contamination in the lubrication oil because there are already compounds containing the elements in the oil formulation. Some of the additives containing calcium, phosphorus and zinc are used during operation which is shown by a reduction in the concentration of zinc and phosphorus in the used oil. Zinc, which is not present in the chars in substantial quantities reduced in concentration by the highest proportion, whereas calcium, the most abundant trace element in the chars, increased in concentration. This shows that it is likely that some of the calcium and phosphorus in the used oil is from the slurry ash.

Table 7-5 Lubrication oil analysis before and after the 10%wt. slurry tests.

	<i>Unused oil</i>	<i>Oil after 10% tests (8 hours usage)</i>
<i>Aluminium (ppm in oil)</i>	1	29
<i>Chromium (ppm in oil)</i>	0	34
<i>Iron (ppm in oil)</i>	1	195
<i>Silicon (ppm in oil)</i>	0	55
<i>Calcium (ppm in oil)</i>	2538	2543
<i>Magnesium (ppm in oil)</i>	12	31
<i>Phosphorus (ppm in oil)</i>	1766	1722
<i>Zinc (ppm in oil)</i>	1948	1889
<i>Copper (ppm in oil)</i>	0	11
<i>Viscosity at 40°C (centistokes)</i>	98.5	86.40

Based on the amount of char burned in the fuel, the soot concentration and contaminant concentration in the lubrication oil, the amount of ash accounted for is small compared to the total that has passed through the combustion chamber. This suggests another possibility for the fate of the ash in the char added, that the ash is deposited in the exhaust system. There is a significant length of exhaust before the sampling ports- a silencer and several metres of sampling lines before the analytical instruments, all areas which the ash could leave the exhaust stream. One possibility is that the high temperature of the engine causes the ash to melt, leave through the exhaust then condense on the cooler surfaces of the exhaust.

During the 10%wt. slurry tests, approximately 600mg of silicon passed through the combustion chamber as part of the char. Multiplying the concentration of silicon in the used oil by the amount of oil in the engine sump, 15% of the total silicon is estimated to have ended in the oil sump. The amount of calcium entering the engine during the test was approximately 7000mg which means only a small proportion has entered the lubrication oil based on the analysis in table 7-5. As the amount of soot in the exhaust gases and found in the lubrication oil is far less than the amount of ash created then the ash must be deposited on the surfaces of the exhaust. Whilst these deposits collecting in the exhaust can cause issues in the long term, it is more favourable than to be emitted as harmful particulates or to remain in the lubrication oil continuing to cause wear.

It, therefore, appears that the tendency for ash to deposit in the lubrication oil is dependent on the elemental content with silicon more likely the calcium to end up in the sump. To prevent long-term wear it would be beneficial to use a special lubrication oil or cleaning systems which can stop abrasion by deposited silicon.

7.4 Conclusions

The objective of this chapter was to incorporate char into diesel as a co-fuel to the traditionally used fossil fuel. The results have shown that, at loads above 75%, a 10%wt. slurry can be used in a high-speed diesel engine with a similar efficiency to neat diesel. At low loads, however, the temperature of the engine was not high enough to burn the slurry to produce more energy than if the diesel fuel in the slurry was used solely. At the highest achieved load using 10%wt. char slurries, the efficiency was marginally less than neat diesel, the difference was under 0.5%. The maximum attained efficiency of 10%wt. char slurries in the high-speed diesel engine was 22.6%.

Comparison of the two char slurries; one containing pyrochar and another containing hydrochar from the same initial material showed differences when used in an engine generator. The emissions data shows the 10%wt. hydrochar slurry burned more cleanly, producing less CO, THC and soot, measures of incomplete combustion, compared to the pyrochar slurry at every load tested. The cause of the first two emission types being lower, and to some extent, the third is the less aromatised carbon structure of hydrochar, which means that it burns at a lower temperature and contains fewer compounds with a high tendency to soot. Another potential reason for less particulate emissions on a mass basis released by the hydrochar is the lower level of ash which can add to this value.

The 10%wt. char slurries used increased NO_x emissions compared to neat diesel. The increased exhaust temperature points to higher in-cylinder temperatures caused by a delayed

onset in combustion is a possible cause. The concentration of NO₂ in the exhaust was significantly reduced by the use of char slurries, especially pyrochar. The reduction in NO₂ achieved was more than when 1%wt. slurry chars were used. The reason for this is that NO₂ is consumed by the late burning char.

The alterations in emissions caused by the surfactant were found to be highly important to the total, something which has been overlooked in previous studies. The use of lecithin at 0.5%wt. caused the number of particles released to over double at some loads. The total increase in particles produced from using 10%wt. slurries compared to neat diesel can be mainly attributed to the surfactant used rather than the char added. The surfactant, lecithin, increased THC and CO, but reduced NO_x compared to neat diesel. The change in emissions shows that the surfactant has reduced the quality of atomisation, possibly by increasing the viscosity. Choosing a surfactant which can reduce viscosity would improve efficiency and reduce soot emissions. The surfactant is therefore important from an emissions, as well as a rheological perspective and should be investigated further.

Despite improvements to the injector to help the flow of particles in the slurry, problems were still encountered, especially at full load which meant operation could not be maintained long enough to collect accurate measurements. On dismantling of the injector, compacted char was found inside the cavity, causing the needle to not lift or shut properly, which prevented smooth operation. The spray pattern was affected by the build-up of particles also.

Wear of the engine was found to be a key problem encountered using these slurry fuels. During preliminary tests, the cast iron cylinder liner became so worn that it had to be replaced. Analysis of the engine lubrication oil after testing the 10%wt. char slurries showed wear had taken place and silicon in the ash had contaminated it. The contamination of the lubrication oil is concerning as it will continue to wear parts until it is removed. Special lubrication oils and systems for slurry engines is another important area for investigation.

Except for the injector and cylinder liner, the other parts of the engine appeared to be undamaged by the slurry fuel. The high-pressure fuel pump which was thought might have trouble handling the particle-filled slurry fuel, was unaffected. The crankshaft, valves and cylinder head had no adverse wear.

The fate of the ash in the char is important because it has the ability to increase the amount of particulates by over double compared to neat diesel or damage the engine. Evidence was found that ash ends in the lubrication oil and emitted with the soot in the exhaust. However, the amount accounted for was less than what would be expected from the mass of char used. It suggested that some of the ash has been deposited in the exhaust system. The temperatures in the cylinder during combustion were high enough that the ash can melt then solidify on the cooler exhaust sections. Approximately 15% of the silicon passing through the engine as fuel ended in the lubrication oil and may continue to cause wear. The results showed that silicon in biomass for producing slurries should be avoided where possible.

7.5 References

- British Standards Institution. 2013. 2013. *BS EN 590:2013+A1:2017 Automotive fuels. Diesel. Requirements and test methods*. London UK: British Standards Institution.
- British Standards Institution. 2014. 2014. *BS EN14214:2012+A1:2014 Liquid petroleum products. Fatty acid methyl esters (FAME) for use in diesel engines and heating applications. Requirements and test methods*. London, UK: British Standards Institution.
- Brown, D.Gassner, M.Fuchino, T. and Maréchal, F. 2009. Thermo-economic analysis for the optimal conceptual design of biomass gasification energy conversion systems. *Applied Thermal Engineering*. **29**(11), pp.2137-2152.
- Das, D.D.McEnally, C.S.Kwan, T.A.Zimmerman, J.B.Cannella, W.J.Mueller, C.J. and Pfefferle, L.D. 2017. Sooting tendencies of diesel fuels, jet fuels, and their surrogates in diffusion flames. *Fuel*. **197**, pp.445-458.
- Flynn, P.L.Leonard, G.L. and Mehan, R.L. 1989. Component Wear in Coal-Fueled Diesel Engines. *Journal of Engineering for Gas Turbines and Power*. **111**(3), pp.521-529.
- Inyang, H. 2008. Decommissioning of Diesel-Fueled Electric Power Generators in Developing Countries. *Journal of Energy Engineering*. **134**(1), pp.1-1.
- Kanagawa, M. and Nakata, T. 2008. Assessment of access to electricity and the socio-economic impacts in rural areas of developing countries. *Energy Policy*. **36**(6), pp.2016-2029.
- Matyshak, V.A.Sadykov, V.A.Kuznetsova, T.G.Ukharskii, A.A.Khomenko, T.I.Bykhovskii, M.Y.Sil'chenkova, O.N. and Korchak, V.N. 2006. Role of nitrogen dioxide in the oxidation of diesel soot on promoted mixed catalysts with fluorite and perovskite structures. *Kinetics and Catalysis*. **47**(3), pp.400-411.
- Motamen Salehi, F.Morina, A. and Neville, A. 2017. The effect of soot and diesel contamination on wear and friction of engine oil pump. *Tribology International*. **115**, pp.285-296.
- Needelman, W.M. and Madhavan, P.V. 1988. Review of Lubricant Contamination and Diesel Engine Wear. In. SAE International.
- Rahman, M.M.Pourkhesalian, A.M.Jahirul, M.I.Stevanovic, S.Pham, P.X.Wang, H.Masri, A.R.Brown, R.J. and Ristovski, Z.D. 2014. Particle emissions from biodiesels with different physical properties and chemical composition. *Fuel*. **134**, pp.201-208.
- Ryan, T.W.Likos, W.E. and Moses, C.A. 1980. The Use of Hybrid Fuel in a Single-Cylinder Diesel Engine. In. SAE International.
- Sautermeister, F. 2012. *Piston Ring Lubrication - Influence of Sulphuric Acid Formation From High Sulphur Content Fuel*. Doctor of Philosophy thesis, University of Leeds.
- Schwalb, J.A. 1991. *Wear Mechanism and Wear Prevention in Coal-Fueled Diesel Engines Task III: Traditional Approaches to Wear Prevention*. San Antonio, Texas, USA: Southwest Research Institute.

- Sendilvelan, R. and Anandanatarajan, S. 2016. Controlling Silicon and Soot Content in the Crank Case Oil to Improve Performance of Diesel Engine. *Global Journal of Research In Engineering*.
- Shackelford, J. and Alexander, W. 2001. Mechanical Properties of Materials. In: Shackelford, J. and Alexander, W. eds. *CRC Materials Science and Engineering Handbook*. Third ed. Boca Raton, US: CRC.
- Shameer, P.M. and Ramesh, K. 2017. Experimental evaluation on performance, combustion behavior and influence of in-cylinder temperature on NO_x emission in a D.I diesel engine using thermal imager for various alternate fuel blends. *Energy*. **118**, pp.1334-1344.
- Shehata, M.S. and Razek, S.M.A. 2011. Experimental investigation of diesel engine performance and emission characteristics using jojoba/diesel blend and sunflower oil. *Fuel*. **90**(2), pp.886-897.
- Soloiu, V.Lewis, J.Yoshihara, Y. and Nishiwaki, K. 2011. Combustion characteristics of a charcoal slurry in a direct injection diesel engine and the impact on the injection system performance. *Energy*. **36**(7), pp.4353-4371.
- GDP per capita (current US\$)*. 2018a. [Online database]. Washington DC, USA: The World Bank.
- Pump price for diesel fuel (US\$ per liter)*. 2018b. [Online database]. Washington DC, USA: The World Bank.

Chapter 8: Energy and economics

8.1 Introduction

The main barrier to the uptake of any new energy technology in developing countries is cost. Unlike developed countries which are aiming to reduce greenhouse gases and pollutants for environmental reasons and would pay a premium for it, in developing countries the choice is more basic- the cheaper, the better. In Nepal, for example, the GDP per capita is US\$2,700 and is less in rural areas of the country where the lack of electricity is an issue (Central Intelligence Agency, 2017). Therefore, the cost is a major limiting factor.

Another concern beyond cost is the strain a system can place on the natural resources in an area. In the case of slurry fuels, the amount of woody biomass used per unit of electricity should be minimised to help preserve the important natural resource. If the system can use less biomass than other technological options, such as gasification, then slurry fuel technology could have an added benefit to rural communities in developing countries.

The chapter aims to address objective 8 of the thesis- to compare slurry fuel engines with other energy generation technologies used in developing countries. The most similar alternative to slurry fuels is gasification which uses biomass and converts it to a fuel suitable for internal combustion engines. Hence, if producing a slurry fuel can be a cheaper route to an engine fuel than gasification, then it may have a future as a general use fuel, rather than one for special circumstances, like an emergency back-up. Another important comparison to be made is between slurry fuel engines and a diesel generator as it could be cheaper to buy diesel rather than converting an engine generator and making a slurry fuel.

Also, another aim is to predict the amount of biomass needed through the process by Sankey diagrams. Gasification and slurry fuels are compared on the basis of the amount of biomass used during each part of the process from fuel production to electricity generation.

8.2 Energy requirements for the production of electricity with a slurry engine

Figure 8-1 shows the energy flow through the laboratory scale slurry fuels process demonstrated in this thesis. The energy efficiency of the pyrolysis process was assumed to be 22%. The efficiency of traditional earth pit kilns, the oldest and one of the most popular methods today, have an efficiency in the region of 10-22%, therefore the value represents the upper limit (Adam, 2009). The overall efficiency of the slurry fuel process from harvesting of biomass to producing electricity was found to be 1.3%. The energy lost during the pyrolysis

process is the most significant, meaning that investment in a high-quality retort would be particularly beneficially to the overall sustainability of the system. The added benefit of purchasing a more efficient retort is that the charcoal making reactor is useful for other processes in developing countries. The most important is fuel for cooking which would require less time spent harvesting branches if a more efficient retort was used.

The electricity needed for the mill is 0.75MJ to produce 1MJ of electricity, which is most of what the engine produces. To produce this electricity, more charcoal needs to be made, milled and burned in the slurry engine to yield a net of 1MJ. The wet ball milling process, therefore, is consuming most of the electricity the engine is creating from the char.

The engine generator used had a low efficiency compared to many models available. Being the final process means there is a knock-on effect that more fuel is needed, therefore more pyrolysis and milling is needed. The efficiency attainable by the diesel engine in a developing country scenario may be limited to what is already available in the area, as a brand new model is likely too expensive. Using older engines would have a negative effect on efficiency but the greater tolerances might make them more resilient to slurry fuels.

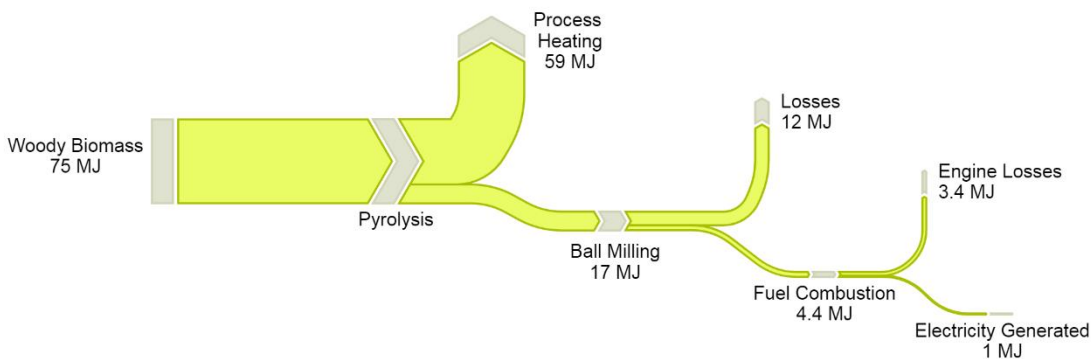


Figure 8-1 Sankey diagram showing input energy and losses associated with producing 1MJ net of electricity via an engine slurry generator. Note: The energy required for pyrolysis is based on the typical efficiency of a traditional earth pit kiln ($\eta=22\%$).

Figure 8-2 is a Sankey diagram showing the best practice found through a review of literature for producing electricity from a char-slurry fuel. The overall efficiency which was estimated to be achievable was 10.7%. The efficiency of the pyrolysis process was assumed to be 48% which was found by Adam (2009) using a low-cost retort kiln. It was also stated that common retort kilns have an efficiency of 35-40%. Improving this part of the process roughly halves the amount of woody biomass needed to produce electricity through char-slurries, compared to traditional earth pit kilns. Improving the pyrolysis process is therefore vital to sustainability. Furthermore, retort kilns produce a more homogeneous product through a more controlled process compared to earth pit kilns, which is also advantageous because the quality of charcoal in slurries must be strictly controlled (Adam, 2009).

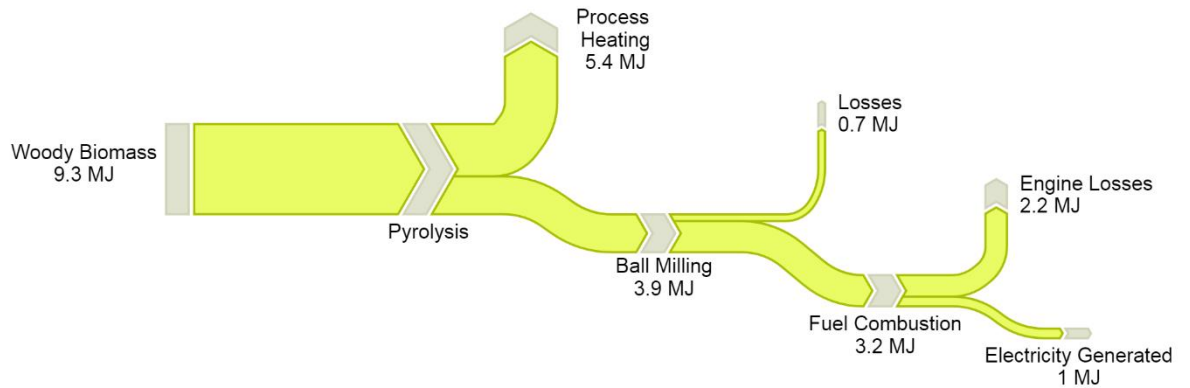


Figure 8-2 Sankey diagram for the production of electricity using a slurry engine based on the best practice processes in literature which are feasible in a developing country.

There is a significant improvement possible in the energy requirements as there is high scalability in the milling processes. Also, the wet ball mill used for the milling studies in the thesis is smaller than what would be used in a real-life situation. Only 1L of fuel could be made at a time, which is not enough to keep up with the rate it is being used. Cui et al. (2008) used wet ball milling to make a coal-water slurry with a size distribution suitable for an engine, consuming 442kWh t^{-1} . The amount of energy needed for the process in terms of electricity is 0.18MJ or 0.7MJ of woody biomass converted to electricity via a slurry fuel, still a significant proportion of the electricity being generated. It should be noted that the energy requirement from Cui et al. (2008) is based on coal and thus the energy for milling char could be different. The type of char will also affect this value. In this example, milling accounts for 7.5% of the total energy input.

Soloiu et al. (2011) used a char-diesel slurry at 31% efficiency which is used for the engine efficiency value in the Sankey diagram in figure 8-2. The losses in the engine generator account for 23.7% of the total energy input.

The main limiting factor in terms of efficiency remains the pyrolysis stage which is energy intensive. Wet ball milling can feasibly produce particles small enough for a slurry fuel without significant energy expense.

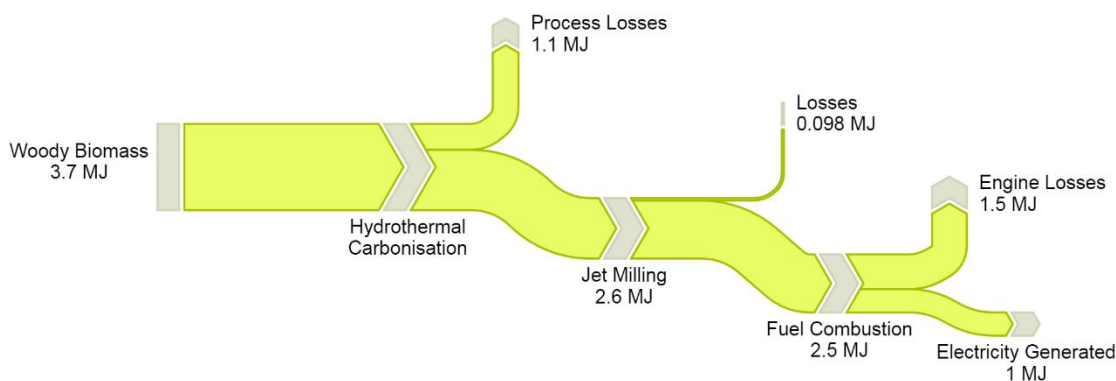


Figure 8-3 Sankey diagram based on all available technologies for running a slurry engine for electricity generation.

The best possible conversion efficiency of biomass to electricity via a slurry engine is estimated to be 27%. To maximise the amount of char which can be produced, hydrothermal carbonisation should be used instead of pyrolysis. The engine tests in the thesis showed that hydrochars burn better than pyrolysis chars which is an additional benefit. Figure 8-3 shows a Sankey diagram of the flow of energy from feedstock to electricity being produced in the most efficient scenario. The efficiency of the hydrothermal carbonisation process was assumed to be 70% which was found by Lucian and Fiori (2017) for the production of hydrochar from grape pomace at 250°C. The efficiency includes drying which may not be necessary as the mixture could be directly micronised. The hydrothermal carbonisation efficiency found was similar to other studies (Kim et al., 2015; Oh and Yoon, 2017). Lucian and Fiori (2017) also found that reducing the process temperature to 220°C improved the efficiency to 78%. As hydrochar produced at this temperature was not assessed for grindability it is unknown if it is suitable for slurrying.

The maximum efficiency found in literature for slow pyrolysis was 90-95% from a reactor made by Carbon Terra (Gustafsson, 2013). However, only 60% of the input energy remains in the char, with an additional 30% in the pyrolysis gas produced. If this was substituted with hydrothermal carbonisation in the model, it was assumed that the pyrolysis gas could be used elsewhere, and only the 5-10% loss was considered, then the overall efficiency would be 34.6%. Another option would be to dual fuel the engine with pyrolysis gases produced during the carbonisation stage.

By using jet milling demonstrated by Cui et al. (2008), the energy consumption can be further reduced to almost negligible levels. The Hardgrove Grindability Index (HGI) is usually higher for hydrochars produced at 250°C than coal, thus the energy expenditure might be even less than shown in figure 8-3 (Smith et al., 2018).

The more efficient carbonisation process means that the biggest energy loss occurs in the engine combustion stage of the slurry fuel process. The efficiency of the engine was assumed to be 40%, which is in the typical range for large stationary engines and was the value used in a techno-economic study of coal-water slurries by Red'kina et al. (2013). However, the overall generation efficiency of using coal-water slurries in a 50MWe engine has been estimated by others to be as high as 48.1% based on the higher heating value of the fuel (Nicol, 2014). Wilson (2007) suggested the target generation efficiency for slurry engines is 45% for 14MW+ engines and 40% for smaller engines. If 48.1% efficiency were possible and a highly efficient pyrolysis reactor was used with 90% efficiency, then the overall efficiency of using woody biomass as a slurry fuel would be as high as 41.5%. With the utilisation of modern carbonisation reactors and mills, then the technical limit for generation efficiency becomes engine technology and laws of thermodynamics.

The potential generation efficiency of an advanced char slurry engine compares well to some other technologies. Modern biomass steam turbines can reach approximately 25% efficiency (Jurado et al., 2003). Another potential modern biomass technology is a steam injection gas turbine which is estimated to reach 40% electrical generation efficiency at 51.4MW which is higher than the estimate for an advanced slurry fuel system in figure 8-3 but less than the efficiency target set by Wilson (2007) for slurry engines (Larson and Williams, 1990). However, if the capital cost of a slurry engine power plant was significantly less, it could still have a place in the electricity mix.

8.3 Energy requirements for producing electricity through an engine gasification alternative

In developing countries, the most comparable technology to slurry engines is gasification which some engines have been converted to run using. Some systems use gas engines connected to a gasifier which can run purely on syngas. Others use diesel engines which are dual fuelled, often for the convenience of operation. Figure 8-4 shows a typical small-scale gasifier system fuelling a diesel engine. Systems usually use downdraft gasifiers which produce a fuel containing less tar which can cause deposits in the engine. Before the syngas enters the engine, it passes through cyclones to remove ash, condensers to improve fuel density and filters to remove tar.



Figure 8-4 An example of a diesel generator converted to run on syngas.

Table 8-1 shows a review of gasification engine systems and the electricity generation efficiency found. There are two key areas to optimise: firstly is the cold gas efficiency, which is the ratio of energy in the fuel into the gasifier to the energy in the gas being produced (Lee et al., 2017). It does not account for the heat energy in the gas produced. The review shows that 65-70% is the typical cold gas efficiency of gasifiers used in systems with a similar output to that of the engine generator used in chapter 6 and 7. The cold gas efficiency varies between 38.6-82% in the literature which is a large discrepancy. Considering in developing countries there is less technical expertise than is available for lab tests, the cold gas efficiency could be significantly lower than 65% in real-world applications. Producing a consistent quality of syngas, especially during start-up is an issue which will cause a variation in engine thermal efficiency (Zainal et al., 2002).

The second area to optimise is the engine thermal efficiency. Only one study in table 8-1 reports higher engine thermal efficiency than was found by Soloiu et al. (2011) using a 25%wt charcoal-diesel slurry. The average thermal efficiency of the tests in table 8-1 is 22.8%, which is similar to what was found using a 10%wt. charcoal diesel slurry in chapter 7 of 22.6%. Chaves et al. (2016) achieved an engine thermal efficiency of 16.5% using the most similar in size engine to the one used in this study. The efficiency of using syngas in a gas engine is generally low for two reasons. Firstly, spark ignition engines are less efficient than diesel engines which are used for slurry fuels. Secondly, the low calorific value of syngas reduces the efficiency the engine can achieve because the combustion temperature decreases (Indrawan et al., 2017; Kan et al., 2018).

Table 8-1 Efficiency reported of engine gasifier systems.

Study	Fuel	Cold gas efficiency (CGE) (%)	Engine thermal efficiency (%)	Total efficiency (%)	Notes
<i>Ding et al. (2018)</i>	Carbonised pellets	38.6-45.6	27.8	10.7-12.7	30kW gas engine used.
<i>Elsner et al. (2017)</i>	Sewage/wood pellets blend	69	29.0	20	Large, 75kWe maximum electrical power output
<i>Zainal et al. (2002)</i>	Wood, charcoal	67-82	10-22	8-15	65kW gasifier. Better CGE with charcoal.
<i>Hollingdale et al. (1988)</i>	Charcoal, coconut shell	60-71.2	30-32.8	19.7-21.2	20kW system
<i>Kotowicz et al. (2013)</i>	Wood chips	63	24.6	15.5	60kW system
<i>Chaves et al. (2016)</i>	Wood waste	70	16.5	11.6	5.5kWe system. Only 2.5KWe achieved with syngas.
<i>Boloy et al. (2011)</i>	Wood	69	18.6	12.8	20kW system
<i>Nhuchhen and Salam (2012)</i>	Wood	69.2	20.1	13.9	Dual fuel system 10 kWe output achieved.

Another practical issue is that the low calorific value of syngas limits the maximum power output for a given engine displacement compared to slurry fuels which can still be used to run engines at the maximum output. Typical de-rating for a gas engine running on syngas is 20-35% (Indrawan et al., 2017). System operating dual-fuel diesel-syngas also experience a reduction in thermal efficiency with increasing syngas ratio (Mahgoub et al., 2015).

The choice of fuel for gasification is important. The main criterion is that the feedstock material has low moisture, which harms the cold gas efficiency. The articles reviewed in table 8-1 generally used wood or charcoal. The reason for using charcoal is to reduce the amount of tar formed which, even when using a downdraft gasifier with after treatment, can cause issues. Hollingdale et al. (1988) encountered issues with tar when using wood blocks in a downdraft reactor, but less with charcoal or coconut shell. Additionally, charcoal was always used during the ignition procedure to prevent tar carry-over. Tar deposits had to be removed from the engine inlet manifold, valves and piston crown after 360 hours and 124 hours of operation on charcoal and coconut shell respectively. The feasibility of using materials without prior pyrolysis is questionable and affects the overall suitability of gasification engines in developing countries. Need for regular maintenance may be difficult in developing countries

where little mechanical expertise is available. Systems may end up lying dormant for long periods while they are fixed.

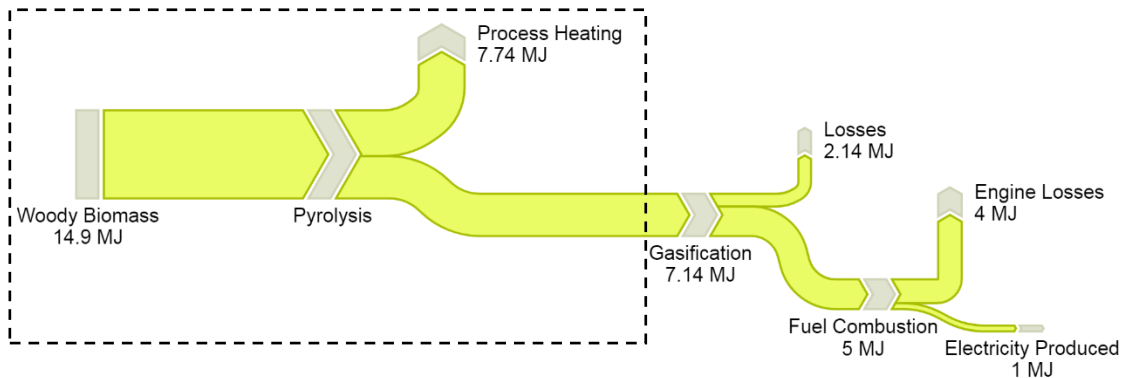


Figure 8-5 Sankey diagram showing the energy flow for producing electricity through an engine gasifier system. In the dotted box is the energy flow during pyrolysis, a pre-treatment to gasification which is not necessarily needed.

Figure 8-5 shows a Sankey diagram of a gasifier system based on the previous studies in table 8-1. Cold gas efficiency was assumed to be 70% and engine efficiency to be 20%, which are typical from the previous studies. The overall efficiency of the system in figure 8-5 is therefore 14% which is similar to the average in table 8-1 of 14.6%. In the dotted box in figure 8-5, is the pyrolysis process which is potentially needed to prevent tar problems. If used, the overall efficiency is reduced by over half. Compared to the slurry best practice in figure 8-2, the efficiency is lower for a gasification system if a pyrolysis pre-treatment is used- 6.7% vs. 10.8%. Without the need for pyrolysis before gasification gives a better efficiency than the best practice slurry engine by 3.2%.

The energy efficiency of possible gasification systems and slurry engines suitable for microgeneration in developing countries are in a similar range. The preference between systems would likely consider more practical issues like what maintenance is needed, costs, equipment and feedstocks available.

8.4 Projected cost of microgeneration systems

The cost of generating electricity by conversion of a diesel generator to use either char slurries or syngas was assessed. Table 8-2 shows the assumptions made in the model for the cost of the two systems and an unmodified generator for comparison. The assumptions for costs were taken from previous studies. It should be noted that few studies exist for the cost of slurry engines and certainly not for the size, 10kW, being investigated. The cost of electricity is based on the amount needed to break even after five years from the initial investment.

Table 8-2 Economic model assumptions for a 10kW system.

<i>Parameter</i>	<i>Cost</i>	<i>Source</i>
<i>Genset</i>	US\$5000-7000	A cost estimate based on gensets on sale.
<i>Slurry engine equipment. Mill, retort, modification</i>	\$2794-7794	Chapter 5 of the thesis, Cost of retort (Adam, 2005), and additional cost for a slurry engine estimated to be 47% more than a standard engine. (Wilson, 2007).
<i>Gasifier and cleaning systems</i>	\$3750-12250	\$500/kW for 500kW gasifier (Susanto et al., 2018), \$1000/kW for 100kW gasifier engine system (Fracaro et al., 2011), \$784-1869/kW for less than 30kW system (V. Siemons, 2001), and \$1000/kW for small systems (U.S. Congress Office of Technology Assessment, 1992).
<i>Cost of diesel</i>	0.89-1.13\$/kg	Based on the cost in Nepal in the last five years (Nepal Oil Corporation Limited, 2018).
<i>Cost of biomass</i>	0-0.045 \$/kg	Significant differences. 0.045\$/kg (Susanto et al., 2018). 0.0004\$/kg (Si, 2018).
<i>Surfactant cost</i>	0.06-0.12 \$/kg char	Estimate in Wilson (2007).
<i>Unskilled/skilled labour</i>	7.8/9.25 \$ per day	Based on minimum wage in Delhi, India (Govt. of NCT of Delhi, 2017).
<i>The capacity factor of the generator</i>	0.25-0.75	Estimate based on assumptions about times energy is needed.
<i>Diesel engine efficiency</i>	31%	From Soloiu et al. (2011).
<i>Gas engine efficiency</i>	20-25%	Table 8-1
<i>Cold gas efficiency</i>	65-70%	Table 8-1
<i>Pyrolysis efficiency</i>	30-48%	From Adam (2009).
<i>Milling energy</i>	5% of charcoal energy	From Cui et al. (2008) and investigation in chapter 5.
<i>Maintenance</i>	1-3% of the initial cost	From Wilson (2007). Factor commonly used in other studies
<i>Maintenance for slurry engine</i>	2.7-7.4% of engine cost	Wilson (2007) estimated maintenance cost to be 178% more than an engine running conventional diesel.
<i>Maintenance of gasifier system</i>	2-5% of gasification system cost	Low estimate. Studies predict maintenance can be anywhere between 3-10%. (Brown et al., 2009; Nouni et al., 2007; Si, 2018; Susanto et al., 2018; Tripathi et al., 1999).

Continuous labour was assumed to be required for both the slurry and syngas systems, but not for the diesel generator which can be started and left to operate unattended. Gasifiers, on the other hand, must be regularly stoked with biomass. They also need regular, ongoing maintenance and checked to ensure that the quality of syngas is good. For these reasons, it was assumed to be operated by one skilled and one unskilled employee.

Char slurry fuel systems also need people to operate the engine and make the fuel. Three days of skilled labour were assigned for the production of charcoal and conversion to the slurry per load created in a retort. It was also assumed that the generator was operated by an unskilled employee as operation tasks are simpler than with gasification systems. Another reason why fewer people are needed to run the slurry system is, once the fuel is produced, it can theoretically be used like any other liquid fuel.

Figure 8-6 shows the projected cost of electricity for several types of biomass engine system which could be used versus capacity factor. Under certain conditions, producing 20% of the total energy from char in a diesel generator could be economical compared to using diesel (figure 8-6a). For 20% char by energy to be economical it is predicted that the capacity factor must be at least 40%. Producing 50% of the electricity from char is expected to be more economical than 20%. The minimum capacity factor of the generator which is needed to justify conversion of a diesel generator to a 50% slurry fuel system is 27%. It is projected that using a char-water slurry system could nearly half the cost of electricity compared to using diesel only if the capacity factor is high. As there are currently no systems in demonstration, there is high uncertainty as to the viability of producing electricity from slurries, shown by the large bars in figure 8-6a.

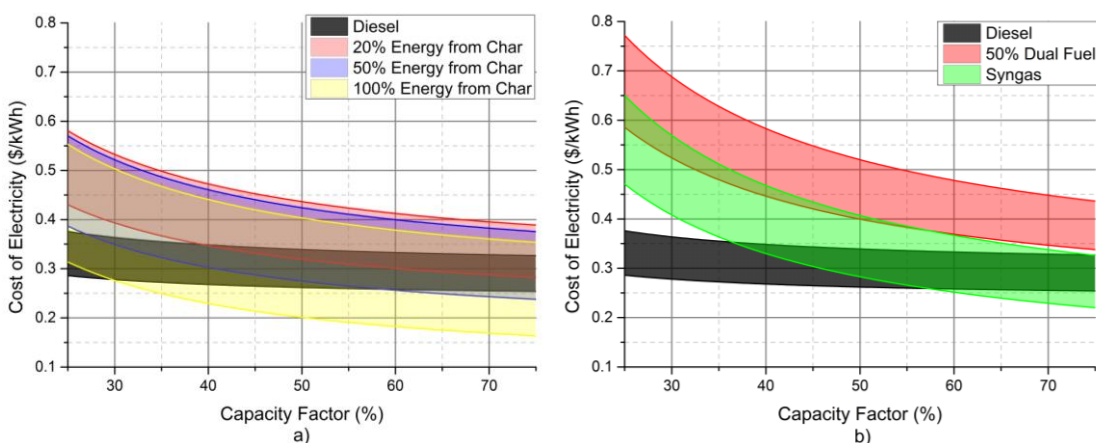


Figure 8-6 Estimated cost of electricity for diesel engine conversions to biofuels. a) Char slurry fuels, and b) gasification systems.

An alternative to char slurries for an engine fuel is syngas from gasification. Two potential systems are compared to diesel in figure 8-6b. Dual fuelling with 50% syngas and diesel is projected, with such a small generator system, to never be economical compared to using diesel. This is because the labour requirement is high to operate. It is also why, at low capacity factors, the cost of electricity is expensive from gasification systems. Producing electricity via 100% syngas becomes potentially viable at a capacity factor of 36% based on the usual cost of diesel. Based on previous studies, it is expected that using a syngas generator over a diesel version would be cheaper at high capacity factors. The current information suggests that more savings could be made using a 100% char slurry system than a gasification system. However, the upper prediction suggests that a syngas system could be cheaper than slurry systems in some instances.

Another potential cost advantage of using slurry fuels instead of gasification as a thermochemical conversion route is economies of scale. Gasification systems require syngas to be produced next to and fed directly to the engine. Slurry fuels, however, can be made at an alternative site and distributed to the point of use. This means that a single, large pyrolysis and slurrying site close to the location of suitable feedstock could be used, then distributed to generators in different micro-grids.

Figure 8-7 shows the estimated cost breakdown of a kWh of electricity produced by several methods for a 10kW system operating at a capacity factor of 75%. Figure 8-7a is the breakdown for a conventional, diesel-powered generator. The majority of the cost occurs from the purchase of the fuel used to power the engine. This means the affordability is strongly determined by fluctuating oil markets and local distribution networks. The cost of the generator and its maintenance is small in comparison which suggests it may be beneficial to spend more on a more efficient generator to save diesel.

The cost breakdown of the dual fuel system using char and diesel in figure 8-7b shows over half of the total cost of the electricity is associated with the cost of the fuel used. The need for operators to produce the fuel and keep the engine running is a significant cost also. Creating a system which is reliable enough to need less supervision or scaling up the pyrolysis and slurrying process, reducing the time to produce the fuel would be particularly beneficial to the electricity cost.

The proportion of the cost of electricity produced associated with the fuel materials is reduced but is still significant in a 100% char powered system shown in figure 8-7c. The cost of the fuel is roughly split 50:50 between the biomass and the surfactants used. The largest proportion of the cost is estimated to be from the operators needed. The cost of electricity produced

associated with the initial capital investment for the equipment, and maintenance is still low compared to other costs but would be higher if the capacity factor was reduced.

The cost breakdown of the gasification engine in figure 8-7d estimates the most significant cost to be for the operators. The fuel cost is significantly less than the other three options because no diesel or surfactants are needed, and the biomass used does not need to be treated by pyrolysis, which increases the amount of fuelwood needed. If the gasification system needs pretreatment of the feedstock by pyrolysis, then the fuel cost would be roughly double, which has the potential to notably raise the cost of the electricity production. The initial capital cost of the gasification system is estimated to be the highest and so ensuring a long lifespan of the equipment is important.

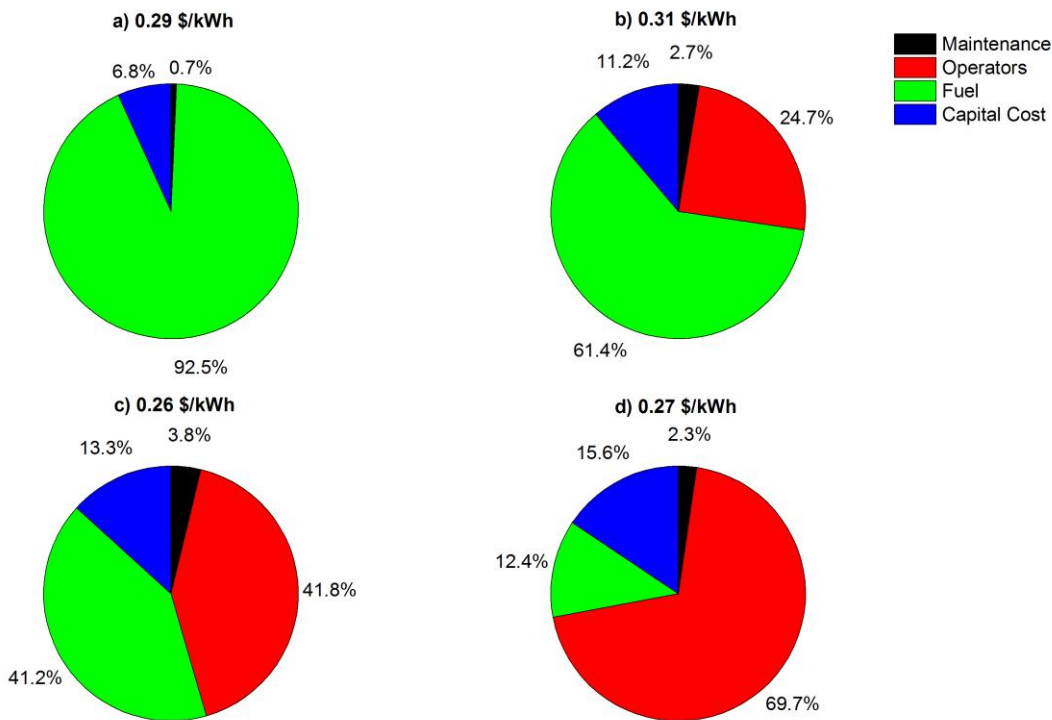


Figure 8-7 Cost breakdown of electricity produced by 10kW, operating at a capacity factor of 75%. a) Generator using diesel, b) A slurry fuel system achieving 50% of energy from char, c) A fully char powered slurry engine system, and d) A 100% gasification engine generator.

The cost of biomass in developing countries is usually low, or potentially free if a community has control of suitable resources, like in Nepal where much of the forests are managed by community forestry user groups (CFUGs). One of the main costs of the slurry fuel will be the cost of the surfactants used to improve stability and viscosity. Figure 8-8 shows the variation in the cost of electricity generation against the cost of surfactant used. The capacity factor was set at 75% for a 10kW system. In a system where 50% of the energy comes from the addition of charcoal, then it is predicted that the cost of the surfactant should be kept to below 0.155

\$/kg of char used to remain economical. This would be the case when diesel prices are comparatively high, roughly 1.13\$/kg, represented by the top horizontal black line in figure 8-8. For the worst-case scenario, when diesel is cheap, shown by the lower horizontal black line, even with no surfactant used, a 50% charcoal system might not be cost effective because of the high setup costs. Based on the margin of error, for systems achieving 50% of electricity from charcoal, the cost of the surfactant must be no more than 0.11\$/kg of char when diesel costs less than 0.89\$/kg. To be economical, the system would have a low maintenance cost and initial capital cost.

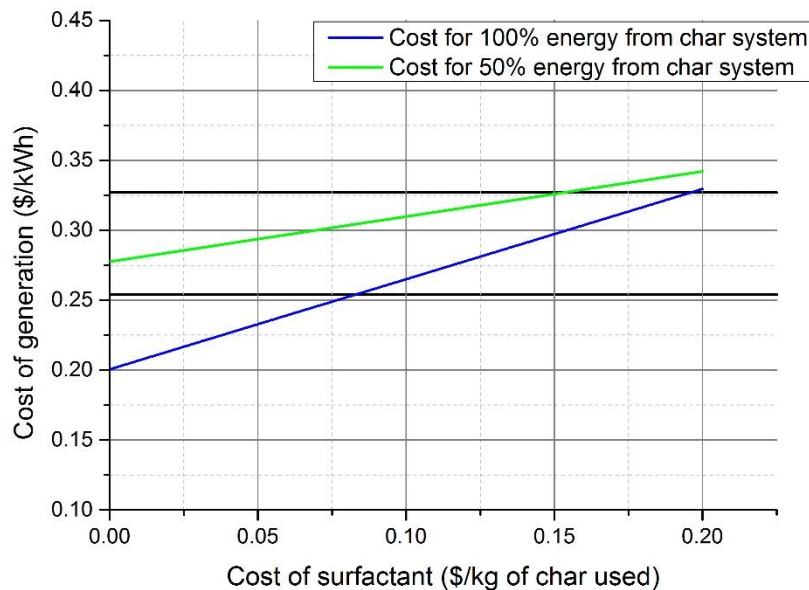


Figure 8-8 Cost variation of electricity generated versus the cost of surfactant used for the slurry. 75% capacity factor system. Horizontal lines project the predicted cost for operating a diesel only generator system. The diesel cost represented by the top and bottom line is 1.13 and 0.89\$/kg respectively.

A system which achieves 100% of energy from charcoal can use more surfactant per kilogram of char than a system that still uses some diesel. It is estimated that for high diesel prices, the surfactant cost should be below 0.195\$/kg to make the conversion of a diesel generator to slurry fuels profitable. For periods when diesel is cheap, roughly 0.89\$/kg then the cost of surfactant should be kept to below 0.08\$/kg of char.

Wilson (2007) estimated surfactants cost 0.06\$/kg of coal in coal-water slurries which suggests that achieving a surfactant cost of 0.08\$/kg of char is achievable. Furthermore, it shows that achieving a cost-effective surfactant mix for slurry fuels when the diesel price is high is a realistic possibility. The required cost of surfactants used in systems where 50% of the energy comes from char is lower than for the 100% system, thus 50% char systems are only possible when the cost of diesel is high.

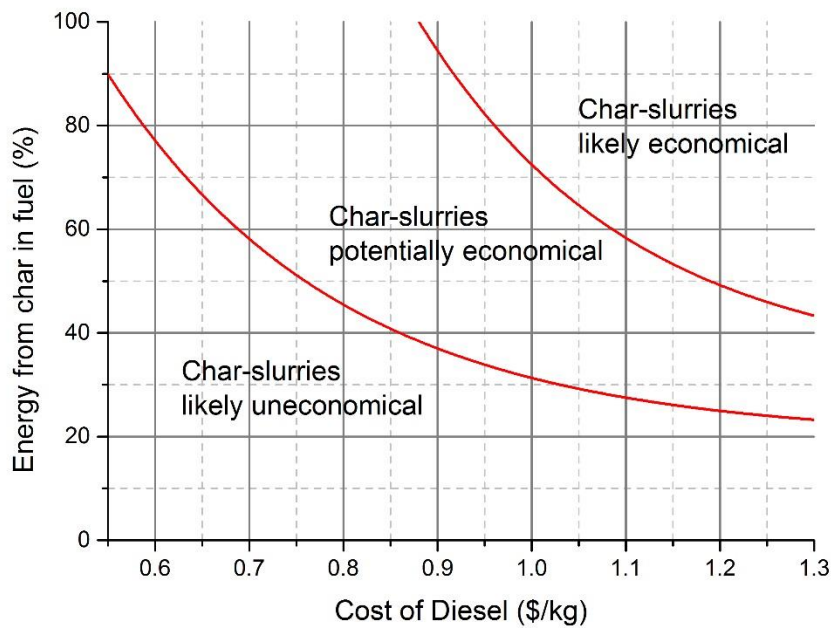


Figure 8-9 Prediction of the economic feasibility of slurry fuel generation systems based on the cost of diesel and the proportion of char used to create electricity.

Figure 8-9 shows a prediction of the economic feasibility of converting a diesel generator to handle char slurries based on the price of diesel. Higher proportions of char used instead of diesel means that there is more opportunity for making cheaper electricity, but more technical barriers to overcome. In figure 8-9 it is predicted that 100% char slurry systems (i.e. char-water slurries are solely used) are potentially economical across the full range of realistic diesel prices. 100% char systems are likely to be feasible in regions where the cost of diesel is over 0.88\$/kg (0.73\$/L). At the other end, small 10kW systems using 20% charcoal or less on an energy basis of the fuel used are unlikely to be economical. Systems operating using char-diesel slurries which can potentially reach 50%wt. of char and 35% on an energy basis, may be economical when the cost of diesel is over 0.925\$/kg. Between 35% and 100%, char systems could be run in a number of ways. They could be char-water slurry engines with a diesel pilot injector to initiate combustion. Emulsion fuels could also be produced whereby diesel or another fuel is added to a char-water slurry.

As of August 2018, a number of developing countries have a diesel price which suggests that using slurry fuels would be economical. Table 8-3 shows the current diesel price per kilogram is in the region of \$0.9-1.2 which is estimated in figure 8-9 to likely make 50-100% charcoal powered slurry engine systems economical. One exception is Nigeria, which has a low price because it is an oil producing country. Still, 100% charcoal powered engine systems may be economical. Rwanda, Tanzania and Uganda are neighbouring countries in East Africa, all of which have high-cost diesel making the region a possible location for slurry fuel production.

The Indian sub-continent containing Bangladesh, India and Nepal is another area where an economic benefit could be achieved with slurry fuels.

Table 8-3 Cost of diesel in a number of developing countries as of August 2018 (GlobalPetrolPrices.com 2018).

<i>Country</i>	<i>Cost of Diesel (US\$/kg)</i>
<i>Bangladesh</i>	0.94
<i>India</i>	1.23
<i>Indonesia</i>	0.91
<i>Nepal</i>	1.00
<i>Nigeria</i>	0.69
<i>Rwanda</i>	1.51
<i>Tanzania</i>	1.20
<i>Uganda</i>	1.20

8.5 Conclusions

Energy efficiency analysis using Sankey diagrams showed the amount of woody biomass needed to produce 1MJ of electricity using best practice in developing countries is 9.3MJ. This is larger than the amount needed for gasification which is 7.14MJ, providing pretreatment of the biomass used in gasification is not needed. If pyrolysis is needed before gasification, then the amount of biomass needed for 1MJ of electricity is 14.9MJ, 60% more than estimated for slurry systems. The optimum slurry system, incorporating advanced milling, hydrothermal carbonisation and an efficient engine could need just 3.7MJ of woody biomass to produce 1MJ of electricity. The key benefit is the reduction in losses during the thermal pretreatment.

The cost of 10kW char slurry systems is predicted to be competitive or cheaper than either diesel generators or gasification systems in developing countries. Slurry systems receiving 50-100% of the energy from char are likely to be economical based on the current cost of diesel in developing countries. Slurry fuels incorporating just 20% char on an energy basis or unlikely to be economical so are perhaps best as an emergency fuel, a way of bulking out the available diesel with cheaper char.

The target price for a surfactant mixture for char-water slurries is below 0.195\$/kg of char in areas where the cost of diesel is relatively high at 1.13\$/kg which is more than achievable based on previous studies. In systems where 50% of energy is derived from char, the rest coming from using diesel, the surfactant must be cheaper at 0.155\$/kg of char. In places and at times where diesel is cheap at 0.89\$/kg, the cost of using 50% energy from char slurry systems is predicted to be higher than using an unmodified engine running on diesel, regardless of the cost of the surfactants used in the mixture. In the case of a low diesel price at 0.89\$/kg, pure char-water slurry systems can be economical given the surfactant price is kept to below 0.08\$/kg of char which can also be achieved based on previous work.

8.6 References

- Adam, J.C. 2005. Improved charcoal production saves energy. *Appropriate Technology*. **32**(4), pp.63-64.
- Adam, J.C. 2009. Improved and more environmentally friendly charcoal production system using a low-cost retort–kiln (Eco-charcoal). *Renewable Energy*. **34**(8), pp.1923-1925.
- Boloy, R.A.M.Silveira, J.L.Tuna, C.E.Coronado, C.R. and Antunes, J.S. 2011. Ecological impacts from syngas burning in internal combustion engine: Technical and economic aspects. *Renewable and Sustainable Energy Reviews*. **15**(9), pp.5194-5201.
- Brown, D.Gassner, M.Fuchino, T. and Maréchal, F. 2009. Thermo-economic analysis for the optimal conceptual design of biomass gasification energy conversion systems. *Applied Thermal Engineering*. **29**(11), pp.2137-2152.
- Central Intelligence Agency. 2017. *Country Comparison: GDP- Per Capita (PPP)*. [Online]. Available from: <https://www.cia.gov/library/publications/the-world-factbook/rankorder/2004rank.html>.
- Chaves, L.I.da Silva, M.J.de Souza, S.N.M.Secco, D.Rosa, H.A.Nogueira, C.E.C. and Frigo, E.P. 2016. Small-scale power generation analysis: Downdraft gasifier coupled to engine generator set. *Renewable and Sustainable Energy Reviews*. **58**, pp.491-498.
- Cui, L.An, L. and Jiang, H. 2008. A novel process for preparation of an ultra-clean superfine coal–oil slurry. *Fuel*. **87**(10), pp.2296-2303.
- Ding, L.Yoshikawa, K.Fukuhara, M.Kowata, Y.Nakamura, S.Xin, D. and Muhan, L. 2018. Development of an ultra-small biomass gasification and power generation system: Part 2. Gasification characteristics of carbonized pellets/briquettes in a pilot-scale updraft fixed bed gasifier. *Fuel*. **220**, pp.210-219.
- Elsner, W.Wysocki, M.Niegodajew, P. and Borecki, R. 2017. Experimental and economic study of small-scale CHP installation equipped with downdraft gasifier and internal combustion engine. *Applied Energy*. **202**, pp.213-227.
- Fracaro, G.P.M.Souza, S.N.M.Medeiros, M.Formentini, D.F. and Marques, C.A. 2011. Economic feasibility of biomass gasification for small-scale electricity generation in Brazil. In: *World Renewable Energy Congress 2011, Sweden*. Bioenergy Technology, pp.295-302.
- GlobalPetrolPrices.com 2018. *Diesel prices, liter*. [Online]. [Accessed 18/08/2018]. Available from: https://www.globalpetrolprices.com/diesel_prices/.
- Govt. of NCT of Delhi. 2017. *Labour Department Notification*. [Online]. Available from: http://www.delhi.gov.in/wps/wcm/connect/doi_labour/Labour/Home/Minimum+Wages/.
- Gustafsson, M. 2013. *PYROLYSIS FOR HEAT PRODUCTION Biochar – the primary byproduct*. Masters in Energy Systems thesis, University of Gävle.
- Hollingdale, A.C.Breag, G.R. and Pearce, D. 1988. *Producer gas fuelling of a 20kW output engine by gasification of solid biomass (ODNRI Bulletin No. 17)*. University of Greenwich.
- Indrawan, N.Thapa, S.Bhoi, P.R.Huhnke, R.L. and Kumar, A. 2017. Engine power generation and emission performance of syngas generated from low-density biomass. *Energy Conversion and Management*. **148**, pp.593-603.
- Jurado, F.Cano, A. and Carpio, J. 2003. Modelling of combined cycle power plants using biomass. *Renewable Energy*. **28**(5), pp.743-753.
- Kan, X.Zhou, D.Yang, W.Zhai, X. and Wang, C.-H. 2018. An investigation on utilization of biogas and syngas produced from biomass waste in premixed spark ignition engine. *Applied Energy*. **212**, pp.210-222.
- Kim, D.Yoshikawa, K. and Park, K. 2015. Characteristics of Biochar Obtained by Hydrothermal Carbonization of Cellulose for Renewable Energy. *Energies*. **8**(12), p12412.
- Kotowicz, J.Sobolewski, A. and Iluk, T. 2013. Energetic analysis of a system integrated with biomass gasification. *Energy*. **52**, pp.265-278.
- Larson, E.D. and Williams, R.H. 1990. Biomass-Gasifier Steam-Injected Gas Turbine Cogeneration. *Journal of Engineering for Gas Turbines and Power*. **112**(2), pp.157-163.

- Lee, J.W., Lee, S.J., Jamal, Y. and Yun, Y. 2017. Partial slagging coal gasifier operational performance and product characteristics for energy sustainability in an integrated gasification combined cycle system. *Journal of the Energy Institute*.
- Lucian, M. and Fiori, L. 2017. Hydrothermal Carbonization of Waste Biomass: Process Design, Modeling, Energy Efficiency and Cost Analysis. *Energies*. **10**(2), p211.
- Mahgoub, B., Sulaiman, S. and Abdul Karim, Z.A. 2015. *Performance study of imitated syngas in a dual-fuel compression ignition diesel engine*.
- Nepal Oil Corporation Limited. 2018. *Selling Price Archive*. [Online]. Available from: <http://www.nepaloil.com.np/selling-price-archive-16.html>.
- Nhuchhen, D.R. and Salam, P.A. 2012. Experimental study on two-stage air supply downdraft gasifier and dual fuel engine system. *Biomass Conversion and Biorefinery*. **2**(2), pp.159-168.
- Nicol, K. 2014. *The direct injection carbon engine*. London, UK: IEA Clean Coal Centre.
- Nouni, M.R., Mullick, S.C. and Kandpal, T.C. 2007. Biomass gasifier projects for decentralized power supply in India: A financial evaluation. *Energy Policy*. **35**(2), pp.1373-1385.
- Oh, S.-Y. and Yoon, Y.-M. 2017. Energy Recovery Efficiency of Poultry Slaughterhouse Sludge Cake by Hydrothermal Carbonization. *Energies*. **10**(11), p1876.
- Red'kina, N.I., Khodakov, G.S. and Gorlov, E.G. 2013. Coal fuel slurry for internal combustion engines. *Solid Fuel Chemistry*. **47**(5), pp.306-314.
- Si, K.H. 2018. Cost Analysis and Economic Evaluation of Gasifier Engine and Conventional IC Engine. *International Journal of Science, Engineering and Technology Research*. **7**(7), pp.521-524.
- Smith, A.M., Whittaker, C., Shield, I. and Ross, A.B. 2018. The potential for production of high quality bio-coal from early harvested Miscanthus by hydrothermal carbonisation. *Fuel*. **220**, pp.546-557.
- Soloiu, V., Lewis, J., Yoshihara, Y. and Nishiwaki, K. 2011. Combustion characteristics of a charcoal slurry in a direct injection diesel engine and the impact on the injection system performance. *Energy*. **36**(7), pp.4353-4371.
- Susanto, H., Suria, T. and Pranolo, S.H. 2018. Economic analysis of biomass gasification for generating electricity in rural areas in Indonesia. In: *3rd ICChESA 2017*. Institute of Physics.
- Tripathi, A.K., Iyer, P.V.R. and Chandra Kandpal, T. 1999. Financial analysis of biomass gasifier based water pumping in India. *Energy*. **24**(6), pp.511-517.
- U.S. Congress Office of Technology Assessment. 1992. *Fueling Development: Energy Technologies for Developing Countries*. Washington D.C., USA: Government Printing office.
- V. Siemons, R. 2001. Identifying a role for biomass gasification in rural electrification in developing countries: the economic perspective. *Biomass and Bioenergy*. **20**(4), pp.271-285.
- Wilson, R. 2007. *Clean coal diesel demonstration project: Final report*. Cambridge, USA: TIAX.
- Zainal, Z.A., Rifau, A., Quadir, G.A. and Seetharamu, K.N. 2002. Experimental investigation of a downdraft biomass gasifier. *Biomass and Bioenergy*. **23**(4), pp.283-289.

Chapter 9: Conclusions

9.1 Summary

The overarching objective of the thesis was to investigate if char-diesel slurries are a viable fuel for electricity generation in developing countries. It was found that most woody biomass materials are suitable as long as they are low in ash, especially silicon and calcium. The majority of agricultural residues were found not to be suitable.

Using a 10%wt. char-diesel slurry in a high-speed diesel engine proved challenging. The main issue was with the fuel injector, which could get blocked with the fuel or seize, preventing the engine operating properly. Another problem was that when using a high ash char in a slurry, the cylinder liner wore away quickly until the engine would no longer work. It was found that a harder cylinder liner is needed for slurries. The 10%wt. char-diesel slurries burned poorly at low load, causing a drop in efficiency because the temperature inside the combustion chamber was too low to effectively burn the char particles. However, at the highest load tested the generation efficiency of using 10%wt. char-diesel slurries approached that of pure diesel. The hydrochar slurry tested was found to be more suitable than the pyrochar because the emissions were generally lower.

Economic analysis of slurry fuel systems for developing countries found that the engine generator would have to run on at least 20% char by energy to make the conversion economical. The estimated cost for a slurry fuel system was similar to the most relevant alternative, gasification.

9.1.1 Selection of char

Analysis of several potential biomass materials for conversion to slurry fuels showed that the most suitable is woody biomass that is low in ash. Analysis of some of the most common woody biomass in Nepal showed that some were more suitable for slurry fuels, such as *Eupatorium adenophorum*, *Pinus roxburghii* and *Shorea robusta*, but most are potentially useable. Nepal was found to be a nation with a large number of materials suitable for conversion to slurry fuels which means the nation could benefit from the technology. Another woody biomass *Rhododendron ponticum* sourced from the UK was also found to be suitable and was therefore used to produce slurry fuels for experiments.

Using agricultural residues is more problematic because of the high ash content, especially silicon, which is usually present. Analysis of agricultural residues in Nepal showed that only sugarcane bagasse was of similar quality as the woody biomass materials tested. The next best

were maize stems and cobs but would likely need an exceptionally durable diesel engine if used because silicon content was still comparatively high compared to woody biomass. Shea residue, a common agricultural waste in much of Africa was also studied and used. Whilst there were positives about the material, it had a high calorific value and high volatile matter, ultimately the wear it caused to the engine showed that the silicon content made it unsuitable.

A potentially novel feedstock is *Chlorella vulgaris*, the hydrochar from which may be suitable for slurry fuels. Silicon and calcium content in the hydrochar was similar to those derived from woody biomass produced under the same thermal process conditions. The main difference is that chlorella hydrochar contains magnesium, an element that can cause wear, which the other materials tested did not.

The most important trace elements in the biomass materials tested for determining their suitability for slurry fuels are silicon and calcium. Silicon is the second most abrasive element likely to be in biomass, after aluminium, but is usually more abundant. Calcium is important because it has medium abrasiveness and is often the most abundant trace element. To overcome the issues from ash content it might be worthwhile to strip bark from the biomass before use.

The structure of the chars produced is dependent on the thermal treatment used. The carbon structures in the hydrochars produced are less aromatic than pyrolysis chars. Aromatic carbon is associated with increased soot emissions from diesel engines. Another benefit of hydrothermal carbonisation is that lipids, which have a high calorific value, remain during the process whereas in pyrolysis they are carbonised to compounds which are poor for slurry fuels. The hydrochars produced have a lower recalcitrance, meaning that they begin to burn earlier in diesel engines and emit less soot than pyrochars. The emission results also showed that hydrochar slurries have a shorter ignition delay. However, the high proportion of volatile matter in hydrochars made them hard to micronise dry but milled well under wet conditions.

Pyrolysis as a thermal conversion route is more suitable for developing countries as it is already a method which is widely used. The optimum pyrolysis temperature for producing char for a slurry engine was found to be 400°C because it makes the material brittle enough to grind, retains some volatile matter, has a low recalcitrance for charcoal, and the low process temperature saves energy. Raising the pyrolysis temperature to 600°C improved grindability but means the fuel produced more particulates than the 400°C pyrochar when 0.1%wt. of char was added to diesel.

9.1.2 Using char slurries

Rhododendron char was added to diesel at three concentrations, 0.1, 1 and 10%wt.. Table 9-1 shows a summary of the percentage change in emissions at 3.5kW of power output from the diesel baseline. Generally, the addition of char decreases THC and NO₂ but increases particulates and NOx. At high concentrations of char, an increase in CO was found, but a decrease was found at concentrations of 1%wt. and below.

Table 9-1 Percentage change in emissions from adding rhododendron char to diesel at three different concentrations when the engine is operated at 3.5kW, the highest power achieved with the highest concentration of particles. The baseline for comparison used is diesel fuel with the surfactant concentration corresponding to the amount of char added.

Fuel		Temperature (°C)	CO (%)	THC (%)	Particle number (%)	NOx (%)	NO ₂ (%)
Hydrochar	0.1%wt.	250	1.2	-11.6	19.5	0.0	-10.3
	1%wt.	250	-30.4	-38.7	14.9	7.3	-81.0
	10%wt.	250	5.1	-17.2	55.1	2.7	-100.0
Pyrochar	0.1%wt.	400	-6.8	-24.4	21.7	-6.7	-17.4
		600	-20.6	-37.2	255.1	-7.0	-71.8
	1%wt.	400	-8.8	-43.0	27.1	1.9	-81.0
	10%wt.	400	7.9	-21.0	72.8	0.6	-100.0

There were differences in emissions depending on the type of char added. Pyrochars outperformed hydrochars in terms of THC emissions, and increasing the pyrolysis temperature reduced THC emissions when char was used as an additive at 0.1%wt.. However, at concentrations above 1%wt. and low engine loads, hydrochar slurries produced less THC than pyrochars because they burn better at lower temperatures. The CO emissions did not show a pattern depending on the type of char, but the effect of increasing the pyrochar temperature when 0.1%wt. was added was to reduce CO emissions. NOx concentrations were reduced with both pyrochars when added at 0.1%wt.. The most significant reduction was that of NO₂ emissions. This was further reduced when the pyrolysis temperature was increased. As NO₂ emissions reduce at high loads in a diesel engine anyway, the reduction in these emissions found when adding char at lower powers is more important. The reduction in NO₂ emissions was found to be greater when pyrochar was used over hydrochar. Particle number emissions increased significantly at all solid loadings. Increasing pyrolysis temperature more than tripled the particle number emissions, showing that minimising the pyrolysis temperature is beneficial.

The concentration of char in diesel had an effect on the percent change in emissions at 3.5kW. CO emissions decreased with respect to the baseline with loadings of 0.1 and 1%wt. and increased when 10%wt. was added. THC emissions were reduced by the most when 1%wt. was added to diesel. Particle number emissions increased by similar percentages at 0.1 and 1%wt. but underwent a marked increase when the solid loading was raised to 10%wt. The change in NO_x emissions with solid loadings was the lowest or negative at 0.1%wt. and was highest at 1%wt.. The NO₂ emissions consistently decreased with the addition of char of both types.

Both the carbon structure and elements contained in the ash have an effect on emissions. NO₂ emissions were found to be heavily influenced by the carbon structure, with a larger reduction occurring with increasing aromatisation. As a NO_x emissions reduction of similar intensity was found with rhododendron pyrochar at two different pyrolysis temperatures, it suggests that the trace elements are causing the effect because similar quantities are present in both instances. The reduction in NO_x occurred only with pyrochars at concentrations below 1%wt. When tested at 10%wt. solid loading, NO_x emissions increased because of increasing ignition delay. Particle number emissions increased with the degree of aromatisation, with hydrochars consistently producing less than pyrochars produced from the same feed material and at equal solid loadings. CO and THC emissions, caused by incomplete combustion are potentially affected by both the carbon structure and catalytic effects caused by the ash. CO caused by the incomplete combustion of char became more important to the overall emission as the solid loadings increased, affecting pyrochar slurries more. At lower solid loadings, the CO emissions could be reduced compared to the baseline possibly because of a catalytic effect with the trace elements in the ash. THC emissions were affected in a similar way to CO.

The investigation into using chars as additives to diesel for high-speed engines showed that 1%wt. was too much and could affect the smooth operation of the engine. Pyrochars had the greater benefit as an additive than hydrochars, reducing NO_x, THC and CO emissions. The main drawback was the increase in particle emissions. There was no notable positive effect found from adding char to biodiesel.

Benefits could be optimised by doping char and aiming to negate particulate emissions. Investigating even lower concentrations of char in diesel than 0.1%wt. may provide the same benefits but without the increase in particulates. Another option for producing char additives for diesel would be to use hydrothermal processes to produce nanoparticles which will cause fewer issues with sedimentation and blockages.

Producing a stable char-diesel slurry was challenging. The particles in the most stable 10%wt. char-diesel slurry remained in suspension for approximately 12.5 days but used a large amount of surfactant to do so, 1%wt.. As minimising the cost of the surfactant is important, ideally less should be used. For the engine tests using 10%wt. char in diesel slurries, 0.5%wt. lecithin was used as the surfactant which was sufficient. It may be better from an economic perspective to sacrifice the stability of the slurries for lower costs fuels, instead ensuring that the fuel remains constantly stirred when in use.

Adding char at 10%wt. to diesel for the direct injection, high-speed engine used proved difficult. Using a high silicon content char was catastrophic to the engine after just a couple of hours, meaning that in a real-life situation, accidentally choosing a poor fuel will ruin the equipment quickly. The issue caused by the poor char was wear to the cylinder liner which in the case of the engine used for tests, is not replaceable. It is therefore recommended that an engine with a replaceable cylinder liner is used and that a harder material than cast iron is chosen.

Another concern of using char as a fuel for diesel engines is the poor combustion shown by the increase in particulates and carbon monoxide. A potential solution would be to use a slower speed engine, allowing more time for combustion to finish. A longer window for fuel injection from using a slower speed engine would also be beneficial, improving the smoothness of operation.

The most persistent issue, and one which was also regularly found in previous studies was inconsistent atomisation and blocking within the injector. The need for special injectors with larger gaps between the moving parts seems necessary for direct injection engines. The issue with the injector used was that the gap between the needle and the injector body must be small to ensure that injection pressure is achieved, forcing back against the spring used to hold the injector shut. A design where the actuation of the injector is not dependent on the fuel pressure forcing a spring would be better. Some blocking occurred inside the injector holes, reducing the quality and consistency of atomisation. To prevent blocking, the injector holes should be made larger. An issue with this, however, is that smaller injector holes produce better atomisation. To counteract, injection pressure may have to be increased which could cause other problems. An alternative is to use indirect injection for slurry fuels as good atomisation is achieved with low pressures and large injector hole sizes. The drawback is that indirect injection engines have a lower thermal efficiency than direct injection.

Another part which has tight gaps between moving parts is the high-pressure fuel pump. A piston type high-pressure fuel pump was used and no issues were found during the operation.

One of the more surprising results was the fate of ash in the fuel. Whilst an increase in particulates measured both as the total on a mass and a number basis occurred when char was added to diesel, the total was less than expected based on the total ash in the fuel used. The total particulate mass was found to be less than a third of the total ash which passed through the engine when 10%wt. char-diesel slurries were used. Analysis of the lubrication oil showed that some of the ash, especially silicon entered the oil sump, but the difference was less than if all the remaining ash ended here. It suggests that somewhere along the exhaust system of the engine the ash is being deposited.

The presence of trace elements from char such as silicon within the lubrication oil presents another challenge which has not been discussed much in literature. Formulating a special lubrication oil with detergents to help alleviate wear from these deposits should be considered.

Two types of rhododendron char were tested at 10%wt. in diesel- one produced by pyrolysis at 400°C and another by hydrothermal carbonisation at 250°C. Generation efficiency was significantly less when using the slurry fuels at low engine power than neat diesel. However, as power increased, the difference between neat diesel and the slurries in terms of efficiency decreased, to a point at which they were nearly equal.

In terms of emissions for using 10%wt. slurries, there is a clear benefit to using hydrochar instead of pyrochar. CO emissions from both 10%wt. slurries were higher than neat diesel at low power but eventually converged at 3.5kW. The hydrochar slurry emitted consistently less CO emissions than the pyrochar equivalent. Total hydrocarbon (THC) and particulate emissions were less when using a hydrochar slurry than a pyrochar slurry because it burns at lower temperatures. The particulate emissions also showed the importance of surfactant selection as much of the difference compared to neat diesel was caused by the lecithin surfactant used. As particle emissions are harmful, it is recommended to install an exhaust filtration system to address this increase. The soot data for char slurries in the thesis contradicts previous work in Soloiu et al. (2011) which stated smoke reduced when diesel was exchanged for a 25%wt. char-diesel slurry.

9.2.3 Energy and economics

Analysis of the energy consumption showed that the greatest loss occurs during the pyrolysis process which could be reduced by using a good retort kiln, a relatively inexpensive investment. Another important process is the micronisation needed for the char to be able to pass through the injectors. The process requires electricity, provided by the engine, meaning that you can end up “chasing your tail” if the milling process efficiency is low. The more energy

needed for the micronisation process, the more char must be burned to produce the electricity which also needs to be milled down. The laboratory scale process was too inefficient to prevent this cycle from happening. However, literature suggests that wet ball milling of char to the required size can be achieved, consuming just 7.5% of the energy inputted into the process in the form of biomass. The efficiency of the engine is less important than the other two main processes, milling and thermal conversion, in regards to the overall energy input. Investing in more expensive but more efficient engines is, therefore, less crucial. Also, in a developing country, it is likely that engines already available would be converted to slurry systems, rather than new state-of-the-art models.

An economic analysis was performed and it was found that real-world systems in developing countries should aim to gain a contribution to electricity produced of 20% from the char to have a chance for the conversion of a generator to be economical. This means that under 25%wt. diesel slurries would be used only under special circumstances, like an emergency shortage of diesel. The only exception would be if little modification of the engine is needed and economies of scale could be achieved by making slurry fuels in a central production site.

The economic analysis predicted that converting an engine to run on char-water slurries would be financially beneficial when the cost of diesel is over 0.9US\$/kg. After the initial implementation and optimisation of the whole production system on a pilot scale, it could be beneficial to further roll out the technology in regions where the cost of diesel is 0.55\$/kg or higher.

A major cost in the production process is the surfactants used to improve stability and flow properties. The maximum cost of the surfactant used whilst remaining profitable was predicted to be between 0.08 and 0.195\$/kg of char, depending on the cost of diesel, when char-water slurries are used.

A financial comparison was made with using a gasifier to run an engine on biomass. A prediction of the costs per unit of electricity produced from the two different technological approaches was similar, but potentially cheaper through slurry fuels if cheap technical solutions to some of the problems, such as part wear, can be found. Another potential benefit is the economies of scale that could be achieved with slurry fuels. Unlike gasification, where the syngas unit must be connected to the engine used, a single site could be used for the production of slurries and then distributed to decentralised generators.

9.2 Review of objectives

The section reviews to what extent the objectives set out in the introduction have been achieved. The first objective was to conduct a literature review which is found in chapter 2.

The second objective was to investigate suitable feedstocks and thermal conversion routes for creating slurry fuels. Feedstock selection and thermal conversion routes were covered in chapter 4. Also, the chapters 5, 6 and 7 provided supplementary information regarding the appropriateness of materials. Analysis of biomass feedstocks in Nepal was performed to estimate the amount of suitable material in the developing country. It was found that charcoal made from maize cob and sugarcane bagasse are potentially suitable because of the high volatile matter. Whilst the silicon content in the charcoal produced from these feedstocks were low compared to other agricultural residues tested, it was significantly higher than the majority of charcoal produced from woody biomass. Sugarcane bagasse is a potential feedstock for slurry fuels especially in the low lying Terai region of Nepal, along the south of the country. Most of the woody, herbaceous and shrub biomass tested were suitable, but the most suitable were *Eupatorium adenophorum*, *Pinus roxburghii* and *Shorea robusta*. The aim of finding suitable and abundant resources in Nepal which could be used for making slurries was met.

The scope of types of biomass was also broadened to include algae. It was found that macroalgae was unsuitable regardless of how it was thermally treated. Microalgae char produced via HTC, however, may be suitable depending on how corrosion resistant the engine used is.

A general rule was found that thermal treatment temperature should be minimised so that it is just enough to break down the fibrous structure of the biomass. In chapter 6 it was found that the char produced at a lower pyrolysis temperature produced fewer particle emissions than a higher temperature pyrochar, and in chapter 5 it was found that the grindability of the two chars were similar. Another benefit was that less energy was required in the treatment process. One exception for when a high pyrolysis temperature char might be more useful is as an additive in reducing THC, CO and NO₂ emissions if the increasing particulate emissions can be overcome.

Of the two thermal conversion pathways investigated, HTC and pyrolysis, HTC produced the most suitable chars for slurry fuels. They were generally more stable, produced less soot emissions and had higher yields of solid product than pyrolysis chars. Currently, however, hydrothermal carbonisation is not a technology that is or could be used in a developing country.

Overall, the second objective was met as a wide selection of feedstock materials were investigated. The effect of altering the pyrolysis temperature on slurry fuel emissions has been shown, which was not found in literature. Furthermore, a direct comparison between HTC and pyrolysis as a treatment method has not previously been researched.

The next objective set was to investigate how to achieve a suitable degree of micronisation for a slurry fuel used in a diesel engine. This was addressed in chapter 5. The small-scale milling tests on each of the chars used as a slurry fuel in later chapters showed that all could be reduced in size to a value which was suitable for use in a diesel engine. It was found that wet milling in diesel was the best system because every type of char could be milled to the required fineness whereas dry milling caused some to agglomerate.

A two-stage milling process was found to be the most efficient, an initial dry grinding method to produce a comparatively coarse powder, then wet ball milling to produce micronised particles. It was found that without the initial dry grinding, the wet milling would not break the large pieces down. The most energy efficient wet milling speed and time required was found. An analysis of the energy consumption in chapter 8 showed that the amount of energy used in the laboratory scale setup was too high to be realistically viable. This means that the third objective was only partially met as the sufficient micronisation was achieved but questions remain over the energy consumption. However, previous studies in literature do suggest that wet milling methods exist which are more energy efficient and could be suitable for producing slurry fuels in developing countries.

Objective 4 investigated the formulation of slurries with surfactants to improve stability. It was found that char was more stable in RME biodiesel than in diesel, which means that biodiesel potentially could be used as a stabiliser in char-diesel slurries. It was also found that hydrochar slurries were more stable, a further benefit of using hydrothermal carbonisation as the thermal conversion route. The most effective surfactant for stabilising was lecithin, an amphoteric surfactant. The use of the surfactant increased the stability of the slurry from a few hours to over a week, depending on the char used. Lecithin was found to be more effective for stabilising pyrolysis chars than hydrochars. Despite the improvement, the slurries should still be stirred before use to remove any sediment. The degree of stability achieved was good compared to other studies, but further optimisation is still needed to see if the cost and quantity of the surfactant can be reduced.

One of the most important objectives was the fifth, to construct a slurry engine test bed. The system designed produced repeatable results in terms of emissions. One issue occurred that

the fuel consumption rate was inaccurate, but was later improved upon. Overall, the objective was met because the test bed could be used to appraise the quality of slurry fuels produced.

Objective 6 was to investigate using char as an additive to diesel to reduce emissions. At just 0.1%wt. of char added, the amount of emissions produced changed and depended on the initial feedstock, thermal conversion conditions and type of fuel it was added to. As an additive, pyrolysis chars were most effective and reduced THC, CO and NO_x when added at 0.1%wt. to diesel. The major drawback, however, was the increase in particulates produced.

The increase in char added to 1%wt. required modification to the injector system which immediately reduces the suitability of adding this much char to standard liquid fuels. Emissions of NO₂, THC and CO were again reduced by the presence of char. As the modifications significantly increased the amount of particulates produced, under some power conditions the presence of char actually reduced the particle number emissions.

The objective to investigate char as an additive was partially fulfilled as it was shown that the effect of adding a small amount of char could reduce the emissions of certain undesirable compounds. Whilst each char used as an additive had drawbacks, it did show that potentially pyrolysis could be used to create additives for diesel providing the issue of increasing particulates can be overcome.

The most important objective of the thesis, and in many ways the one the other objectives ultimately feed into, was to use a char-diesel slurry where the carbonised solid makes a significant contribution to the overall calorific value of the fuel. Whilst there were significant difficulties with wear from using high silicon char and injector design, it was shown that a 10%wt. char-diesel slurry could be used in a small, high-speed diesel generator in chapter 7. At higher loads, the efficiency came close to that of neat diesel. The direct comparison between pyrolysis and hydrothermal carbonisation showed that slurry made from using the latter produces less particulates, THC and CO compared to pyrochar. The difference can be attributed to the lower recalcitrance of hydrochar.

There are some issues which have occurred in literature that were still not overcome in chapter 7. Mainly, these problems were with the injector which jammed regularly, especially at higher powers. Another point not completely satisfied is the fate of the ash in the fuel, as the amount in the lubrication oil and the smoke is less than expected. The results suggested that most ash was deposited in the exhaust system which could cause other problems. Overall, the objective of using a char-diesel slurry as a fuel was mostly met because the fuels were demonstrated to work in the engine and provided a useful comparison between pyrochar and

hydrochar slurries. Further issues such as the fate of the ash from the char used were found which are not discussed in much detail in the literature.

The final objective aimed to compare slurry fuels to the alternative of gasification in terms of projected cost and energy use. It was found that the amount of energy that is needed for producing electricity from a slurry engine in terms of biomass is similar to gasification. Also, the cost projections show that a lower cost of electricity could be achieved using slurry fuels than diesel or syngas. The objective was met in showing the points in the process most in need to optimise to reduce biomass usage and cost.

9.3 Limitations

There were some limitations to the work which should be noted and avoided in future research. The first was the choice of engine was not ideal for the type of fuel. Issues continued with the injector throughout the work. The use of multi-hole direct injectors has always been a challenge in the literature, regardless of the engine size. The decision not to heavily alter the injectors was taken on the basis of lack of resources and time to create a new one. However, the removal of the needle stem material was partially successful and potentially better than the alternative in previous studies- to make a high-pressure lubrication channel into the needle guide.

The speed of the engine used was higher than the ideal. Reducing the engine speed may also help with smoothing the injection because there is more time available with the injector to open and close. The speed of the engine reduced the combustion period which may have contributed to particle emissions and loss of efficiency, especially at low loads. Reducing speed means that the char is subjected to higher temperatures for longer which is especially important at the lower combustion temperatures at low loads. However, using a high-speed engine did show it was possibly suitable if kept running close to full load.

The choice of engine certainly was limiting, but it is not yet clear what the most suitable engine for slurries is, especially for low power applications in developing countries. This might be a slower speed direct injection or an indirect injection engine.

The size of machinery used to produce the slurry fuels in this study was smaller than what would be needed to continuously run an engine of the size used. For example, the stirred mill could be used to produce approximately 2 litres of 10%wt. slurry fuel an hour, which is about the rate the engine consumes it. Ideally, more would be produced at once to save the amount of labour needed. Also, the pyrolysis reactor could produce just 150g of char a day, much less than is needed. Hence, there is a question of if a process of realistic scale can achieve the energy efficiency needed.

The inability to make large quantities of slurry fuel meant it was not feasible to thoroughly investigate the effect of long-term use on the lifespan of the engine. Some information about wear on the engine was gained in the study through inspecting parts and analysis of lubrication oil. However, a solution to the issue was not found to reduce wear to acceptable levels.

The accuracy of the cost estimate for producing electricity from slurry fuels was limited because the concept of using them for developing countries is at the beginning of the research. The evidence used to predict the cost was mostly based on much larger systems, in developed countries using more abrasive coal slurries.

9.4 Recommendations for further work

A continuing issue has been wear which still occurred despite the use of biomass chars, which are less abrasive than coal, the most common slurry fuel choice. By doing so, it was hoped that the relative absence of aluminium and silicon would reduce the wear rate sufficiently so no further modifications were needed. Choosing low ash materials such as some types of woody biomass is one realistic wear preventative measure that can be used in developing countries. Nevertheless, other investigations should be done to develop engine modifications which are cheap enough for use in developing countries but will increase the lifespan of parts to an amount similar if the engine was using conventional fuels. Investigating adding detergents to the engine oil is one way which could significantly alleviate wear. Increasing alkali content in the lube oil could also be considered as a method to reduce increasing sulphur from using char. Also, harder materials should be investigated for key parts. The cylinder liner and rings are components which require hardening to prevent failure of the engine. A cheaper alternative to tungsten carbide coatings, but has sufficient wear resistance to char fuels would be ideal.

Investigating other types of engine is recommended as the high-speed engine used in this study was not well suited, particularly at low loads, to using slurry fuels. The emissions and performance of slower engines (1500rpm and less) should be studied. Another potentially viable alternative is to use an indirect injection engine, which can achieve good atomisation of fuel without the need for small injector holes.

The most persistent challenge in the running of slurry fuels in this study and many others was the injector which can become blocked or seized by the slurry particles. To find or design a suitable slurry fuel injector is necessary for engines to be run for long periods on slurry fuel. Small injector hole sizes might have to be sacrificed in favour of smoother running. The main area of interest in the injector design will be the needle guide area which can seize. Ensuring the needle sits properly when closed is also important.

Another potentially interesting area would be to investigate turbocharging slurry engines, especially in the case when char-water slurries are used. The greater combustion temperature achieved would help with the burning of char.

Further work is recommended regarding the fate of the ash in the char that enters the engine. It is thought that the majority is deposited in the exhaust system from the results of this thesis. The mechanism for this is unknown. Potentially, molten ash accumulates and solidifies on cooler parts of the engine exhaust. Installing a cyclone on the exhaust could be used to collect any ash that exits the engine for quantification and understanding of formation.

The end goal of the research area is to eventually have a suitable system which can provide electricity to people in rural regions of developing countries, cleanly and reliably. Operating in a laboratory environment with skilled technical staff is different to in the field where replacement parts and mechanics are harder to access. Proving the fuel can be produced and used by villagers in developing countries is important. The research in the thesis has identified many issues which occur using the fuel and how they can be prevented. It has also been shown that the fuel can likely be used in small engine generators which are typically found in developing countries with some modification. Designing a facility for a real developing country situation also raises the possibility of investigating the effect of the continued operation of an engine on slurry fuel, something which is important for calculating long-term maintenance costs.

A simple test procedure for chars that can be used in developing countries would be useful to minimise issues, particularly wear from using the fuel. The needed test would have to include determination of ash content and ideally calcium and silicon content. Some tests are unlikely to be possible in a developing country such as particle size and autoignition temperature of char. Instead, developing a predictive method based on common materials would be more suitable.

Upgrading of the solid fuel in slurries is often performed so that the lifespan of the key parts of the engine are improved. In previous studies, this has involved removing ash from the fuel by separation. Past studies have focussed on quite elaborate methods such as acid washing and froth flotation separation techniques which are unsuitable for the purpose set out in the thesis. However, as the silicon content is low in char compared to that in the more commonly used coal, the level of de-ashing required might be less. Simpler techniques could be investigated such as water leaching and size separation through sieving. Previous studies have shown ash in biomass can be significantly reduced through size separation (Lacey et al., 2016;

Liu and Bi, 2011). The local economy may have uses for the higher ash component of the separated char, including for producing briquettes for cooking and heating.

Further development of char slurries is needed to determine how much diesel fuel can be replaced. The economic assessment predicted that at least 20% of char by energy must be added to diesel for it to be viable to convert the engine from neat diesel to slurry fuels. Increasing the char content in the fuel is one way to reduce the reliance on diesel to produce energy. The higher percent weight of char in the slurry raises concerns about viscosity which, in turn, causes problems with atomisation and poor combustion. This is particularly problematic in small, high-speed engines, such as the one used in the thesis because the time for combustion is more limited. Unburned char will reduce fuel efficiency and potentially increase wear. Detailed viscosity tests and spray pattern investigations would be useful in determining what percentage weight of char could be added to fuel for use in typical engines found in developing countries. An investigation into how viscosity is affected by char feedstock, pyrolysis temperature and micronisation would also be beneficial because, in a real-world process in a developing country, these parameters could change on a daily basis or vary by site.

Another area of study is to further reduce the need for expensive diesel fuel by using another liquid medium such as water or another locally produced biofuel. Ethanol is one which could potentially be used because it is relatively easy to produce. Char could be added to an ethanol-water mixture, with the ethanol acting as a heating value improver, counteracting the heat loss from the water. At present, this has never been demonstrated as a viable fuel for diesel engines. Another option is to dual fuel with a gaseous fuel such as biogas which can also be made locally. Integrating bio oil by-products from the production of char through pyrolysis into the fuel mixture would further increase the amount of biofuel used. Other slurry mixtures using char particles and other locally available biofuels such as plant oils, virgin or used, could be investigated further expanding the fuel-flexibility of diesel generators.

To run slurry fuels in rural regions of developing countries requires the import of certain chemicals which can improve the rheology and stability of the fuel. Development of an affordable surfactant package is, therefore, an important area which needs to be investigated further. Also, reducing the amount of surfactant needed would reduce costs significantly in char-water slurries where it is the main cost. A surfactant package could also improve other properties, by including a cetane improver for char-water slurries or an emissions reducer. Creating a surfactant package that works well with all chars would be the most convenient for end users.

Finally, a life-cycle assessment is recommended to investigate feasibility. Whilst char slurries can be carbon neutral, pollution throughout the production process and end-use occur. There is a requirement for wood which forests would have to supply. The sustainability of the source of feedstock for making char must be considered in a slurry making process. Smoke, carbon monoxide and pyroligneous acid are emitted during the charcoal making process (Cornelissen et al., 2016; Mathew and Zakaria, 2015). The production process for the surfactants must also be considered.

9.5 References

- Cornelissen, G. et al. 2016. Emissions and Char Quality of Flame-Curtain "Kon Tiki" Kilns for Farmer-Scale Charcoal/Biochar Production. *PLoS ONE*. **11**(5), pp.1-16.
- Lacey, J.A. et al. 2016. Ash reduction strategies in corn stover facilitated by anatomical and size fractionation. *Biomass and Bioenergy*. **90**, pp.173-180.
- Liu, X. and Bi, X.T. 2011. Removal of inorganic constituents from pine barks and switchgrass. *Fuel Processing Technology*. **92**(7), pp.1273-1279.
- Mathew, S. and Zakaria, Z.A. 2015. Pyroligneous acid—the smoky acidic liquid from plant biomass. *Applied Microbiology and Biotechnology*. **99**(2), pp.611-622.
- Soloiu, V. et al. 2011. Combustion characteristics of a charcoal slurry in a direct injection diesel engine and the impact on the injection system performance. *Energy*. **36**(7), pp.4353-4371.

Appendix 1: Images of reactors and equipment

Sample preparation

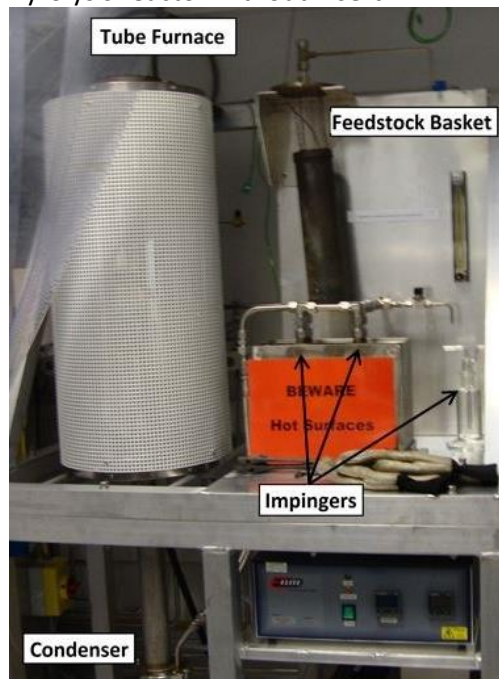
Retsch Cutting mill SM300



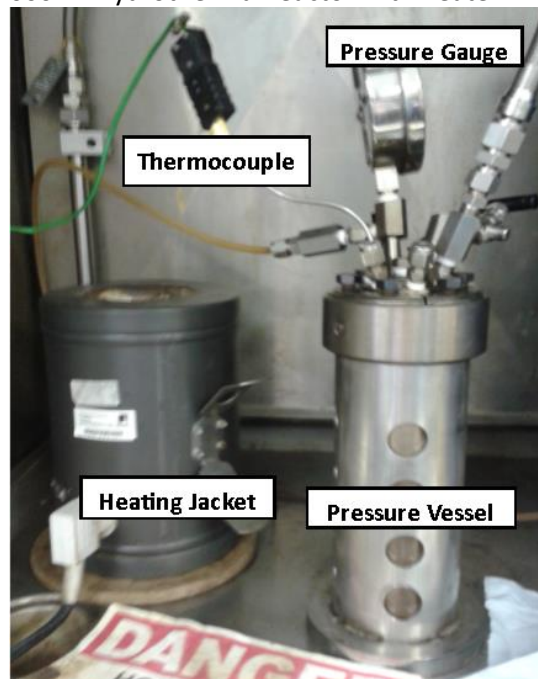
Retsch Cryomill



Pyrolysis reactor without insert



600 ml hydrothermal reactor with heater



Anton Parr Multiwave 3000



Physical and chemical analysis

Mettler-Toledo TGA/DSC 1



Thermo-Scientific EA112 Flash analyser



Thermo-Scientific iCAP7600



Varian 240FS



Varian Unity INOVA spectrometer



Thermo-Scientific Multiskan GO



Malvern Mastersizer 2000E



LUM LUMiSizer



Fuel preparation

Retsch vibratory disc mill RS 200



Tencan JM-3L stirred media ball mill



Engine test facility

Cambustion DMS500



Horiba MEXA-7100D



Engine test bed. Far left: Load bank. Front: Exhaust with sampling ports. Right: fuel tank



Left: Andersen cascade impactor, Right: Single stage filter



Front Panel

Start Program

Real-time thermocouple value

Graph of temperatures since beginning of recording

Fuel remaining in tank

Error handler

Real-time and graph of NOx and oxygen from zirconia sensor

End measurement

Fuel Warning

.txt datalogger

Elapsed Time (s) 0

Fuel Tank Mass (kg) 0

Thermocouples: Lube Oil, Ext Manifold, Exhaust, Inlet Air, RT, Pre Cat, Exhaust sec, Post Cat

Fuel Mass

Temperature

Zirconia Output

Oxygen (%)

NOx (100ppm)

Zirconia sensor

Fuel level: Low Fuel Warning, Very Low Fuel

Data Transfer Timeout

STOP/END

Engine Test.lvproj/NI-cRIO-9066-03088.cdc

Appendix 2: Labview program for datalogging engine test data

Illustrative example of outputted .txt file in Excel table

Wed,
Jun 07,
2017

shea250 7617 0.1 4kw

Time (s)	Lube Oil	Engine outlet	Exhaust	Air Intake	T5	T6	T7	T8
2649.843	65.39205	479.2375	262.0512	28.33125	1372	1372	1372	1372
2650.843	65.40643	479.6301	262.3091	28.33073	1372	1372	1372	1372
2651.842	65.43429	479.278	262.5023	28.34513	1372	1372	1372	1372
2652.84	65.45372	479.34	262.6948	28.3573	1372	1372	1372	1372
2653.838	65.49168	479.5502	262.8977	28.37273	1372	1372	1372	1372
2654.842	65.54324	479.6625	263.075	28.35341	1372	1372	1372	1372
2655.842	65.57005	479.6323	263.244	28.35041	1372	1372	1372	1372
2656.839	65.65904	479.6954	263.4514	28.35473	1372	1372	1372	1372
2657.843	65.69679	479.6311	263.6643	28.36558	1372	1372	1372	1372
2658.843	65.73554	478.9777	263.8885	28.35999	1372	1372	1372	1372

Time (s)	Fuel Mass (kg)
2650.581	4.44
2679.105	4.43
2702.926	4.42
2725.518	4.41

Time (s)	Oxygen (%)	NOx (PPM)
2649.843	6.574707	437.5
2650.843	6.550293	442.8711
2651.842	6.472168	447.7539
2652.84	6.601562	437.5
2653.838	6.496582	447.7539
2654.842	6.652832	442.8711
2655.842	6.472168	442.8711
2656.839	6.601562	442.8711
2657.843	6.420898	442.8711
2658.843	6.601562	453.125
2659.84	6.445312	453.125
2660.841	6.677246	453.125
2661.844	6.523438	442.8711
2662.842	6.601562	447.7539

Appendix 3: Supplementary tests undertaken on biomass and chars from Nepal

Analysis of untreated samples collected from Nepal

Table A3-1 Proximate and ultimate analysis of untreated samples collected from Nepal

Sample	Moisture (% As received (% AR))	Volatile matter (% Dry basis (%DB))	Fixed carbon (% DB)	Ash (% DB)	Carbon (% DB) ^a	Hydrogen (% DB) ^a	Nitrogen (% DB) ^a	Sulphur (% DB) ^a	Oxygen (% DB) ^b	Higher Calorific value (MJ/kg) DB ^c
<i>Alnus nepalensis</i>	3.55	80.37	14.43	5.19	47.82	5.89	0.38	N.D.	40.71	17.35
<i>Castanopsis indica</i>	3.77	76.65	16.95	6.40	46.67	5.75	0.34	N.D.	40.84	16.74
<i>Choerospondias axillaris</i>	3.39	81.28	12.96	5.76	46.07	5.66	0.29	N.D.	42.22	16.15
<i>Ficus semicordata</i>	5.20	75.59	17.21	7.20	46.60	5.55	0.31	N.D.	40.34	16.51
<i>Lagerstroemia parviflora Roxb</i>	4.51	75.31	16.64	8.05	46.07	5.51	0.41	N.D.	39.97	16.34
<i>Lyonia ovalifolia</i>	4.19	76.79	18.72	4.49	48.92	6.68	0.40	N.D.	39.50	19.09
<i>Melia azedarach</i>	4.53	74.92	17.88	7.20	48.03	6.37	0.50	N.D.	37.90	18.62
<i>Myrica esculenta</i>	4.97	74.60	18.74	6.67	47.47	5.44	0.51	0.06	39.86	16.72
<i>Quercus semecarpifolia</i>	5.49	74.32	19.51	6.17	47.45	5.30	0.39	N.D.	40.70	16.37
<i>Pinus roxburghii</i>	4.41	76.17	19.31	4.52	49.72	5.86	0.15	N.D.	39.76	18.12
<i>Rhododendron arboreum</i>	3.90	75.59	18.10	6.31	48.49	5.87	0.25	N.D.	39.08	17.84
<i>Schima wallichii</i>	3.90	75.08	19.30	5.62	47/89	6.20	0.27	N.D.	40.01	17.94
<i>Shorea robusta</i>	4.83	84.33	11.72	3.94	50.55	5.26	0.39	N.D.	39.85	17.52

Table A3-1 continued

Sample	Moisture (% As received (% AR))	Volatile matter (% Dry basis (%DB))	Fixed carbon (% DB)	Ash (% DB)	Carbon (% DB) ^a	Hydrogen (% DB) ^a	Nitrogen (% DB) ^a	Sulphur (% DB) ^a	Oxygen (% DB) ^b	Higher Calorific value (MJ/kg) DB ^c
<i>Zanthoxylum armatum</i>	3.50	77.80	15.35	6.85	46.79	5.84	0.49	0.02	40.02	17.04
<i>Artemisa indica</i>	4.30	75.16	18.40	6.44	47.19	5.83	0.72	N.D.	39.82	17.20
<i>Eupatorium adenophorum</i>	4.54	80.76	13.12	6.12	45.81	6.00	0.32	N.D.	41.74	16.65
<i>Gaultheria fragrantissima</i>	3.49	78.70	15.35	6.85	47.52	5.71	0.17	N.D.	41.26	16.89
<i>Lantana camara</i>	3.38	76.51	17.09	6.40	45.65	6.02	0.54	0.04	41.36	16.68
<i>Woodfordia fruticosa</i>	4.92	74.53	18.97	6.49	47.33	6.06	0.41	N.D.	39.70	17.61
<i>Brassica campestris</i>	5.12	70.98	12.99	16.02	41.51	5.26	1.76	0.05	35.40	15.25
<i>Saccharum officinarum</i>	2.79	80.68	14.77	4.56	45.81	5.94	0.12	0.11	43.47	16.23
<i>Thysanolaena maxima</i>	4.03	73.60	18.53	7.87	45.34	5.56	0.34	N.D.	40.89	16.00
Finger millet	5.26	69.73	13.88	16.39	40.61	5.66	1.50	N.D.	35.84	15.46
Maize cob	4.44	76.92	17/61	5/47	46.27	5.96	0.34	N.D.	41.96	16.69
Maize stem	3.51	76.81	15.29	7.90	47.27	5.75	0.31	0.14	38.62	17.33
Maize cover	4.81	80.68	14.77	4.56	45.42	5.94	0.42	N.D.	42.56	16.27
Rice husk	4.42	61.69	12.37	25.94	36.23	4.77	0.95	N.D.	32.11	13.37

^aDenotes measured used an elemental analyser

^bEstimated by difference from the sum of 100 minus C,H,N and S

^cCalculated by Dulong's formula

Table A3-2 Proximate and ultimate analysis of Pyrolysis chars produced at 600°C from samples collected in Nepal

Sample and pyrolysis temperature (°C)	Char Yield (%)	Moisture (% AR)	Volatile matter (% DB)	Fixed carbon (% DB)	Ash (% DB)	Carbon (% DB) ^b	Hydrogen (% DB) ^b	Nitrogen (% DB) ^b	Sulphur (% DB) ^b	Oxygen (% DB) ^c	HHV (MJ/kg) DB ^d	Energy recovery (%)
<i>Alnus nepalensis</i> 600°C	25.2	1.37	12.75	75.98	11.27	78.29	2.08	1.29	N.D.	7.08	28.23	40.95
<i>Castanopsis inidica</i> 600°C	27.3	2.60	13.68	77.42	8.90	83.34	2.20	0.97	N.D.	4.59	30.57	49.92
<i>Choerospondias axillaris</i> 600°C	23.1	1.57	12.71	78.66	8.63	81.28	2.29	1.11	N.D.	6.70	29.61	42.40
<i>Ficus semicordata</i> 600°C	27.9	2.38	16.46	70.17	13.37	72.79	1.52	0.45	N.D.	11.87	24.70	41.72
<i>Lagerstroemia parviflora</i> Roxb 600°C	27.7	1.78	14.58	74.66	10.75	81.93	1.86	0.73	N.D.	4.72	29.58	50.21
<i>Lyonia ovalifolia</i> 600°C	27.2	2.02	10.87	80.49	8.64	79.40	1.55	0.55	N.D.	9.86	27.35	38.96
<i>Melia azedarach</i> 600°C	27.1	1.97	13.61	77.89	8.50	83.28	2.41	0.82	N.D.	5.00	30.77	44.71
<i>Myrica esculenta</i> 600°C	28.1	1.95	13.34	77.21	9.45	80.52	2.10	1.41	N.D.	6.52	29.12	48.91
<i>Quercus semecarpifolia</i> 600°C	28.7	2.06	12.38	76.38	11.24	80.11	2.11	0.74	N.D.	5.80	29.13	51.05
<i>Pinus roxburghii</i> 600°C	26.1	1.09	10.50	83.52	5.98	83.06	1.97	0.27	N.D.	8.72	29.39	41.88
<i>Rhododendron arboreum</i> 600°C	27.2	1.72	12.69	77.41	9.90	82.56	2.28	0.95	N.D.	4.31	30.46	46.44
<i>Schima wallichii</i> 600°C	28.4	2.56	13.02	76.13	10.85	77.16	1.41	0.36	N.D.	10.23	26.31	41.70
<i>Shorea robusta</i> 600°C	27.0	0.39	10.82	82.86	6.32	87.36	2.44	0.39	N.D.	3.48	32.48	50.04
<i>Zanthoxylum armatum</i> 600°C	24.9	2.24	13.74	75.73	10.54	82.73	2.10	1.84	N.D.	2.80	30.54	44.60
<i>Artemisa indica</i> 600°C	27.3	3.44	13.03	75.64	11.32	80.39	1.90	2.74	N.D.	3.65	29.31	46.51

Table A3-2 continued

Sample and pyrolysis temperature (°C)	Char Yield (%)	Moisture (% AR)	Volatile matter (% DB)	Fixed carbon (% DB)	Ash (% DB)	Carbon (% DB) ^a	Hydrogen (% DB) ^a	Nitrogen (% DB) ^a	Sulphur (% DB) ^a	Oxygen (% DB) ^b	HHV (MJ/kg) DB ^c	Energy recovery (%)
<i>Eupatorium adenophorum</i> 600°C	23.9	3.57	15.60	68.44	15.96	79.35	1.67	0.59	N.D.	9.50	27.56	39.50
<i>Gaultheria fragrantissima</i> 600°C	24.7	1.69	11.30	80.54	8.16	81.61	2.08	0.88	N.D.	7.27	29.33	42.90
<i>Lantana camara</i> 600°C	26.2	4.10	16.78	70.85	12.37	78.53	1.71	1.29	N.D.	6.10	27.96	43.92
<i>Woodfordia fruticosa</i> 600°C	27.9	1.91	14.30	74.69	11.01	80.43	2.17	0.45	N.D.	5.93	29.30	46.39
<i>Brassica campestris</i> 600°C	32.8	3.92	21.31	53.42	25.27	59.44	0.97	1.45	0.48	12.39	19.25	41.39
<i>Saccharum officinarum</i> 600°C	25.3	1.57	9.93	81.83	8.24	84.57	2.21	0.40	N.D.	4.57	31.01	48.36
<i>Thysanolaena maxima</i> 600°C	28.4	3.33	12.24	67.82	19.94	70.14	1.15	0.41	N.D.	8.36	23.90	42.45
Finger millet 600°C	32.5	4.97	19.69	48.77	31.54	57.47	1.56	1.39	N.D.	8.04	20.27	42.55
Maize cob 600°C	24.4	2.51	10.91	78.75	10.34	80.35	2.04	1.09	N.D.	6.17	29.04	42.50
Maize stem 600°C	28.6	3.57	15.60	68.44	15.96	74.56	1.82	1.32	N.D.	6.33	26.74	44.13
Maize cover 600°C	24.6	2.56	11.08	75.39	13.53	81.14	2.09	1.34	N.D.	1.89	30.15	45.58
Rice husk 600°C	38.5	1.85	8.42	37.59	54.00	39.72	0.94	1.05	N.D.	4.29	14.03	40.45

^aDenotes measured used an elemental analyser

^bEstimated by difference from the sum of 100 minus C,H,N and S

^cCalculated by Dulong's formula